U.S. Department
of Commerce

Volume 109
Number 4
October 2011

Fishery Bulletin

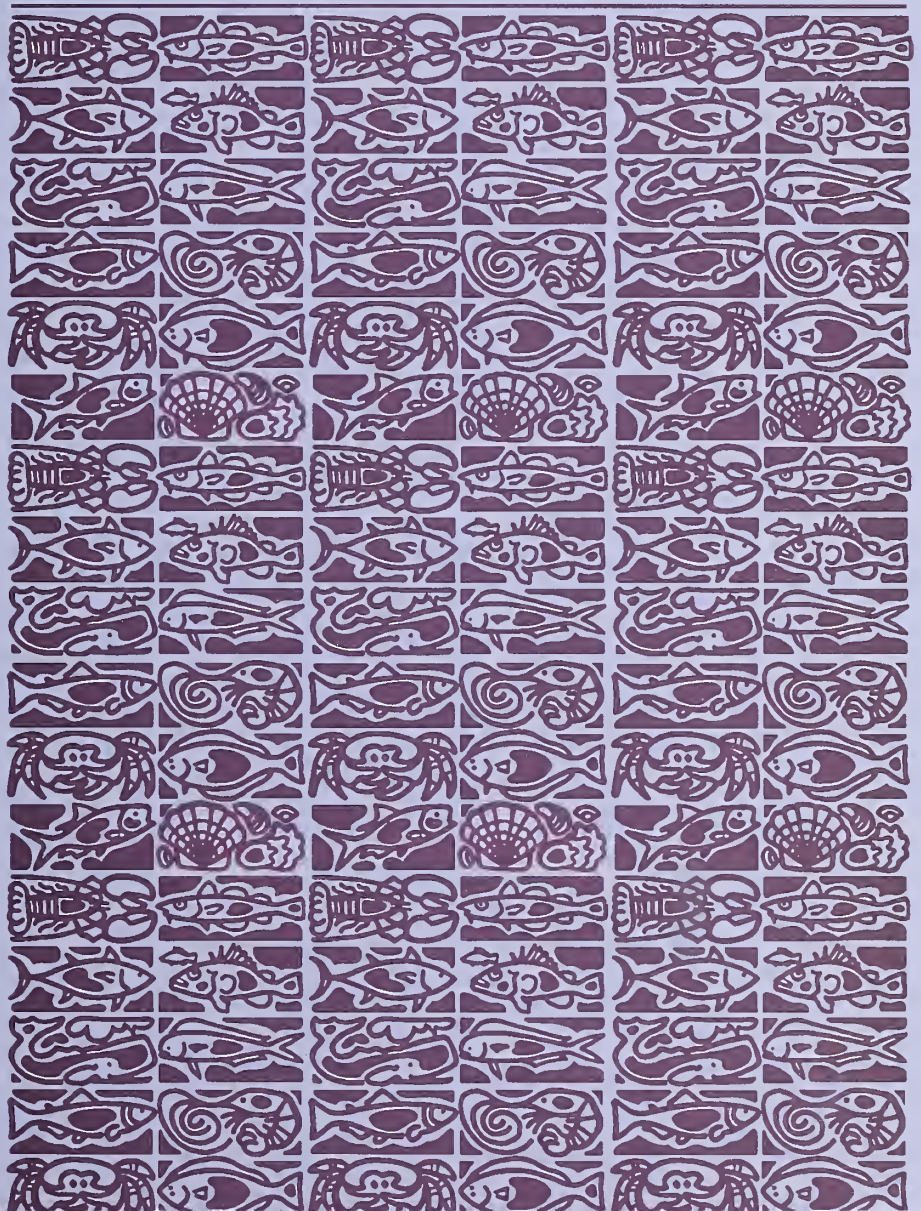

Fishery Bulletin

***Fishery Bulletin* web site: www.fisherybulletin.noaa.gov**

The *Fishery Bulletin* (ISSN 0090-0656) is published quarterly by the Scientific Publications Office, National Marine Fisheries Service, NOAA, 7600 Sand Point Way NE, Seattle, WA 98115-0070.

The Secretary of Commerce has determined that the publication of this periodical is necessary according to law for the transaction of public business of this Department. Use of funds for printing of this periodical has been approved by the Director of the Office of Management and Budget.

For sale by the Superintendent of Documents, U.S. Government Printing Office, Washington, DC 20402. Subscription price per year: $36.00 domestic and $50.40 foreign. Cost per single issue: $21.00 domestic and $29.40 foreign. **See back for order form.**

The *Fishery Bulletin* carries original research reports and technical notes on investigations in fishery science, engineering, and economics. It began as the Bulletin of the United States Fish Commission in 1881; it became the Bulletin of the Bureau of Fisheries in 1904 and the *Fishery Bulletin* of the Fish and Wildlife Service in 1941. Separates were issued as documents through volume 46; the last document was No. 1103. Beginning with volume 47 in 1931 and continuing through volume 62 in 1963, each separate appeared as a numbered bulletin. A new system began in 1963 with volume 63 in which papers are bound together in a single issue of the bulletin. Beginning with volume 70, number 1, January 1972, the *Fishery Bulletin* became a periodical, issued quarterly. In this form, it is available by subscription from the Superintendent of Documents, U.S. Government Printing Office, Washington, DC 20402. It is also available free in limited numbers to libraries, research institutions, State and Federal agencies, and in exchange for other scientific publications.

U.S. Department of Commerce
Seattle, Washington

Volume 109
Number 4
October 2011

Fishery Bulletin

Contents

Articles

341–368 **Musyl, Michael K., Richard W. Brill, Daniel S. Curran, Nuno M. Fragoso, Lianne M. McNaughton, Anders Nielsen, Bert S. Kikkawa, and Christopher D. Moyes**
Postrelease survival, vertical and horizontal movements, and thermal habitats of five species of pelagic sharks in the central Pacific Ocean

369–381 **Riemer, Susan D., Bryan E. Wright, and Robin F. Brown**
Food habits of Steller sea lions (*Eumetopias jubatus*) off Oregon and northern California, 1986–2007

382–393 **Wildes, Sharon L., Johanna J. Vollenweider, Hanhvan T. Nguyen, and Jeffrey R. Guyon**
Genetic variation between outer-coastal and fjord populations of Pacific herring (*Clupea pallasii*) in the eastern Gulf of Alaska

394–401 **O'Connell, Craig P., Daniel C. Abel, Eric M. Stroud, and Patrick H. Rice**
Analysis of permanent magnets as elasmobranch bycatch reduction devices in hook-and-line and longline trials

402–415 **Javor, Barbara, Nancy Lo, and Russ Vetter**
Otolith morphometrics and population structure of Pacific sardine (*Sardinops sagax*) along the west coast of North America

416–428 **Carson, Evan W., Eric Saillant, Mark A. Renshaw, Nancie J. Cummings, and John R. Gold**
Population structure, long-term connectivity, and effective size of mutton snapper (*Lutjanus analis*) in the Caribbean Sea and Florida Keys

429–439 **Muto, Nozomu, Yoshiaki Kai, and Tetsuji Nakabo**
Genetic and morphological differences between *Sebastes vulpes* and *S. zonatus* (Teleostei: Scorpaeniformes: Scorpaenidae)

440–453 **Pearcy, William G., and Joseph P. Fisher**
Ocean distribution of the American shad (*Alosa sapidissima*) along the Pacific coast of North America

454–465 **Andrews, Allen H., Lisa J. Natanson, Lisa A. Kerr, George H. Burgess, and Gregor M. Cailliet**
Bomb radiocarbon and tag-recapture dating of sandbar shark (*Carcharhinus plumbeus*)

466 **List of reviewers**

467–468 **Guidelines for authors**

Subscription form (inside back cover)

Postrelease survival, vertical and horizontal movements, and thermal habitats of five species of pelagic sharks in the central Pacific Ocean

Michael K. Musyl (contact author)[1]
Richard W. Brill[2]
Daniel S. Curran[3]
Nuno M. Fragoso[4]
Lianne M. McNaughton[1]
Anders Nielsen[5]
Bert S. Kikkawa[3*]
Christopher D. Moyes[6]

Email address for contact author: michael.musyl@noaa.gov

[*] Deceased

[1] University of Hawaii
Joint Institute for Marine and Atmospheric Research (JIMAR)
Kewalo Research Facility/NOAA
1125B Ala Moana Boulevard
Honolulu, Hawaii 96814

[2] Northeast Fisheries Science Center
National Marine Fisheries Service
Woods Hole, Massachusetts and
Virginia Institute of Marine Science
P.O. Box 1346
Gloucester Point, Virginia 23062

[3] Pacific Islands Fisheries Science Center
NOAA Fisheries
2570 Dole Street
Honolulu, Hawaii 96822

[4] Large Pelagics Research Center
108 East Main Street
Gloucester, Massachusetts 01930

[5] Technical University of Denmark
National Institute of Aquatic Resources
Jægersborg Allé 1
2920 Charlottenlund, Denmark

[6] Department of Biology
Queen's University
Kingston, ON, K7L 3N6, Canada

Abstract—From 2001 to 2006, 71 pop-up satellite archival tags (PSATs) were deployed on five species of pelagic shark (blue shark [*Prionace glauca*]; shortfin mako [*Isurus oxyrinchus*]; silky shark [*Carcharhinus falciformis*]; oceanic whitetip shark [*C. longimanus*]; and bigeye thresher [*Alopias superciliosus*]) in the central Pacific Ocean to determine species-specific movement patterns and survival rates after release from longline fishing gear. Only a single postrelease mortality could be unequivocally documented: a male blue shark which succumbed seven days after release. Meta-analysis of published reports and the current study (n=78 reporting PSATs) indicated that the summary effect of postrelease mortality for blue sharks was 15% (95% CI, 8.5–25.1%) and suggested that catch-and-release in longline fisheries can be a viable management tool to protect parental biomass in shark populations. Pelagic sharks displayed species-specific depth and temperature ranges, although with significant individual temporal and spatial variability in vertical movement patterns, which were also punctuated by stochastic events (e.g., El Niño-Southern Oscillation). Pelagic species can be separated into three broad groups based on daytime temperature preferences by using the unweighted pair-group method with arithmetic averaging clustering on a Kolmogorov-Smirnov D_{max} distance matrix: 1) epipelagic species (silky and oceanic whitetip sharks), which spent >95% of their time at temperatures within 2°C of sea surface temperature; 2) mesopelagic-I species (blue sharks and shortfin makos, which spent 95% of their time at temperatures from 9.7° to 26.9°C and from 9.4° to 25.0°C, respectively; and 3) mesopelagic-II species (bigeye threshers), which spent 95% of their time at temperatures from 6.7° to 21.2°C. Distinct thermal niche partitioning based on body size and latitude was also evident within epipelagic species.

Manuscript submitted 11 January 2011.
Manuscript accepted 16 May 2011.
Fish. Bull. 109(4):341–368 (2011).

The views and opinions expressed or implied in this article are those of the author (or authors) and do not necessarily reflect the position of the National Marine Fisheries Service, NOAA.

Although there is considerable disagreement and uncertainty about the current state of pelagic fish populations (Burgess et al., 2005; Hampton et al., 2005; Sibert et al., 2006), there is general agreement that large apex predators, particularly sharks, are at greatest risk of overfishing (Baum et al., 2003; Baum and Myers, 2004; Camhi, 2008). Possessing life-history characteristics (e.g., slow growth, long gestation, late maturity) that evolved in the absence of industrial fishing, pelagic shark species are susceptible to overfishing, and declining trends in some populations need to be reversed for parental biomass to rebuild stocks (Camhi, 2008; Chang and Liu, 2009; Dulvey et al., 2008). With food web models, Schindler et al. (2002) predicted that continued mortality of blue shark (*Prionace glauca*) in longline fisheries in the central Pacific could adversely affect their populations and the role of this species as apex predators. Moreover, commercial and recreational fishing activities generally remove the largest animals (i.e., parental biomass) and heavy selection pressure over several decades can potentially cause evolutionary effects (e.g., heritable changes in life-history traits such as body size, growth, age-at-maturity, and fecundity; Law, 2000; DiBattista et al., 2009; Genner et al., 2009).

Large pelagic sharks, particularly blue sharks, which form a large part of the international shark fin trade (Clarke et al., 2006), are generally not targeted but are by far the majority of the bycatch in pelagic gill nets and longline fisheries targeting swordfish (*Xiphias gladius*) (Camhi, 2008; Mandelman et al., 2008; Nakano and Stevens, 2008). Effective strategies to mitigate shark bycatch requires knowledge of species-specific horizontal and, more importantly, vertical movement patterns (e.g., Wat-

son et al., 2009). Knowledge of these vertical movement patterns may allow fishing crews to target the opportunity of mismatch between hook depth and the sharks' vertical distributions and thus possibly minimize bycatch (Beverly et al., 2009). For effective management measures to be implemented, it is also beneficial to have accurate estimates of both at-vessel and postrelease mortality rates (Carruthers et al., 2009). These data are necessary for estimating total fishery-induced mortality and for improving stock assessments (Kitchell et al., 2004). Mitigation strategies could then be given special consideration for species with high rates of postrelease mortality (Carruthers et al., 2009).

Information on postrelease mortality in blue sharks (Carey and Scharold, 1990; Weng et al., 2005; Moyes et al., 2006; Campana et al., 2009a; Queiroz et al., 2010; Stevens et al., 2010), bigeye threshers (*Alopias superciliosus*) (Nakano et al., 2003; Weng and Block, 2004), shortfin makos (*Isurus oxyrinchus*) (Holts and Bedford, 1993; Klimley et al., 2002; Sepulveda et al., 2004; Loefer et al., 2005), and common thresher sharks (*A. vulpinus*) (Heberer et al., 2010) is available from studies with acoustic tracking and pop-up satellite archival tags (PSATs). In two studies (Moyes et al., 2006; Campana et al., 2009a), the investigation of postrelease mortality of blue sharks released from longline fishing gear was the primary goal, but mortality rates may have been confounded by specific aspects of fishing practices (Musyl et al., 2009). Hook type, time spent hooked on the line, fight time, leader material, fish size, and handling and discard practices can influence the at-vessel and postrelease mortality of pelagic shark species (e.g., Diaz and Serafy, 2005; Moyes et al., 2006; Campana et al. 2009a; Carruthers et al., 2009; Heberer et al. 2010; Hoey and Moore[1]).

Our goals were to measure postrelease mortality rates and vertical movement patterns in the five most commonly captured pelagic shark species in the Hawaii-based commercial longline fishery: blue sharks, bigeye threshers, oceanic whitetip sharks (*Carcharhinus longimanus*), shortfin makos, and silky sharks (*C. falciformis*)(Walsh et al., 2009). All five species represent a significant portion of the shark bycatch in global fisheries and their life history characteristics make populations vulnerable to fishing pressure (Cortés, 2000; Camhi, 2008; Dulvy et al., 2008; Stevens, 2008; Chang and Liu, 2009). Moreover, there is little or no information about their postrelease survival, population ecology, and movement patterns in the central Pacific Ocean. As far as we know, there are no published reports on the movements and postrelease mortality of silky sharks and oceanic whitetip sharks, and several authors have commented on the paucity of information on the biology and ecology of these apex predators (Bonfil, 2008; Bonfil, et al., 2008; Dulvy et al., 2008). Results from this study extend the work presented in Moyes et al. (2006) and are expected to be useful in the mitigation of shark bycatch and mortality.

Materials and methods

Sharks were caught by pelagic longline fishing gear (from March 2001 through November 2006) deployed from the NOAA research vessels *Townsend Cromwell* and *Oscar Elton Sette* and by using methods described in Moyes et al. (2006). In brief, longline gear (~400–800 hooks per set) was deployed at night (usually immediately after dusk) and retrieved in the morning. Because we used four to six hooks between floats; hook depths were generally <100 m as determined by attached time-temperature-depth recorders (Wildlife Computers, Redmond, WA).

Soak times ranged from 10 to 24 hours with an average of 15 hours, and before 2004, we employed 15/0 size circle hooks, squid (*Illex* spp.) bait, and green chemical light sticks attached to the monofilament nylon leader ~90 cm above each hook. However, because of regulations introduced in 2004 to reduce sea turtle bycatch in the Hawaii-based shallow-set (nighttime) commercial longline fishery targeting swordfish (Gilman et al., 2007; Walsh et al., 2009), we began using 16/0 and 18/0 circle hooks (no offset), and Pacific saury (sanma, *Cololabis saira*) as bait. In addition, to improve shark catch rates by reducing bite-offs from monofilament leaders, we added ~25 cm of seven-strand braided stainless steel cable immediately above the hook.

Sharks were hoisted aboard by a sling and restrained by the crew as described in Moyes et al. (2006). Sharks showing an absence of movements or reaction of the nictitating membrane to light touching of the eye were deemed dead and were not tagged (i.e., these samples would bias the postrelease mortality estimate). Tagged sharks were measured to the nearest centimeter for total length (TL), and hooks were removed by cutting them in half with bolt cutters unless they were too deeply ingested, in which case, the leader line was cut as close to the mouth of a shark as possible. PSATs (model PTT-100, Microwave Telemetry, Columbia, MD) were affixed to the dorsal fin by drilling a 10–15 mm diameter hole near the base of the fin and threading seven-strand braided stainless steel cable encased in soft plastic tubing (which acted as the harness) through the wound. Next, a second tether (made of ~123-kg breaking strength fluorocarbon leader material) was used to attach (with stainless steel crimps and thimbles) the PSAT to the dorsal fin harness. The only exception was applied to bigeye threshers, which were tagged in the water by using a harpoon, and for these sharks the tag head was affixed to the end of the tethers on the PSAT. For these sharks, total lengths were visually estimated.

PSATs were programmed to acquire temperature and pressure (depth) readings every 15–60 minutes and

[1] Hoey, J. J., and N. Moore. 1999. Captain's report: multispecies catch characteristics for the U.S. Atlantic pelagic longline fishery. National Fisheries Inst. report to NOAA, National Marine Fisheries Service, Silver Spring, MD, 78 p. [Available from http://www.sefsc.noaa.gov/seaturtlecontractreports.jsp, accessed May 2011.]

pop-up dates were set at 8–13 months after deployment of the tags. Depth and temperature data were measured as 8-bit numbers, yielding a depth resolution of ~5.4 m and temperature resolution of ~0.17°C. Fail-safe options were also programmed into the PSAT software whereby stationary PSATs (i.e., those experiencing no significant changes in pressure) or shed tags would begin transmitting archived data to the ARGOS satellite system after four days. In the event of mortality, once the shark sank to ~1200 m and remained there for ~15 minutes, the PSAT would separate from the shark, float to the surface, and begin transmitting stored data to ARGOS.

Daily (raw) geolocation estimates were calculated by the manufacturer using ambient light-level irradiance data during postprocessing of the satellite data with a proprietary algorithm (Gunn and Block, 2001). From the raw geolocations, most probable tracks (MPTs), movement parameters, and associated error estimates were calculated by a state-space Kalman filter algorithm with position estimates refined with the use of sea surface temperature (SST) (Nielsen et al., 2006). Depth and temperature data were assigned to daytime or nighttime according to times of local dusk and dawn derived from longitude and latitude estimates (from the MPTs) with the use of standard astronomical formulae (Meeus, 1998).

Resampling techniques were used to construct 95% parametric bootstrap confidence intervals (CI*) (with the assumption of a binomial distribution with 10,000 replicates) for postrelease mortality estimates and PSAT reporting rates (Manly, 2007). Meta-analysis was used to estimate a summary effect for postrelease mortality in blue sharks from published studies (Weng et al., 2005; Campana et al., 2009a; Stevens et al., 2010) and the present report, by assuming that these studies represent random samples of some population in which the underlying (infinite-sample) effect sizes have a distribution rather than a single value (i.e., random effects model, Borenstein et al., 2009). The analysis was conducted on the logit (log odds ratio) of the proportion of blue sharks that ultimately died as identified from PSATs across studies by using Comprehensive Meta Analysis, vers. 2.2 (www.Meta-Analysis.com, accessed November 2010). Postrelease mortality estimates and 95% confidence intervals were weighted by sample size and the number of studies where heterogeneity was assumed (i.e., with the random-effects model where each study was assumed to have its own postrelease mortality rate and variance). The Q statistic, a measure of heterogeneity, was calculated to test whether postrelease mortality estimates across studies were similar, and the Z test was used to determine whether the postrelease mortality estimate was significantly greater than zero (Borenstein et al., 2009). If postrelease mortality is consistent across studies, then the meta-analysis yields a combined estimate that is more precise than any of the separate estimates (Borenstein et al., 2009). For presentation purposes, logits were converted back into percentages.

Data provided by the PSATs were divided into six data streams by parsing depth data into day depth (DD), night depth (ND), and "all" depth (=both day and night) (AD); and temperature data into day temperature (DT), night temperature (NT), and combined temperature (AT). Nonparametric tests were used to examine variation by species with Kruskal-Wallis ANOVAs (to compare equality of medians across individuals) for each of the data streams where the test statistic (H_c) was adjusted for ties (Zar,1996) because data distributions were not normally distributed (Lillifors tests, $P<0.01$). For each species, multiple *post-hoc* pairwise Mann-Whitney W-tests, with Bonferroni corrected P-values to account for inflation of type-I error based on multiple tests of the same hypothesis (MWBC), were used to compare equality of medians within and between individuals for each of the data streams (Zar, 1996). When only a single Mann-Whitney test could be performed, Monte Carlo methods (10,000 random assignments) were used to obtain an empirical P-value that approximated the exact P-value without reliance on asymptotic distributional theory or exhaustive enumeration (Manly, 2007). The greatest vertical distance (D_{max}) between cumulative distribution functions among tags from two-sample Kolmogorov-Smirnov (KS) tests was formatted into distance matrices as input for the unweighted pair-group method by using arithmetic average (UPGMA) clustering (Sneath and Sokal, 1973; Musyl et al., 2003). This procedure allowed us to observe patterns of depth and temperature preferences across pelagic species. Electronic tag data from Pacific bigeye tuna (*Thunnus obesus*) (Musyl et al., 2003), swordfish, black marlin (*Istiompax indica*), and blue marlin (*Makaira nigricans*) (Musyl et al.[2]) served as outgroups to help clarify and define relationships (Sneath and Sokal, 1973). The cophenetic correlation was used as a measure of goodness-of-fit between the matrices and resultant clustering dendrograms (e.g., 0.7–0.8 is considered "poor," >0.8 is considered "good," and >0.9 is considered "very good" [Rohlf, 1992]).

Time-at-depth and time-at-temperature data were aggregated into 20-m and 1°C bins, respectively. These data were subsequently expressed as a fraction of the total time of observation for each shark, and the fractional data bins were averaged across all sharks within each category. For sharks experiencing several lunar cycles, the correlation coefficient (R) was determined between average nighttime depth (m) and lunar illumination (Zar, 1996). Lunar illumination data were obtained from the United States Naval Observatory (http://aa.usno.navy.mil/data/docs/MoonFraction.php, accessed June 2010) and were uncorrected for cloud

[2] Musyl, M. K., L. M. McNaughton, J. Y. Swimmer, and R. W. Brill. 2004. Convergent evolution of vertical movement behavior in swordfish, bigeye tuna and bigeye threshers. Vertical niche partitioning in the pelagic environment as shown by electronic tagging studies. Pelagic Fisheries Research Program, Univ. Hawaii Manoa, Newsletter 9:1–4.

cover. Unless indicated otherwise, all statistical tests were performed at the P=0.05 level of significance.

Results

Rates of at-vessel and postrelease mortality

Capture date, sizes, deployment location, set pop-off date, ARGOS reporting location, days-at-liberty, and linear displacement for tagged sharks are summarized in Table 1. The overall PSAT reporting rate was 62% (CI*=50–73%), although reporting rates varied by species: 100% for silky sharks; 81% (CI*=63–98%) for oceanic whitetip sharks; 50% (CI*=34– 65%) for blue sharks; 40% (CI*= 0–80%) for shortfin makos; and 38% (CI*=13–75%) for bigeye threshers. Median days-at-liberty were likewise species-specific: bigeye threshers, 240 days (range: 181–240 days); shortfin makos, 165 days (155–174 days); oceanic whitetip sharks, 164 days (10–243 days); blue sharks, 86 days (1–247 days); and silky sharks, 73 days (12–194 days).

The fraction of sharks found dead during gear retrieval was species-specific and was concordant with estimates derived from the commercial fishery (Table 2). More importantly, we were able to document only one case of postrelease mortality out of the 44 sharks (2.3%, CI*=0–6.8%) whose PSAT transmitted data. One blue shark (male, 173 cm TL) expired seven days after being released (one mortality in 16 reporting tags affixed to blue shark; 6.3%, CI*=0–19%).

Meta-analysis indicated the summary effect (Table 3) for postrelease mortality in blue sharks was 15% (95% CI, 8.5–25.1%). The Z statistic indicated that postrelease mortality was significantly different from zero (P<0.001) and the Q statistic indicated studies were measuring the same parameter (P=0.680). Although the narrower 95% CI bounds for the summary effect (Table 3) indicated increased power over individual studies; a comparison of postrelease mortality estimates between Campana et al. (2009a) and the present study for blue sharks (with the assumption that sharks have equal chance of survival) at 80% power would require ~275 reporting PSATs (two-tailed Z-tests between two independent proportions at α=0.05, Zar, 1996).

Horizontal movements

For each of the pelagic shark species, estimated most probable tracks are shown in Figure 1. Error estimates for longitude were much lower than those for latitude in the movement model (Appendix 1). Geolocations could not be calculated for PSATs attached to bigeye threshers (Fig. 1F) because of extreme and rapid vertical excursions coinciding at crepuscular times and the inability of the light sensor to record these changes (Musyl et al., 2001, 2003).

For species where geolcation data were available, some individuals exhibited more directed movements as indicated by their advection-diffusion parameters whereas other movement patterns were more complex or cyclical (Fig. 1, Appendix 1). For example, the advection parameters for longitude (u=9.23) and latitude (v=3.84) indicated primarily east–west movements by the shortfin mako with ID 38572 (female, 210 cm TL) when it swam from subtropical waters near Hawaii to temperate waters in the North Pacific, including California Current coastal waters off central California (Fig. 1E). Tagged silky sharks traveled west and southwest of the Hawaiian Islands in 20–2004, but south of 10°N in 2005, near the North Equatorial Countercurrent (NEC) (Fig. 1C). The diffusion parameters estimated from the movement model indicated that six sharks exhibited relatively meandering swimming behaviors whereas three individuals (IDs 46585, 38581, 38573) exhibited more north–south directed movements. Oceanic whitetip sharks showed a complex movement pattern generally restricted to central Pacific tropical waters north of the NEC (Fig. 1D). Nine individuals exhibited meandering swimming behavior, whereas three sharks (IDs 13113, 38582, 46568) generally adopted more straight-line swimming modes, of which one shark (ID 38582) made a directed southward movement across the equator into the South Pacific. Although restricted to central Pacific tropical waters north of the NEC, blue sharks showed complex movement patterns (Fig. 1, A and B) from waters near Hawaii into the Subtropical Convergence Zone. As determined from deployment and pop-up locations, blue sharks tagged in 2001 occupied latitudes from 7.92° to 30.75°N (Fig. 1A), but individuals tagged in 2002 did not travel farther south than 17.6°N (Fig. 1B).

Vertical movements

Blue sharks remained significantly deeper and experienced significantly cooler temperatures during the day than during the night (Fig. 2; Appendices 2 and 3). Moreover, the significant daytime and nighttime differences in depth and temperature preferences were evident within and across individuals, and also when the data were grouped by sex (Figs. 2 and 3; Appendices 2 and 3). As identified by the coefficient of variability, daytime and nighttime vertical movement patterns were similar, but the vertical movements of male blue sharks were significantly more variable than those of females. Coefficients of variability over 1.0 have been used to indicate possible mixtures in samples (Simpson et al., 1960) and values over 1.0 in blue sharks are reflective of individuals switching from a typical deep-daytime to shallow-nighttime vertical movement pattern, or exhibiting a mixture of the two patterns (Fig. 2). The aggregated temperature-depth profile (Fig. 2B) shows that blue sharks regularly undertake movements beneath the uniformed temperature surface layer, but with considerable variability at crepuscular transitions (Fig. 2E). Several blue sharks adjusted their nighttime behaviors simultaneously with changing lunar illumination (Appendix 2).

Bigeye threshers showed the most striking differences in depth and temperature preferences and all MWBC

Table 1

Tagging details for pop-up satellite archival tags (PSATs) affixed to blue shark (*Prionace glauca*), shortfin mako (*Isurus oxyrinchus*), silky shark (*Carcharhinus falciformis*), oceanic whitetip shark (*C. longimanus*) and bigeye thresher (*Alopias superciliosus*). Total length (TL) was measured to the nearest cm. Set pop-off date is the programmed time PSATs were scheduled to report data after deployment. The locations where the PSATs were deployed and reported from in latitude and longitude east are given in decimal degree format. DAL=days-at-liberty, nr=nonreporting tag, M=male, F=female, and linear displacement of PSATs from deployment to reporting locations in nautical miles (nmi).

PSAT no. and sex	TL (cm)	Tagging date	Set pop-off date	Deployment latitude	Deployment longitude	Reporting date	Reporting latitude	Reporting longitude	DAL	Linear displac. (nmi)
Blue shark (*Prionace glauca*)[1]										
13081F	168	03/30/01	06/29/01	29.06	199.09	03/31/01	21.76	201.10	4	451.31
13083F[a]		04/05/01	10/03/01	18.79	201.61	05/10/01	23.36	197.99	35	340.92
13085F	168	04/02/01	09/30/01	18.77	201.68				nr	
13087M	204	04/05/01	05/05/02	18.81	201.64	04/27/01	25.82	194.77	22	567.47
13088M	152	04/10/01	05/10/02	18.88	201.72				nr	
13089F[a]	160	04/10/01	05/10/02	29.07	199.05				nr	
13091M[b]	173	04/11/01	05/11/02	28.29	201.28	04/16/01	18.91	201.10	5	562.89
13093F	160	04/11/01	05/11/02	28.30	201.33	07/22/01	29.40	216.34	102	791.03
13094F[a]		04/05/01	05/05/02	28.28	201.24				nr	
13095F	160	04/03/01	05/03/02	29.08	199.02	05/23/01	17.21	192.93	50	787.07
13096F	173	04/03/01	05/03/02	30.31	201.50	06/11/01	7.92	200.05	69	1345.87
13097F	183	04/02/01	05/02/02	30.75	200.01	08/23/01	26.45	199.50	143	259.39
13098F[a]	150	04/05/01	05/05/02	30.31	201.50	11/24/01	22.38	188.62	233	839.20
13111F[c1]	152	04/14/01	05/14/02	30.26	201.93	06/10/01	13.91	199.54	41	989.87
13209M	140	04/09/02	12/10/02	28.48	202.09				nr	
13215F	200	04/07/02	12/08/02	31.02	199.97	12/10/02	28.56	191.30	247	474.81
13218F[a]	145	04/06/02	12/07/02	31.02	199.97				nr	
13225M	131	04/05/02	12/06/02	31.01	199.96				nr	
13226M	133	04/10/02	12/11/02	31.01	199.97				nr	
13475M	120	04/10/02	12/11/02	31.03	199.99				nr	
13478M[d]		04/10/02	12/11/02	30.24	201.93				nr	
13491F	215	04/10/02	12/11/02	31.01	199.96	12/10/02	24.06	189.58	244	691.39
13497F[a]	200	04/10/02	12/11/02	21.56	201.43	05/16/02	35.18	206.29	36	856.19
13499F[c2]	175	04/06/02	12/07/02	31.01	199.96	12/08/02	17.60	183.69	246	1196.73
13501M	196	04/10/02	12/11/02	30.70	199.93				nr	
13503F	187	04/02/02	12/03/02	31.10	199.90	07/31/02	25.08	209.39	120	618.26
27322M	148	04/10/02	12/11/02	30.96	199.92	12/10/02	34.07	206.03	244	360.98
27323M	180	04/09/02	12/10/02	31.13	199.94				nr	
29149F	200	04/12/02	12/13/02	30.99	199.95				nr	
29537M	160	04/10/02	12/11/02	26.64	201.97				nr	
29541M	158	04/12/02	12/13/02	30.93	198.59				nr	
29872M	180	04/10/02	12/11/02	19.10	201.83				nr	

continued

Table 1 (continued)

PSAT no. and sex	TL (cm)	Tagging date	Set pop-off date	Deployment latitude	Deployment longitude	Reporting date	Reporting latitude	Reporting longitude	DAL	Linear displac. (nmi)
Shortfin mako (*Isurus oxyrinchus*)[2]										
13496M	185	04/04/02	12/05/02	26.64	201.97				nr	
28721M	118	04/13/02	12/14/02	30.93	198.59				nr	
30371M	190	04/24/02	12/25/02	19.10	201.83				nr	
38572F	210	12/03/02	08/06/03	21.78	203.70	05/07/03	28.94	231.81	155	1579.10
46583F		11/15/06	07/17/07	18.83	201.68	05/08/07	18.55	199.45	174	127.85
Silky shark (*Carcharhinus falciformis*)[3]										
38573M	170	12/09/02	08/12/03	19.01	203.90	04/20/03	9.67	197.05	132	687.15
38581F	140	12/12/02	08/15/03	19.34	202.92	01/12/03	13.80	195.27	31	551.20
38599M	200	04/02/03	12/02/03	19.25	203.71	05/08/03	18.85	200.25	36	197.69
38601M	200	12/11/02	08/14/03	19.47	203.95	06/23/03	21.42	200.22	194	240.12
46564M		02/11/05	10/13/05	7.34	197.06	03/03/05	6.63	198.09	20	74.68
46566M		02/07/05	10/09/05	6.86	197.22	03/04/05	6.88	205.56	25	496.80
46571M	168	05/20/04	01/19/05	19.37	202.83	06/01/04	19.90	201.48	12	82.65
46585M	120	02/05/05	10/07/05	5.24	198.50	05/26/05	6.01	191.44	110	424.08
46588M	137	05/09/04	01/08/05	18.13	201.59	10/01/04	18.41	199.66	145	111.24
46590F	116	02/01/05	10/03/05	8.13	199.73	03/01/05	7.71	206.31	28	391.84
Oceanic whitetip shark (*Carcharhinus longimanus*)[4]										
13092F	120	04/13/01	05/13/02	19.46	203.90	09/24/01	23.84	186.61	164	998.57
13113M		02/07/05	10/09/05	8.10	199.64	08/01/05	7.82	182.46	175	1020.93
29487F	107	04/25/02	12/26/02	19.27	203.97				nr	
29918F	225	04/21/02	12/22/02	19.21	203.85	05/01/02	18.88	198.20	10	321.04
38574M	100	12/07/02	08/09/03	18.36	201.71				nr	
38575M	200	12/04/02	08/07/03	21.36	204.14	07/07/03	25.40	201.73	215	276.34
38576M	200	12/05/02	08/07/03	19.42	203.92	05/03/03	19.02	207.41	149	199.18
38582M	115	12/07/02	08/10/03	29.08	199.01	03/12/03	−9.30	195.01	95	2314.41
38598M	200	04/03/03	06/03/03	19.58	203.73	06/03/03	16.48	198.06	61	373.10
46568M		05/16/04	01/15/05	18.55	204.52	08/10/04	23.77	193.07	86	712.72
46569M	127	02/01/05	10/03/05	19.49	203.98	06/18/05	8.73	191.71	137	961.60
46570F		05/14/04	01/13/05	18.25	201.51	01/02/05	15.28	202.12	233	181.61
46579M	120	02/06/05	10/08/05	5.97	197.57				nr	
46581M	100	05/22/04	01/21/05	19.60	203.71	12/14/04	16.26	200.23	206	282.15
46587M		05/09/04	01/08/05	18.13	201.55	01/07/05	16.18	201.58	243	117.01
46589F		05/20/04	01/19/05	19.37	202.88	01/17/05	19.21	201.53	242	77.05

continued

Table 1 (continued)

PSAT no. and sex	TL (cm)	Tagging date	Set pop-off date	Deployment latitude	Deployment longitude	Reporting date	Reporting latitude	Reporting longitude	DAL	Linear displac. (nmi)
Bigeye thresher (*Alopias superciliosus*)[5]										
28476[e]		04/28/02	12/29/02	18.52	201.97	12/24/02	16.45	234.67	240	1872.98
29290[e]		04/27/02	12/28/02	18.55	202.17				nr	
29481[e]	200	04/27/02	12/28/02	18.57	202.08	12/23/02	19.84	198.66	240	208.22
29896[e]		04/27/02	12/28/02	18.56	202.11				nr	
30028[e]		04/28/02	12/29/02	18.52	201.96				nr	
30373[e]		04/27/02	12/28/02	18.55	202.13				nr	
38597[f]	200	04/01/03	05/31/03	18.71	203.19				nr	
46582[f]		05/21/04	01/20/05	19.39	202.84	11/18/04	19.72	229.97	181	1532.40

[1–5] Estimated lengths at maturity (given in cm of total length [TL]), M=male, F=female.

[1] Blue shark: ~200 cm for both sexes (M: 182–235 cm, F: 173–229 cm, Nakano and Stevens, 2008).

[2] Shortfin mako, M: 195–202 cm, F: 265–312 cm (Stevens, 2008).

[3] Silky shark, M: 180–210 cm, F: 180–218 cm (Bonfil, 2008).

[4] Oceanic whitetip, M: 168–196 cm, F: 175–189 cm (Bonfil et al., 2008).

[5] Bigeye thresher, M: 270–288 cm, F: 332–341 cm (Smith et al., 2008).

[a] Nuptial bites present on dorsal, pectoral fins and body.

[b] Postrelease mortality (see also Moyes et al., 2006).

[c1] Hook ingested and stomach everted at capture; specimen recaptured by Japanese longline fishing vessel on 25 May, 2001; 41 days at-liberty, conventional plastic tag no.1649 recovered in addition to PSAT and harness (no cuts, abrasions on PSAT or harness)

[c2] Hook ingested, stomach everted.

[d] PSAT likely damaged during release.

[e] PSATs affixed with metal tag heads near base of dorsal fin by using a harpoon (Musyl et al. 2011).

[f] PSATs affixed with flopper tag heads (i.e., nylon tag head augmented with stainless steel spear gun blades, Musyl et al., 2011) near base of dorsal fin by using a harpoon.

Table 2

Number of pelagic sharks caught and those retrieved dead from shallow-set longline gear targeting swordfish (*Xiphias gladius*). Mortality estimates from the Hawaii-based commercial longline fishery are provided for comparison (na=not available).

Species	No. caught	Samples[1] taken	No. dead	% dead	% dead commercial fishery[2]	
					Shallow	Deep
Blue shark (*Prionace glauca*)	203	37	12	5.9	5.7	4.0
Crocodile shark (*Pseudocarcharias kamoharai*)	3	2	2	66.7	na	13.6
Oceanic whitetip shark (*Carcharhinus longimanus*)	19	6	1	5.3	7.4	20.7
Shortfin mako (*Isurus oxyrinchus*)	8	4	0	0	20.5	7.5
Silky shark (*Carcharhinus falciformis*)	35	3	4	11.4	na	21.8
Bigeye thresher (*Alopias superciliosus*)	12	1	3	25.0	22.6	16.5
Pelagic thresher shark (*Alopias pelagicus*)	28	0	10	35.7	na	na
Total	308	53	32	10.4	na	na

[1] Sampled for biochemical correlates of morbidity and mortality (Moyes et al., 2006).

[2] At-vessel mortality estimates of pelagic sharks from the shallow-set longline gear targeting swordfish (*Xiphias gladius*) and deep-set longline gear targeting bigeye tuna (*Thunnus obesus*) in the Hawaii-based longline fishery, 2004–06 (Walsh et al., 2009).

Table 3

Meta-analysis of postrelease mortality of blue sharks (*Prionace glauca*) as determined from pop-up satellite archival tags (PSATs). The postrelease mortality rate estimate was determined with a random-effects model, where each study was assumed to have its own postrelease mortality rate and variance. Details of the analysis can be found in the text and in Borenstein et al. (2009). Nonreporting PSATs were not used in the analysis.

Study	Samples[1]	Postrelease mortality rate	95% confidence interval
Weng et at. (2005)	2/17	0.118	0.030–0.368
Campana et al. (2009b)	7/37	0.189	0.093–0.347
Stevens et al. (2010)	1/8	0.125	0.017–0.537
Musyl et al. (present study)	1/16	0.063	0.009–0.335
Summary effect	11/78	0.150	0.085–0.251

[1] Postrelease mortality in blue sharks (*Prionace glauca*) determined with PSATs over (/) the total number of reporting PSATs for each study

tests were significantly different among daytime and nighttime comparisons (Figs. 3 and 4; Appendices 2 and 3). The dichotomy between coefficients of variability indicates that bigeye threshers are significantly more active at nighttime than during daytime. The aggregated temperature-depth profile (Fig. 4B) and vertical movements indicate that bigeye threshers spend most of their time beneath the uniformed temperature surface layer, and that increased variability in vertical movement patterns occurs during crepuscular transitions (Fig. 4E).

Oceanic whitetip sharks and silky sharks showed similar vertical movement patterns (Figs. 5 and 6, respectively), and the depth and temperature data indicated that both species were largely confined to the uniform temperature surface layer (Figs. 3, 5, and 6; Appendices 2 and 3). Although oceanic whitetip sharks and silky sharks exhibited plasticity in their daytime and nighttime vertical movements, both species spent >95% of their time at temperatures that were within 2°C of the uniform temperature surface layer (Table 4). Oceanic whitetip sharks (Fig. 5E) and silky sharks (Fig. 6E) exhibited pronounced movements at crepuscular periods and both species showed significant correlations between average nighttime depths and lunar illumination (Appendix 2).

Further analysis of silky shark data indicated distinct depths and temperatures occupied north and south of 10°N, delimited by the NEC (Fig. 1C). Comparisons of pooled day and night data showed that silky sharks north of 10°N remained significantly deeper (median=54 m, mean=57 m ±0.4 SE, interquartile range [IQR]=22–86 m) than immature silky sharks south of 10°N (median=32 m, mean=32 m ±0.3 SE, IQR=11–48 m) (MWBC, z= –108.9, Monte Carlo P<0.0001). Likewise silky sharks north of 10°N experienced significantly cooler temperatures (median=25.5°C, mean=25.4°C ±0.01 SE, IQR=24.7–25.9°C) than silky sharks south of 10°N (median=28.4°C, mean=28.3°C ±0.007 SE,

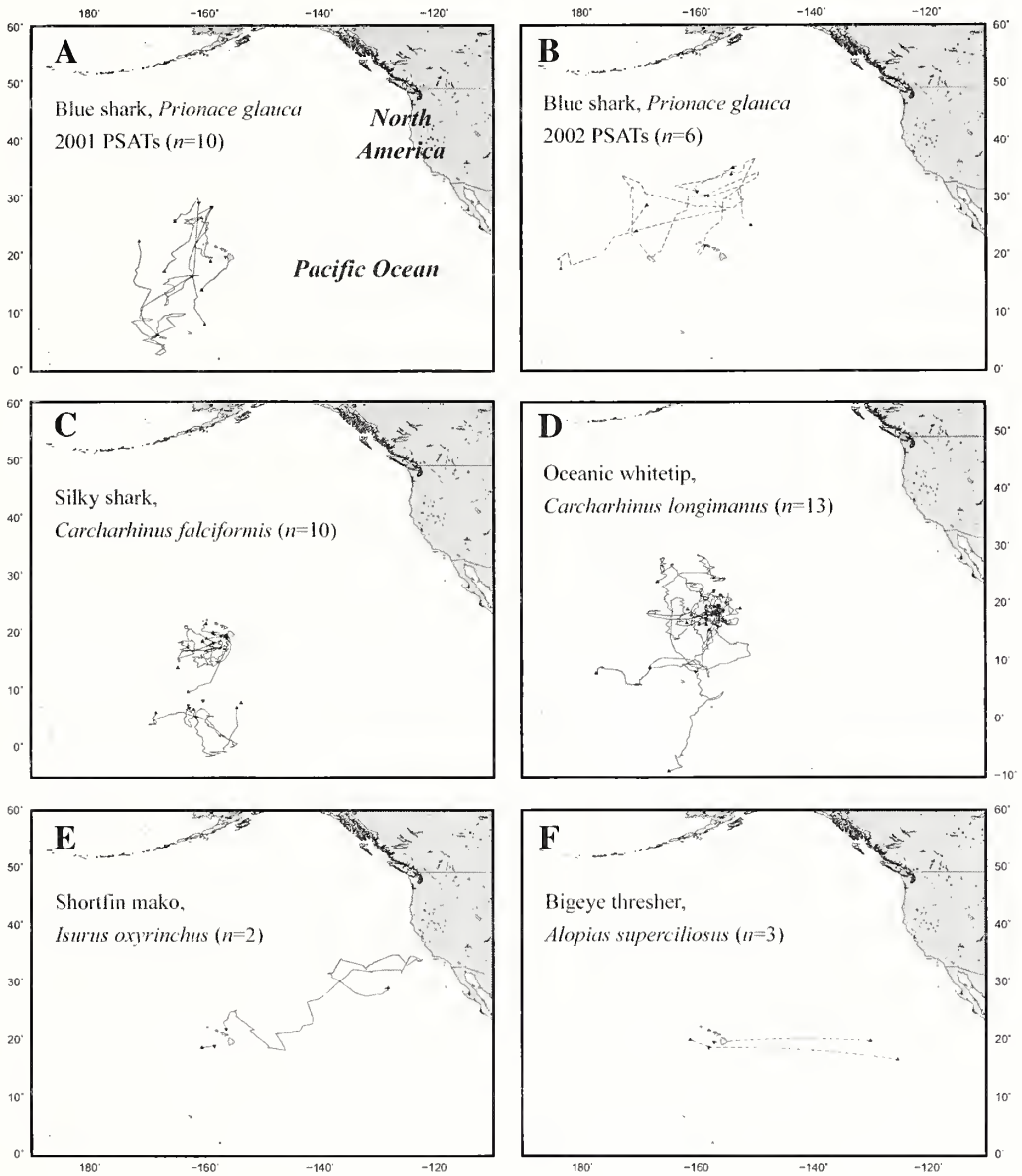

Figure 1

Most probable tracks for five species of pelagic sharks tagged with PSATs and released in the central Pacific Ocean were estimated from the raw geolocations using the Kalman filter-sea surface temperature state-space model (Appendix 1). Downward triangles indicate pop-up satellite archival tag (PSAT) deployment locations and upward triangles indicate PSAT pop-up locations. In situations where no geolocation data were returned, movements of sharks with from PSAT deployment to pop-up locations are indicated as a straight line. (**A**) Blue sharks (*Prionace glauca*) tagged in 2001, where male shark movement patterns are shown in gray; (**B**) blue sharks (*Prionace glauca*) tagged in 2002, where male shark movement patterns are shown in gray; (**C**) silky sharks (*Carcharhinus falciformis*), where female movement patterns are shown in gray; (**D**) oceanic whitetip sharks (*C. longimanus*), where female movement patterns are shown in gray; (**E**) shortfin makos (*Isurus oxyrinchus*) (n=2, both female); and (**F**) bigeye threshers, (*Alopias superciliosus*).

IQR=28.2–28.6°C) (MWBC, z= −39.47, Monte Carlo P<0.0001). Within and between these two geographic groups, significantly different trends for depth and temperature preferences during daytime and nighttime were also observed.

Female shortfin makos remained significantly deeper and at cooler temperatures during the daytime than at nighttime (Figs. 3 and 7; Appendices 2 and 3). Unlike pronounced crepuscular patterns exhibited by blue sharks, bigeye threshers, silky sharks, and oceanic

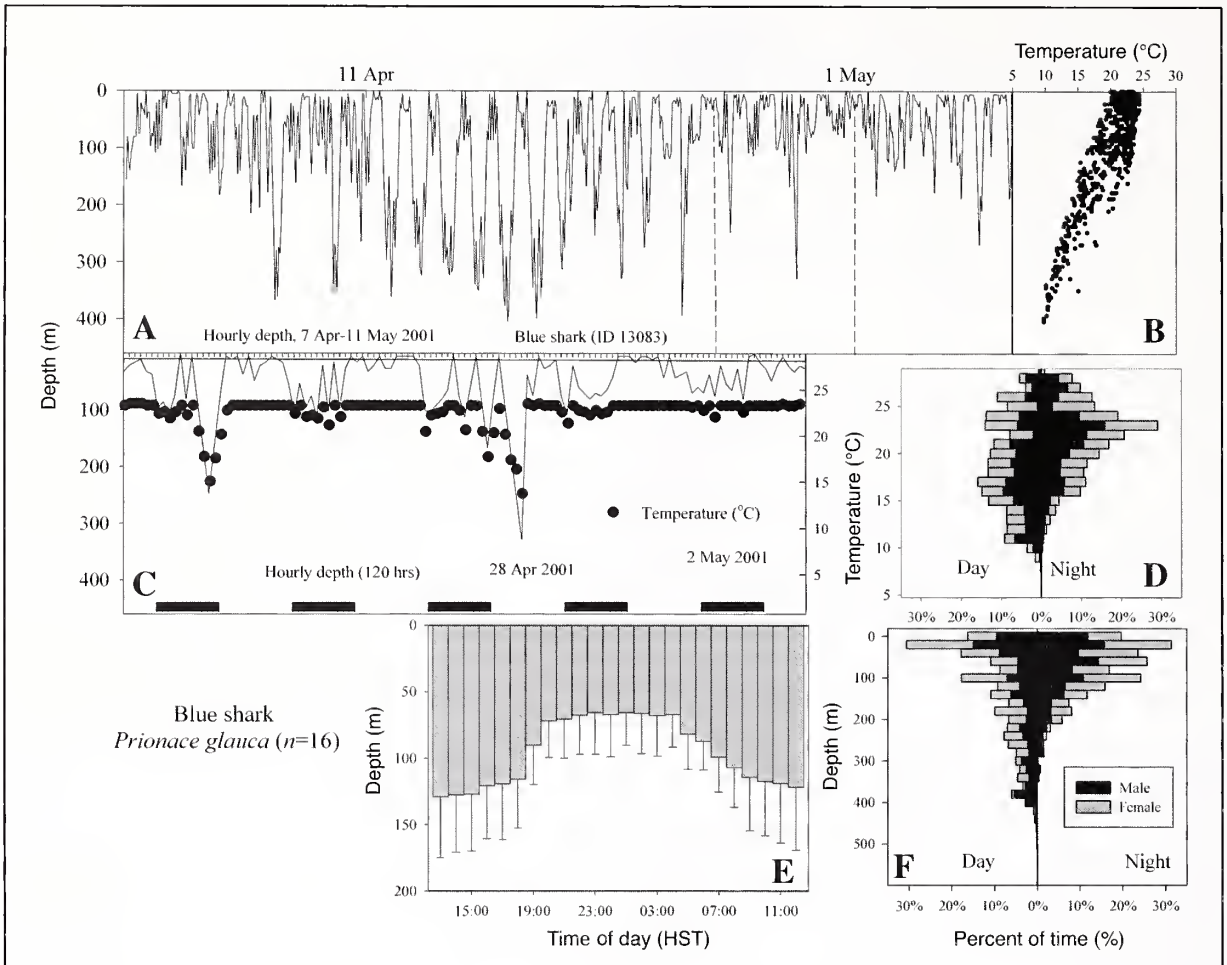

Figure 2

Blue shark (*Prionace glauca*) depth and thermal ranges as identified by pop-up satellite archival tags (PSATs). (**A**) Representative vertical movements. Dashed lines indicate expanded area shown in C. (**B**) Temperature-depth profiles obtained from the aggregated data from all sharks. (**C**) Expanded section from panel A with horizontal black bars representing nighttime. (**D**) Percentage of time spent in individual temperature strata for daytime and nighttime diving activities (all tags). (**E**) Average hourly depth (±standard deviation, SD) readings calculated for all samples, illustrating variability at crepuscular times (all tags). (**F**) Percentage of time spent in individual depth strata for daytime and nighttime diving activities (all tags). (Note: to prevent excessive clutter, SDs were not shown in some panel figures).

whitetip sharks; shortfin makos did not display striking changes in behavior during crepuscular transitions (Fig. 7E). Traveling west to east from deployment to pop-up location can alter times of sunrise and sunset by as much as −4 and −1.5 h, respectively, but one shortfin mako (ID 38572) made no obvious depth corrections to account for spatial changes in the times of local sunrise and sunset as did bigeye threshers (*cf.* Fig. 4E). Shortfin makos made regular excursions beneath the uniform temperature surface layer, and vertical movement patterns were more variable during daytime than at nighttime (Figs. 3 and 7). Around 27 January 2003, a shortfin mako (ID 38572) crossed the ~18°C SST isotherm, the southern boundary of the North Pacific Transition Zone (Polovina et al., 2001), at 31.34°N, 135.18°W (Fig. 1E) and moved into cooler water. Comparisons of pooled daytime and nighttime data showed that this individual remained significantly deeper (median=113 m, mean=125 m ±2 SE, IQR=91– 161 m) in warmer water than after it crossed the boundary and entered cooler water (median=87 m, mean=90 m ±2 SE, IQR=39–118 m) (MWBC, z= −16.45, Monte Carlo P<0.0001). Temperature data indicated that significantly warmer temperatures were encountered before 27 January 2003 (median=21.02°C, mean=20.5°C ±0.01 SE, IQR=19–22°C) than after this date (median=14.9°C, mean=14.8°C ±0.05 SE, IQR=14–16°C) (MWBC, z= −35.04, Monte Carlo P<0.0001). The switching between water masses is clearly seen in the temperature-depth profile (Fig. 7B).

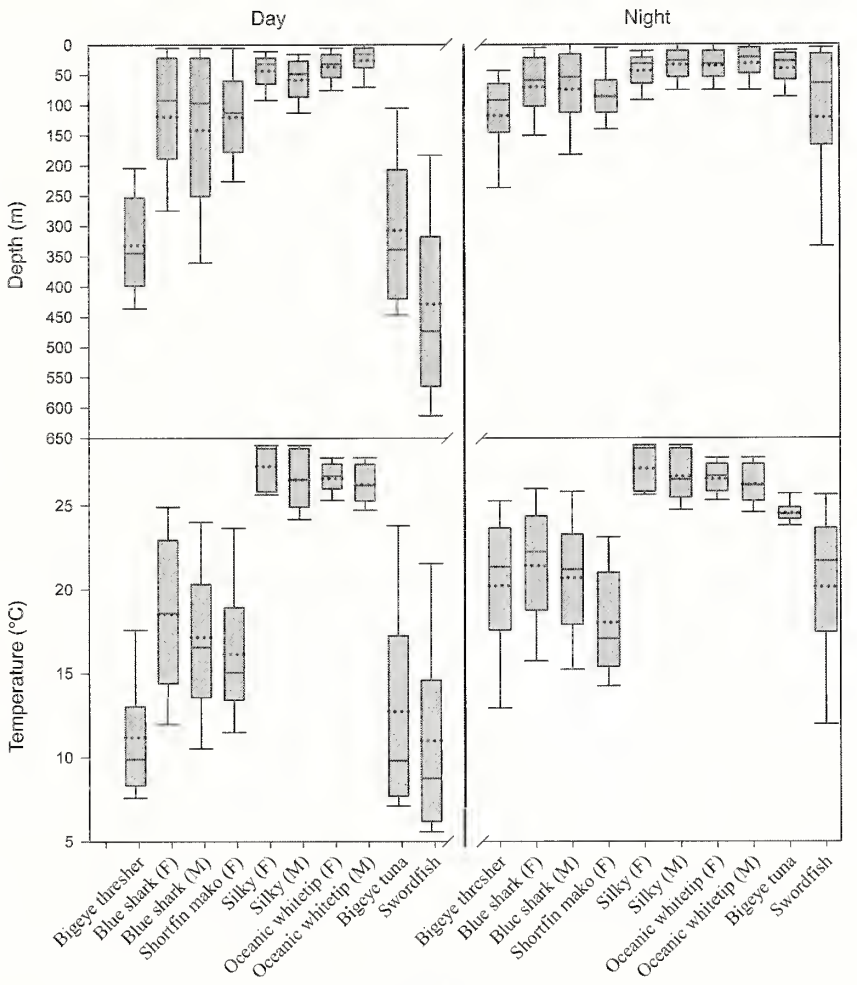

Figure 3

Daytime and nighttime depth and thermal ranges for pelagic species: bigeye thresher (*Alopias superciliosus*), blue shark (*Prionace glauca*), shortfin mako (*Isurus oxyrinchus*), silky shark (*Carcharhinus falciformis*), oceanic whitetip shark (*C. longimanus*), bigeye tuna (*Thunnus obesus*), and swordfish (*Xiphias gladius*). The box represents the interquartile range. The position of the mean (dashed horizontal line) and median (solid horizontal line) are indicated and the "whiskers" represent the 10–90th deciles. M=male and F=female.

Grouping of vertical movement patterns

Kruskal-Wallis ANOVAs showed that medians of depth and temperature data across individuals for each pelagic shark species (24 total tests) were all significantly different for the six PSAT data streams, indicating substantial amounts of individual variability in vertical movement patterns (Appendix 3). This result was confirmed by *post-hoc* pairwise MWBC tests (Appendix 3). Significantly different daytime and nighttime median depths and temperatures (DD vs. ND, DT vs. NT) were evident in most pooled comparisons (including those by sex) and in the majority of comparisons within and between individuals. Results from two-sample KS tests for each of the pelagic shark samples paralleled the results given for the MWBC tests. For the entire sample of 394 possible two-sample KS tests in which depth distributions between individuals were compared, 94% of tests were significantly different. And of 394 possible tests for temperature comparisons, 98% of tests were significantly different.

Although individuals exhibited high levels of variability, we were able to partition shark species into three major groups based on daytime temperature preferences by using UPGMA clustering with the D_{max} distance (Fig. 8). These were 1) epipelagic species that included silky sharks and oceanic whitetip sharks, plus the outgroups black marlin and blue marlin; 2) mesopelagic-I species that included blue sharks and shortfin makos;

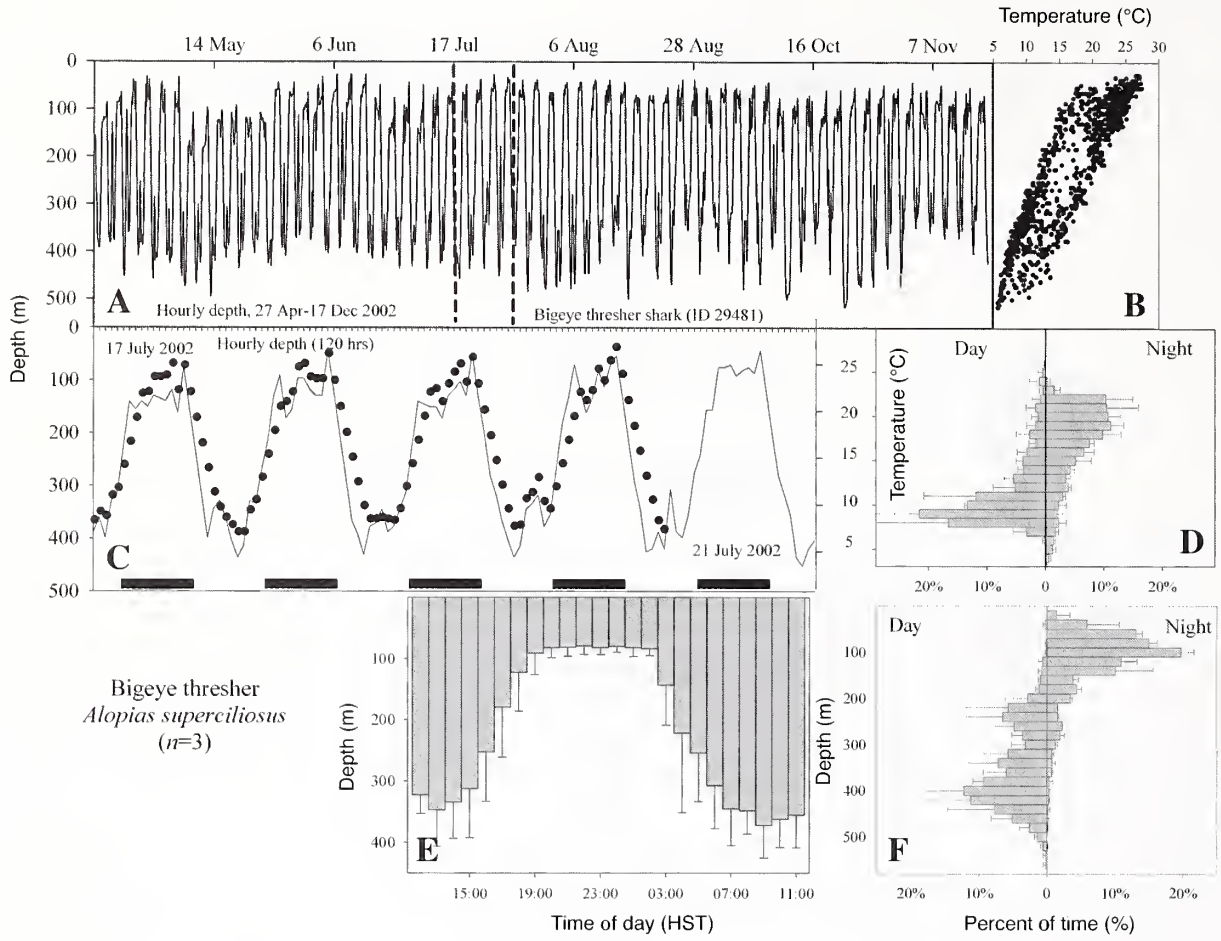

Figure 4

Bigeye thresher (*Alopias superciliosus*) depth and thermal ranges as identified by pop-up satellite archival tags (PSATs). (**A**) Representative vertical movements. Dashed lines indicate expanded area shown in C. (**B**) Temperature-depth profiles obtained from the aggregated data from all sharks. (**C**) Expanded section from panel A with horizontal black bars representing nighttime. (**D**) Percentage of time spent in individual temperature strata (±standard deviation, SD) for daytime and nighttime diving activities (all tags). (**E**) Average hourly depth (±SD) readings calculated for all samples, illustrating variability at crepuscular times (all tags). (**F**) Percentage of time spent individual depth strata (±SD) for daytime and nighttime diving activities (all tags).

3) mesopelagic-II species that included bigeye threshers plus outgroups bigeye tuna and swordfish. The epipelagic group could be further broken down by body size and latitude because juvenile silky sharks south of 10°N formed the most distinctive cluster (i.e., exhibited the longest branch lengths). Moreover, another distinctive epipelagic cluster was composed entirely of presumably mature silky and oceanic whitetip sharks >200 cm TL whose PSATs separated from the sharks at latitudes above 18°N. The cophenetic correlation (0.86) indicated "good" fit between the data matrix and resultant dendrogram. A similar clustering pattern was obtained with daytime depth data (cophenetic correlation=0.88) but it included five mismatches to the pattern observed with daytime temperature (i.e., black marlin ID 13208, silky shark IDs 38573, 38581, 38601 were placed in mesopelagic-I and blue shark ID 13095 was placed in the epipelagic group). The mismatches, however, may have been attributable to the relatively poor resolution of PSAT depth data in comparison with the temperature data. There was, however, no discernible pattern with nighttime depth (cophenetic correlation=0.77) and temperature data (cophenetic correlation=0.88) because all species generally remained near the surface.

Discussion

Rates of at-vessel and postrelease mortality

Mortality for blue sharks at the time of gear retrieval in commercial longline fisheries operating in the

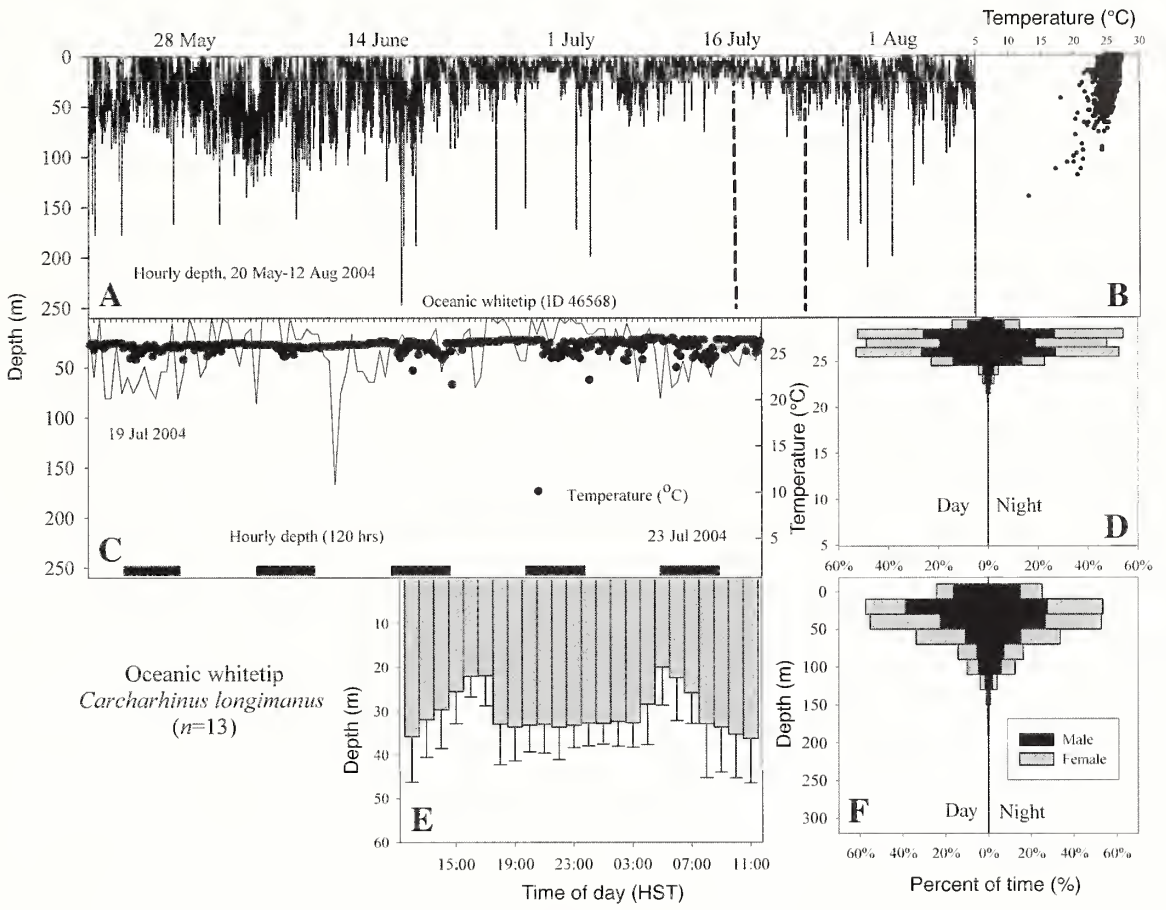

Figure 5

Oceanic whitetip shark(*Carcharhinus longimanus*), depth and thermal ranges as identified by pop-up satellite archival tags (PSATs). (**A**) Representative vertical movements. Dashed lines indicate expanded area shown in C. (**B**) Temperature-depth profiles obtained from the aggregated data from all sharks. (**C**) Expanded section from panel A with horizontal black bars representing nighttime. (**D**) Percentage of time spent in individual temperature strata for daytime and nighttime diving activities (all tags). (**E**) Average hourly depth (±standard deviation, SD) readings calculated for all samples, illustrating variability at crepuscular times (all tags). (**F**) Percentage of time spent in individual depth strata for daytime and nighttime diving activities (all tags). (Note: To prevent excessive clutter, SDs were not shown in some panel figures).

Atlantic range from 10–32% (32%, Hoey and Moore[1]; 31%, Diaz and Serafy, 2005; 13.2%, Beerkircher et al., 2008; ~10%, Carruthers et al., 2009; 16%, Campana et al., 2009a). By contrast, in central Pacific longline fisheries, Walsh et al. (2009) reported that only 4% and 6% of blue sharks were dead on retrieval from deep-set tuna and shallow-set swordfish gear, respectively. Our sample sizes, except for those for blue sharks, were not large enough to have a strong statistical impact; nevertheless, our estimates of at-vessel mortality appear to be species-specific and correlate with observations for the shallow-set sector of the Hawaii-based longline fishery (Walsh et al., 2009). The at-vessel mortality estimates for blue sharks were also concordant with those reported in the Pacific by Yokota et al. (2006, 2–11%) and Hight et al. (2007, ~6%).

Our reporting rate for PSATs attached to blue sharks (50%) was similar to that reported by Weng et al. (2005) for 28 PSATs (61%, CI*=43–79%). Non-reporting tags, however, cannot be considered synonymous with mortality because other factors can cause failure in electronic tags (Goodyear, 2002; Hays et al., 2007; Campana et al., 2009a; Musyl et al., 2011. PSATs can, however, provide less ambiguous identification of mortality because they will automatically release from the animal at programmed depths (Moyes et al., 2006). This is especially true for sharks because dead sharks are negatively buoyant and sink, thus carrying the PSATs to depths where the pressure-activated release mechanism will be engaged (Moyes et al., 2006; Campana et al., 2009a).

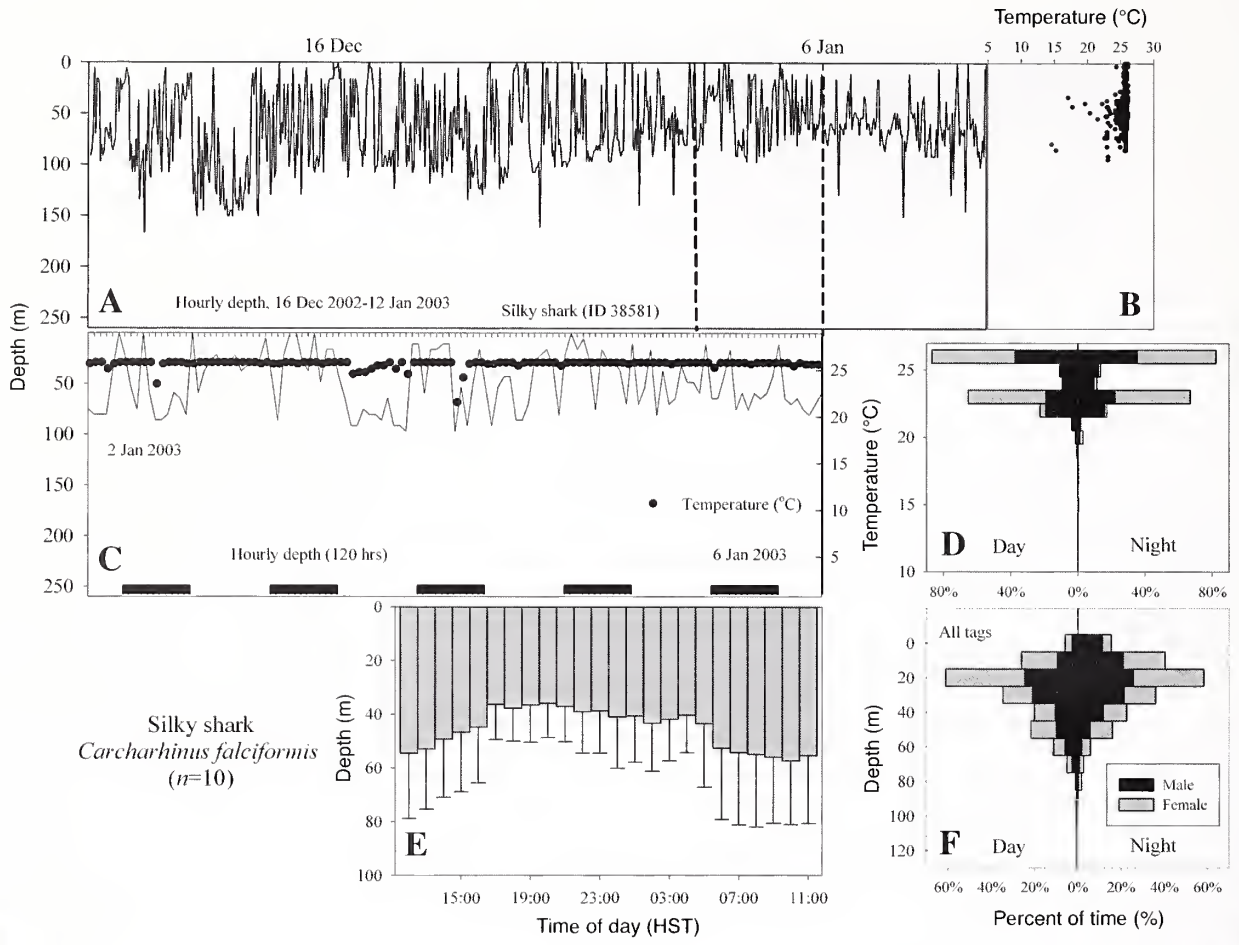

Figure 6

Silky shark (*Carcharhinus falciformis*) depth and thermal habitat as identified by pop-up satellite archival tags (PSATs). (**A**) Representative vertical movements. Dashed lines indicate expanded area shown in C. (**B**) Temperature-depth profiles obtained from the aggregated data from all sharks. (**C**) Expanded section from panel A with horizontal black bars representing nighttime. (**D**) Percentage of time spent in individual temperature strata for daytime and nighttime diving activities (all tags). (**E**) Average hourly depth (± standard deviation, SD) readings calculated for all samples illustrating variability at crepuscular times (all tags). (**F**) Percentage of time spent in individual depth strata for daytime and nighttime diving activities (all tags). (Note: To prevent excessive clutter, SDs were not shown in some panel figures).

Campana et al. (2009a), using PSATs, determined that 19% (CI*=8–32%) of blue sharks tagged in the North Atlantic longline fishery targeting swordfish and released alive subsequently died. We could find only two other published studies where PSATs had been used with blue sharks and that provided postrelease mortality estimates. Weng et al. (2005) and Stevens et al. (2010) reported 11.8% (CI*=0–29%) and 14.3% (CI*=0–42%) postrelease mortality, respectively. As determined by meta-analysis with all available data from 78 reporting PSATs, the summary effect of postrelease mortality of blue sharks was 15% (95% CI, 8.5–25.1%). However, because only two of four studies were specifically designed to estimate mortality, experimental bias could be a confounding factor, as well as small and unrepresentative sample sizes (Campana et al., 2009b; Musyl et al., 2009).

We could find no equivalent postrelease mortality estimates for bigeye thresher, shortfin mako, silky sharks, or oceanic whitetip sharks. Heberer et al. (2010), using PSATs, reported a 26% postrelease mortality rate of common thresher sharks released from recreational gear where fight-times ≥85 minutes identified survivors from moribund individuals. Our postrelease mortality rates for pelagic sharks were similar to PSAT tagged istiophorid billfish released from commercial pelagic longline gear in the Atlantic (average postrelease mortality rate was 9%, CI*=2–18%) (Kerstetter et al., 2003; Kerstetter and Graves, 2005, 2008).

Table 4

Cumulative percentage of temperature readings from pop-up satellite archival tags (PSATs) attached to silky and oceanic whitetip sharks expressed as differences from daily calculated sea surface temperature (ΔSST°C) for daytime and nighttime diving behavior.

Silky shark (*Carcharhinus falciformis*)									
Day	52.56	87.06	95.78	98.26	99.53	99.84	99.96	100	
Night	63.30	91.63	96.93	98.80	99.26	99.48	99.71	99.83	100
Total	57.71	89.25	96.33	98.52	99.40	99.66	99.84	99.92	100
ΔSST (°C)	0	−1	−2	−3	−4	−5	−6	−7	−8
Oceanic whitetip shark (*Carcharhinus longimanus*)									
Day	63.89	91.53	96.88	98.59	99.36	99.63	99.87	99.95	100
Night	61.40	89.98	95.92	98.39	99.21	99.58	99.86	99.94	100
Total	62.67	90.77	96.41	98.49	99.29	99.61	99.86	99.95	100

Methods for determining postrelease mortality in large pelagic fishes and sharks

Implementing survival studies for pelagic species is challenging because of logistics, cost, experimental design, and obtaining sufficient samples. There are only a few methods for estimating survival, and each has limitations. Historically, long-term survival of pelagic species has been estimated by large-scale conventional tagging programs with low return rates (<5%, blue shark, Kohler et al., 1998; ~1%, blue marlin, Ortiz et al., 2003). Such results are consistent with a high postrelease mortality but could also be attributed to large population sizes, dispersal, tag loss, or uncooperative fishermen. Direct observation in tank or pen studies (e.g., Mandelman and Farrington, 2007) may not be practical for large pelagic species. Although they are the right tool to indicate postrelease mortality, the cost of PSATs precludes their widespread application. Moyes et al. (2006) introduced a biochemical approach that reduces experimental bias and increases sample size and would therefore optimize experimental design. Once the method is operational, about 40 samples can be assayed for the cost of one PSAT (~US$ 4000) (Musyl et al., 2009). Other potential methods that could achieve sufficient sample sizes have shown promise for other species (e.g., reflex action mortality predictors; Davis, 2007), but it is not known how well these methods would translate for large pelagic species. For example, we used the absence of movement in the nictitating membrane to determine at-vessel mortality, but it is not known whether variability in this response (or other responses) would be useful to predict postrelease mortality. Lastly, bioelectrical impedance analysis (Cox and Heintz, 2009) may be feasible if body condition correlates with long-term survival.

Factors that influence mortality

Presumably the effects of stress and injury during capture are additive and unless there are overriding factors, we suggest that, under similar conditions (and with adequate sample sizes), the at-vessel and postrelease mortality rates for pelagic species should be roughly concordant (e.g., Moyes et al., 2006; Campana et al., 2009a). For survival studies on blue sharks, the at-vessel and postrelease mortality estimates show close agreement. For example, Campana et al. (2009a) reported 16% at-vessel and 19% postrelease mortality rates and we reported 5.9% at-vessel and 6.3% postrelease mortality rates. Although we did not find this relationship for other pelagic sharks, it is possible our sample sizes were not sufficient to detect differences between these two mortality rates.

Clearly additional research is required to determine whether at-vessel mortality correlates with postrelease mortality across a range of shark species and to determine which biological and anthropogenic factors account for variability in mortality estimates. As discussed in Musyl et al. (2009), postrelease mortality estimates in Campana et al. (2009a) may have been strongly influenced by handling. Hoey and Moore[1] suggested that a 20% difference in mortality for blue sharks discarded from longlines was attributable to handling practices in the Atlantic fishery where the Campana et al. (2009a) study took place. Campana et al. (2009a) also reported a significant vessel effect in their survival model of retrieved dead sharks, which the authors attributed to handling. Carruthers et al. (2009) and Diaz and Serafy (2005) also suggested discard and handling practices may have been responsible for differences in at-vessel mortality rates of blue sharks in the Atlantic longline fishery. If differences in handling practices strongly correlate with variable survival, a logical extension would be to develop discard-and-release regulations that could significantly improve survival (Carruthers et al., 2009).

Circle hooks were used throughout our study which probably increased both the at-vessel survival (Diaz and Serafy, 2005; Kerstetter and Graves, 2006; Campana et al., 2009a; Carruthers et al., 2009; Musyl et al., 2009) and postrelease survival of blue sharks (Moyes

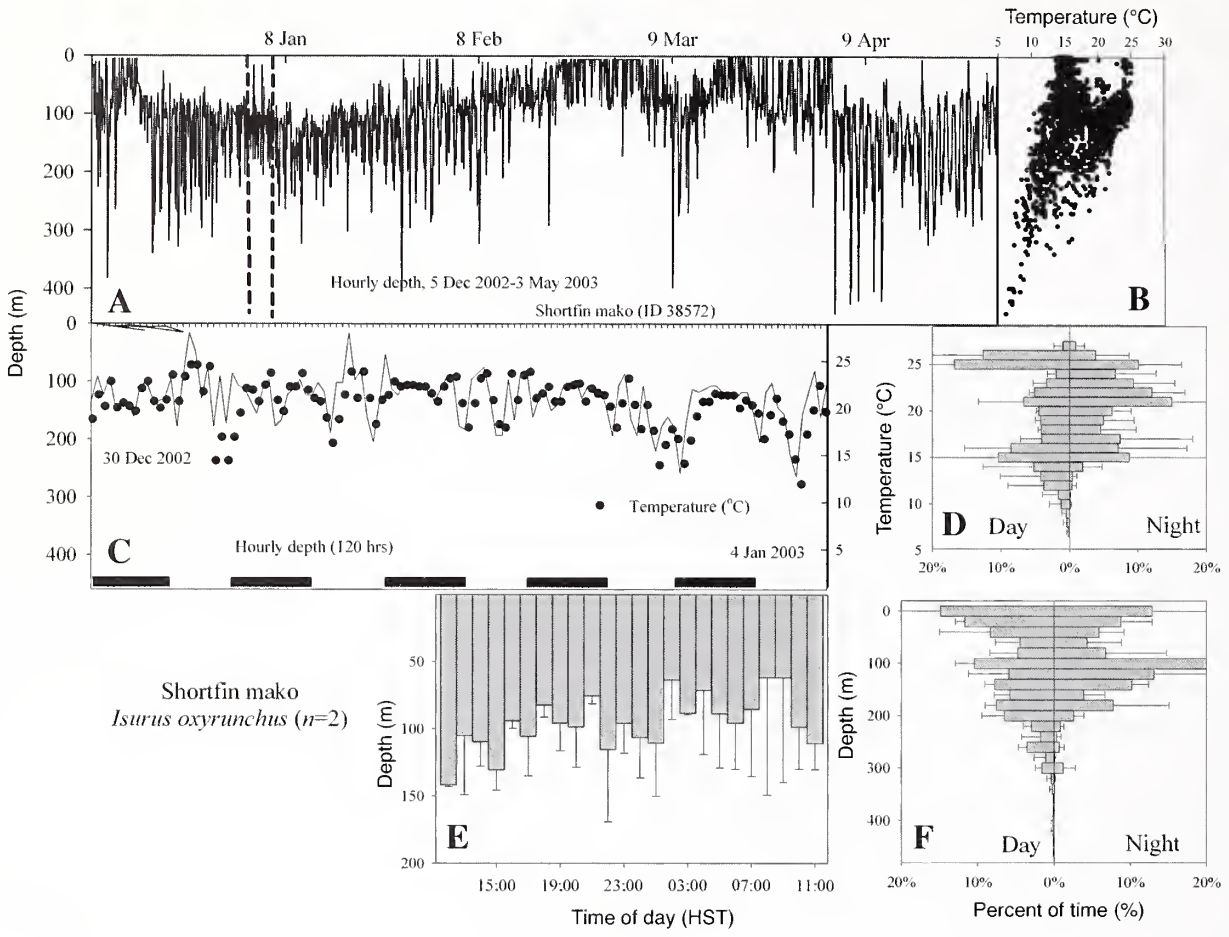

Figure 7

Shortfin mako (*Isurus oxyrinchus*) depth and thermal ranges as identified by pop-up satellite archival tags (PSATs). (**A**) Representative vertical movements. (**B**) Temperature-depth profiles obtained from the aggregated data from all sharks. (**C**) Expanded section from panel A with horizontal black bars representing nighttime. (**D**) Percentage of time spent in individual temperature strata (±standard deviation, SD) for daytime and nighttime diving activities (all tags). (**E**) Average hourly depth (±SD) readings calculated for all samples (all tags). (**F**) Percentage of time spent in individual depth strata (±SD) for daytime and nighttime diving activities (all tags).

et al. 2006; Campana et al., 2009a; Musyl et al., 2009) captured and released from longline gear. Similar findings have been reported for istiophorid billfish, which showed significantly lower at-vessel mortality (Diaz, 2008; Serafy et al., 2008) and postrelease mortality (Horodysky and Graves, 2005) with the use of circle hooks over J-hooks. Campana et al. (2009a; 2009b) did not mention the hook type used on blue shark that ultimately died when released from commercial longline gear. However, we argue that given their observed rates of at-vessel mortality, it is likely that this factor, along with handling and time spent hooked, were important factors to explain their rates of postrelease mortality (Musyl et al., 2009).

The amount of time spent on the hook shows a positive relationship with mortality for a variety of pelagic species, presumably because the captured animal experiences increased stress over time and is more vulnerable to predation (Boggs, 1992; Erickson and Berkeley, 2008; Carruthers et al., 2009). Many authors suggested that shorter soak times could significantly reduce bycatch mortality (Diaz and Serafy, 2005; Erickson and Berkeley, 2008; Carruthers et al., 2009). Without the benefit of hook timers (Boggs, 1992; Erickson and Berkeley, 2008) however, it would be challenging to test the correlation between time spent on the line and mortality. Our samples probably consisted of both mature and immature sharks, but we could not determine any significant trends between mortality and size as reported in Diaz and Serafy (2005).

Lastly, we also observed species-specific differences in the at-vessel mortality rates which other authors

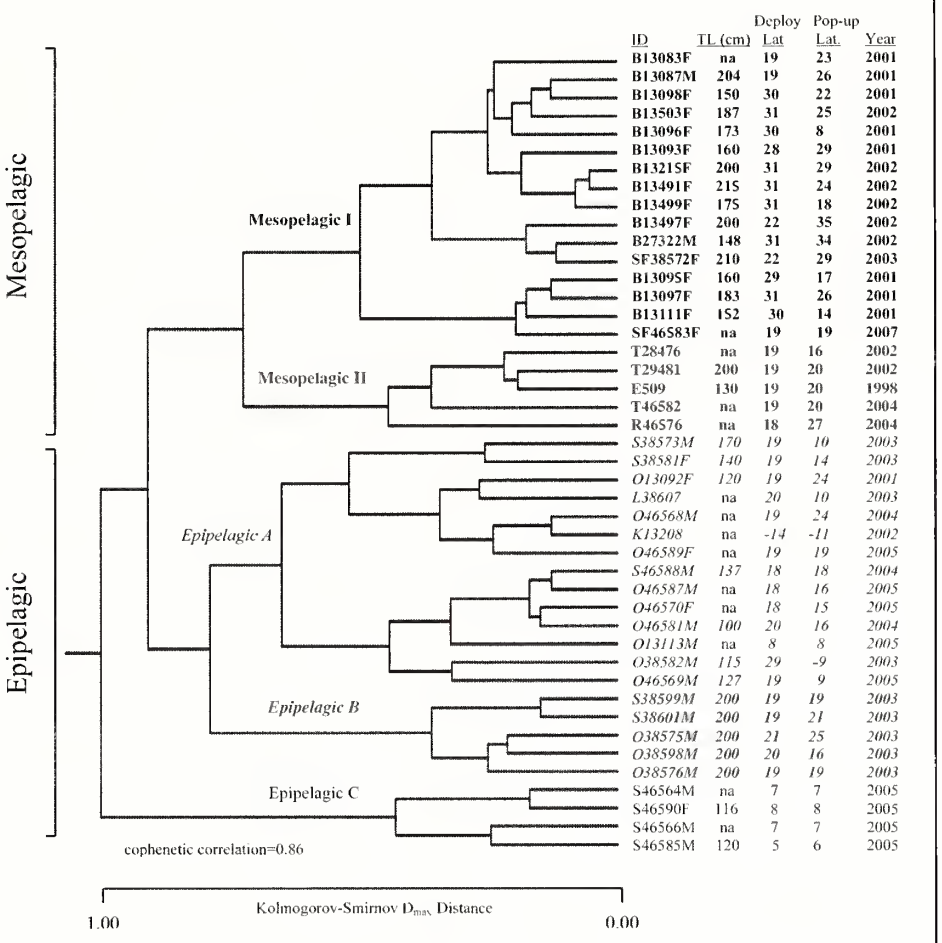

Figure 8

Dendrogram of epipelagic and mesopelagic species clusterings for five species of sharks, determined with unweighted pair-group method using arithmetic averages (UPGMA) and daytime temperature preference readings from pop-up satellite tags (PSATs). ID abbreviations: B=blue shark (*Prionace glauca*), SF=shortfin mako (*Isurus oxyrinchus*), T=bigeye thresher (*Alopias superciliosus*), E=bigeye tuna (*Thunnus obesus*), R=swordfish (*Xiphias gladius*), S=silky shark (*Carcharhinus falciformis*), O=oceanic whitetip shark (*C. longimanus*), K=black marlin (*Istiompax indica*), L=blue marlin (*Makaira nigricans*), M=male, and F=female, TL=total length (cm) and PSAT deployment and pop-up latitude are provided with pop-up year. na=not available. Outgroup data were taken from Pacific swordfish, black marlin, blue marlin (Musyl et al.[2]) and bigeye tuna (Musyl et al., 2003). Italic and bold fonts are used to distinguish the various species groupings.

have noted (e.g., Hight et al., 2007; Erickson and Berkeley, 2008; Walsh et al., 2009), presumably because of species-specific tolerances to stress and injuries (Hight et al., 2007; Mandelman et al., 2008; Mandelman and Skomal, 2009). For example, in the Pacific, Hight et al. (2007) reported blue sharks to exhibit significantly lower catecholamine levels than shortfin makos during retrieval of longline gear. The difference agrees with results indicating much lower at-vessel mortality for blue sharks (Walsh et al., 2009).

Species-specific vertical and horizontal movements

Our results strongly indicate that pelagic sharks exhibit high levels of individual variability in their vertical movement patterns and these are significantly influenced by time of day, and the transitions from daytime to nighttime diving activity can be dramatic. Plasticity in diel vertical movement patterns has also been documented in bigeye tuna (Musyl et al., 2003) and southern bluefin tuna (*T. maccoyii*, Bestly et al., 2009) and other pelagic species (Arnold and Dewar, 2001; Gunn and

Block, 2001). Our data also indicate that vertical mobility patterns are species-specific. Moreover, the vertical movement patterns of bigeye thresher and blue sharks and shortfin makos appear to allow them to remain in the vicinity of prey organisms in the deep sound scattering layer (SSL), as is the case for swordfish and bigeye tuna (Childress and Nygaard, 1974; Carey, 1990; Josse et al., 1998; Musyl et al., 2003, Musyl et al.[2]), during their extensive daytime vertical migrations, with additional adjustment of nighttime vertical movement behaviors to lunar illumination (e.g., Musyl et al., 2003). By contrast, the epipelagic silky and oceanic whitetip sharks remain in the upper mixed layer (~120 m) both night and day. Diet studies (Tricas, 1979; Harvey, 1989; Preti et al., 2008) and observations from submersibles (Davies and Bradley, 1972) indicate overlap among pelagic shark species which are in concordance with the overlap in diel vertical movement patterns, especially at nighttime when species remain near the surface.

With the exception of shortfin makos, the pelagic sharks in our study displayed distinct changes in vertical movement patterns during crepuscular transitions. Pronounced or regular activity at crepuscular periods has been hypothesized to aid in orientation and navigation (e.g., by detecting sun angles and geomagnetic or electric fields; Carey and Scharold, 1990; Musyl et al., 2001, 2003; Klimley et al., 2002; Willis et al., 2009). Other authors have suggested this strategy reflects movements of the organisms of the SSL (Josse et al., 1998; Musyl et al., 2003). Klimley et al. (2002) postulated that shortfin makos occasionally dive deep to sample magnetic gradients, but also need to sample the earth's main dipole field at the surface where it is strongest. The absence of pronounced vertical movements during crepuscular transitions indicates sun elevations or changes in light-intensity may not be critical for navigation.

Examining data from 22 blue sharks carrying ultrasonic transmitters, Carey and Scharold (1990) noted the largest vertical oscillations during the day (descents to 620 m and 7°C) and smaller excursions at night. Blue sharks appear to have no unique anatomical or physiological adaptations (e.g., thermoconserving mechanisms necessary for regional endothermy) and Carey and Scharold (1990) suggested this "up and down movement" pattern might be a hunting tactic, behavioral thermoregulation, or an efficient way to sample odor plumes that tend to spread horizontally throughout the water column. Lastly, divergent vertical movement behaviors could be specific search behaviors tailored to finding the availability of specific resources (Sims et al., 2008; Humphries et al., 2010). For example, when resources are scarce and patchily distributed, pelagic sharks adopt a Lévy flight behavior, but at thermal fronts, where there are abundant resources, they switch to Brownian movement (Humphries et al., 2010).

PSAT data from blue sharks in eastern Australia have shown diel vertical movement patterns (i.e., deeper in daytime and near the surface at nighttime) with the majority of the time spent between 17° and 20°C and approximately 80% of vertical movements above ~200 m, but maximum depths reached may have been constrained by bathymetry (Stevens et al., 2010). In contrast, blue sharks in our study experienced a larger range in temperatures (e.g., 80% of temperatures occupied were from 13–26°C) as a result of their greater vertical mobility. In the tropical Indian Ocean, catch data indicated the abundance of blue sharks was greatest at depths of 80–220 m and at temperatures from 12° to 25°C (Compagno, 1984)—data that correlate with our results. Nakano et al. (1985) offered that 14–21°C was the preferred temperature of blue sharks in the North Pacific, whereas Strasburg (1958) claimed that 99% of the blue shark catch in the Pacific was taken by longline hooks in waters between 7° and 20.5°C—hooks that were in or immediately below the thermocline.

The horizontal movements of blue sharks that we observed generally followed the seasonal and ontogenetic north–south migratory patterns reported by Strasburg (1958) and Nakano and Stevens (2008). Weng et al. (2005) reported movements of blue sharks from the eastern Pacific into the central Pacific, but it is unclear if populations of blue sharks in the central Pacific are regularly supplemented by recruits from the eastern Pacific. Moreover, to our knowledge, movements of blue sharks from the central to eastern Pacific have not been documented. Understanding these movement patterns would be helpful for stock assessments.

Apart from anecdotal and taxonomic information (Compagno, 1984; Bonfil et al., 2008) very little data exist about the life history and ecological requirements of oceanic whitetip sharks. The movement data reported herein are in agreement with published summaries on the biology of this species (Bonfil et al., 2008), which generally indicate their habitat to be primarily in the uniform temperature surface layer. We found that oceanic whitetip sharks spend >95% of their time at temperatures within 2°C of SST. Strasburg (1958) concluded that the whitetip "was surface dwelling north of the equator and bathypelagic to the south," whereas Compagno (1984) suggested that this species can tolerate temperatures from 18° to 28°C but normally prefers water above 20°C. Bonfil et al. (2008) suggested that blue and oceanic whitetip sharks—the most abundant oceanic sharks—have evolved an efficient partitioning of the oceanic environment," and our data clearly support this conclusion.

Silky sharks have been reported to be limited to water temperature >23°C (Last and Stevens, 2009) which agrees with our data. Compagno (1984), however, suggested that silky sharks could inhabit depths below 500 m, something we did not observe. Watson et al. (2009) reported finding smaller, immature silky sharks captured by purse seine north of the equator in the eastern tropical Pacific. In our cluster analysis, the most unique cluster was composed of immature silky sharks south of the NEC, and silky sharks segregated by body size and also by latitude. Presumably this topology is temporary and changes through ontogeny.

The most striking diel vertical movement behavior among pelagic shark species was observed in bigeye threshers. Our observations were similar to those of Nakano et al. (2003) who acoustically tracked two immature females (175 and 124 cm precaudal length) for 96 and 70 h, respectively; their vertical movements were centered between 200 and 500 m during the day and 80 and 130 m at night. Moreover, the diel vertical movement patterns we observed were comparable to the PSAT data reported by Weng and Block (2004).

Movement data of the shortfin makos that we observed were similar to those recorded by Loefer et al. (2005) for this species in the Atlantic, in that both studies recorded adjustment of vertical behavior when the sharks entered water masses with different thermal characteristics. However, shortfin makos in the Atlantic made excursions from the surface to 556 m (temperatures from 10.4° to 28.6°C), whereas we never observed movements below ~441 m.

Thermal niche partitions and habitat structure

Our results show that pelagic shark species display distinct thermal niche partitioning (as identified by UPGMA clustering) and that habitat structure for the epipelagic silky and oceanic whitetip sharks can be adequately estimated from two dimensions (these species spend most of their time in the warmest available water). By contrast, three dimensions will be required to describe the extended vertical habitat of the species that we classified as mesopelagic I (blue sharks, shortfin makos) and mesopelagic II (bigeye threshers).

Except for the oceanic whitetip shark and silky shark clusters, which showed familial affinities based on phylogeny and life history, the topology of the dendrogram for pelagic shark species appeared to correlate with body size and latitudinal gradient, but not with phylogeny (Shirai, 1996), life history (Cortés, 2000), ecomorphotype (Compagno, 1990), neural anatomy (Lisney and Collin, 2006; Yopak and Montgomery, 2008; Yopak and Frank, 2009), relative eye size (Lisney and Collin, 2007), or the presence of regional endothermy (Bernal et al., 2001; Dickson and Graham, 2004). It also does not appear that clustering was greatly influenced by the El Niño-Southern Oscillation (www.esrl.noaa.gov/psd/people/klaus.wolter/MEI/, accessed November 2010) or Pacific Decadal Oscillation (cses.washington.edu/cig/pnwc/compensopdo.shtml, accessed November 2010) climate patterns.

Dickson and Graham (2004) argued that endothermy *per se* was not required for niche expansion and that other adaptations were necessary to allow for vertical movements below the thermocline. This hypothesis implies that other factors (e.g., ontogeny, latitude, locomotion, diet, and dimensionality of the environment) probably influence thermal niche partitions (Yopak and Montgomery, 2008; Yopak and Frank, 2009). Dietary studies based on accumulation of mercury in prey items, which is depth-dependent, have revealed vertical niche preferences among pelagic species (Choy et al., 2009). Dagorn et al. (2000) suggested, on the basis of their simulation model, that "different solutions for exploiting the same environment" had evolved among tropical pelagic species; their findings reflected a diverse array of species-specific vertical movement patterns and vertical niche partitions similar to those observed in our study on pelagic sharks. Numerous authors (e.g., Brill et al., 2005; Bernal et al., 2009; Musyl et al.[2]; and others) have suggested that evolution of the ability to make extensive daily vertical movements in pelagic species may have arisen from predator-prey dynamics. In other words, predator and prey may be locked in a physiological race driving the biological and physiological adaptations and tolerances of both and thus expanding their vertical niche.

For comparative purposes, shark species from other locations could be analyzed with our clustering methods to determine thermal niche clusters. From a practical standpoint, pelagic shark species that form thermal clusters may also experience similar fishing pressures and this association may have direct application to mitigating bycatch. For example, from longline catch data in the Atlantic, Rey and Muñoz-Chapuli (1992) calculated that blue sharks were more likely to be captured in association with shortfin makos rather than with bigeye threshers and this calculation supported our groupings in the cluster analysis.

Conclusions

Results from PSAT tagging indicate that pelagic shark species can have high survival rates when released alive from longline fishing gear, and therefore catch-and-release may be a viable option to protect parental biomass in this fishery. Additional research is warranted to determine which biological and anthropogenic factors correlate with at-vessel and postrelease survival. Furthermore, information on the temporal and spatial vertical distribution patterns and community structure of pelagic species can assist in the formulation of management strategies to modify fishing gear, and thus reduce bycatch. This information should also provide more confidence in predicting catch rates and the species captured in different gear types by managers regulating fishing practices. As the tools and techniques for differentiating postrelease mortality become more refined allowing for larger sample sizes, it should be feasible to design fishing methods and practices that significantly reduce bycatch mortality.

Acknowledgments

This project was funded by Cooperative Agreements NA37RJ0199 and NA67RJ0154 of the National Oceanic and Atmospheric Administration (NOAA) with the Joint Institute for Marine and Atmospheric Research (JIMAR), University of Hawaii. We thank crew and officers of the NOAA RV *Townsend Cromwell* and *Oscar*

Elton Sette for their outstanding support. K. Bigelow, M. Laurs, C. Boggs, and three anonymous referees provided comments on an earlier draft that improved the manuscript. The assistance of A. Au, Head Librarian, Pacific Islands Fisheries Science Center, Honolulu, was greatly appreciated. This paper is dedicated to the memory of our colleague, Bert Kikkawa.

Literature cited

Arnold, G., and H. Dewar.
2001. Electronic tags in marine fisheries research: a 30-year perspective. *In* Electronic tagging and tracking in marine fisheries reviews: Methods and technologies in fish biology and fisheries (J. R. Sibert and J. L. Nielsen, eds.), p. 7–64. Dordrecht Kluwer, Academic Press, New York.

Baum, J. K., and R. A. Myers.
2004. Shifting baselines and the decline of pelagic sharks in the Gulf of Mexico. Ecol. Let. 7:135–145.

Baum, J. K., R. A. Myers, D. G. Kelhler, B. Worm, S. J. Harley, and P. A. Doherty.
2003. Collapse and conservation of shark populations in the northwest Atlantic. Science 299:389–392.

Beerkircher, L. R., E. Cortés, and M. S. Shivji.
2008. Case study: elasmobranch bycatch in the pelagic longline fishery off the southeastern United States, 1992–1997. *In* Sharks of the open ocean: biology, fisheries and conservation (M. D. Camhi, E. K. Pikitch, and E. A. Babcock, eds.), p. 242–246. Blackwell Scientific Publications, Oxford, U.K.

Bernal, D., K. A. Dickson, R. E. Shadwick, and J. B. Graham.
2001. Review: analysis of the evolutionary convergence for high performance swimming in lamnid sharks and tunas. Comp. Biochem. Physiol., pt. A 129:695–726.

Bernal, D., C. Sepulveda, M. Musyl, and R. Brill.
2009. The eco-physiology of swimming and movement patterns of tunas, billfishes, and large pelagic sharks. *In* Fish locomotion—an etho-ecological perspective (P. Domenici and D. Kapoor, eds.), p. 436–483. Scientific Publs., Enfield, NH.

Bestley, S., J. S. Gunn, and M. A. Hindell.
2009. Plasticity in vertical behaviour of migrating juvenile southern bluefin tuna (*Thunnus maccoyii*) in relation to oceanography of the south Indian Ocean. Fish. Ocean. 18: 237–254.

Beverly, S., D. Curran, M. Musyl, and B. Molony.
2009. Effects of eliminating shallow hooks from tuna longline sets on target and non-target species in the Hawaii based pelagic tuna fishery. Fish. Res. 96:281–88.

Boggs, C. H.
1992. Depth, capture time, and hooked longevity of longline-caught pelagic fish: timing bites of fish with chips. Fish. Bull. 90:642–658.

Bonfil, R.
2008. The biology and ecology of the silky shark, *Carcharhinus falciformis*. *In* Sharks of the open ocean: biology, fisheries and conservation (M. D. Camhi, E. K. Pikitch, and E. A. Babcock, eds.), p. 114–127. Blackwell Sci. Publ., Oxford, U.K.

Bonfil, R., S. Clarke, and H. Nakano.
2008. The biology and ecology of the oceanic whitetip shark, *Carcharhinus longimanus*. *In* Sharks of the open ocean: biology, fisheries and conservation (M. D. Camhi, E. K. Pikitch, and E. A. Babcock, eds.), p. 128–139. Blackwell Scientific Publ., Oxford, UK.

Borenstein, M., L. V. Hedges, J. P. T. Higgins, and H. R. Rothstein.
2009. Introduction to meta-analysis, 421 p. Wiley Press, West Sussex, U.K.

Brill, R. W., K. A. Bigelow, M. K. Musyl, K. A. Fritsches, and E. J. Warrant.
2005. Bigeye tuna behavior and physiology and their relevance to stock assessments and fishery biology. Col. Vol. Sci. Pap. ICCAT 57(2):141–162.

Burgess, G. H., L. R. Beerkircher, G. M. Cailliet, J. K. Carlson, E. Cortes, K. J. Goldman, R. D. Grubbs, J. A. Musick, M. K. Musyl, and C. A. Simpfendorfer.
2005. Is the collapse of shark populations in the northwest Atlantic Ocean and Gulf of Mexico real? Fisheries 30:20–26.

Camhi, M. D.
2008. Conservation status of pelagic elasmobranchs. *In* Sharks of the open ocean: biology, fisheries and conservation (M. D. Camhi, E. K. Pikitch, and E. A. Babcock, eds.), p. 397–417. Blackwell Scientific Publications, Oxford, U.K.

Campana, S. E., W. Joyce, and M. J. Manning.
2009a. Bycatch and discard mortality in commercially caught blue sharks *Prionace glauca* assessed using archival satellite pop-up tags. Mar. Ecol. Prog. Ser. 387:241–253.

Campana, S. E., W. Joyce, M. P. Francis, and M. J. Manning.
2009b. Comparability of blue shark mortality estimates for the Atlantic and Pacific longline fisheries. Mar. Ecol. Prog. Ser. 396:161–164.

Carey, F. G.
1990. Further acoustic telemetry observations of swordfish. *In* Planning the future of billfishes, research and management in the 90s and beyond (R. H. Stroud, ed.), p. 103–122. National Coalition for Marine Conservation, Inc., Savannah, GA.

Carey, F. G., and J. V. Scharold.
1990. Movements of blue sharks (*Prionace glauca*) in depth and course. Mar. Biol. 106:329–342.

Carruthers, E. H., D. C. Schneider, and J. D. Neilson.
2009. Estimating the odds of survival and identifying mitigation opportunities for common by catch in pelagic longline fisheries. Biol. Conserv. 142:2620–2630.

Chang, J-H, and K-M Liu.
2009. Stock assessment of the shortfin mako shark (*Isurus oxyrinchus*) in the Northwest Pacific Ocean using per recruit and virtual population analyses. Fish. Res. 98: 92–101

Childress, J. J. and M. H. Nygaard.
1974. The chemical composition and relative buoyancy of midwater crustaceans as a function of depth off Southern California. Mar. Biol. 27:225–238.

Clarke, S., M. K. McAllister, E. J. Milner-Gulland, G. P. Kirkwood, C. G. J. Michielsens, D. J. Agnew, E. K. Pikitch, H. Nakano, and M. S. Shivji.
2006. Global estimates of shark catches using trade records from commercial markets. Ecol. Let. 9:1115–1126.

Choy, C. A., B. N. Popp, J. J. Kaneko, and J. C. Drazen.
2009. The influence of depth on mercury levels in pelagic fishes and their prey. Proc. Nat. Acad. Sci. 106:13865–13869.

Compagno, L. J. V.
1984. FAO species catalogue. Vol. 4: Sharks of the world. An annotated and illustrated catalogue of shark spe-

cies known to date. Part 2: Carcharhiniformes. FAO Fish. Synop. 125:251–655. FAO, Rome.

1990. Alternate life history styles of cartilaginous fishes in time and space. Environ. Biol. Fishes 28:33–75.

Cortés, E.

2000. Life history patterns and correlations in sharks. Rev. Fish. Sci. 8:299–344.

Cox, M. K., and R. Heintz.

2009. Electrical phase angle as a new method to measure fish condition. Fish. Bull. 107:477–487.

Dagorn, L., F. Menczer, P. Bach, and R. J. Olson.

2000. Co-evolution of movement behaviours by tropical pelagic predatory fishes in response to prey environment: a simulation model. Ecol. Model. 134:325–341.

Davis, M. W.

2007. Simulated fishing experiments for predicting delayed mortality rates using reflex impairment in restrained fish. ICES J. Mar. Sci. 64:1535–1542.

Davies, I. E, and R. P. Bradley.

1972. Deep observations of anchovy and blue sharks from Deepstar 4000. Fish. Bull. 70:510–511.

Diaz, G. A.

2008. The effect of circle hooks and straight (J) hooks on the catch rates and numbers of white marlin and blue marlin released alive by the U.S. pelagic longline fleet in the Gulf of Mexico. N. Am. J. Fish. Manage. 28:500–506.

Diaz, G. A., and J. E. Serafy.

2005. Longline-caught blue shark (*Prionace glauca*): factors affecting the numbers available for live release. Fish. Bull. 103:720–724.

DiBattista, J. D., K. A. Feldham, D. Garant, S. H. Gruber, and A. P. Hendry.

2009. Evolutionary potential of a large marine vertebrate: quantitative genetic parameters in a wild population. Evolution 63:1051–1067.

Dickson, K. A., and J. B. Graham.

2004. Evolution and consequences of endothermy in fishes. Physiol. Biochem. Zool. 77:998–1018.

Dulvy, N. K., J. K. Baum, S. Clarke, L. V. J. Compagno, E. Cortés, A. Domingo, S. Fordham, S. Fowler, M. P. Francis, C. Gibson, J. Martínez, J. A. Musick, A. Soldo, J. D. Stevens, and S. Valenti.

2008. You can swim but you can't hide: the global status and conservation of oceanic pelagic sharks. Aquat. Cons. Mar. Freshw. Ecosys. 18:459–482.

Erickson, D. L., and S. A. Berkeley.

2008. Methods to reduce bycatch mortality in longline fisheries. *In* Sharks of the open ocean: biology, fisheries and conservation (M. D. Camhi, E. K. Pikitch, and E.A. Babcock, eds.), p. 462–471. Blackwell Scientific Publ., Oxford, UK.

Genner, M. J., D. W. Sims, A. J. Southwood, G. C. Budd, P. Masterson, M. McHugh, P. Rendle, E. J. Southall, V. J. Wearmouth, and S. J. Hawkins.

2009. Body size-dependent responses of a marine fish assemblage to climate change and fishing over a century-long scale. Global Change Biol. 16:517–527.

Gilman, E., D. Kobayashi, T. Swenarton, N. Brothers, and P. Dalzell.

2007. Reducing sea turtle interactions in the Hawaii-based longline swordfish fishery. Biol. Cons. 139:19–38.

Goodyear, C. P.

2002. Factors affecting robust estimates of the catch-and-release mortality using pop-off tag technology. Am. Fish. Soc. Symp. 30:172–179.

Gunn, J., and B. Block.

2001. Advances in acoustic, archival, and satellite tagging of tunas. *In* Tuna physiology, ecology, and evolution (B. A. Block and E. D. Stevens, eds.), p. 167–224. Academic Press, New York.

Hampton, J., J. R. Sibert, P. Klieber, M. N. Maunder, and S. J. Harley.

2005. Decline of Pacific tuna populations exaggerated? Nature 434:E1–E2.

Harvey, J. T.

1989. Food habits, seasonal abundance, size, and sex of the blue shark, *Prionace glauca*, in Monterey Bay, California. Calif. Fish Game Fish Bull. 75:33–44.

Hays, G. C., C. J. A. Bradshaw, M. C. James, P. Lovell, and D. W. Sims.

2007. Why do Argos satellite tags deployed on marine animals stop transmitting? J. Exp. Mar. Biol. Ecol. 349:52–60.

Heberer, C., S. A. Albers, D. Bernal, S. Kohin, B. DiFiore, and C. A. Sepulveda.

2010. Insights into catch-and-release survivorship and stress-induced blood biochemistry of common thresher sharks (*Alopias vulpinus*) captured in the southern California recreational fishery. Fish. Res. 106:495–500.

Hight, B. V., D. Holts, J. B. Graham, B. P. Kennedy, V. Taylor, C. A. Sepulveda, D. Bernal, D. Ramon, R. Rasmussen, and N. C. Lai.

2007. Plasma catecholamine levels as indicators of the postrelease survivorship of juvenile pelagic sharks caught on experimental drift longlines in the Southern California Bight. Mar. Freshw. Res. 58:145–151.

Holts, D. B., and D. W. Bedford.

1993. Horizontal and vertical movements of the shortfin mako shark, *Isurus oxyrinchus*, in the southern California Bight. Aust. J. Mar. Freshw. Res. 44:901–909.

Horodysky, A. Z., and J. E. Graves.

2005. Application of pop-up satellite archival tag technology to estimate postrelease survival of white marlin (*Tetrapturus albidus*) caught on circle and straight-shank ("J") hooks in the western North Atlantic recreational fishery. Fish. Bull. 103:84–96.

Humphries, N. E., J. R. M. Dyer, N. Queiroz, N. G. Pade, M. K. Musyl, K. Schaefer, J. M. Brunnschweiler, T. K. Doyle, J. D. R. Houghton, G. C. Hays, C. S. Jones, L. R. Noble, V. J. Wearmouth, E. J. Southall, and D. W. Sims.

2010. Environmental context explains Lévy and Brownian movement patterns of marine predators. Nature 465:1066–1069.

Josse, E., P. Bach, and L. Dagorn.

1998. Simultaneous observations of tuna movements and their prey by sonic tracking and acoustic surveys. Hydrobiologia 371/373:61–69.

Kerstetter, D. W., and J. E. Graves.

2005. Survival of white marlin (*Tetrapturus albidus*) released from commercial pelagic longline gear in the western North Atlantic. Fish. Bull. 104:434–444.

2006. Effects of circle versus J-style hooks on target and non-target species in a pelagic longline fishery. Fish. Res. 80:239–250.

2008. Postrelease survival of sailfish caught by commercial pelagic longline gear in the southern Gulf of Mexico. N. Am. J. Fish. Manage. 28:1578–1586.

Kerstetter, D. W., B. E. Luckhurst, E. D. Prince, and J. E. Graves.

2003. Use of pop-up satellite archival tags to demonstrate survival of blue marlin (*Makaira nigricans*) released from pelagic longline gear. Fish. Bull. 101:939–948.

Kitchell, J. F., I. C. Kaplan, S. P. Cox, S. J. D. Martell, T. E. Essington, C. H. Boggs, and C. J. Walters.
2004. Ecological and economic components of managing rare or endangered species in a tropical pelagic ecosystem. Bull. Mar. Sci. 74:607–619.

Klimley, A. P., S. C. Beavers, T. H. Curtis, and S. J. Jorgensen.
2002. Movements and swimming behaviour of three species of sharks in La Jolla Canyon, California. Environ. Biol. Fishes 63:117–135.

Kohler, N. E., J. G. Casey, P. A. Turner.
1998. NMFS Cooperative Tagging Program, 1962–1993: an atlas of shark tag and recapture data. Mar. Fish. Rev. 60:1–87.

Last, P. R., and J. D. Stevens.
2009. Sharks and rays of Australia, 644 p. CSIRO, Hobart, Australia.

Law, R.
2000. Fishing, selection, and phenotypic evolution. ICES J. Mar. Sci. 57:659–668.

Lisney, T. J., and S. P. Collin.
2006. Brain morphology in large pelagic fishes: a comparison between sharks and teleosts. J. Fish. Biol. 68:532–554.
2007. Relative eye size in elasmobranchs. Brain Behav. Evol. 69:266–279.

Loefer, J. K., G. R. Sedberry, and J. C. McGovern.
2005. Vertical movements of a shortfin mako in the Western North Atlantic as determined by pop-up satellite tagging. SE Nat. 4:237–246.

Mandelman, J. W., P. W. Cooper, T. B. Werner, and K. M. Lagueux.
2008. Shark bycatch and depredation in the U.S. Atlantic pelagic longline fishery. Rev. Fish. Biol. Fish. 18:427–442.

Mandelman, J. W., and M. A. Farrington.
2007. The physiological status and mortality associated with otter-trawl capture, transport, and captivity of an exploited elasmobranch, *Squalus acanthias*. ICES J. Mar. Sci. 64:122–130.

Mandelman, J. W., and G. B. Skomal.
2009. Differential sensitivity to capture stress assessed by blood acid–base status in five carcharhinid sharks. J. Comp. Physio. B Biochem. Syst. Environ. Physiol. 179:267–277.

Manly, B.
2007. Randomization, bootstrap and Monte Carlo methods in biology, 455 p. CRC Press, Boca Rotan, FL.

Meeus, J.
1998. Astronomical algorithms, 2nd ed., 477 p. Willman-Bell, Richmond, VA.

Moyes, C. D., N. Fragoso, R. W. Brill, and M. K. Musyl.
2006. Predicting postrelease survival in large pelagic fish. Trans. Am. Fish. Soc.135:1389–1397.

Musyl, M. K., R. W. Brill, C. H. Boggs, D. S. Curran, T. K. Kazama, and M. P. Seki.
2003. Vertical movements of bigeye tuna (*Thunnus obesus*) associated with islands, buoys, and seamounts near the main Hawaiian Islands from archival tagging data. Fish. Oceanogr. 12:152–169.

Musyl, M. K., R. W. Brill, D. S. Curran, J. S. Gunn, J. R. Hartog, R. D. Hill, D. W. Welch, J. P. Eveson, C. H. Boggs, and R. E. Brainard.
2001. Ability of archival tags to provide estimates of geographical position based on light intensity. *In* Electronic tagging and tracking in marine fisheries reviews: Methods and technologies in fish biology and fisheries (J. R. Sibert and J. L. Nielsen, eds.), p. 343–368. Dordrecht Kluwer, Academic Press, New York.

Musyl, M. K., M. L. Domeier, N. Nasby-Lucas, R. W. Brill, L. M. McNaughton, J. Y. Swimmer, M. S. Lutcavage, S. G. Wilson, B. Galuardi, and J. B. Liddle.
2011. Performance of pop-up satellite archival tags. Mar. Ecol. Prog. Ser. 433:1–28.

Musyl, M. K., C. D. Moyes, R. W. Brill, and N. Fragoso.
2009. Factors influencing mortality estimates in postrelease survival studies. Mar. Ecol. Prog. Ser. 396:157–159.

Nakano, H., H. Matsunaga, H. Okamoto, and M. Okazaki.
2003. Acoustic tracking of bigeye thresher *Alopias superciliosus* in the eastern Pacific Ocean. Mar. Ecol. Prog. Ser. 265:255–261.

Nakano, H., M. Makihara, and K. Shimazaki.
1985. Distribution and biological characteristics of the blue shark in the central North Pacific. Bull. Faculty Fish., Hokkaido Univ. 36:99–113.

Nakano, H., and J. D. Stevens.
2008. The biology and ecology of the blue shark, *Prionace glauca*. *In* Sharks of the open ocean: biology, fisheries and conservation (M. D. Camhi, E. K. Pikitch, and E. A. Babcock, eds.), p. 140–151. Blackwell Scientific Publ., Oxford, U.K.

Nielsen, A., K. A. Bigelow, M. K. Musyl, and J. R. Sibert.
2006. Improving light-based geolocation by including sea surface temperature. Fish.Oceanogr. 15:314–325.

Ortiz, M., E. D. Prince, J. E. Serafy, D. B. Holts, K. B. Davy, J. G. Pepperell, M. B. Lowry, and J. C. Holdsworth.
2003. Global overview of the major constituent-based billfish tagging programs and their results since 1954. Mar. Freshw. Res. 54:489–507

Polovina, J. J., E. Howell, D. R. Kobayashi, and M. P. Seki.
2001. The transition zone chlorophyll front, a dynamic global feature defining migration and forage habitat for marine resources. Prog. Oceanog. 49:469–483.

Preti, A. P., S. Kohin, H. Dewar, and D. Ramon.
2008. Feeding habits of the bigeye thresher (*Alopias superciliosus*) sampled from the California-based drift gillnet fishery. Cal. COFI Rep. 49:202–211.

Queiroz, N., N. E. Humphries, L. R. Noble, A. M. Santos, and D. W. Sims.
2010. Short-term movements and diving behaviour of satellite-tracked blue sharks *Prionace glauca* in the northeastern Atlantic Ocean. Mar. Ecol. Prog. Ser. 406:265–279.

Rey, J. C., and R. Muñoz-Chápuli.
1992. Intra and interspecific association of large pelagic fishes inferred from catch data of surface longline. Environ. Biol. Fishes 35:95–103.

Rohlf, F.J.
1992. NTSYS-pc: Numerical taxonomy and multivariate analysis system. Exeter Software, Setauket, NY.

Schindler, D. E., T. E. Essington, J. F. Kitchell, C. Boggs and R. Hilborn.
2002. Sharks and tunas: fisheries impacts on predators with contrasting life histories. Ecol. Appl. 12:735–748.

Sepulveda, C. A., S. Kohin, C. Chan, R. Vetter, and J. B. Graham.
2004. Movement patterns, depth preferences, and stomach temperatures of free-swimming juvenile mako sharks, *Isurus oxyrinchus*, in the Southern California Bight. Mar. Biol. 145:191–199.

Serafy, J. E., D. W. Kerstetter, and P. H. Rice.
2008. Can circle hook use benefit billfishes? Fish Fisheries 9:1–11.

Shirai, S.
1996. Phylogenetic interrelationships of neoselachains (Chondrichthyes: Euselachii). *In* Interrelationships of fishes (M. L. J. Stiassny, L. R. Parenti, and G. D. Johnson, eds.), p. 9–34. Academic Press, San Diego, CA.

Sibert, J., J. Hampton, P. Kleiber, and M. Maunder.
2006. Biomass, size, and trophic status of top predators in the Pacific Ocean. Science 314:1773–1776.

Simpson, G. G., A. Roe, and R. C. Lewontin.
1960. Quantitative zoology, 440 p. Harcourt, Brace and Company, Inc., New York.

Sims, D. W., E. J. Southall, N. J. Humphries, G. C. Hays, C. J. A. Bradshaw, J. W. Pitchford, A. James, M. Z. Ahmed, A. S. Brierley, M. A. Hindell, D. Morritt, M. K. Musyl, D. Righton, E. L. C. Shepard, V. J. Wearmouth, R. P. Wilson, M. J. Witt, J. D. Metcalfe.
2008. General scaling laws of predator search behaviour and adaption to complex prey assemblage structure. Nature 451:1098–1102.

Smith, S. E., R. C. Rasmussen, D. A. Ramon, and G. M. Cailliet.
2008. The biology and ecology of thresher sharks (Alopiidae). *In* Sharks of the open ocean: biology, fisheries and conservation (M. D. Camhi, E. K. Pikitch, and E. A. Babcock, eds.), p. 60–68. Blackwell Scientific Publications, Oxford, U.K.

Sneath, P. H. A., and R. R. Sokal.
1973. Numerical taxonomy, 573 p. W.H. Freeman, New York.

Stevens, J. D.
2008. The biology and ecology of the shortfin mako shark, *Isurus oxyrinchus*. *In* Sharks of the open ocean: biology, fisheries and conservation (M. D. Camhi, E. K. Pikitch, and E. A. Babcock, eds.), p. 87–94. Blackwell Scientific Publ., Oxford, U.K.

Stevens, J. D., R. W. Bradford, and G. J. West.
2010. Satellite tagging of blue sharks (*Prionace glauca*) and other pelagic sharks off eastern Australia: depth behaviour, temperature experience and movements. Mar. Biol. 157:575–591.

Strasburg, D. W.
1958. Distribution, abundance, and habits of pelagic sharks in the Central Pacific Ocean. Fish. Bull. 138: 335–361.

Tricas, T. C.
1979. Relationships of the blue shark, *Prionace glauca*, and its prey species near Santa Catalina Island, California. Fish. Bull. 77:175–182.

Walsh, W. A., K. A. Bigelow, and K. L. Sender.
2009. Decreases in shark catches and mortality in the Hawaii-based longline fishery as documented by fishery observers. Mar. Coast. Fish. Dynam. Manage. Ecosys. Sci. 1:270–282.

Watson, J. T., T. E. Essington, C. E. Lennert-Cody, and M. A. Hall.
2009. Trade-offs in the design of fishery closures: management of silky shark bycatch in the eastern Pacific Ocean tuna fishery. Conserv. Biol. 23:626–635

Weng, K. C., and B. A. Block.
2004. Diel vertical migration of the bigeye thresher (*Alopias superciliosus*), a species possessing orbital retia mirabilia. Fish. Bull. 102:221–229.

Weng, K. C., P. C. Castilho, J. M. Morrissette, A. M. Landeira-Fernandez, D. B. Holts, R. J. Schallert, K. J. Goldman, and B. A. Block.
2005. Satellite tagging and cardiac physiology reveal niche expansion in salmon sharks. Science 310:104–106.

Willis, J., J. Phillips, R. Muheim, F. J. Diego-Rasilla, and A. J. Hobday.
2009. Spike dives of juvenile southern bluefin tuna (*Thunnus maccoyii*): a navigational role? Behav. Ecol. Sociobiol. 64:57–68.

Yokota, K., M. Kiyota, and H. Minami.
2006. Shark catch in a pelagic longline fishery: comparison of circle and tuna hooks. Fish. Res. 81:337–341.

Yopak, K. E., and L. R. Frank.
2009. Variation in cerebellar foliation in cartilaginous fishes: Ecological and behavioral considerations. Brain Behav. Evol. 74: 121–142.

Yopak, K. E., and J. C. Montgomery.
2008. Brain organization and specialization in deep-sea chondrichthyans. Brain Behav. Evol. 71: 287–304.

Zar, J. H.
1996. Biostatistical analysis, 3rd ed., 622 p. Prentice Hall, New York.

Appendix 1

Movement parameter estimates for tagged sharks determined from the Kalman filter (KF)-sea surface temperature (SST) state-space model (Nielsen et al., 2006). Blank spaces indicate models in which the parameters were set to zero, i.e., have no influence on the model, and were not estimated. u and v are advection parameters in longitude and latitude, respectively; D=all estimated diffusive parameters, b_x, b_{y0}, b_{sst} are the bias estimates for longitude, latitude and SST, respectively; σ_x ,σ_{y0}, σ_{sst}, are the standard deviations, a_0, is the upper bound for the latitude variance, b_0 is the estimated number of days before the equinox (when latitude error is maximal), and nlogL is the log-likelihood function. u and v are expressed in nautical mile (nmi) day^{-1}, D in nmi^2 day^{-1}, b_x, b_y, b_{sst}, σ_x, σ_y, and σ_{sst} in degrees, and a_0 and b_0 in days. Numbers in parentheses after pop-up satellite archival tag (PSAT) no. are number of days with geolocations with M=male, F=female.

PSAT no.	u	v	D	b_x	b_{y0}	b_{sst}	σ_x	σ_{y0}	σ_{sst}	a_0	b_0	nlogL
Blue shark (*Prionace glauca*)												
13087M (9)			949.50				4.57	100	0.09			166.51
13093F (43)			1285.63				3.37	2.65	0.49	0.07	52.3	332.34
13095F (13)			916.80				0.76	10.41	0.36			91.69
13096F (13)	−0.75	−19.70	759.08				2.18	7.01	2.32			109.13
13097F (41)			539.67				1.90	5.29	0.31			282.71
13098F (98)			2990.00			−11.76	2.50	8.73	3.91			1099.83
13111F (18)			480.75				3.54	7.27	1.05			186.23
13215F (26)			1567.10				0.95	3.07	2.27			259.22
13491F (28)			1373.44				1.26	3.83	0.49			260.59
13497F (6)			785.47				0	2.40	1.26			76.48
13499F (11)			1204.47				1.56	5.32				72.60
13503F (17)			698.28				0.79	2.70	0.38			141.51
27322M (36)			582.41				1.97	4.24				198.50
Shortfin mako (*Isurus oxyrinchus*)												
38572F (77)	9.23	3.84	1483.27				0.78	3.57	0.28	0.36	−41.58	708.59
Silky shark (*Carcharhinus falciformis*)												
38573M (87)	−2.74	−3.54	602.29				0.51	2.13	0.16	0.02	−18.54	508.62
38581F (25)	−12.4	−11.8	165.58				0.9	2.13	0.46			140.68
38599M (31)			265.48				0.62	2.93	0.18			169.64
38601M (185)			119.16				0.61	4.46	2.45		−0.89	1573.87
46564M (20)			624.34				0.59	5.91	0.61			163.68
46566M (25)			2357.41				0.48	4.07	0.91			274.26
46571M (8)			105.30				0.26	1.99	0.53			80.79
46585M (91)	−3.70	4.25	701.27				0.73	3.43	0.59	0.02	−0.69	859.75
46588M (91)			791.38				0.42	1.33	0.38		1.03	821.53
46590F (23)			451.12				0.73	5.10	1.30			203.05
Oceanic whitetip shark (*Carcharhinus longimanus*)												
13092F (62)			351.17				1.10	3.26	0.40			510.81
13113M (123)	−5.75	−0.37	358.36				0.97	4.34	0.76		1.28	1170.24
29918F (8)			413.89				0.23	2.47	0.12			58.93
38575M (200)			554.91				0.39	1.98	2.15		2.14	1416.63
38576M (102)			471.92				0.47	1.42	0.22	0.05	−8.24	523.42
38582M (87)	−6.22	−17.05	596.56				0.53	3.82	0.15			372.53
38598M (51)			750.42				0.19	1.33	0.14	0.02	4.35	169.85
46568M (80)	−6.89	2.74	427.95			0.53	0.52	2.08	0.29	0.35	37.74	565.44
46569M (40)			571.16			0.12	0.57	3.88	0.01		−2.59	383.19
46570F (182)			377.06				0.48	8.95	0.36			1605.19
46581M (173)			760.70				0.48	2.35	0.39		0.42	1214.86
46587M (196)			532.79				0.58	3.06	0.37		−3.57	1569.85
46589F (175)			453.52				0.76	2.27	0.30		−1.84	1614.75

Appendix 2

Descriptive statistics of daytime and nighttime vertical movement behavior of blue shark (*Prionace glauca*), shortfin mako (*Isurus oxyrinchus*), silky shark, (*Carcharhinus falciformis*), oceanic whitetip shark (*C. longimanus*) and bigeye thresher (*Alopias superciliosus*) tagged with pop-up satellite archival tags (PSATs). For sharks experiencing several lunar cycles, the correlation coefficient (R) is given between average nighttime depth (m) and lunar illumination, where $^{*}P<0.05$; $^{**}P<0.01$; $^{***}P<0.001$. CV is the coefficient of variation, SE is the standard error, and M=male, F=female. The following percentages of PSAT data were received for each species based on days-at-liberty and data acquisition interval: blue shark; depth (48%), temperature (49%); shortfin mako; depth (38%), temperature (38%); silky shark, depth (50%), temperature (55%); oceanic whitetip shark, depth (53%), temperature (48%); bigeye thresher, depth (18%), temperature (19%).

PSAT no. and sex	Day depth (m)			Night depth (m)				Day temperature (°C)			Night temperature (°C)		
	Mean ±SE	Min–max	CV	Mean ±SE	Min–max	CV	Lunar (R)	Mean ±SE	Min–max	CV	Mean ±SE	Min–max	CV
Blue shark (*Prionace glauca*)													
13081F	209 ±41	81–323	0.44					18 ±1	14–23	0.17			
13083F	108 ±6	0–403	1.04	66 ±3	0–274	0.82	0.03	19 ±0	10–24	0.23	22 ±0	13–24	0.10
13087M	124 ±9	0–371	0.82	97 ±6	0–280	0.71		20 ±0	11–28	0.21	22 ±0	14–28	0.15
13093F	65 ±3	0–398	1.17	38 ±2	0–307	1.22	0.14	18 ±0	8–29	0.25	19 ±0	10–28	0.22
13095F	61 ±5	0–403	1.38	81 ±3	0–323	0.68	0.07	22 ±0	9–26	0.17	22 ±0	11–26	0.11
13096F	160 ±8	0–522	0.92	93 ±4	0–479	0.91	0.62***	19 ±0	7–28	0.33	22 ±0	8–28	0.20
13097F	98 ±3	5–430	0.93	81 ±2	5–317	0.71	0.44***	22 ±0	9–27	0.17	23 ±0	12–27	0.10
13098F	73 ±2	0–178	0.76	103 ±1	0–178	0.47	0.31**	19 ±0	8–29	0.26	23 ±0	10–29	0.17
13111F	124 ±7	0–581	0.77	119 ±4	0–296	0.49		21 ±0	8–26	0.18	22 ±0	14–26	0.13
13215F	176 ±3	5–581	0.58	65 ±1	5–344	0.71	0.12	17 ±0	5–28	0.29	21 ±0	8–27	0.21
13491F	149 ±2	0–479	0.70	54 ±1	0–328	0.97	0.12	17 ±0	6–29	0.28	21 ±0	9–28	0.20
13497F	110 ±4	0–350	0.85	46 ±2	0–247	0.92	0.39*	16 ±0	9–22	0.17	18 ±0	12–22	0.10
13499F	130 ±11	0–317	0.63	72 ±10	0–225	0.97		18 ±1	9–29	0.3	22 ±0	14–29	0.19
13503F	92 ±3	0–403	1	55 ±2	0–296	1	0.005	19 ±0	9–26	0	20 ±0	10–26	0
27322M	153 ±11	0–435	0.97	55 ±5	0–328	1.22		16 ±0	9–26	0.29	20 ±0	10–27	0.20
Male	141 ±7	0–435	0.94	74 ±4	0–328	0.95		17 ±0	9–28	0.28	21 ±0	10–28	0.19
Female	119 ±1	0–581	0.87	70 ±1	0–479	0.82		19 ±0	5–29	0.27	21 ±0	8–29	0.18
Mean	120 ±1	0–581	0.87	70 ±1	0–479	0.82		19 ±0	5–29	0.27	21 ±0	8–29	0.18
Shortfin mako (*Isurus oxyrinchus*)													
38572F	121 ±2	0–441	0.67	86 ±1	0–328	0.57	0.18*	16 ±0	6–25	0.25	18 ±0	9–25	0.18
46583F	76 ±3	0–290	1.11	89 ±8	0–290	0.85		23 ±0	14–26	0.14	22 ±0	18–26	0.09
Female	119 ±2	0–441	0.68	86 ±1	0–328	0.59		16 ±0	6–26	0.26	18 ±0	9–26	0.18
Silky shark (*Carcharhinus falciformis*)													
38573M	82 ±1	0–253	0.44	42 ±1	0–237	0.82	0.28**	25 ±0	20–27	0.03	26 ±0	19–27	0.02
38581F	65 ±2	0–161	0.53	62 ±2	0–167	0.63	0.45*	26 ±0	23–26	0.02	25 ±0	15–26	0.05
38599M	51 ±1	0–134	0.52	42 ±2	0–178	0.74	0.42*	25 ±0	22–25	0.03	25 ±0	16–26	0.04
38601M	92 ±1	0–237	0.38	42 ±1	0–151	0.75	0.16	24 ±0	19–27	0.04	25 ±0	22–27	0.02
46564M	50 ±1	0–215	0.38	50 ±1	5–215	0.43		28 ±0	22–29	0.02	28 ±0	23–29	0.02
46566M	35 ±1	0–86	0.49	45 ±1	0–97	0.48		28 ±0	25–29	0.02	28 ±0	22–29	0.03
46585M	34 ±0	0–145	0.61	15 ±0	0–199	1.34	0.04	28 ±0	22–29	0.02	28 ±0	22–29	0.02

continued

Appendix 2 (continued)

PSAT no. and sex	Day depth (m)			Night depth (m)				Day temperature (°C)			Night temperature (°C)		
	Mean ±SE	Min–max	CV	Mean ±SE	Min–max	CV	Lunar (R)	Mean ±SE	Min–max	CV	Mean ±SE	Min–max	CV
Silky shark (*Carcharhinus falciformis*) *continued*													
46588M	30 ±1	0–161	0.72	24 ±1	0–167	0.99	0.23	27 ±0	20–28	0.03	27 ±0	18–29	0.05
46590F	27 ±1	0–86	0.55	30 ±1	0–183	0.65		28 ±0	27–29	0.01	28 ±0	18–29	0.03
Male	58 ±0	0–253	0.65	34 ±0	0–237	0.90		27 ±0	19–29	0.07	27 ±0	16–29	0.06
Female	43 ±1	0–161	0.73	43 ±1	0–183	0.76		27 ±0	23–29	0.05	27 ±0	15–29	0.07
Mean	56 ±0	0–253	0.66	34 ±0	0–237	0.89		27 ±0	19–29	0.08	27 ±0	15–29	0.06
Oceanic whitetip shark (*Carcharhinus longimanus*)													
13092F	46 ±1	0–140	0.60	37 ±1	0–145	0.86	0.29	26 ±0	22–28	0.04	26 ±0	22–28	0.04
13113M	31 ±1	0–172	1.08	31 ±1	0–167	0.99	0.35**	27 ±0	17–28	0.05	27 ±0	22–28	0.03
38575M	28 ±1	0–264	1.20	30 ±1	0–178	1.03	0.20**	25 ±0	12–28	0.04	25 ±0	19–27	0.04
38576M	19 ±1	0–156	1.25	25 ±1	0–124	0.95	0.07	25 ±0	21–26	0.02	25 ±0	22–26	0.02
38582M	22 ±1	0–118	0.94	40 ±1	0–172	0.81	0.07	28 ±0	21–31	0.06	27 ±0	20–30	0.06
38598M	31 ±1	0–172	0.93	33 ±1	0–231	0.97	0.04	25 ±0	21–26	0.03	25 ±0	19–26	0.03
46568M	23 ±0	0–140	1.03	27 ±1	0–247	0.98	0.25*	26 ±0	20–28	0.03	26 ±0	13–29	0.04
46569M	24 ±1	0–108	0.82	33 ±1	0–151	0.77	0.45*	2 7±0	22–29	0.04	27 ±0	20–28	0.05
46570F	36 ±1	0–231	0.80	38 ±1	0–194	0.76	0.05	27 ±0	20–29	0.04	27 ±0	19–29	0.04
46581M	31 ±1	0–178	0.91	35 ±1	0–210	0.81	0.26**	27 ±0	21–30	0.04	27 ±0	21–30	0.04
46587M	27 ±1	0–242	1.19	35±1	0–280	1.02	0.12	27 ±0	19–29	0.04	27 ±0	18–29	0.05
46589F	32 ±1	0–167	0.77	30 ±1	0–317	0.89	0.07	26 ±0	20–29	0.04	26 ±0	18–28	0.04
Male	26 ±0	0–264	1.08	32 ±0	0–280	0.95		26 ±0	12–31	0.05	26 ±0	13–30	0.05
Female	36 ±1	0–231	0.77	35 ±1	0–317	0.82		27 ±0	20–29	0.04	26 ±0	18–29	0.04
Mean	28 ±0	0–264	1.02	32 ±0	0–317	0.93		26 ±0	12–31	0.05	26 ±0	13–30	0.05
Bigeye thresher (*Alopias superciliosus*)													
28476	297 ±4	22–506	0.29	105 ±2	5–409	0.67	0.009	11 ±0	6–21	0.28	19 ±0	7–27	0.22
29481	339 ±3	102–516	0.24	127 ±3	27–500	0.64	0.31*	12 ±0	6–24	0.35	20 ±0	6–27	0.23
46582	380 ±5	38–543	0.22	125 ±6	22–430	0.83	0.22	10 ±0	5–25	0.39	21 ±0	8–27	0.21
Mean	331 ±2	22–543	0.27	118 ±2	5–500	0.70		11 ±0	5–25	0.35	20 ±0	6–27	0.23

Appendix 3

Summary of Kruskal-Wallis nonparametric ANOVA tests with the data streams available in pop-up satellite archival tags (PSATs) for depth (day depth=DD, night depth=ND, combined depth=AD) and temperature data (day temperature=DT, night temperature=NT, combined temperature=AT) for each of the pelagic shark species. The Kruskal-Wallis test statistic (*Hc*) was adjusted for ties (Zar, 1996). Results for post-hoc pairwise Mann-Whitney (Bonferroni corrected *P*-values) (MWBC) tests are summarized for each of the pelagic shark species. Sample sizes and possible number of pairwise tests used in the comparisons are given for each species. Two sample Kolmogorov-Smirnov tests paralleled the results from pairwise MWBC tests (results not shown).

Species	Kruskal-Wallis	PSAT data stream/ comparison	Possible no. of pairwise Mann-Whitney tests (MWBC)	No. of significant MWBC tests	Percentage of significant MWBC tests
Blue shark	H_c=1152, P=4.898–238	AD	91	71	78.02
(*Prionace glauca*)	H_c=209, P=1.945–37	DD	91	57	62.64
n=14	H_c=298.1, P=5.988–56	ND	91	54	59.34
	H_c=292.5, P=8.916–55	AT	91	60	65.93
	H_c=175.1, P=1.758–30	DT	91	58	63.74
	H_c=423.2, P=2.945–82	NT	91	74	81.32
			Total 546	374	68.50
		DD vs. ND			
			1 (pooled)[1]	1	100.00
			1 (pooled: male)[1]	1	100.00
			1 (pooled: female)[1]	1	100.00
			14 (within)	12	85.71
			4 (between×pooled gender)	4	100.00
			182 (between)	150	82.42
		DT vs. NT			
			1 (pooled)[1]	1	100.00
			1 (pooled: male)[1]	1	100.00
			1 (pooled: female)[1]	1	100.00
			14 (within)	6	42.86
			4 (between×pooled gender)	3	75.00
			182 (between)	131	71.98
Bigeye thresher	H_c=567.2, P=6.933–124	AD	3	3	100.00
(*Alopias superciliosus*)	H_c=62.38, P=2.861–14	DD	3	3	100.00
n=3	H_c=238.6, P=1.567–52	ND	3	2	66.67
	H_c= 2.83 , P=3.375–12	AT	3	2	66.67
	H_c=56.01, P=6.921–13	DT	3	3	100.00
	H_c=45.85, P=1.107–10	NT	3	2	66.67
			Total 18	15	83.33
		DD vs. ND			
			1 (pooled)[1]	1	100.00
			3 (within)	3	100.00
			6 (between)	6	100.00
		DT vs. NT			
			1 (pooled)[1]	1	100.00
			3 (within)	3	100.00
			6 (between)	6	100.00
Oceanic whitetip	H_c=1206, P=1.078–249	AD	66	58	87.88
(*Carcharhinus*	H_c=267.7, P=8.6–51	DD	66	50	75.76
longimanus)	H_c=556.3, P=4.121–112	ND	66	56	84.85
n=12	H_c=2101, P=0	AT	66	56	84.85
	H_c=463.4, P=2.726–92	DT	66	54	81.82
	H_c=978.2, P=1.71–202	NT	66	59	89.39
			Total 396	333	84.09

continued

Appendix 3 (continued)

Species	Kruskal-Wallis	PSAT data stream/ comparison	Possible no. of pairwise Mann-Whitney tests (MWBC)	No. of significant MWBC tests	Percentage of significant MWBC tests
Oceanic whitetip *continued*		DD vs. ND			
			1 (pooled)[1]	1	100.00
			1 (pooled: male)[1]	1	100.00
			1 (pooled: female)[1]	1	100.00
			12 (within)	9	75.00
			4 (between × pooled gender)	3	75.00
			132 (between)	105	78.79
		DT vs. NT			
			1 (pooled)[1]	0	0
			1 (pooled: male)[1]	1	100.00
			1 (pooled: female)[1]	1	100.00
			12 (within)	9	75.00
			4 (between×pooled gender)	4	100.00
			132 (between)	121	91.67
Silky shark	H_c=2265 , P=0	AD	36	33	91.67
(*Carcharhinus*	H_c=643.7, P=1.347–133	DD	36	30	83.33
falciformis)	H_c=259.5, P=2.092–51	ND	36	26	72.22
n=9	H_c=581.4, P=2.938–120	AT	36	32	88.89
	H_c=907.2, P=2.154–189	DT	36	30	83.33
	H_c=1514, P=1.161–319	NT	36	35	97.22
			Total 216	186	86.11
		DD vs. ND			
			1 (pooled)[1]	1	100.00
			1 (pooled: male)[1]	1	100.00
			1 (pooled: female)[1]	1	100.00
			9 (within)	5	55.56
			4 (between×pooled gender)	4	100.00
			72 (between)	57	79.17
		DT vs. NT			
			1 (pooled)[1]	1	100.00
			1 (pooled: male)[1]	1	100.00
			1 (pooled: female)[1]	0	0
			4 (between×pooled gender)	4	100.00
			9 (within)	8	88.89
			72 (between)	62	86.11
Shortfin mako					
(*Isurus oxyrinchus*)		AD	11	1	100.00
n=2		DD	11	1	100.00
		ND	11	1	100.00
		AT	11	0	0
		DT	11	0	0
		NT	11	0	0
			Total 6	3	50.00
		DD vs. ND			
			1 (pooled)[1]	1	100.00
			2 (within)	2	100.00
			2 (between)	2	100.00
		DT v. NT			
			1 (pooled)[1]	1	100.00
			2 (within)	1	50.00
			2 (between)	1	50.00

[1] For Mann-Whitney tests involving single comparison, Monte Carlo P-values are based on 10,000 random assignments.

Food habits of Steller sea lions (*Eumetopias jubatus*) off Oregon and northern California, 1986–2007

Susan D. Riemer[1] **(contact author)**
Bryan E. Wright[2]
Robin F. Brown[2]

Email address for contact author: susan.d.riemer@state.or.us

[1] Oregon Department of Fish and Wildlife
Marine Mammal Research Program
1495 E. Gregory Road
Central Point, Oregon 97502

[2] Oregon Department of Fish and Wildlife
Marine Mammal Research Program
7118 NE Vandenberg Avenue
Corvallis, Oregon 97330

Abstract—We described the diet of the eastern stock of Steller sea lions (*Eumetopias jubatus*) from 1416 scat samples collected from five sites in Oregon and northern California from 1986 through 2007. A total of 47 prey types from 30 families were identified. The most common prey was Pacific hake (*Merluccius productus*), followed by salmonids (*Oncorhynchus* spp.), skates (Rajidae), Pacific lamprey (*Lampetra tridentata*), herrings (Clupeidae), rockfish (*Sebastes* spp.), and northern anchovy (*Engraulis mordax*). Steller sea lion diet composition varied seasonally, annually, and spatially. Hake and salmonids were the most commonly identified prey in scats collected during the summer (breeding season), whereas hake and skate were most common in the nonbreeding season. Continued research on Steller sea lion diet and foraging behavior in the southern extent of their range is necessary to address issues such as climate change, interaction with competing California sea lions, and predation impacts on valuable or sensitive fish stocks.

Manuscript submitted 27 October 2010.
Manuscript accepted 18 May 2011.
Fish. Bull. 109:369–381 (2011).

Knowledge of an animal's diet is important for understanding its foraging behavior, habitat use, and population dynamics, and this knowledge is of particular importance when considering threatened and endangered species. Steller sea lions (*Eumetopias jubatus*) are a case in point. Ranging throughout the North Pacific Rim from California to Japan (Loughlin et al., 1984; Pitcher et al., 2007), Steller sea lion populations in western Alaska underwent dramatic declines from the late 1970s to early 1990s (Braham et al., 1980; Merrick et al., 1987; Loughlin et al., 1992; Trites and Larkin, 1996). This population was listed as "threatened" under the Endangered Species Act (ESA) in 1990, and later the western stock was listed as "endangered" (Loughlin, 1997; NMFS, 2008). The primary hypothesis for the decline has been chronic nutritional stress related to changes in diet (Springer, 1992; Merrick and Loughlin, 1997; Trites and Donnelly, 2003; NMFS, 2008).

With the nutritional stress hypothesis (Springer, 1992; Merrick et al., 1997; Trites and Donnelly, 2003), and its successor, the ocean climate hypothesis (Trites et al., 2007a), declines in the Steller sea lion western distinct population segment (WDPS) were proposed to be the result of changes in the quantity, quality, and availability of prey, brought about by an ocean climate regime shift in 1976–77 (but see Fritz and Hinckley, [2005]). This shift is hypothesized to have forced Steller sea lions to change their diet and to have resulted in chronic nutritional stress manifested by reductions in body size, productivity, and juvenile and pup survival (York, 1994; Trites and Donnelly, 2003). Other explanations for the decline of the WDPS that were considered but rejected included population redistribution, commercial and subsistence harvest, predation, pollution, and entanglement in marine debris (Merrick et al., 1987).

Although the Steller sea lion WDPS experienced annual declines in abundance ranging between 1.6% and 5.2% (Merrick et al., 1987), the abundance in the eastern distinct population segment (EDPS) increased at 3.1% per year from 1977 through 2002 (Pitcher et al., 2007; NMFS, 2008). The hypothesized role of poor diet in the decline of the WDPS, contrasted with the increasing EDPS, begs the question as to what type of prey the Steller sea lion EDPS consumes and how does it compare with that of the WDPS. The majority of information on Steller sea lion diet, however, has come from Alaska (e.g., Pitcher, 1981; Merrick et al., 1997; Sinclair and Zeppelin, 2002; Womble and Sigler, 2006; Trites et al., 2007b; McKenzie and Wynne, 2008). In this

study, we provide data on Steller sea lion diet from the southern extent of the EDPS range based on 1416 scat (fecal samples) collected from five sites in Oregon and northern California from 1986 through 2007. We tested for seasonal, annual, and spatial differences in diet composition and discuss our results in relation to findings from Alaska.

Materials and methods

Field and laboratory

We collected scat from four locations off Oregon and one location off northern California from 1986 through 2007 (Fig. 1; Table 1). Three of the five locations were occupied seasonally as rookeries (Orford Reef, Rogue Reef, St. George Reef), whereas the other two were strictly nonbreeding haul-outs (Columbia River South Jetty, Cascade Head). Scats collected from May through August were classified samples from the "breeding season" and scats from the remainder of the year, as samples from the "nonbreeding season." Scats were collected opportunistically as part of other research activities or during dedicated food habit collection trips.

Scat samples were collected and processed according to the method described in Lance et al.[1] Collections made after 2003 were processed with a standard washing machine according to collection and processing procedures described in Orr et al. (2003). Recovered hard parts were examined with a dissecting microscope and identified to the lowest possible taxonomic level by comparing all identifiable prey remains (e.g., bones, otoliths, cartilaginous parts, lenses, teeth, and cephalopod beaks) with a comparative reference collection of fish from the northeastern Pacific Ocean and Oregon estuaries. Individual samples that contained both identified prey and remains too eroded to be identified (unidentified fish) were included in this analysis, whereas samples with only unidentified remains (n=11) or no remains (n=22) were not.

Data analysis

We summarized the relative importance of prey in sea lion diet by calculating the frequency of occurrence (FO) of each prey type. Frequency of occurrence was defined as the number of scat containing a given prey type divided by the number of scat with identifiable prey. Although other summary statistics are possible, FO is a simple calculation, widely used, and probably least affected by differences in prey recovery (Tollit et al., 2010). We calculated exact 95% confidence intervals

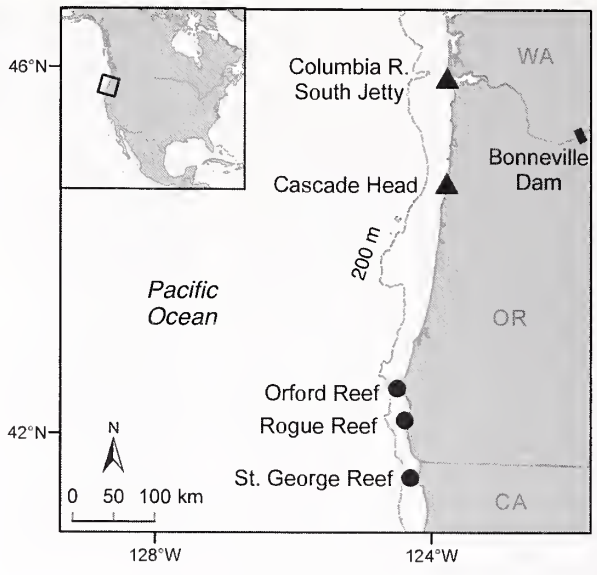

Figure 1

Locations (solid circles=rookeries, solid triangles=haul-outs) where Steller sea lion (*Eumetopias jubatus*) scat was collected off Oregon and northern California, 1986–2007. See Table 2 for detailed information on sampling locations and effort.

for FO by assuming that the number of scat in a collection containing a given prey was binomially distributed.

In addition to univariate summaries, we were also interested in testing whether multivariate diet composition differed between collections. Wright (2010) and Lemons et al. (2010) noted that the common practice of using chi-square tests to compare diets violates the assumption of independence for that test by ignoring the nesting of multiple prey items within a scat. Violation of the assumption of independence results in psuedoreplication and biased chi-square statistics. More appropriate alternatives for comparing multivariate diet composition between groups include distance-based permutation methods (e.g., Luo and Fox, 1996; Anderson, 2001; Berry and Mielke, 2003); multiple-response categorical variable methods (e.g., Agresti and Liu, 1999; Bilder and Loughlin, 2009; Nandram et al., 2009); and mark-recapture methods (Lemons et al., 2010). We chose the distance-based Mantel test (Mantel, 1967; Luo and Fox, 1996) because it could be formulated to address our questions of interest, was easy to implement in existing software, and has been used by other researchers studying animal diets (e.g., Hudon and Lamarche, 1989; Green and Burton, 1993; Jones and Barmuta, 1998).

We implemented Mantel tests, using package "vegan" (Oksanen et al., 2009) in R (R Development Core Team, 2009). We tested whether diet composition differed by month (after controlling for year and site), year (after controlling for month and site), or site (after controlling for month and year). Distances among scat samples were computed using the Jaccard coefficient which is an asymmetrical binary coefficient commonly used to compare sampling units using species presence-absence

[1] Lance, M. M., A. J. Orr, S. D. Riemer, M. J. Weise, and J. L. Laake. 2001. Pinniped food habits and prey identification techniques protocol. AFSC (Alaska Fisheries Science Center) Proc. Rep. 2001-04, 36 p. Alaska Fisheries Science Center, NMFS, NOAA, 7600 Sand Point Way NE, Seattle, WA 98115.

Table 1

Total number of Steller sea lion (*Eumetopias jubatus*) scat collected by site, month, and year from haul-outs and rookeries in northern California and Oregon, 1986–2007.

		Breeding season month				Nonbreeding season month								
Location	Year	May	Jun	Jul	Aug	Sep	Oct	Nov	Dec	Jan	Feb	Mar	Apr	Total
Columbia River[1]	2004		55		38	45							51	189
	2006				48									48
	2007			20	61	3								84
Cascade Head[2]	2003							13		11				24
Orford Reef[3]	1990			41										41
	2002			15										15
Rogue Reef[4]	1986		18											18
	1987		40											40
	1988		20											20
	1990			47										47
	1993		36											36
	1994		33											33
	1995		12											12
	1996	60												60
	2001		70		48								46	164
	2002			33	37							42	78	190
	2003			12				54					57	123
	2004			33										33
	2005	2		13									20	35
	2006			25										25
St. George Reef[5]	1990			4										4
	1994		37											37
	2002			35										35
	2003			29									7	36
	2004			34										34
	2006			33										33
Total		62	321	374	232	48	67	0	0	11	0	42	259	1416

[1] South Jetty (46.233 lat. N, 124.070 long. W).

[2] Sea Lion Cove (45.067 lat. N, 124.013 long. W).

[3] Long Brown Rock (42.791 lat. N, 124.605 long. W).

[4] Primarily Pyramid Rock (42.444 lat. N, 124.469 long. W), but also surrounding sites including Needle Rock (42.448 lat. N, 124.483 long. W), Double Rock (42.449 lat. N, 124.490 long. W), and South Seal Rock (42.436 lat. N, 124.465 long. W).

[5] South Seal Rock (41.813 lat. N, 124.351 long. W).

data (Legendre and Legendre, 1998). A Jaccard distance of zero indicates that two scat shared all of the same prey items, whereas a distance of one indicates that they had no prey items in common. We paired the Jaccard distance matrix with a design matrix consisting of zeros for between-population distances and $1/(n_i-1)$ for within-population distances (where i indicates population membership; see Manly, 1997). When used with a design matrix the Mantel test is equivalent to a nonparametric multivariate analysis of variance (Sokal and Rohlf, 1995).

We compared diets based on prey identified to the lowest possible taxon in order to limit the potential for spurious differences arising from an arbitrary categorization of prey types, although this procedure resulted in some comparisons where data were not at an equivalent taxonomic level. Analysis based on additional categorization of prey—such as size, ecology, or abundance—although potentially useful, was beyond the limits of what the data could support. We restricted statistical comparisons to selected unpooled collections with at least 30 samples. For each test, 9999 randomizations were used to obtain the distribution for the Mantel test statistic (r_M) and to calculate probability (P) values. A significance level of $\alpha=0.002$ was used based on a Bonferroni adjustment of $\alpha=0.05$ for 26 multiple comparisons.

Results

We collected 1416 Steller sea lion scat samples during 42 collection trips from 1986 through 2007. The number

of scat collected per trip ranged from 2 to 78 (mean of 34) (Table 1). Of the 1416 scat, 22 were discarded from analysis because they had no prey and 11 were discarded because they contained only unidentified prey, resulting in a working data set of 1383 scat. The majority of samples came from Rogue Reef during the breeding (n=526) and nonbreeding (n=290) seasons, followed by collections at the Columbia River South Jetty (n=219) and St. George Reef (n=165) during the breeding season. Only minor collections were made at Orford Reef during the breeding season (n=56), and Cascade Head (n=24) and St. George Reef (n=7) during the nonbreeding season (Table 1).

A total of 47 Steller sea lion prey taxa from 30 families were identified (33 to species) (Table 2). Overall percent frequency of occurrence for the most common (FO>10%) prey in decreasing order were Pacific hake (*Merluccius productus*, FO=78.6%), salmonids (*Oncorhynchus* spp.; FO=28.6%), skates (Rajidae; FO=23.4%), Pacific lamprey (*Lampetra tridentata*; FO=20.8%), clupeids (Clupeidae; FO=18.7%), rockfish (*Sebastes* spp.; FO=17.4%), northern anchovy (*Engraulis mordax*; FO=13.2%), and unidentified teleost fishes (FO=10.8%) (Table 2, Fig. 2). Scat during the breeding season were dominated by hake (87.1%), followed by salmonids (27.1%) and Pacific lamprey at 20.1%. Hake, with an FO of 59%, was also a primary prey in samples collected during the nonbreeding season and skate species increased in frequency to 40.3%, followed by salmonids (32.1%), and rockfish (29.7%) (Table 2). Prey diversity within scat samples ranged from one to 25 types, although 64% of all samples had ≤3 prey types. Of the 222 scat collected during the breeding season that contained a single prey item, 85.1% contained Pacific hake and 4.1% contained rockfish. Scat collected during the nonbreeding season that contained a single prey species (n=63), 49.2% contained hake and 22.2% rockfish.

By site and season (Fig. 2), Pacific hake occurred in more scats than any other prey taxa among all sites and seasons except at Cascade Head and St. George Reef during the nonbreeding season. For example, Pacific hake was the dominant prey in scats collected at Rogue Reef, the largest rookery in the study area, both during breeding (87.3%) and nonbreeding (62.1%) seasons. Although salmonids occurred with high frequency at all sites and seasons, except at Cascade Head, the highest frequency was found at Rogue Reef during the nonbreeding season. Skates, although consumed at all sites and seasons, occurred most frequently in scats collected during the nonbreeding season. For example, skate FO increased at Rogue Reef from 16.2% to 45.5% during the breeding and nonbreeding seasons, respectively. Pacific staghorn sculpin (*Leptocottus armatus*) was common only at the northern sites (i.e., Columbia River and Cascade Head), whereas rockfish were common only at the southern sites (particularly Rogue Reef).

In general, diet composition varied seasonally, annually, and spatially. After controlling for site and year (10 of 11 comparisons; Table 3), we found that diet differed by month; after controlling for site and month, we found that diet differed by year (10 of 12 comparisons; Table 4); and after controlling for year and month (2 of 3 comparisons; Table 5), we found that diet differed by site. Average Jaccard distance within collections ranged from 0.206 to 0.807 (median of 0.724), whereas average Jaccard distance between collections ranged from 0.425 to 0.911 (median of 0.771).

Discussion

Like other researchers (e.g., Pitcher, 1981; Merrick et al., 1997; Sinclair and Zeppelin, 2002; Womble and Sigler, 2006; Trites et al., 2007b; McKenzie and Wynne, 2008), we found that Steller sea lion diet was diverse yet dominated by only one or two species (Fig. 3). In Oregon and northern California the diet was dominated by Pacific hake, whereas in Alaska diet was dominated by walleye pollock (*Theragra chalcogramma*) in the Bering Sea and Gulf of Alaska, and Atka mackerel (*Pleurogrammus monopterygius*) in the Aleutians Islands. Prey types shared between Alaskan and Oregon–northern California collections included salmonids, clupeids (e.g., Pacific herring [*Clupea pallasii*]), rockfish, and skate.

The dominance of Pacific hake in Steller sea lion diets in Oregon and northern California is probably related to the widespread abundance of this species in the California current (as is the case with the widespread distribution of walleye pollock in Alaskan waters). Dorn et al.[2] reported that Pacific hake, ranging from southern California to the Queen Charlotte Sound, British Columbia, was the most abundant groundfish in the California Current system. During summer months adult Pacific hake move north along the Oregon coast while juveniles stay further south off central California (Bailey et al., 1982). From 1966 to 2007 the Pacific Coast (U.S, and Canadian waters) Pacific hake fishery landings averaged 219,000 metric tons (t), with a low of 90,000 t in 1980 and a peak harvest of 364,000 t in 2006 (Helser et al., 2008). Pacific hake are similar in caloric density to cod and pollock, which are prominent in the diet of Steller sea lions in the WDPS. This gadid diet has been hypothesized to result in chronic nutritional stress and ultimately population declines (Trites and Donnelly, 2003, Trites et al., 2007a). However, despite the dominance of Pacific hake in the diet from Oregon and northern California, Steller sea lions in the EDPS have been increasing at approximately 3% per year since the 1970s (Pitcher et al., 2007). This fact was cited by Fritz and Hinckley (2005) as evidence that was inconsistent with the nutritional stress hypothesis.

[2] Dorn, M. W., M. W. Saunders, C. D. Wilson, M. A. Guttormsen, K. Cooke, R. Kieser, and M. E. Wilkins. 1999. Status of the coastal Pacific hake/whiting stock in U.S. and Canada in 1998, 102 p. [Available at Pacific Fishery Management Council, 7700 NE Ambassador Place, Suite 101, Portland, OR. 97220 1384.]

Table 2

Sample information and frequency of occurrence (FO) of prey identified from Steller sea lion (*Eumetopias jubatus*) scat collected in Oregon and northern California from 1986 through 2007. FO is presented by collection site (CR=Columbia River, OR=Orford Reef, RR=Rogue Reef, and SGR=St. George Reef; CH=Cascade Head, see Fig. 1 and Table 1) and season (breeding=May–August, nonbreeding=September–April). Prey are sorted by family in decreasing order of total FO.

		Season		Breeding season				Nonbreeding season			
	Total	Breeding	Nonbreeding	CR	OR	RR	SGR	CR	CH	RR	SGR
Samples											
Total scat collected	1416	989	427	222	56	539	172	99	24	297	7
Scat containing ≥1 identifiable prey	1383	966	417	219	56	526	165	96	24	290	7
Scat containing no identifiable prey	11	6	5	0	0	4	2	0	0	5	0
Empty scat	22	17	5	3	0	9	5	3	0	2	0
Prey item											
Hakes: family Merlucciidae											
Pacific hake (*Merluccius productus*)	78.6	87.1	59.0	80.8	98.2	87.3	90.9	64.6	4.2	62.1	42.9
Salmon: family Salmonidae											
Pacific salmon (*Oncorhynchus* spp.)	28.6	27.1	32.1	27.9	21.4	27.6	26.7	22.9	4.2	37.9	14.3
Skate: family Rajidae											
Skate, unidentified	23.4	16.1	40.3	21.5	8.9	16.2	11.5	26.0	25.0	45.5	71.4
Lamprey: family Petromyzontidae											
Pacific lamprey (*Lampetra tridentata*)	20.8	20.1	22.3	12.3	3.6	28.5	9.1	19.8	0.0	25.2	14.3
Herring, shad, sardine: family Clupeidae											
Unidentified clupeid	18.7	17.7	20.9	27.4	7.1	14.8	17.6	18.8	37.5	20.3	14.3
Pacific herring (*Clupea pallasii*)	9.9	12.4	4.1	6.8	5.4	18.1	4.2	2.1	4.2	4.8	0.0
Pacific sardine (*Sardinops sagax*)	9.2	10.5	6.2	10.5	19.6	6.7	19.4	16.7	8.3	2.8	0.0
American shad (*Alosa sapidissima*)	2.2	1.9	3.1	4.6	1.8	1.1	0.6	5.2	8.3	2.1	0.0
Rockfish: family Sebastidae											
Rockfish (*Sebastes* spp.)	17.4	12.1	29.7	3.2	5.4	14.8	17.6	6.3	0.0	40.3	14.3
Anchovies: family Engraulidae											
Northern anchovy (*Engraulis mordax*)	13.2	11.9	16.1	33.8	8.9	4.2	8.5	24.0	33.3	11.4	42.9
Class Osteichthyes											
Teleost fishes, unidentified	10.8	10.1	12.5	5.9	5.4	11.6	12.7	13.5	4.2	12.8	14.3
Sculpins: family Cottidae											
Pacific staghorn sculpin (*Leptocottus armatus*)	9.4	7.2	14.4	26.5	1.8	1.7	1.2	35.4	54.2	4.5	0.0
Sculpins, unidentified	5.5	5.8	4.8	8.7	5.4	5.7	2.4	1.0	4.2	6.2	0.0
Irish lord (*Hemilepidotus* spp.)	1.6	2.0	0.7	0.0	1.8	1.1	7.3	0.0	0.0	1.0	0.0
Buffalo sculpin (*Enophrys bison*)	0.2	0.1	0.5	0.0	0.0	0.0	0.6	0.0	0.0	0.7	0.0
Sand lances: family Ammodytidae											
Pacific sand lance (*Ammodytes hexapterus*)	9.0	5.6	16.8	1.4	17.9	6.5	4.2	4.2	8.3	20.7	57.1

continued

Table 2 (continued)

	Total	Season		Breeding season				Nonbreeding season			
		Breeding	Nonbreeding	CR	OR	RR	SGR	CR	CH	RR	SGR
Smelts: family Osmeridae											
Smelts, unidentified	6.8	6.3	7.9	3.7	0.0	8.2	6.1	6.3	8.3	8.3	14.3
Eulachon (*Thaleichthys pacificus*)	0.1	0.0	0.2	0.0	0.0	0.0	0.0	1.0	0.0	0.0	0.0
Surf smelt (*Hypomesus pretiosus*)	0.1	0.0	0.2	0.0	0.0	0.0	0.0	0.0	0.0	0.3	0.0
Stickleback: family Gasterosteidae											
Threespine stickleback (*Gasterosteus aculeatus*)	6.1	5.5	7.4	0.0	7.1	4.6	15.2	0.0	0.0	9.7	42.9
Squids and octopus: class Cephalopoda											
Squid and octopus, unidentified	5.7	5.6	6.0	0.5	3.6	6.8	9.1	3.1	0.0	7.6	0.0
Squids, unidentified	4.3	3.9	5.0	0.0	5.4	5.9	2.4	0.0	0.0	7.2	0.0
Octopus, unidentified	2.8	2.6	3.4	0.0	0.0	4.0	2.4	1.0	8.3	3.8	0.0
Jack mackerels: family Carangidae											
Pacific jack mackerel (*Trachurus symmetricus*)	5.4	7.1	1.2	2.3	14.3	5.9	15.2	1.0	0.0	1.4	0.0
Codfishes: family Gadidae											
Pacific tomcod (*Microgadus proximus*)	4.3	3.0	7.4	0.5	1.8	4.2	3.0	6.3	12.5	7.6	0.0
Codfishes, unidentified	1.5	1.2	2.2	0.0	0.0	1.3	3.0	1.0	0.0	2.8	0.0
Pacific cod (*Gadus macrocephalus*)	0.1	0.0	0.2	0.0	0.0	0.0	0.0	0.0	0.0	0.3	0.0
Righteye flounders: family Pleuronectidae											
Starry flounder (*Platichthys stellatus*)	4.3	3.3	6.7	12.8	0.0	0.6	0.6	18.8	4.2	3.1	0.0
Dover sole (*Microstomus pacificus*)	2.1	2.1	2.2	3.2	0.0	1.7	2.4	0.0	0.0	3.1	0.0
Righteye flounder, unidentified	1.9	1.6	2.6	3.7	0.0	1.0	1.2	1.0	8.3	2.8	0.0
Rex sole (*Glyptocephalus zachirus*)	1.2	1.1	1.4	0.9	0.0	1.1	1.8	0.0	0.0	2.1	0.0
Sand sole (*Psettichthys melanostictus*)	1.2	0.8	2.2	0.5	0.0	1.0	1.2	2.1	0.0	2.4	0.0
Slender sole (*Lyopsetta exilis*)	1.2	1.0	1.7	0.0	0.0	0.8	3.6	0.0	0.0	2.4	0.0
Butter sole (*Isopsetta isolepis*)	1.2	0.6	2.4	0.5	0.0	0.8	0.6	4.2	4.2	1.4	14.3
English sole (*Parophrys vetulus*)	0.7	0.8	0.5	0.9	0.0	1.0	0.6	1.0	0.0	0.3	0.0
Arrowtooth flounder (*Atheresthes stomias*)	0.1	0.1	0.2	0.0	0.0	0.0	0.6	1.0	0.0	0.0	0.0
Rock sole (*Lepidopsetta bilineata*)	0.1	0.1	0.0	0.0	0.0	0.2	0.0	0.0	0.0	0.0	0.0
Flatfishes: order Pleuronectiformes											
Flatfishes, unidentified	3.1	2.6	4.3	2.3	1.8	3.2	1.2	5.2	4.2	3.8	14.3
Dogfish sharks: family Squalidae											
Spiny dogfish (*Squalus acanthias*)	2.7	2.8	2.4	5.0	0.0	2.5	1.8	2.1	0.0	2.8	0.0
Sanddabs: family Paralichthyidae											
Sanddabs (*Citharichthys* spp.)	2.7	2.2	4.1	2.3	0.0	1.7	4.2	5.2	20.8	2.1	14.3
Hagfishes: family Myxinidae											
Pacific hagfish (*Eptatretus stoutii*)	1.6	2.1	0.5	0.0	0.0	2.9	3.0	0.0	0.0	0.7	0.0

continued

Table 2 (continued)

		Season		Breeding season				Nonbreeding season			
	Total	Breeding	Nonbreeding	CR	OR	RR	SGR	CR	CH	RR	SGR
Mackerel and tuna: family Scombridae											
Pacific chub mackerel (*Scomber japonicus*)	1.4	2.1	0.0	0.0	0.0	3.4	1.2	0.0	0.0	0.0	0.0
Greenlings: family Hexagrammidae											
Greenling/lingcod, unidentified	0.7	0.8	0.2	0.0	1.8	0.6	2.4	0.0	0.0	0.0	14.3
Lingcod (*Ophiodon elongatus*)	1.3	0.6	2.9	0.0	0.0	1.0	0.6	1.0	4.2	3.4	0.0
Greenling (*Hexagrammos* spp.)	0.3	0.2	0.5	0.0	0.0	0.0	1.2	1.0	0.0	0.3	0.0
Poachers: family Agonidae											
Poachers, unidentified	1.3	1.6	0.7	3.7	0.0	0.4	3.0	1.0	0.0	0.7	0.0
Sturgeon poacher (*Podothecus accipenserinus*)	0.1	0.1	0.0	0.5	0.0	0.0	0.0	0.0	0.0	0.0	0.0
Subclass Elasmobranchii											
Sharks and rays, unidentified	1.2	1.3	1.0	3.7	0.0	0.8	0.6	1.0	0.0	1.0	0.0
Sharks, unidentified	0.3	0.1	0.7	0.0	0.0	0.2	0.0	0.0	0.0	1.0	0.0
Surfperch: family Embiotocidae											
Surfperch, unidentified	1.1	0.7	1.9	0.0	0.0	1.1	0.6	3.1	0.0	1.7	0.0
Gunnel: family Pholidae											
Gunnel, unidentified	1.0	0.9	1.2	0.5	0.0	0.8	2.4	0.0	0.0	1.7	0.0
Wolffishes: family Anarhichadidae											
Wolf eel (*Anarrhichthys ocellatus*)	0.8	1.1	0.0	0.0	1.8	1.3	1.8	0.0	0.0	0.0	0.0
Snailfish: family Liparidae											
Snailfish and lumpfish, unidentified	0.7	0.9	0.2	1.4	1.8	1.0	0.0	0.0	0.0	0.3	0.0
Cusk-eels: family Ophidiidae											
Spotted cusk-eel (*Chilara taylori*)	0.3	0.3	0.2	0.0	0.0	0.2	1.2	0.0	0.0	0.3	0.0
Prickleback: family Stichaeidae											
Pricklebacks, unidentified	0.3	0.4	0.0	0.0	0.0	0.8	0.0	0.0	0.0	0.0	0.0
Class Agnatha											
Jawless fishes, unidentified	0.1	0.1	0.0	0.0	0.0	0.2	0.0	0.0	0.0	0.0	0.0
Clingfish: family Gobiesocidae											
Clingfishes, unidentified	0.1	0.2	0.0	0.0	0.0	0.4	0.0	0.0	0.0	0.0	0.0
Northern clingfish 0.1 (*Gobiesox maeandricus*)	0.1	0.0	0.0	0.0	0.2	0.0	0.0	0.0	0.0	0.0	
Eelpout: family Zoarcidae											
Eelpouts, unidentified	0.1	0.1	0.2	0.0	0.0	0.0	0.6	0.0	0.0	0.3	0.0
Pipefish: family Syngnathidae											
Bay pipefish (*Syngnathus leptorhynchus*)	0.1	0.1	0.0	0.0	0.0	0.0	0.6	0.0	0.0	0.0	0.0
Sandfish: family Trichodontidae											
Pacific sandfish (*Trichodon trichodon*)	0.1	0.1	0.0	0.0	0.0	0.2	0.0	0.0	0.0	0.0	0.0
Sandfishes, unidentified	0.1	0.0	0.2	0.0	0.0	0.0	0.0	0.0	0.0	0.3	0.0

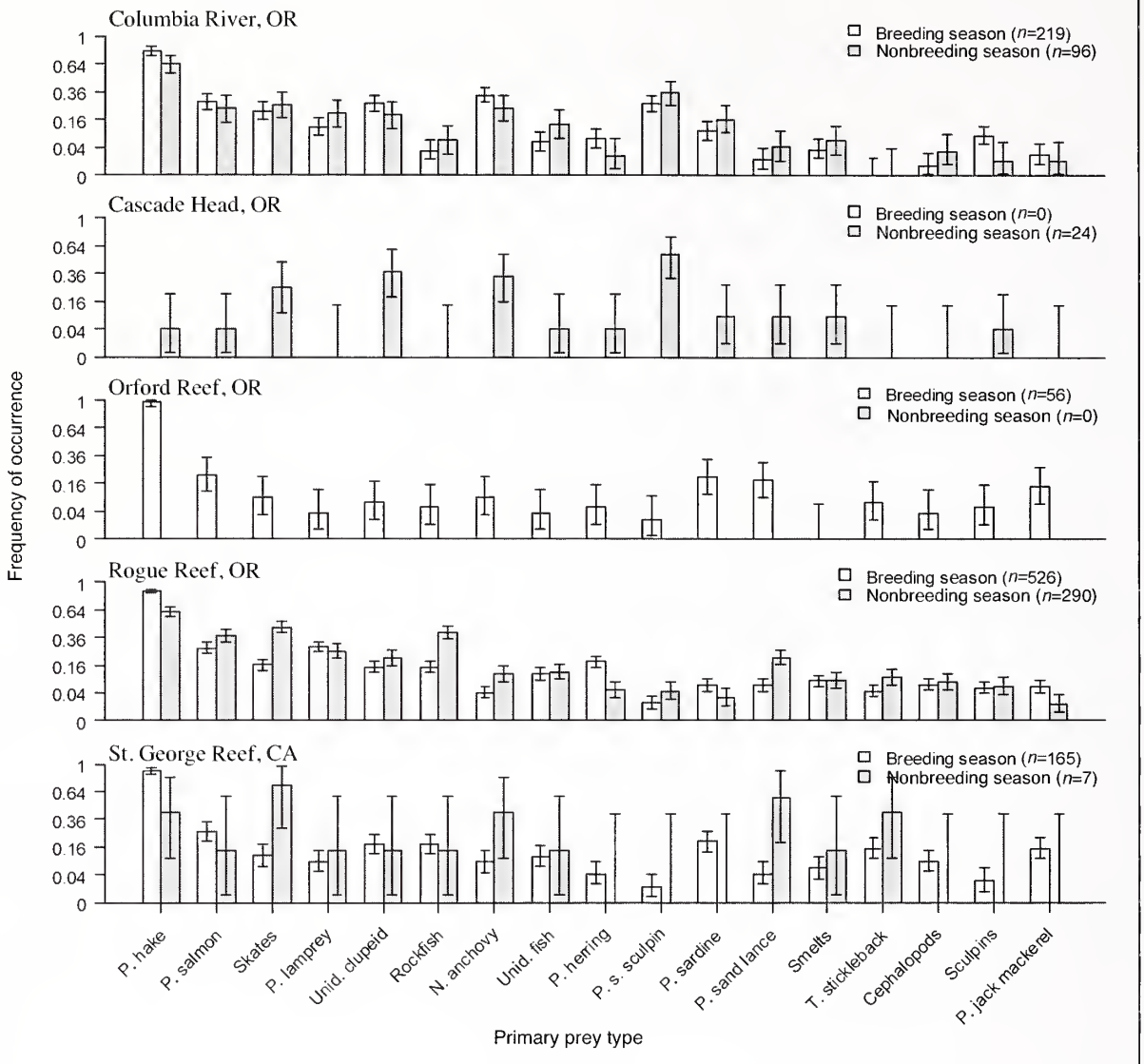

Figure 2

Frequency of occurrence (FO) of primary prey (prey with total FO values≥0.05) identified from Steller sea lion (*Eumetopias jubatus*) scat collected in Oregon and northern California from 1986 through 2007. FO is presented by collection site and season (breeding season=May–August, nonbreeding season=September–April) in descending order of overall pooled FO. Error bars indicate exact 95% binomial confidence intervals. Scientific names for prey types can be found in Table 1. P=Pacific; N=northern; s=staghorn; T=threespine.

How important a specific type of prey is to the survival of an opportunistic marine pinniped predator is unknown. Abundance of prey may have more impact on survival when a predator feeds on schooling fish rather than on more solitary types of prey, such as flatfish and sculpin. Furthermore, a diversity of prey types may be important in sustaining populations and help buffer the effects of ocean climate changes. For example, analyses by Merrick et al. (1997) and Trites et al. (2007b) showed a strong positive correlation between diet diversity and rate of population change. Our data are consistent with this finding; we identified 17 primary (≥5%) prey types (Fig. 3) and the population has been growing at approximately 3% per year (Pitcher et al., 2007).

Perhaps as a reflection of their diverse diet, we found a surprisingly high number of statistical differences in diet composition between months (Table 3), years (Table 4), and sites (Table 5). Although simulation exercises (not presented) indicated that the Mantel test was not overly sensitive (e.g., it did not reject a null hypothesis simply due to a large difference in a single prey type), the procedure is only a hypothesis test and does not lend itself to estimation of effect sizes or biologically

Table 3

Comparison of Steller sea lion (*Eumetopias jubatus*) diet composition by month, after controlling for collection site and year. Sample size (n=number of scat analyzed) and individual number of prey types (D) are given for each diet; pooled number of unique prey types (D_p), correlation coefficient (R_M), and permutation-based P-value (based on 9999 replications) are given for each comparison. * indicates significance at the a=0.002 level (based on Bonferroni adjustment of α=0.05 for 26 multiple comparisons).

		Diet 1			Diet 2				Mantel test	
Site	Year	Month	n	D	Month	n	D	D_p	R_M	P value
Columbia R.	2004	June	53	25	August	37	13	27	0.061	0.0017*
		June	53	25	September	43	17	28	0.145	0.0001*
		August	37	13	September	43	17	19	0.047	0.0105
Rogue Reef	2001	April	45	32	August	48	32	44	0.089	0.0001*
	2002	March	39	27	April	49	30	36	0.264	0.0001*
		March	39	27	July	33	27	35	0.409	0.0001*
		March	39	27	August	37	35	38	0.251	0.0001*
		April	49	30	July	33	27	36	0.173	0.0001*
		April	49	30	August	37	35	39	0.147	0.0001*
		July	33	27	August	37	35	40	0.117	0.0002*
	2003	April	57	29	October	53	31	42	0.101	0.0001*

Table 4

Comparison of Steller sea lion (*Eumetopias jubatus*) diet composition by year, after controlling for collection site and month. Sample size (n) and individual number of prey types (D) are given for each diet; pooled number of unique prey types(D_p), correlation coefficient (R_M), and permutation-based P-value (based on 9999 replications) are given for each comparison. * indicates significance at the α=0.002 level (based on Bonferroni adjustment of α=0.05 for 26 multiple comparisons).

		Diet 1			Diet 2				Mantel test	
Site	Month	Year	n	D	Year	n	D	D_p	R_M	P value
Columbia R.	August	2004	37	13	2007	31	16	20	0.105	0.0004*
Rogue Reef	April	2001	45	32	2002	49	30	40	0.109	0.0001*
		2001	45	32	2003	57	29	40	0.018	0.0682
		2002	49	30	2003	57	29	38	0.126	0.0001*
	June	1987	34	14	1993	36	29	32	0.222	0.0001*
	July	1990	43	16	2002	33	27	29	0.199	0.0001*
		1990	43	16	2004	33	20	26	0.216	0.0001*
		2002	33	27	2004	33	20	29	0.097	0.0001*
	August	2001	48	32	2002	37	35	41	0.123	0.0001*
St. George Reef	July	2002	33	13	2004	33	21	22	0.008	0.2515
		2002	33	13	2006	33	21	25	0.122	0.0001*
		2004	33	21	2006	33	21	29	0.203	0.0001*

interpretable parameters. Nonetheless, it does indicate that researchers should be cautious about pooling samples across space and time before investigating whether those samples differ.

Athough analysis of pinniped fecal matter is a standard technique for studying diet (e.g., Pitcher, 1980; Beach et al.[3]; Olesiuk et al., 1990; Orr et al., 2004), there are some limitations. For example, the use of otoliths to identify prey can lead to biased diet composition estimates (Jobling and Breiby, 1986). We minimized this problem by including all bony skeletal structures (vertebrae, gillrakers, etc.) to identify prey. Another potential bias can occur when drawing inference to a particular population from opportunistically collected

[3] Beach, R. J., A.C. Greiger, S. J. Jeffries, S. D. Treacy, and B. L. Troutman. 1985. Marine mammals and their interactions with fisheries of the Columbia River and adjacent waters, 1980–1982: third annual report, March 1, 1980 to October 31, 1982. National Marine Mammal Laboratory, Northwest and Alaska Fisheries Center, NMFS, NOAA Proc. Rep. 85-03, 316 p. [Available at www.lib.noaa.gov, accessed May 2011.]

Table 5

Comparison of Steller sea lion (*Eumetopias jubatus*) diet composition by site, after controlling for collection year and month. Sample size (n) and individual number of prey types (D) are given for each diet; pooled number of unique prey types(D_p), correlation coefficient (r_M), and permutation-based P-value (based on 9999 replications) are given for each comparison. * Indicates significance at the α=0.002 level (based on Bonferroni adjustment of α=0.05 for 26 multiple comparisons).

		Diet 1			Diet 2				Mantel test	
Year	Month	Site	n	D	Site	n	D	D_p	r_M	P value
1990	July	Orford Reef	41	6	Rogue Reef	43	16	17	0.079	0.0002*
2002	July	Rogue Reef	33	27	St. George Reef	33	13	28	0.075	0.0023
2004	July	Rogue Reef	33	20	St. George Reef	33	21	25	0.096	0.0008*

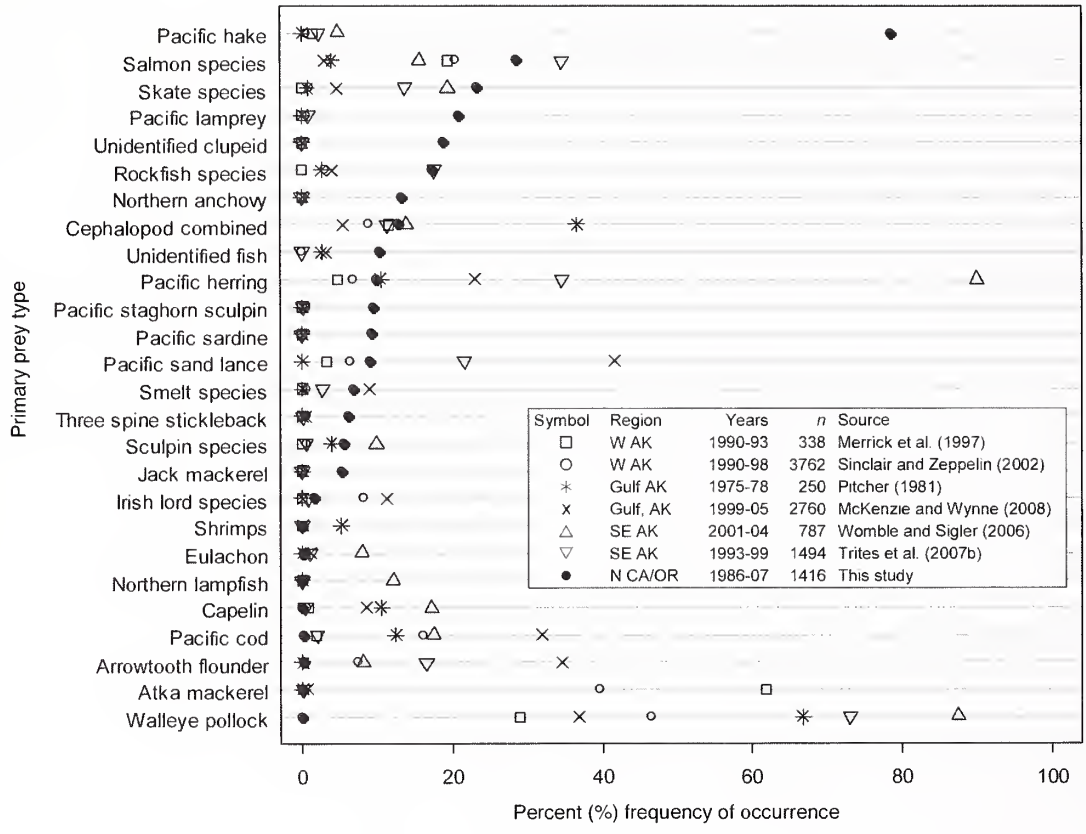

Figure 3

Percent frequency of occurrence (FO) of primary prey reported for Steller sea lions (*Eumetopias jubatus*) in Alaska (n=6 studies) and northern California and Oregon (this study). FO summary for Trites et al. (2007b) and Merrick et al. (1997) was calculated by the authors of the present study. Scientific names for prey types can be found in Table 1.

samples. For example, scat that we collected on rookeries (i.e., Rogue Reef, Orford Reef, St. George Reef) during the summer breeding season primarily reflect adult female diet because males often fast during the breeding season and juveniles are not generally present at rookery sites.

The Steller sea lion recovery plan (NMFS, 2008) notes that although several factors affecting the endangered WDPS also affect the threatened EDPS, those threats do not appear to be affecting the sustained growth or recovery of the EDPS. It is noted in the plan, however, that concerns regarding climate change,

particularly on the southern part of the species range, warranted continued research and monitoring. Population growth in California sea lions (Carretta et al., 2010) may also be a concern for the EDPS because these sympatric ottariids potentially compete for prey resources and habitat. Steller sea lions in the Channel Island rookeries in California experienced a similar situation in the late 1950s as California sea lion populations increased and potentially out-competed Steller sea lions for food and habitat (Bartholomew and Boolootian, 1960). Additionally, as the Steller sea lion EDPS increases, its real and perceived impacts on sport and commercial fish harvests; as well as threatened and endangered fish populations, will likely increase. For example, Steller sea lion abundance at Bonneville Dam on the Columbia River (Fig. 1), 235 km from the ocean, increased from zero individuals in 2002 to at least 53 in 2010 and these sea lions have consumed hundreds of threatened and endangered salmonids and thousands of white sturgeon (*Acipenser transmontanus*) (Stansell et al.[4]). Ongoing uncertainties over the role of diet in the decline of the WDPS, impacts of climate change on the EDPS, and emerging management concerns all argue for continued and refined research on Steller sea lion diet and foraging behavior in the southern extent of their range.

Conclusions

Identification of prey from 1383 Steller sea lions scats collected in Oregon and northern California during 1986–2007 resulted in a list of 47 prey taxa consumed. Primary prey items included Pacific hake, Pacific salmon, skate, Pacific lamprey, rockfish and clupeid species. Prey identified from scat during the breeding and nonbreeding seasons were fairly similar but rockfish and skate species had a higher frequency of occurrence during the nonbreeding season. Data analysis showed that, in general, diet composition varied seasonally, annually, and spatially. When compared to previous diet studies for Steller sea lions in Alaska, this population was shown to depend on hake as the primary prey rather than on the gadid and hexagrammid species identified in the northern populations studied. Salmonids were important prey in all the studies compared. Continued study of Steller sea lion food habits is necessary to evaluate their interactions with important fish populations (such as salmonids and rockfish), to assess the increasing pressure from migrating California sea lions for limited prey resources, and to begin to address the effects of climate change on population abundance.

[4] Stansell, R. J, K. M. Gibbons, and W. T. Nagy. 2010. Evaluation of pinniped predation on adult salmonids and other fish in the Bonneville Dam tailrace, 2008–2010. U.S. Army Corps of Engineers, Cascade Locks, OR. [Available online at http://www.nwd-wc.usace.army.mil/tmt/documents/fish/2010/2008-2010_Pinniped_Report.pdf, accessed 2 March 2011.]

Acknowledgments

This article summarizes over 25 years of research on Steller sea lions in Oregon that would not have been accomplished without the help of many individuals and agencies. We would like to thank the following for support, guidance, and assistance: Oregon Department of Fish and Wildlife, National Marine Fisheries Service (J. Scordino, P. Gearin, R. DeLong), U.S. Fish and Wildlife Service Oregon Coast National Wildlife Refuge (P. Sekora, R. Lowe, D. Pitkin), M. Tennis, J. Jenniges, J. Scordino, M. Dhruv, A. Ougzin, S. Jeffries, J. Harvey, J. Stein, and many others who assisted in the field with collection of data and samples over the years. R. Emmett, P. Gearin, D. Fox, and R. Stauff and three anonymous reviewers provided beneficial comments on the manuscript. This research was conducted under Marine Mammal Protection Act scientific research permit numbers 499, 835, 854, 782-1446, 434-1669, and 434-1892.

Literature cited

Agresti, A., and I. Liu.
1999. Modeling a categorical variable allowing for arbitrarily many category choices. Biometrics 55:936–943.

Anderson, M. J.
2001. A new method for non-parametric multivariate analysis of variance. Austral Ecology 26:32–46.

Bailey, K. M., R. C. Francis, and P. R. Stevens.
1982. The life history and fishery of Pacific whiting, *Merluccius productus*. Calif. Coop. Oceanic Fish. Invest. Rep. 23:81–98.

Bartholomew, G. A. and R. A. Boolootian.
1960. Numbers and population structures of the pinnipeds on the California Channel Islands. J. Mammal. 41:366–375.

Berry, J. J. and P. W. Mielke Jr.
2003. Permutation analysis of data with multiple binary category choices. Psych. Rep. 92:91–98.

Bilder, C. R. and T. M. Loughin.
2009. Modeling multiple-response categorical data from complex surveys. Can. J. Stat. 37:553–570.

Braham, H. W., R. D. Everitt, and D. J. Rugh.
1980. Northern sea lion population decline in the eastern Aleutian Islands. J. Wildl. Manage. 44:25–33.

Carretta J. V., K. A. Forney, M. S. Lowry, J. Barlow, J. Baker, D. Johnston, B. Hanson, R. L. Brownell Jr., J. Robbins, D. K. Mattila, K. Ralls, M. M. Muto, D. Lynch, and L. Carswell.
2010. U.S. Pacific marine mammal stock assessments: 2009. NOAA Tech. Memo. NOAA-TM-NMFS-SWFSC-453, 336 p.

Fritz, L. W., and S. Hinckley.
2005. A critical review of the regime shift "junk-food" nutritional stress hypothesis for the decline of the western stock of Steller sea lion. Mar. Mamm. Sci. 21:476–518.

Green, K., and H. R. Burton.
1993. Comparison of the stomach contents of southern elephant seals *Mirounga leonina*, at Macquarie and Heard Islands. Mar. Mamm. Sci. 9:10–22.

Helser, T. E., I. J. Stewart, and O. S. Hamel.
2008. Stock assessment of Pacific hake (whiting) in U.S.

and Canada waters in 2008. [Available from Pacific Fishery Management Council, 7700 NE Ambassador Place, Suite 101, Portland, OR. 97220-1384.]

Hudon, C., and G. Lamarche.
1989. Niche segregation between American lobster *Homarus americanus* and rock crab *Cancer irroratus*. Mar. Ecol. Prog. Ser. 53:155–168.

Jobling, M., and A. Breiby.
1986. The use and abuse of fish otoliths in studies of feeding habits of marine piscivores. Sarsia 71:265–274.

Jones, M. E., and L. A. Barmuta.
1998. Diet overlap and relative abundance of sympatric dasyurid carnivores: a hypothesis of competition. J. Anim. Ecol. 67:410–421.

Legendre, P., and L. Legendre.
1998. Numerical ecology, 2nd English ed., 853 p. Elsevier Science, Amsterdam.

Lemons, P. R., J. S. Sedinger, M. P. Herzog, P. S. Gipson, and R. L. Gilliland.
2010. Landscape effects on diets of two canids in northwestern Texas: a multinomial modeling approach. J. Mammal. 91:66–78.

Loughlin, T. R.
1997. Using the phylogeographic method to identify Steller sea lion stocks. *In* Molecular genetics of marine mammals (A. E. Dizon, S. J. Chivers, and W. F. Perrin, eds.), p. 159–171. Soc. Mar. Mammal., spec. publ. no. 3.

Loughlin, T. R., A. S. Perlov, and V. A. Vladimirov.
1992. Range-wide survey and estimation of total abundance of Steller sea lions in 1989. Mar. Mamm. Sci. 8:220–239.

Loughlin, T. R., D. J. Rugh, and C. H. Fiscus.
1984. Northern sea lion distribution and abundance: 1956–80. J. Wildl. Manage. 48:729– 740.

Luo, J., and B. J. Fox.
1996. A review of the Mantel test in dietary studies: effect of sample size and inequality of sample sizes. Wildl. Res. 23:267–288.

Manly, B. F. J.
1997. Randomization, bootstrap, and Monte Carlo methods in biology, 2nd ed., 399 p. Chapman and Hall, London.

Mantel, N. A.
1967. The detection of disease clustering and a generalized regression approach. Cancer Res. 27:209–220.

McKenzie J. and K. M. Wynne.
2008. Spatial and temporal variation in the diet of Steller sea lions in the Kodiak Archipelago, 1999 to 2005. Mar. Ecol. Prog. Ser. 360:265–283.

Merrick, R. L., M. K. Chumbley, and G. V. Byrd.
1997. Diet diversity of Steller sea lions (*Eumetopias jubatus*) and their population decline in Alaska: a potential relationship. Can. J. Fish. Aquat. Sci. 54:1342–1348.

Merrick, R. L., and T. R. Loughlin.
1997. Foraging behavior of adult female and young-of-the-year Steller sea lions in Alaskan waters. Can. J. Zool. 75:776–786.

Merrick, R. L., T. R. Loughlin, and D. G. Calkins.
1987. Decline in abundance of the northern sea lion, *Eumetopias jubatus*, in Alaska, 1956–86. Fish. Bull. 85:351–365.

Nandram, B., M. C. S. Toto, and M. Katzoff.
2009. Bayesian inference for a stratified categorical variable allowing all possible category choices. Journal Stat. Comp. Simulation 79:161–179.

NMFS (National Marine Fisheries Service).
2008. Recovery plan for the Steller sea lion (*Eumetopias jubatus*), 325 p. Revision. NMFS, Silver Spring, MD.

Oksanen, J., R. Kindt, P. Legendre, B. O'Hara, G. L. Simpson, P. Solymos, M. H. H. Stevens, and H. Wagner.
2009. vegan: community ecology package. R package, vers. 1.15-3. http://CRAN.R-project.org/package=vegan, accessed October 2010).

Olesiuk, P. F., M. A. Bigg, G. M. Ellis, S. J. Crockford, and R. J. Wigen.
1990. An assessment of the feeding habits of harbour seals (*Phoca vitulina*) in the Strait of Georgia, British Columbia, based on fecal analysis. Can. Tech. Rep. Fish. Aquat. Sci. No. 1730, 135 p.

Orr, A. J., A. S. Banks, S. Mellman, H. R. Huber, R. L. DeLong and R. F. Brown.
2004. Examination of the foraging habits of Pacific harbor seal (*Phoca vitulina richardsi*) to describe their use of the Umpqua River, Oregon, and their predation on salmonids. Fish. Bull. 102:108–117.

Orr, A. J., J. L. Laake, M. I. Dhruv, A. S. Banks, R. L. DeLong and H. R. Huber.
2003. Comparison of processing pinniped scat samples using a washing machine and nested sieves. Wildl. Soc. Bull. 31:253–257.

Pitcher, K. W.
1980. Stomach contents and feces as indicators of harbor seal, *Phoca vitulina*, foods in the Gulf of Alaska. Fish. Bull. 78:797–798.
1981. Prey of the Steller sea lion *Eumetopias jubatus* in the Gulf of Alaska. Fish. Bull. 79:467–472.

Pitcher, K. W., P. F. Olesiuk, R. F. Brown, M. S. Lowry, S. J. Jeffries, J. L. Sease, W. L. Perryman, C. E. Stinchcomb, and L. F. Lowry.
2007. Abundance and distribution of the eastern North Pacific Steller sea lion (*Eumetopias jubatus*) population. Fish. Bull. 107:102–115.

R Development Core Team.
2009. R: A language and environment for statistical computing. R Foundation for Statistical Computing, Vienna, Austria. [ISBN 3-900051-07-0, URL http://www.R-project.org, accessed October 2010.]

Sinclair, E. H., and T. K. Zeppelin.
2002. Seasonal and spatial differences in diet in the western stock of Steller sea lions (*Eumetopias jubatus*). J. Mammal. 83:973–990.

Springer, A. M.
1992. A review: walleye pollock in the North Pacific—how much difference do they really make? Fish. Oceanogr. 1:80–96.

Sokal, R. R., and F. J. Rohlf.
1995. Biometry: the principles and practice of statistics in biological research, 3rd ed., 887 p. W.H. Freeman and Company, New York.

Tollit, D. J., G. J. Pierce, K. A. Hobson, W. D. Bowen, and S. J. Iverson.
2010. Diet. *In* Marine mammal ecology and conservation (I. L. Boyd, W. D. Bowen, and S. J. Iverson, eds.), p. 191–221. Oxford Univ. Press, Oxford, U.K.

Trites, A. W., A. J. Miller, H. D. G. Maschner, M. A. Alexander, S. J. Bograd, J. A. Calder, A. Capotondi, K. O. Coyle, E. Di Lorenzo, B. P. Finney, E. J. Gregr, C. E. Grosch, S. R. Hare, G. L. Hunt Jr., J. Jahncke, N. B. Kachel, H. Kim, C. Ladd, N. J. Mantua, C. Marzban, W. Maslowski, R. Mendelssohn, D. J. Neilson, S. R. Okkonen, J. E. Overland, K. L. Reedy-Maschner, T. C. Royer, F. B. Schwing, J. X. L. Wang, and A. J. Winship.
2007a. Bottom-up forcing and the decline of Steller sea lions (*Eumetopias jubatus*) in Alaska: assessing the ocean climate hypothesis. Fish. Oceanogr. 16:46–67.

Trites, A. W., D. G. Calkins, and A. J. Winship.
2007b. Diets of Steller sea lions (*Eumetopias jubatus*) in Southeast Alaska, 1993 to 1999. Fish. Bull. 105:234–248.

Trites, A. W., and C. P. Donnelly.
2003. The decline of Steller sea lions *Eumetopias jubatus* in Alaska: a review of the nutritional stress hypothesis. Mamm. Rev. 33:3–28.

Trites, A. W., and P. A. Larkin.
1996. Changes in the abundance of Steller sea lions (*Eumetopias jubatus*) in Alaska from 1956 to 1992: how many were there? Aquat. Mamm. 22.3:153–166.

Womble, J. N., and M. F. Sigler.
2006. Seasonal availability of abundant, energy-rich prey influences the abundance and diet of a marine predator, the Steller sea lion *Eumetopias jubatus*. Mar. Ecol. Prog. Ser. 325:281–293.

Wright, B. E.
2010. Use of chi-square tests to analyze scat-derived diet composition data. Mar. Mamm. Sci. 26:395–401.

York, A. E.
1994. The population dynamics of northern sea lions, 1975–1985. Mar. Mamm. Sci. 10:38–51.

Genetic variation between outer-coastal and fjord populations of Pacific herring (*Clupea pallasii*) in the eastern Gulf of Alaska

Sharon L. Wildes (contact author)
Johanna J. Vollenweider
Hanhvan T. Nguyen
Jeffrey R. Guyon

Email address for contact author: Sharon.Wildes@noaa.gov

Auke Bay Laboratories
Alaska Fisheries Science Center
National Marine Fisheries Service
National Oceanic and Atmospheric Administration
17109 Point Lena Loop Rd.
Juneau, Alaska, 99801-8344

Abstract—Pacific herring (*Clupea pallasii*) from the Gulf of Alaska were screened for temporal and spatial genetic variation with 15 microsatellite loci. Thirteen collections were examined in this study: 11 from Southeast Alaska and 2 from Prince William Sound, Alaska. Although F_{ST} values were low, a neighbor-joining tree based on genetic distance, homogeneity, and F_{ST} values revealed that collectively, the Berners Bay and Lynn Canal (interior) collections were genetically distinct from Sitka Sound and Prince of Wales Island (outer-coastal) collections. Temporal genetic variation within regions (among three years of Berners Bay spawners and between the two Sitka Sound spawners) was zero, whereas 0.05% was attributable to genetic variation between Berners Bay and Sitka Sound. This divergence may be attributable to environmental differences between interior archipelago waters and outer-coast habitats, such as differences in temperature and salinity. Early spring collections of nonspawning Lynn Canal herring were nearly genetically identical to collections of spawning herring in Berners Bay two months later—an indication that Berners Bay spawners over-winter in Lynn Canal. Southeast Alaskan herring (collectively) were significantly different from those in Prince William Sound. This study illustrates that adequate sample size is needed to detect variation in pelagic fish species with a large effective population size, and microsatellite markers may be useful in detecting low-level genetic divergence in Pacific herring in the Gulf of Alaska.

Manuscript submitted 31 August 2010.
Manuscript accepted 22 June 2011.
Fish. Bull. 109:382–393 (2011).

Defining the population structure of a species is fundamental for fishery management and resource conservation. Sustainable management of commercially harvested stocks depends on a clear understanding of the extent of fish movements and migratory behavior, spawning-site fidelity, and degree of immigration and emigration. One means to assess population structure is through genetic analysis. Armed with the knowledge of genetic stock structure, managers can use the appropriate spatial scale to understand life history, essential habitat, migration patterns, distribution, connectivity and isolation of stocks, recruitment, and spawning behavior. Understanding genetic diversity, which allows for adaptation to changing environmental conditions, is vital information for conserving a species. Detecting genetic divergence within pelagic fish species, however, is often difficult because of large population sizes that retard genetic drift and gene flow among cohorts through dispersal and migration (Shaklee and Bentzen 1998; Waples, 1998). Even small numbers of migrants or episodic straying events can lead to increased genetic connectivity among otherwise isolated stocks. Genetic divergence may occur if gene flow is interrupted by a single factor or combination of factors such as physical barriers, temporal variation (time of spawning), and spawning-site and natal-site fidelity.

A particularly large void of genetic information exists for forage fishes in the Gulf of Alaska. These species play a role of great consequence in marine ecosystems, as prey for most commercially important fish species. Without these nutritionally rich fish, many higher trophic level species might lack the resources to overwinter. Yet the amount of genetic information available for forage species is minimal at best. One example of a forage species is the Pacific herring (*Clupea pallasii*), which provides a critical link between lower and higher trophic levels. Herring typically eat crustaceans and small fish, and serve as forage for whales, sea lions, birds, larger fish, (Bakun, 2006; Hart, 1973; Hourston and Haegele, 1980), and humans.

There are few genetic studies of Pacific herring in Alaska, particularly in regions that have experienced a recent decline in stocks, such as Prince William Sound in the central Gulf of Alaska (GOA), and Lynn Canal in southeast Alaska. Herring abundance in Lynn Canal has declined since the late 1970s and has not recovered to pre-1980 levels, despite the closure of the fishery in 1981. One criterion for listing a stock

Table 1

Location and dates for Pacific herring (*Clupea pallasii*) collections from Southeast and Prince William Sound (PWS), Alaska. Sample size (*n*) reflects the number of individuals successfully genotyped and used in analyses. The two Lynn Canal collections in the early spring of 2008 are noted as Lynn Canal 08, a and b.

Sample	Latitute (N)	Longitude (W)	Sampling date	*n*
Spawning fish				
Berners Bay 07	58°40.9′	134°59.1′	4/5/2007	52
Berners Bay 08	58°40.9′	134°59.1′	5/3/2008	126
Berners Bay 09	58°39.3′	134°58.5′	5/5/2009	148
Hobart Bay 08	57°27.6′	133°21.1′	5/9/2008	128
Hoonah Sound 08	57°36.6′	135°21.5′	4/23/2008	100
Sitka Sound 07	57°05.1′	135°30.4′	3/29/2007	75
Sitka Sound 08	57°08.9′	135°28.7′	4/4/2008	131
Nonspawning fish				
Lynn Canal 07	58°27.2′	134°47.0′	11/10/2007	97
Lynn Canal 08a	58°27.2′	134°49.0′	2/23/2008	98
Lynn Canal 08b	58°29.6′	134°49.2′	2/25/2008	98
Nichols Bay 07	54°43.8′	132°08.3′	6/14/2007	97
Western PWS07	60°13.6′	148°11.0′	7/15/2007	99
Eastern PWS07	60°39.2′	134°49.2′	12/2/2007	92

as threatened or endangered under the Endangered Species Act is a stock's discreteness or uniqueness. To date, four genetic studies have been completed in the eastern GOA. One study of allozymes indicated that, in general, GOA populations are genetically distinct from those to the south in British Columbia, Canada and west of Kodiak Island, (Grant and Utter, 1984): one locus in that study indicated heterogeneity among populations within the GOA. In more recent studies of microsatellite DNA variation, genetically discrete stocks of herring were detected in British Columbia (Beacham et al., 2008) and in Puget Sound in Washington State (Small et al., 2005). In both studies, genetic divergence among these discrete stocks was attributed to different spawning times, geographic isolation, or both. In the fourth study, O'Connell et al. (1998a) confirmed genetic differentiation between Prince William Sound and western Alaska Pacific herring populations, using microsatellites.

This study was conducted to determine whether Lynn Canal Pacific herring (hereafter, herring) in Southeast Alaska are genetically distinct from other eastern Gulf of Alaska herring and whether overwintering Lynn Canal herring spawn in Berners Bay. We evaluated 22 existing microsatellite loci developed for Pacific and Atlantic herring (*Clupea harengus*) (Miller et al., 2001; McPherson et al., 2001; Olsen et al., 2002; O'Connell et al., 1998b) for their ability to distinguish herring populations in the eastern Gulf of Alaska. Our results indicate that this class of highly polymorphic nuclear DNA markers, combined with adequate sample sizes, can resolve spatial patterns of genetic heterogeneity consistent with discrete stocks of Pacific herring.

Materials and methods

Sample collections

Thirteen collections of herring were made in seven locations in Southeast Alaska from 2007 to 2009 (Table 1, Fig. 1). These samples included three collections of nonspawning, overwintering herring in Lynn Canal and three collections of spawning herring in associated Berners Bay, which is located on the eastern side of Lynn Canal and hosts a high concentration of spring spawning herring. Three consecutive years of spawning fish were sampled in Berners Bay: about two weeks before spawning in 2007 (Berners07) and during the spawning season in 2008 and 2009 (Berners08 and Berners09, respectively). Three samples of overwintering fish were collected in Lynn Canal during the winter of 2007–08. The Lynn07 collection was made in early winter (November), whereas collections from along the shoreline (Lynn08a) and from a deep trench offshore (Lynn08b) were made several days apart, approximately two months (late February) before the spawning season. In 2008, samples of spawning fish were also collected in Hobart Bay, approximately 200 km south of Berners Bay on the mainland in central Southeast Alaska, and in Hoonah Sound, on northern Chichagof Island. Two collections were made in Sitka Sound, on the outer coast of Baranof Island, during the spawning season in 2007 and 2008, and one collection of immature fish was obtained from Nichols Bay located at southern Prince of Wales Island in 2007. Two additional collections were made in Prince William Sound: one from a postspawning group in Whale Bay in 2007, located on the western side of the sound (wPWS), and one from an

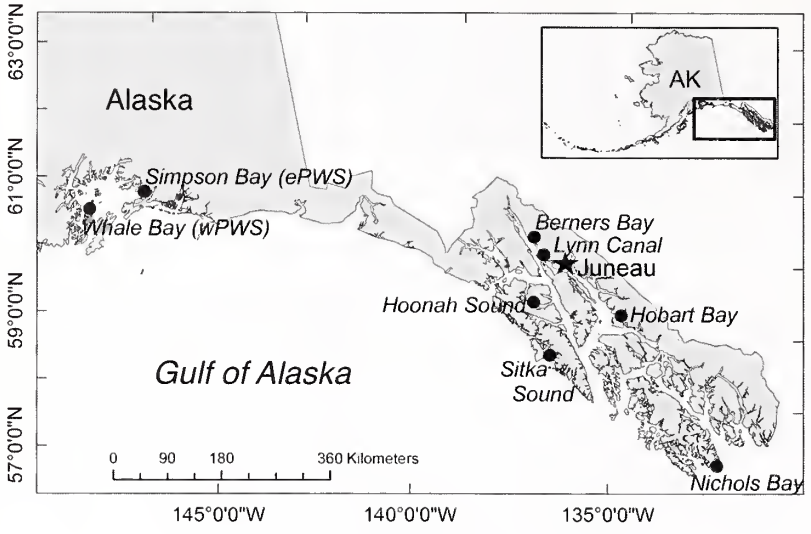

Figure 1

Sampling locations for Pacific herring (*Clupea pallasii*) collected in the Gulf of Alaska for genetic analysis, 2007–09.

overwintering aggregate from Simpson Bay, in eastern Prince William Sound (ePWS) in December, 2007.

All samples were collected by trawl, seine, or castnet. Lynn Cana and Hobart Bay samples were collected with a midwater trawl. Spawning herring in Berners Bay were collected along the shore with a castnet. Hoonah Sound samples were hand netted from the commercial roe-on-kelp fishery. In Sitka Sound, herring were collected from a purse seiner chartered by the Alaska Department of Fish and Game (ADFG) during the test fishery for the Sitka Sound sac roe fishery. Samples from Nichols Bay and Prince William Sound were collected with a beach seine. All samples, except those from Nichols Bay, were mature fish. All collections were shipped as whole frozen fish to the Auke Bay Laboratories in Juneau, AK.

Laboratory procedures

DNA was extracted from tissue samples (heart, muscle, or fin) by following DNeasy genomic DNA extraction methods (Qiagen, Valencia, CA). A master mix of 1 µL 10× PCR buffer, 4.54 µL deionized water, 0.6 µL $MgCl_2$ (25 mM), 0.8 µL dNTPs (10 mM), 0.5 µL forward primer (10 mM), 0.4 µL reverse primer (10 mM), 1.0 µL of fluorescent labeled primer (1 mM), and 0.16 µL of TAQ DNA polymerase was combined with 1 µL of DNA. Initially, 22 microsatellite loci were amplified by polymerase chain reaction (PCR), by using a Gene Amp 9700 thermocycler (Applied Biosystems, Foster City, CA). The resulting PCR products were size fractionated on a DNA sequencer (Licor 4200 and 4300) by using known molecular size standards, and genotypes were scored by using SAGA software (Licor, inc., Lincoln, NE). Loci were double-scored and those with a 2-bp repeat were aligned by allele size and analyzed a second time to ensure data integrity. Individuals for which there were missing data for three or more of the 15 loci were dropped from further analyses. The numbers of individuals used in analyses (n) are given in Table 1.

Genetic analysis

Initial data from 22 loci were examined for the possibility of scoring errors, null alleles, or large allele drop out with MICROCHECKER software (van Oosterhout et al., 2004). Deviation from Hardy-Weinberg expectation (HWE) was tested for each locus for each sample collection by using Fisher's exact test with GENEPOP software, vers. 4.0 (Raymond and Rousset, 1995). Linkage disequilibrium was tested with Slatkin's (1994) method implemented in GENEPOP to confirm that loci were segregating independently. Markov chain parameters of 50,000 dememorizations, 500 batches, and 25,000 iterations were used to calculate an accurate and reliable test. The methods of Weir and Cockerham (1984) implemented in FSTAT, vers. 2.9.3.2 (Goudet, 1995) were used to calculate F_{IS} for each collection by locus, and each locus over all collections. A gene diversity analysis was conducted with GENEPOP software to examine observed and expected heterozygosities per locus and per collection. Allelic richness by collection was calculated in FSTAT. Effective number of alleles was calculated as $1/(1-H_e)$. Chord distances (Cavalli-Sforza and Edwards, 1967) were calculated among all pairs of collections with PHYLIP software, vers. 3.69 (Felsenstein, 1989), and a neighbor-joining tree was constructed to examine the relationships among collections. Data were bootstrapped (1000 replicates) by using allele replacement and loci replacement in PHYLIP, and a summary of the replicates (consensus tree) was constructed to examine the consistency of putative genetic partitions.

Homogeneity tests of allelic frequencies were conducted for all pairs of collections by using χ^2 probabilities (Markov chain algorithm, GENEPOP, vers. 4.0). *P*-values were corrected for multiple testing with the false discovery rate test (Benjamini and Yekutieli, 2001). Pairwise F_{ST} values, a measure of genetic divergence, were calculated with the Weir and Cockerham (1984) algorithm in FSTAT and evaluated with a permutation test.

The amount of molecular diversity was measured within sites at locations for which multiple years of data from the same location were available (Berners Bay and Sitka Sound). The diversity among years was compared with the diversity between locations, by using a hierarchical AMOVA (analysis of molecular variance) with 1000 permutations in ARLEQUIN, vers. 3.5 (Excoffier and Schneider, 2005). The amount of variation was partitioned in the following categories: within the individual sample (Fsc), among collections from different years at the same location (Fct), and between locations (Fst).

Results

Seven of the 22 loci were dropped from further analyses because of either large allele drop out (*Cpa102*), suspected null alleles (*Cpa8*), stutter bands (*Cpa104, Cha123*), one-bp shifts (*Cpa100*), or because of our inability to resolve the loci for all data sets (*Cpa101, Cpa107a*), or because of one-bp shifts (*Cpa100*); however, further optimization in the laboratory may prove these loci useful for future studies. The remaining 15 loci were *Cpa103, Cpa108, Cpa111, Cpa112, Cpa113, Cpa114,* (Olsen et al., 2002) *Cpa4, Cpa6, Cpa27, Cpa107, Cpa125, Cpa134,* (Miller et al., 2001) *Cha1017* and *Cha1020,* (McPherson et al., 2001) and *Cha63* (O'Connell et al., 1998b) (Appendix). These loci were highly polymorphic in general; the average number of alleles was 30.8, ranging from 7 at *Cha1017* to 64 at *Cpa112* (Appendix). Several loci with a large number of unique alleles, such as *Cpa134* (58 alleles), and *Cpa112* (64 alleles), exceeded the number of individuals (n=52) in the Berners07 collection. This finding illustrates the need for ample sample sizes for use with highly polymorphic markers. Average observed heterozygosity across all populations for each locus varied from 0.45 to 0.99. The number of alleles (n_a) found in each collection was similar overall, with the exception of those from the Berners07 collection, which were typically lower. The allelic richness (a) and effective number of alleles (n_{eff}) were also similar overall (Appendix).

Observed and expected heterozygosities were overall in close agreement for all loci. Nine of the 195 tests for Hardy Weinberg equilibrium had an excess of homozygotes—an amount expected by chance alone—and importantly, no excesses of homozygotes at any one locus were found in more than two collections—evidence that null alleles did not contribute significant bias to estimates derived from these 15 microsatellites. Low F_{IS} values for most loci indicate random mating within each collection. *Cha1017* and *Cpa27* had a slightly high overall F_{IS} value of 0.167 and 0.114, respectively. Nine out of 105 linkage disequilibrium tests in GENEPOP were significant. No locus had a significant value at more than two collections, indicating that all loci were likely inherited independently.

Global AMOVA results for the three Berners Bay collections and two Sitka Sound collections revealed that nearly all the variation was within the individuals (99.6%) and within the collection (0.35%). The remainder of the genetic variation was attributable to regional differences between the two locations (0.05%; P=0.058). No variation was attributable to temporal differences among collection years within a region.

Pairwise homogeneity tests of allelic frequency revealed statistically significant genetic differentiation at 10 (7 after correction for multiple testing) of the 21 sample pairs of spawning fish collections (below diagonal of boxed area in Table 2). The most notable result was that Berners08 and 09 spawners were significantly different from the Sitka Sound and Hoonah Sound spawners in all pairwise homogeneity tests of allele frequencies. The Berners07 collection of prespawning fish was generally homogeneous with all other collections, possibly because of small sample size. Berners Bay spawning herring and those collected in the winter from nearby Lynn Canal, were homogeneous, with the exception of the early winter collection (Lynn07). The two Lynn Canal collections in the early spring 2008 (Lynn08, a and b) were nearly identical to each other and were also highly similar to those collections of spawning herring in the nearby Berners08 sample taken several months later.

Among the collections of spawning fish, seven of the 21 F_{ST} estimates were significant before correction. Only one pairwise F_{ST} value was significant after correction: namely the F_{ST} value for Hoonah Sound and Berners08. Berners Bay and Lynn Canal collections, with the exception of Lynn07, exhibited an F_{ST} of 0, indicating a high level of genetic homogeneity in this region over several years of collection.

Significant F_{ST} values and differences in allele frequencies among regional groups were more evident after spatially homogeneous and temporal collections were pooled (Table 3). Collections of herring from Prince William Sound were significantly different (P=0.001) from both outer-coastal and interior collections in Southeast Alaska (except for the single collection of Hobart Bay). Herring samples from the two outer-coastal locations, Sitka Sound and Nichols Bay, were homogeneous (P=0.28), but were collectively divergent from interior Berners Bay and Lynn Canal collections.

Genetic distances and the resulting neighbor-joining tree generally mirrored the results in Tables 2 and 3, however, bootstrap support for the tree was weak. PWS grouped together in 60% of the resamplings, Berners08, Lynn08a, and Lynn08b grouped together 50% of the time, and all other branches grouped less than 50%.

Table 2

F_{ST} values estimated between sample pairs of Pacific herring (*Clupea pallasii*) in the eastern Gulf of Alaska (above diagonal). Below the diagonal are *P*-values from pseudo-exact homogeneity tests between collections. Significances based on 95% confidence intervals from permutation tests (bold) and after correction for multiple testing (asterisk) are indicated. Estimates within shaded area are comparisons between groups of spawning fish; individuals from all other sites were in nonspawning condition. *n*=the number of individuals in the sample. PWS=Prince William Sound.

	Berners Bay 2007 *n*=52	Berners Bay 2008 *n*=126	Berners Bay 2009 *n*=148	Hobart Bay 2008 *n*=128	Hoonah Sound 2008 *n*=100	Sitka Sound 2007 *n*=75	Sitka Sound 2008 *n*=131	Lynn Canal 2007 *n*=97	Lynn Canal 2008a *n*=98	Lynn Canal 2008b *n*=98	Nichols Bay 2007 *n*=97	Western PWS 2007 *n*=99	Eastern PWS 2007 *n*=92
Berners Bay 2007	—	0	0	0.004	0.0009	0.0002	0.0013	0.0008	0.0001	0	0.0018	0	0.0004
Berners Bay 2008	0.5186	—	0	0	**0.0009***	**0.0008**	**0.0004**	**0.0007**	0	0	0.0007	**0.0013**	**0.0003**
Berners Bay 2009	0.2853	0.1045	—	0.0007	**0.0004**	0.0002	**0**	0.0004	0	0	**0.0017***	0.0006	**0.0005**
Hobart Bay 2008	0.2276	**0.0287**	0.1564	—	**0.0009**	0.0002	0.0001	0.0006	0.0007	0	0	0.0015	0.0005
Hoonah Sound 2008	0.1056	**<0.0001***	**0.0027***	**0.0073***	—	0.0002	0.0006	**0.0014**	**0.0011**	**0.0019***	**0.0025**	**0.0010**	**0.0013***
Sitka Sound 2007	0.0567	**<0.0001***	**0.0044***	**0.0318**	0.0558	—	0.0001	0.0021	0.0014	0.0004	0.0012	0.0015	**0.0020**
Sitka Sound 2008	0.5448	**0.0052***	**0.0045***	0.3463	**0.0260**	0.4273	—	0	0.0009	0.0008	0.0011	**0.0012**	**0.0013**
Lynn Canal 2007	0.5566	**0.0063***	0.2992	0.2443	**0.0069***	**0.0050***	0.1494	—	0	0	**0.0015**	**0.0013**	**0.0001**
Lynn Canal 2008a	0.4297	0.5911	0.2555	0.3345	**0.0039***	**0.0370**	**0.0500**	0.4221	—	0	0.0009	0.0007	**0.0012**
Lynn Canal 2008b	0.7783	0.9922	0.2448	0.4537	**0.0004***	0.2216	0.3269	0.5837	0.9988	—	0.0006	0.0003	**0.0002**
Nichols Bay 2007	0.4599	0.1101	**<0.0001***	0.0889	**0.0001***	0.1423	0.2881	**0.0324**	0.2490	0.6419	—	0.0021	**0.0019**
Western PWS	0.5421	**0.0472**	0.1814	0.0536	**0.0076***	0.0859	**0.0466**	0.0742	0.5353	0.9099	0.1254	—	0.0012
Eastern PWS	0.3883	**0.0448**	0.1080	0.0663	**0.0006***	**0.0057***	**0.0151**	**0.0230**	**0.0058***	0.0896	**0.0008***	0.4830	—

Discussion

Genetic structure was evident among herring populations in the eastern Gulf of Alaska. Collections from the fjord system of Berners Bay and Lynn Canal were significantly differentiated from the outer coast collections (Sitka Sound). The level of differentiation was surprising given the small geographical separation of approximately 235 km between the two areas and the higher genetic connectivity typical among marine pelagic species such as herring. Spawning fish from three years of collection in Berners Bay and overwintering fish from Lynn Canal consistently grouped together, indicating these fish may be overwintering in Lynn Canal and spawning in Berners Bay. Early spring collections in Lynn Canal in 2008 (Lynn08a and Lynn08b) were particularly homogeneous with the spring spawning group in Berners Bay (Berners08). These three collections grouped together in the neighbor-joining tree and remained together more than 50% of the time in the consensus tree with both loci replacement and allele replacement bootstrapping methods. Hobart Bay, located several hundred km to the south of Berners Bay in the interior waters of Southeast Alaska, was not genetically distinct from either the fjord group of Berners Bay and Lynn Canal or outer-coastal Sitka Sound, indicating that either there is more extensive gene flow between these regions—Hobart Bay is an interior water body but located along the main waterway that bisects southeast Alaska—or that the sample size of the single collection at Hobart Bay (*n*=100) may not be large enough for detection of differentiation as statistical power decreases considerably if sample sizes are unbalanced (Goudet, 1996; Waples and Gaggiotti, 2006). Pacific herring from Hoonah Sound, however, were genetically distinct from herring in Berners Bay and Lynn Canal interior collections. Herring from this region also had a unique fatty acid signature differing from those at all other locations tested in Southeast Alaska (Otis[1]).

Results of our genetic study tend to verify previous morphological, tagging, and genetic studies that have indicated reduced gene flow among regions within Southeast Alas-

[1] Otis, T., R. Heintz, and J. Maselko. 2010. Investigation of Pacific herring (*Clupea pallasii*) stock structure in Alaska using otolith microchemistry and heart tissue fatty acid composition. Final Rept. submitted to EVOS-TC (*Exxon Valdez* Oil Spill Trustee Council). [Available at http://www/evostc.state.ak.us/Files.cfm?doc=/Store/FinalReports/2007-07769-Final.pdf]

Table 3

F_{ST} values for Pacific herring estimated between sample pairs from geographic regions in the eastern Gulf of Alaska (above diagonal). Below the diagonal are *P*-values from pseudo-exact homogeneity tests of allele frequencies between collections. Significance of tests, based on 95% confidence intervals from permutation tests before (bold) and after (asterisk) corrections for multiple tests are indicated. *n*=the number of individuals in the collection.

	Berners Bay–Lynn Canal *n*=619	Hobart Bay *n*=128	Hoonah Sound *n*=100	Sitka Sound *n*=206	Nichols Bay *n*=97	Prince William Sound *n*=191
Berners Bay–Lynn Canal	—	0.0004	**0.0011***	**0.0008***	**0.0013**	**0.0004***
Hobart Bay	0.1000	—	**0.0009**	0.0001	0	0.0007
Hoonah Sound	**<0.0001***	**0.0070**	—	0.0005	**0.0025**	**0.0009***
Sitka Sound	**<0.0001***	0.1600	**0.0100**	—	0.0011	**0.0011***
Nichols Bay	**0.0020***	0.0890	**0.0001***	0.2750	—	**0.0017**
Prince William Sound	**0.0010***	0.0500	**0.0001***	**0.0010***	**0.0020***	—

ka. McHugh (1954) points out that the expected broad latitudinal clines of morphological characters, such as vertebral counts and growth rates, differ sharply in some geographically adjacent areas within Southeast Alaska, despite similar environmental conditions affecting these phenotypes, and suggests that a degree of isolation may be responsible. Tagging studies corroborate these findings. Herring tagged in the Juneau area were not recovered in the Cape Ommaney reduction fishery on South Baranof Island (Rounsefell and Dahlgren, 1935); however, fish tagged in Sitka Sound and Craig (southern Prince of Wales Island near Nichols Bay) were both detected in this fishery and were interpreted as evidence of an extensive movement and intermingling between these two regions (Skud, 1963). Previous genetic studies indicate that outer-coastal herring from Southeast Alaska were not significantly different from the majority of spawning herring in British Columbia. That study indicated that herring spawning at heads of inlets or ends of fjords migrate relatively short distances to feed in the summer, whereas fish that spawn in exposed, coastal locations may migrate to the continental shelf to feed (Beacham et al., 2008).

Recent genetic studies of herring in the Northeast Pacific Ocean, have indicated that discrete populations exist in British Columbia (Beacham et al., 2008), and Puget Sound, Washington (Small et al., 2005), where some degree of geographic isolation or differences in spawning timing exist. The environments of outer-coastal areas in Southeast Alaska differ from those in interior waterways. This contrast may induce selective pressures on fjord/inland populations owing to selection effects of salinity and may effectively isolate these groups and lead to differentiation at neutral microsatellite loci through drift. A salinity of 21 to 22 ppt (parts per thousand) was reported for the interior waters of Berners Bay (Harris et al.[2]), compared to salinities of outer-coastal seawater. Outer-coastal water salinity is higher and directly affects vertebral counts (Schmidt, 1917). Isolating mechanisms have been associated with specific salinity conditions on spawning locations (Bekkevold et al., 2005), and one microsatellite locus, *Cpa112*, is known to be influenced by divergent selection associated with salinity in Atlantic herring (Andre et al., 2010). *Cpa112* does not appear to be under selection in Pacific herring in the Gulf of Alaska because our study showed this locus to be relatively homogeneous, significantly differentiating only Prince William from Hoonah Sound.

Spawning time for herring varies annually in response to temperature. In 2009, initial spawning occurred 15–16 April for Nichols Bay, directly followed by Sitka Sound, 18–20 April, and three weeks later, 11–12 May for Berners Bay (Pritchett and Hebert[3]). Spawning usually occurs in Berners Bay approximately three weeks later than in Sitka Sound because interior waters remain colder later into the season.

Spawn timing and age of fish can be important considerations for collection of samples for genetic analyses. Spawning waves, where older fish spawn first, followed by younger year classes in the ensuing weeks, have been identified in Atlantic herring (McPherson et al., 2003). In age-structured populations with overlapping generations, allele frequencies are predicted to differ among age classes because of "sweepstakes" recruitment, where a small number of spawners are disproportionately successful in reproducing offspring, compared with the massive number of spawners who fail to leave offspring (Jorde and Ryman, 1996). Age analysis conducted by Pritchett and Hebert[3] revealed that the largest age class of herring in Lynn Canal in 2008 was 6 years, and 8+ years in Sitka Sound. Fish in

[2] Harris, P. M., S. W. Johnson, L. G. Holland, A. D. Neff, J. F. Thedinga, and S. D. Rice. 2005. Hydrocarbons and fisheries habitat in Berners Bay, Alaska: Baseline monitoring associated with the Kensington Gold Mine. Alaska Fisheries Science Center Processed Report 2005–06, 44 p. Alaska Fisheries Science Center, NMFS, NOAA, Juneau, AK.

[3] Pritchett, M., and K. Hebert. 2008. 2009 report to the Alaska Board of Fisheries: Southeast Alaska–Yakutat herring fisheries. Fishery Management Report 08-65, 25 p. Alaska Department of Fish and Game, Anchorage, AK.

our collections from 2008 were about two years younger (on average 4.6 years for Berners Bay herring and 6 years for Sitka Sound herring) than those in the ADFG database for that year. Analysis by year class may be beneficial in future studies in order to examine allele frequencies by age and possible heterogeneity among year classes or spawning waves.

Genetic differences were significant between Southeast Alaska (collectively) and the two collections from Prince William Sound, although no inference about population structure within Prince William Sound is made here, because both of the collections comprised nonspawning fish obtained from a single year. Larger sample sizes and multiyear collections and the use of microsatellite markers may be useful for further genetic studies within Prince William Sound.

Large numbers of alleles at some of the microsatellites and the large effective population size of herring necessitate analysis of adequate numbers of samples to detect population structure. Accordingly, samples sizes were increased during the course of the present study, effectively increasing the power of the analyses. Results of earlier analyses after one and two years of sampling did not reveal significant genetic differences among collections in our study, and notably the number of alleles at several loci exceeded the number of individuals in a collection—an important consideration when using highly polymorphic markers. Low F_{ST} values might be expected because highly polymorphic loci negatively correlate with F_{ST} values (O'Reilly et al., 2004). Berners07 was generally homogeneous with all other collections in pairwise tests of differentiation (homogeneity and F_{ST}), possibly owing to small sample size, which reduces the reliability of the estimate.

Low F_{ST} values, weak bootstrap support for some of the branches of the neighbor-joining tree, and an AMOVA illustrating high genetic variation within individual samples, indicate that population structure among regional groups of herring in Southeast Alaska is detectable but weak. This inference would further indicate low-level or episodic gene flow among these regions.

Conclusion

In conclusion, Pacific herring from Berners Bay and over-wintering fish in Lynn Canal, in the archipelago of Southeast Alaska, were genetically divergent from the spawners along the outer coast of the eastern Gulf of Alaska. Lack of recovery of the Berners Bay population despite closure of the fisheries, may be due to spatial isolation and adaptation to local environmental conditions. Other potential causes for the lack of recovery may be increased predation from expanding populations of sea lions and humpback whales (Rice et al.[4]) or water disturbance in spawning areas and water pollution. Additional pressures on this stock could lead to substantial declines in Lynn Canal herring abundance and in the abundances of fish and marine mammals that forage on them.

Acknowledgments

We thank all who contributed samples: R. Brenner, D. Harris, S. Moffitt (ADFG); C. Gabriele (Glacier Bay National Park); S. Johnson, J. Thedinga, F. Sewall, A. Eller, and K. Cox (Alaska Fisheries Science Center-[AFSC]). We thank C. Marvin (AFSC), N. Rutecki, and L. Miller for their assistance in the laboratory. M. Canino, M. Carls, C. Kondzela, A. Moles, T. McCraney, J. Rice (AFSC), D. Tallmon (University of Alaska Fairbanks), Stew Grant (ADFG) and Jeff Olsen (United States Fish and Wildlife Service [USFWS]) for early reviews of the manuscript, R. Waples (Northwest Fisheries Science Center) and J. Maselko (AFSC) for technical assistance, and J. Hudson (USFWS) for aging fish.

Literature cited

Andre, C., L. C. Larsson, L. Laikre, D. Bekkevold, J. Brigham, G. R. Carvalho, T. G. Dahlgren, W. F. Hutchinson, S. Mariani, K. Mudde, D. E. Ruzzante, and N. Ryman.
2010. Detecting population structure in a high gene-flow species, Atlantic herring (*Clupea harengus*): direct, simultaneous evaluation of neutral vs. putatively selected loci. Heredity, doi:10.1038, 11 p.

Bakun, A.
2006. Wasp-waist populations and marine ecosystem dynamics: navigating the "predator pit" topographies. Prog. Oceanogr. 68:271–288.

Beacham, T. D., J. F. Schweigert, C. MacConnachie, K. D. Le, and L. Flostrand.
2008. Use of microsatellites to determine population structure and migration of Pacific herring in British Columbia and adjacent regions. Trans. Am. Fish. Soc. 137:1795–1811.

Bekkevold, D., C. Andre, T. G. Dahlgren, L. A. W. Clausen, E. Torstensen, H. Mosegaard, G. R. Carvalho, T. B. Christensen, E. Norlinder, and D. E. Ruzzante.
2005. Environmental correlates of population differentiation in Atlantic herring. Evolution 59:2656–2668.

Benjamini, Y., and D. Yekutieli.
2001. The control of the false discovery rate in multiple testing under dependency. Ann. Stat. 29:1165–1188.

Cavalli-Sforza, L. L., and A. W. Edwards.
1967. Phylogenetic analysis. Models and estimation procedures. Am. J. Human Genet. 19:233–257.

Excoffier, L. G. L., and S. Schneider.
2005. Arlequin version 3.5: An integrated software package for population genetics data analysis. Evol. Bioinformatics Online 1:47–50.

Felsenstein, J.
1989. PHYLIP—phylogeny inference package (vers. 3.2). Cladistics 5:164–166.

[4] Rice, S., R. Heintz, J. Moran, T. Quinn, and J. Straley. 2008. Significance of whale predation on natural mortality rate of Pacific herring in Prince William Sound. Annual Progress Report to the Exxon Valdez Oil Spill Trustee Council for Restoration Project 080804, 9 p. Alaska Fisheries Science Center, NMFS, NOAA, Juneau, AK. [Available at: http://www.evostc.state.ak.us/Projects/, accessed June 2011.]

Goudet, J.
1995. FSTAT: A computer program to calculate F-statistics. J. Heredity 86:485–486.
Goudet, J., M. Raymond, T. de Meeüs, and F. Rousset.
1996. Testing differentiation in diploid populations. Genetics 144:1933–1940.
Grant, W. S., and F. M. Utter.
1984. Biochemical population genetics of Pacific herring. Can. J. Fish. Aquat. Sci. 41:856–864.
Hart, J. L.
1973. Pacific fishes of Canada, 180 p. Fish. Res. Board Canada, Ottawa, Ontario.
Hourston, A. S. and C. W. Haegele.
1980. Herring on Canada's Pacific coast. Can. Spec. Publ. Fish. Aquat. Sci. 48:734–750.
Jorde, P. E., and N. Ryman
1996. Demographic genetics of brown trout (*Salmo trutta*) and estimation of effective population size from temporal change of allele frequencies. Genetics 143:1369–1381.
McHugh, J. L.
1954. Geographic variation in the Pacific herring. Copeia 1954:139–151.
McPherson, A. A., P. T. O'Reilly, T. L. McParland, M. W. Jones, and P. Bentzen.
2001. Isolation of nine novel tetranucleotide microsatellites in Atlantic herring (*Clupea harengus*). Mol. Ecol. Notes 1:31–32.
McPherson, A. A., R. L. Stephenson, and C. T. Taggart.
2003. Genetically different Atlantic herring (*Clupea harengus*) spawning waves. Mar. Ecol. Prog. Ser. 247:303–309.
Miller, K. M., K. Laberee, A. D. Schulze, and K. H. Kaukinen.
2001. Development of microsatellite loci in Pacific herring (*Clupea pallasi*). Mol. Ecol. Notes 1:131–132.
O'Connell, M., M. C. Dillon, and J. M. Wright
1998b. Development of primers for polymorphic microsatellite loci in the Pacific herring (*Clupea harengus pallasi*). Mol. Ecol. 7:358–360.
O'Connell, M., M. C. Dillon, J. M. Wright, P. Bentzen, S. Merkouris, and J. Seeb.
1998a. Genetic structuring among Alaskan Pacific herring populations identified using microsatellite variation. J. Fish Biol. 53:150–163.
Olsen, J. B., C. J. Lewis, E. J. Kretschmer, S. L. Wilson, and J. E. Seeb.
2002. Characterization of 14 tetranucleotide microsatellite loci derived from Pacific herring. Mol. Ecol. Notes 2:101–103.
O'Reilly, P. T., M. F. Canino, and K. M. Bailey.
2004. Inverse relationship between F_{ST} and microsatellite polymorphism in the marine fish, walleye pollock (*Theragra chalcogramma*): implications for resolving weak population structure. Mol. Ecol. 13:1799–1814.
Raymond, M., and F. Rousset.
1995. GENEPOP: population genetics software for exact tests and ecumenicism, vers. 1.2. J. Heredity 86:248–249.
Rounsefell, G., and H. Dahlgren.
1935. Races of herring, *Clupea pallasii*, in southeastern Alaska. U.S. Dept. Comm. Bull. Bureau of Fish. 17:119–141.
Schmidt, J.
1917. Racial investigations. I. *Zoarces viviparus* L. and local races of the same. Compt.-Rend. Lab, Carlsberg 13:279–397.
Shaklee, J. B., and P. Bentzen.
1998. Genetic identification of stocks of marine fish and shellfish. Bull. Mar. Sci. 62:589–621.
Skud, B. E.
1963. Herring tagging experiments in Southeastern Alaska. Fish. Bull. 63:19–32.
Slatkin, M.
1994. Linkage disequilibrium in growing and stable populations. Genetics 137:331–336.
Small, M. P., J. L. Loxterman, A. E. Frye, J. F. Von Bargen, C. Bowman, and S. F. Young.
2005. Temporal and spatial genetic structure among some Pacific herring populations in Puget Sound and the southern Strait of Georgia. Trans. Am. Fish. Soc. 134:1329–1341.
Van Oosterhout, C. H., W. F. Hutchinson, D. P. M. Wills, and P. F. Shipley.
2004. MICROCHECKER: Software for identifying and correcting genotyping errors in microsatellite data. Mol. Ecol. Notes 4: 535–538.
Waples, R. S.
1998. Separating the wheat from the chaff: patterns of genetic differentiation in high-gene flow species. Genetics 89:438–450.
Waples, R. S., and O. Gaggiotti.
2006. What is a population? An empirical evaluation of some genetic methods for identifying the number of gene pools and their degree of connectivity. Mol. Ecol. 15: 1419–1439.
Weir, B. S., and C. C. Cockerham.
1984. Estimating *F*-statistics for the analysis of population structure. Evolution 38:1358–1370.

Appendix

Statistical data on Gulf of Alaska Pacific herring (*Clupea pallasii*) by loci, including name of locus, GENEBANK accession number, allele size range and number of base pair (bp) repeats. Collection: 1=Berners Bay 07, 2=Berners Bay 08, 3=Berners Bay 09, 4=Lynn Canal 07, 5=Lynn Canal 08a, 6=Lynn Canal 08b, 7=Hobart Bay 07, 8=Hoonah Sound 08, 9=Sitka Sound 07, 10=Sitka Sound 08, 11=Nichols Bay 08, 12=west Prince William Sound, and 13=east Prince William Sound. Collection sizes (n), number of alleles (n_a), allele richness (a), observed heterozygosity (H_o), expected heterozygosity (H_e), effective number of alleles (n_{eff}), and estimated inbreeding coefficient (F_{is}). Total is n across all populations. All other values in the total column are an average across all collections.

Cha63	AF019987, allele size range 130–187, 2 bp repeats													
Collection	1	2	3	4	5	6	7	8	9	10	11	12	13	Total
n	49	126	136	98	95	97	128	100	72	131	97	99	92	1320
n_a	19	24	23	21	24	24	24	24	21	25	23	21	23	30
a	17.77	19.22	17.29	17.22	18.08	19.31	18.69	18.88	18.14	18.88	18.29	17.91	19.69	18.42
H_o	0.94	0.92	0.94	0.86	0.86	0.91	0.92	0.91	0.88	0.95	0.84	0.92	0.97	0.91
H_e	0.92	0.91	0.91	0.88	0.90	0.91	0.91	0.92	0.91	0.92	0.89	0.92	0.93	0.91
n_{eff}	12.50	11.11	11.11	8.33	10.00	11.11	11.11	12.50	11.11	12.50	9.09	12.50	14.29	11.33
F_{is}	−0.023	−0.009	−0.040	0.029	0.036	−0.002	−0.003	0.009	0.041	−0.029	−0.029	0.064	−0.004	−0.038

Cha1017	AF289096, allele size range 158–208, 4 bp repeats													
Collection	1	2	3	4	5	6	7	8	9	10	11	12	13	Total
n	52	126	148	98	96	96	128	100	75	131	97	99	91	1337
n_a	6	6	7	5	6	6	6	5	6	5	5	6	6	7
a	5.49	5.31	5.63	4.93	5.45	5.52	4.84	4.74	5.24	4.87	4.76	5.24	5.22	5.16
H_o	0.58	0.57	0.57	0.48	0.54	0.52	0.49	0.54	0.49	0.53	0.49	0.47	0.45	0.52
H_e	0.56	0.55	0.58	0.54	0.58	0.55	0.55	0.58	0.60	0.54	0.53	0.50	0.54	0.55
n_{eff}	2.27	2.22	2.38	2.17	2.38	2.22	2.22	2.38	2.50	2.17	2.13	2.00	2.17	2.25
F_{is}	−0.023	−0.031	0.015	0.109	0.065	0.060	0.101	0.063	0.174	0.005	0.005	0.076	0.046	0.167

Cha1020	AF289095, allele size range 130–239, 2 bp repeats													
Collection	1	2	3	4	5	6	7	8	9	10	11	12	13	Total
n	52	113	148	91	95	98	123	99	70	117	93	98	49	1246
n_a	17	28	33	28	27	26	30	22	23	28	23	28	18	43
a	15.29	18.57	19.03	17.98	18.36	18.05	18.38	15.63	17.16	17.74	15.25	19.15	16.37	17.80
H_o	0.73	0.84	0.83	0.85	0.88	0.82	0.84	0.86	0.87	0.80	0.75	0.88	0.90	0.83
H_e	0.79	0.83	0.81	0.81	0.84	0.85	0.83	0.82	0.83	0.81	0.79	0.85	0.84	0.82
n_{eff}	4.76	5.88	5.26	5.26	6.25	6.67	5.88	5.56	5.88	5.26	4.76	6.67	6.25	5.72
F_{is}	0.074	−0.016	−0.023	−0.041	−0.054	0.035	−0.011	−0.049	−0.050	0.012	0.012	0.048	−0.032	−0.074

Cpa4	AF309800, allele size range 111–195, 4 bp repeats													
Collection	1	2	3	4	5	6	7	8	9	10	11	12	13	Total
n	51	125	144	94	96	95	128	98	73	129	92	97	87	1309
n_a	15	16	18	17	18	17	17	18	17	18	16	18	16	22
a	13.99	13.66	14.37	14.58	14.26	14.53	14.15	14.57	14.62	15.33	14.65	15.23	14.25	14.48
H_o	0.90	0.88	0.92	0.95	0.91	0.88	0.91	0.87	0.95	0.89	0.90	0.96	0.94	0.91
H_e	0.91	0.89	0.90	0.91	0.90	0.90	0.91	0.90	0.90	0.92	0.92	0.91	0.91	0.90
n_{eff}	11.11	9.09	10.00	11.11	10.00	10.00	11.11	9.80	9.62	12.20	12.50	11.11	11.11	10.67
F_{is}	0.009	0.016	−0.021	−0.044	−0.008	0.018	−0.008	0.035	−0.055	0.029	0.029	0.016	−0.052	0.001

continued

Appendix (continued)

Cpa6		AF309801, allele size range 154–250, 4 bp repeats												
Collection	1	2	3	4	5	6	7	8	9	10	11	12	13	Total
n	50	124	145	94	91	98	123	99	75	126	81	98	92	1296
n_a	14	16	17	18	18	17	19	17	17	17	15	16	16	22
a	12.97	12.53	13.00	13.34	13.89	12.87	13.08	13.2	13.59	12.21	12.54	12.17	12.32	12.87
H_o	0.76	0.73	0.82	0.79	0.71	0.80	0.84	0.65	0.73	0.75	0.68	0.79	0.72	0.75
H_e	0.81	0.74	0.78	0.76	0.78	0.80	0.76	0.74	0.75	0.72	0.75	0.74	0.76	0.76
n_{eff}	5.26	3.85	4.76	3.85	4.76	5.00	4.17	3.82	4.07	3.60	4.00	3.82	4.17	4.24
F_{is}	0.009	0.008	−0.054	0.006	0.087	−0.001	−0.096	0.124	0.027	−0.033	−0.033	0.098	−0.058	0.054

Cpa27		AF309799, allele size range 89–199, 4 bp repeats												
Collection	1	2	3	4	5	6	7	8	9	10	11	12	13	Total
n	52	126	147	96	96	97	119	97	73	130	97	98	92	1320
n_a	12	13	13	13	15	14	13	14	15	16	16	11	13	26
a	10.75	10.08	10.86	10.19	11.58	10.32	9.46	10.94	10.85	11.14	11.72	9.90	10.58	10.75
H_o	0.71	0.84	0.84	0.79	0.78	0.74	0.74	0.85	0.85	0.74	0.70	0.81	0.71	0.78
H_e	0.81	0.82	0.83	0.81	0.84	0.79	0.76	0.83	0.81	0.81	0.76	0.83	0.80	0.81
n_{eff}	5.26	5.56	5.88	5.26	6.25	4.76	4.17	5.88	5.26	5.26	4.17	5.88	5.00	5.28
F_{is}	0.124	−0.022	−0.018	0.019	0.070	0.066	0.027	−0.013	−0.052	0.082	0.082	0.072	0.033	0.114

Cpa103		AF406939, allele size range 176–280, 4 bp repeats												
Collection	1	2	3	4	5	6	7	8	9	10	11	12	13	Total
n	51	124	147	98	97	98	127	100	74	131	97	98	91	1333
n_a	13	19	19	18	17	18	15	17	18	17	17	19	17	26
a	12.15	13.64	12.60	14.13	12.68	12.86	11.95	12.75	15.01	13.06	13.18	14.30	13.55	13.16
H_o	0.94	0.86	0.91	0.82	0.88	0.86	0.91	0.86	0.82	0.86	0.85	0.88	0.90	0.87
H_e	0.90	0.88	0.88	0.90	0.88	0.88	0.89	0.89	0.89	0.88	0.88	0.88	0.90	0.89
n_{eff}	10.00	8.33	8.33	10.00	8.33	8.33	9.09	9.09	9.09	8.33	8.33	8.33	10.00	8.89
F_{is}	−0.047	0.034	−0.035	0.094	0.002	0.024	−0.015	0.031	0.069	0.020	0.020	0.035	0.006	−0.003

Cpa107		AF309792, allele size range 100–172, 2 bp repeats												
Collection	1	2	3	4	5	6	7	8	9	10	11	12	13	Total
n	33	126	144	97	85	90	127	99	66	123	97	97	84	1268
n_a	18	25	24	21	22	24	25	25	19	23	20	24	22	31
a	18.00	18.27	16.93	15.96	16.59	17.81	17.65	18.16	14.57	17.29	14.52	18.57	18.07	17.55
H_o	0.94	0.89	0.87	0.84	0.89	0.93	0.91	0.89	0.89	0.84	0.89	0.91	0.94	0.89
H_e	0.90	0.91	0.91	0.90	0.91	0.91	0.91	0.92	0.88	0.91	0.89	0.92	0.93	0.91
n_{eff}	10.00	11.11	10.00	10.00	11.11	11.11	11.11	12.50	8.33	11.11	9.09	12.50	14.29	10.94
F_{is}	−0.044	0.019	0.041	0.073	0.013	0.004	0.001	0.032	−0.012	0.077	0.077	0.005	0.008	−0.013

continued

Appendix (continued)

Cpa108		AF406944, allele size range 227–277, 4 bp repeats												
Collection	1	2	3	4	5	6	7	8	9	10	11	12	13	Total
n	47	120	141	94	90	92	126	99	73	123	95	98	90	1288
n_a	9	9	12	10	11	9	12	11	8	13	10	11	9	13
a	8.02	7.76	9.20	8.49	9.46	7.57	9.54	8.77	7.10	8.42	7.41	8.04	6.68	8.38
H_o	0.79	0.73	0.72	0.64	0.68	0.75	0.75	0.78	0.78	0.72	0.75	0.73	0.68	0.73
H_e	0.71	0.73	0.73	0.70	0.72	0.71	0.74	0.75	0.74	0.72	0.71	0.71	0.68	0.72
n_{eff}	3.45	3.70	3.70	3.33	3.57	3.45	3.85	4.00	3.85	3.57	3.45	3.45	3.13	3.58
F_{is}	−0.112	0.000	0.005	0.091	0.061	−0.053	−0.015	−0.038	−0.054	0.012	0.012	−0.049	−0.042	0.004

Cpa111		AF406947, allele size range 162–342, 4 bp repeats												
Collection	1	2	3	4	5	6	7	8	9	10	11	12	13	Total
n	50	124	141	97	91	94	124	88	67	124	93	87	92	1272
n_a	19	20	19	19	20	21	19	20	19	19	21	19	23	27
a	17.84	17.08	16.58	16.99	17.89	17.81	17.02	16.75	17.47	16.77	18.45	17.04	18.97	17.29
H_o	0.88	0.92	0.92	0.94	0.97	0.95	0.92	0.82	0.96	0.94	0.96	0.92	0.99	0.93
H_e	0.93	0.93	0.92	0.93	0.93	0.93	0.93	0.92	0.93	0.93	0.93	0.93	0.93	0.93
n_{eff}	14.29	14.29	12.50	14.29	14.29	14.29	14.29	12.50	14.29	14.29	14.29	14.29	14.29	14.01
F_{is}	0.052	0.013	−0.001	−0.006	−0.040	−0.021	0.011	0.112	−0.029	−0.020	−0.020	−0.031	0.007	−0.059

Cpa112		AF406948, allele size range 244–472, 4 bp repeats												
Collection	1	2	3	4	5	6	7	8	9	10	11	12	13	Total
n	49	109	137	97	83	94	118	97	74	127	95	99	92	1271
n_a	26	35	32	30	32	34	33	36	35	36	35	38	32	64
a	22.10	24.94	23.02	22.79	23.98	24.61	24.02	24.09	26.02	23.66	23.51	25.12	22.50	23.92
H_o	0.88	0.95	0.99	0.96	0.86	0.93	0.93	0.96	0.91	0.96	0.93	0.95	0.96	0.94
H_e	0.93	0.95	0.95	0.95	0.95	0.95	0.95	0.95	0.95	0.94	0.94	0.95	0.94	0.95
n_{eff}	14.29	20.00	20.00	20.00	20.00	20.00	20.00	20.00	20.00	16.67	16.67	20.00	16.67	18.79
F_{is}	0.055	−0.005	−0.041	−0.011	0.099	0.025	0.020	−0.009	0.047	−0.020	−0.019	0.011	0.000	−0.013

Cpa113		AF406949, allele size range 109–209, 4 bp repeats												
Collection	1	2	3	4	5	6	7	8	9	10	11	12	13	Total
n	49	125	148	96	95	86	126	100	71	113	91	98	90	1288
n_a	18	18	18	20	19	17	17	17	17	18	17	16	16	23
a	16.79	15.13	15.57	17.07	15.90	14.75	14.86	15.59	15.07	15.05	15.15	14.80	14.56	15.36
H_o	0.86	0.90	0.87	0.90	0.92	0.92	0.93	0.92	0.92	0.93	0.96	0.93	0.84	0.91
H_e	0.93	0.91	0.92	0.92	0.92	0.92	0.92	0.92	0.90	0.91	0.92	0.91	0.89	0.92
n_{eff}	14.29	11.11	12.50	12.50	12.50	12.50	12.50	12.50	10.00	11.11	12.50	11.11	9.09	11.86
F_{is}	0.077	0.008	0.051	0.026	0.000	−0.004	−0.013	0.000	−0.016	−0.016	−0.016	−0.037	−0.016	0.056

continued

Appendix (continued)

Cpa114	AF406950, allele size range 196–292, 4 bp repeats													
Collection	1	2	3	4	5	6	7	8	9	10	11	12	13	Total
n	47	59	147	94	95	97	128	99	70	126	91	98	90	1241
n_a	16	16	18	18	17	18	17	17	15	17	18	18	16	24
a	14.37	14.74	13.24	12.97	13.76	14.46	13.28	14.35	12.82	13.19	13.93	14.67	13.54	13.70
H_o	0.83	0.97	0.89	0.82	0.91	0.89	0.88	0.90	0.91	0.89	0.88	0.90	0.94	0.89
H_e	0.90	0.90	0.89	0.88	0.90	0.90	0.88	0.88	0.89	0.88	0.90	0.89	0.90	0.89
n_{eff}	10.00	10.00	9.09	8.33	10.00	10.00	8.33	8.33	9.09	8.33	10.00	9.09	10.00	9.28
F_{is}	0.077	−0.069	0.002	0.063	−0.002	0.019	−0.003	−0.016	−0.026	−0.013	−0.013	0.019	−0.004	−0.054

Cpa125	AF309796, allele size range 207–325, 2 bp repeats													
Collection	1	2	3	4	5	6	7	8	9	10	11	12	13	Total
n	45	121	148	94	94	96	123	100	69	127	97	99	76	1289
n_a	28	31	37	35	36	33	37	32	29	34	32	33	35	47
a	25.33	23.10	25.30	25.42	25.80	25.74	26.02	23.74	21.75	25.08	22.87	25.48	26.36	25.15
H_o	0.96	0.97	0.95	0.96	0.92	0.95	0.94	0.93	0.97	0.96	0.94	0.94	0.95	0.95
H_e	0.96	0.95	0.95	0.95	0.95	0.96	0.96	0.94	0.94	0.95	0.94	0.96	0.96	0.95
n_{eff}	25.00	20.00	20.00	20.00	20.00	25.00	25.00	16.67	16.67	20.00	16.67	25.00	25.00	21.15
F_{is}	0.001	−0.020	0.002	−0.007	0.040	0.008	0.013	0.015	−0.035	−0.010	−0.010	0.005	0.020	0.009

Cpa134	AF309798, allele size range 119–255, 2 bp repeats													
Collection	1	2	3	4	5	6	7	8	9	10	11	12	13	Total
n	52	125	140	92	88	98	125	100	64	125	96	99	91	1295
n_a	20	30	29	27	22	27	27	29	21	26	27	29	29	57
a	17.06	18.12	18.60	18.07	15.77	17.54	17.46	19.27	16.38	15.90	17.62	18.22	18.88	17.90
H_o	0.92	0.90	0.91	0.92	0.93	0.94	0.92	0.93	0.86	0.88	0.94	0.89	0.97	0.92
H_e	0.91	0.92	0.91	0.92	0.90	0.92	0.92	0.92	0.91	0.91	0.91	0.91	0.93	0.92
n_{eff}	11.11	12.50	11.11	12.50	10.00	12.50	12.50	12.50	11.11	11.11	11.11	11.11	14.29	11.80
F_{is}	−0.015	0.027	0.008	−0.009	−0.032	−0.024	0.000	−0.010	0.057	0.032	0.032	−0.026	0.027	−0.042

Analysis of permanent magnets as elasmobranch bycatch reduction devices in hook-and-line and longline trials

Craig P. O'Connell (contact author)[1,2,3]
Daniel C. Abel[2]
Eric M. Stroud[3]
Patrick H. Rice[3,4]

Email address for contact author: coconnell2@umassd.edu

[1] Present address for contact author: School of Marine Science and Technology
University of Massachusetts Dartmouth
New Bedford, Massachusetts 02740

[2] Coastal Marine and Wetlands Studies
Coastal Carolina University
Conway, South Carolina 29526

[3] SharkDefense Technologies, LLC
P.O. Box 2593
Oak Ridge, New Jersey 07438

[4] Florida Keys Community College
5901 College Drive
Key West, Florida 33040

Abstract—Previous studies indicate that elasmobranch fishes (sharks, skates and rays) detect the Earth's geomagnetic field by indirect magnetoreception through electromagnetic induction, using their ampullae of Lorenzini. Applying this concept, we evaluated the capture of elasmobranchs in the presence of permanent magnets in hook-and-line and inshore longline fishing experiments. Hooks with neodymium-iron-boron magnets significantly reduced the capture of elasmobranchs overall in comparison with control and procedural control hooks in the hook-and-line experiment. Catches of Atlantic sharpnose shark (*Rhizoprionodon terraenovae*) and smooth dogfish (*Mustelus canis*) were significantly reduced with magnetic hook-and-line treatments, whereas catches of spiny dogfish (*Squalus acanthias*) and clearnose skate (*Raja eglanteria*) were not. Longline hooks with barium-ferrite magnets significantly reduced total elasmobranch capture when compared with control hooks. In the longline study, capture of blacktip sharks (*Carcharhinus limbatus*) and southern stingrays (*Dasyatis americana*) was reduced on magnetic hooks, whereas capture of sandbar shark (*Carcharhinus plumbeus*) was not affected. Teleosts, such as red drum (*Sciaenops ocellatus*), Atlantic croaker (*Micropogonias undulatus*), oyster toadfish (*Opsanus tau*), black sea bass (*Centropristis striata*), and the bluefish (*Pomatomas saltatrix*), showed no hook preference in either hook-and-line or longline studies. These results indicate that permanent magnets, although eliciting species-specific capture trends, warrant further investigation in commercial longline and recreational fisheries, where bycatch mortality is a leading contributor to declines in elasmobranch populations.

Manuscript submitted 14 April 2011.
Manuscript accepted 5 July 2011.
Fish. Bull. 109:394–401 (2011).

Elasmobranch (sharks, skates, and rays) populations are being subjected to large-scale anthropogenic mortality, resulting in significant population declines of numerous species (Musick et al., 1993; Stevens et al., 2000; Baum and Myers, 2004). Directed commercial fisheries for shark meat and fins, combined with substantial bycatch, are thought to be the main cause of elasmobranch mortality (Bonfil, 1994; McKinnell and Seki, 1998; Megalofonou et al., 2005; Poisson, 2011). Furthermore, recreational impact is increasing as charter boats have redirected their efforts to shark fishing to compensate for the lack of teleost targets such as tuna, marlin, and snapper (Anderson, 1990; Musick et al., 1993; NMFS[1]). The decline of several elasmobranch populations is particularly significant because these animals are K-selected species, and therefore populations do not rebound quickly with changes in management practices (Smith et al., 1998).

One strategy for managing shark fisheries and reducing bycatch is to employ repellents that selectively repel elasmobranchs but do not repel target species. A promising line of research involves the use of permanent magnets to create an abnormally strong electrical stimulus to overwhelm the acute electrosensory system of elasmobranchs and thus repel them (Rigg et al., 2009; O'Connell et al., 2010, 2011). This electrosensory system, comprising many individual ampullae of Lorenzini, is used to detect minute electrical impulses for detection of prey and may also provide geolocation information (Murray, 1962; Kalmijn, 1982; Klimley, 2002).

In laboratory trials, Rigg et al. (2009) evaluated the effects of permanent magnets on five elasmobranch bycatch species: scalloped hammerhead (*Sphyrna lewini*); Australian blacktip shark (*Carcharhinus tilstoni*); gray reef shark (*C. amblyrhynchos*); milk shark (*Rhizoprionodon acutus*); and the speartooth shark (*Glyphis glyphis*); as well as the barramundi (*Lates calcarifer*), a teleost.

[1] NMFS (National Marine Fisheries Service). 1991. Draft Secretarial shark fishery management plan for the Atlantic Ocean (19 April 1991), 127 p. U.S. Dep. Commer. NOAA, NMFS, Southeast Regional Center, St. Petersburg, FL.

This study showed that ferrite magnets induced behavioral responses in all the tested elasmobranchs and that permanent magnets may be able to reduce elasmobranch bycatch. Similarly, O'Connell et al. (2010, 2011) showed that permanent magnets are effective elasmobranch-selective repellents in field and controlled laboratory experiments involving tests with magnets and procedural controls on baited apparatuses. Robbins et al. (2011) concluded that magnetic deterrents in the form of rare-earth magnetic discs have high potential for reducing the bycatch of shark species that occur in low densities, but their use in repelling shark species that occur in high densities, such as the Galapagos shark (*Carcharhinus galapagensis*), was concluded to be minimal.

In addition to magnetic repellents, electropositive metal (EPM) repellents have also been explored for their ability to overstimulate the electrosensory system of an approaching shark (Rice, 2008; Stoner and Kaimmer, 2008). In both laboratory and field studies, EPMs were shown to repel juvenile sandbar sharks (*Carcharhinus plumbeus;* Brill et al., 2009). In laboratory studies, the duration of the EPM repellency was short lived (~three minutes), a phenomenon attributed to competitive interactions among the sharks. In field trials, there was a 62% decrease in the capture of *C. plumbeus* with EPM hook treatments. Additionally, electropositive metals have been shown to deter spiny dogfish sharks (*Squalus acanthias*) from baits in both laboratory (Stoner and Kaimmer, 2008) and field experiments (Kaimmer and Stoner, 2008). Although Kaimmer and Stoner (2008) showed that the capture of *S. acanthias* was reduced by 19% on hooks containing EPMs in the Pacific halibut (*Hippoglossus stenolepis*) commercial fishery, Tallack and Mandelman (2009) conducted both laboratory and field experiments in the Northwest Atlantic, producing contradictory results. The reasoning for the contrasting findings is unclear.

In the present study, we explore the effectiveness of two different permanent magnets on hooks as elasmobranch repellents. We hypothesize that the capture of elasmobranchs would be reduced with hooks containing magnets in comparison with control hooks in hook-and-line and longline studies. Additionally, we further hypothesize that the presence of permanent magnets on hooks would not alter teleost capture because teleosts lack the ampullary organ.

Methods

Longline study

For the present study we employed grade N52 neodymium-iron-boron cylinder magnets on 30 longline sets and grade C8 barium-ferrite permanent cylinder magnets on 54 sets in North Inlet and Winyah Bay, Georgetown County, South Carolina, between April and September 2008. North Inlet (33°19′N, 79°10′W) is a tidally dominated, well-mixed estuary comprising 32 km^2 of mudflats, oyster reefs, tidal creeks, and salt marshes dominated by *Spartina alterniflora* (Dame et al., 1986). It has a mean tidal depth of 2.5 m. Winyah Bay (33°12′N, 79°11′W) is a partially mixed estuary during periods of low to moderate river discharges, and a salt wedge estuary during higher flows. Winyah Bay averages about four meters in depth and has various substrate types: mud, sand, silt, and clay (Patchineelam et al., 1999).

Longlines consisted of a 150-m tar-coated nylon mainline with 24 evenly spaced gangions (branches), each with a single hook. Gangions consisted of 0.75 meters of 317.5-kg 49-strand stainless cable and 0.75 meters of 226.8-kg monofilament line and were attached to the mainline with tuna clips. The hooks were 16/0 Mustad® 3996 open-eye circle hooks and were baited with Atlantic mackerel (*Scomber scombrus*).

The magnetic flux of the longline treatments, with 2.5-cm diameter, 85-g neodymium-iron-boron ($Nd_2Fe_{14}B$) and a 2.5-cm diameter, 85-g grade C8 barium-ferrite ($BaFe_{12}O_{19}$) permanent magnets, was measured with a model 4048 teslameter and a transverse probe, model T-4048-001 (F. W. Bell, Milwaukie, Oregon). The former produced a maximum flux of approximately 14,800 gauss at the surface and were polarized through the diameter. The latter were similar in shape to the neodymium-iron-boron cylinder magnets but were polarized through the height and produced a maximum flux of approximately 3850 gauss at their surface. Before experimentation, the axis of polarization was not assumed to be a contributing factor to repellent effectiveness, which is why the axes differed between magnets.

An alternating experimental design consisted of magnetic gangions (treatment) and control (sham-magnet) gangions that were characterized by having an 85-g lead weight similar in appearance to the magnet (Fig. 1, A and B). Magnet-type (i.e., neodymium-iron-boron or barium-ferrite) was consistent for each longline set. Of critical importance was that treatment and control gangions remained separated throughout the study to prevent the magnetization of the control gangions. Magnets were attached to hooks during deployment and removed during retrieval. Also, to prevent the magnetization of control gangions for subsequent trials, the tuna clips on the magnetic treatment gangions were marked, allowing us to properly separate the control and magnetic treatment gangions when not in use.

Longlines were deployed several times each week during slack tides (for safety and to avoid gear tangling) in daylight (between 0800–1700 h) for one hour. Each longline was set in a double-drape configuration with the use of a polyform buoy attached midway on the mainline. With this configuration, approximately 50% of the hooks (i.e., 12 hooks) rested on the substrate, while the remaining hooks were suspended in the water column.

During longline retrieval, teleost and elasmobranch fishes were identified to species, counted, measured (precaudal length [PCL], fork length [FL], total length [TL], stretch total length [STL]), elasmobranch sex was determined, and treatment type noted.

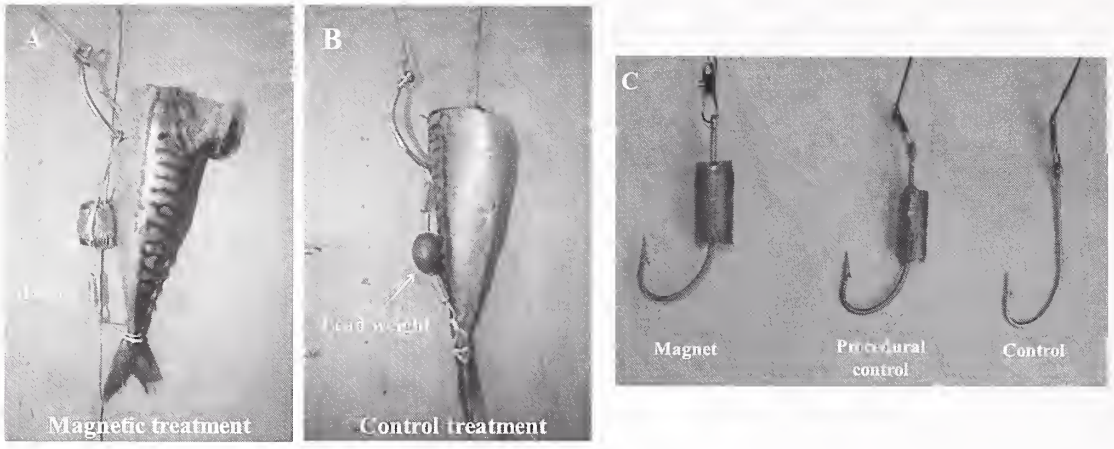

Figure 1

Hook treatments used in the longline and hook-and-line experiments to examine the deterrent effects of permanent magnets on elasmobranchs. (**A**) Configuration of the magnetic treatment used on experimental longlines, (**B**) configuration of the control treatment used on experimental longlines, and (**C**) the magnetic, procedural control, and control treatments used for the recreational fishing experiment.

Hook-and-line study

The hook-and-line fishing experiment was conducted off Springmaid Pier (33°39′N, 78°54′W) in Myrtle Beach, South Carolina, between January 2008 and April 2009. Three medium-action rods and reel combinations were used in each trial. Rods were equipped with Penn Captiva CLL4000 reels with 9.07-kg-test monofilament line, 0.30-m steel leader, and egg-shaped sinkers weighing between 85 and 142 g.

Because elasmobranch fauna varied with water temperature, 6/0 hooks baited with pink shrimp (*Penaeus* spp.), squid (*Loligo* spp.), or freshly caught pinfish (*Lagodon rhomboides*) were used during warmer months (April–October; mean sea surface temperature 24°C), and 2/0 hooks baited with 50 g pieces of Atlantic menhaden (*Brevoortia tyrannus*) were used in colder months (December–March; mean sea surface temperature 11°C).

At equally spaced locations along the pier, the rods were randomly arranged. Lines were cast, fished for fifteen minutes, and then retrieved. Each trial consisted of three hook treatments: 1) control, 2) procedural control (sham magnet), and 3) magnetic treatment (Fig. 1C). The control consisted of an untreated hook (i.e., no addition to the shank). The procedural control contained a lead weight of similar dimensions to those in the magnetic treatment and was attached to the hook shank with duct tape. The magnetic treatment contained a neodymium-iron-boron tube magnet (12-mm outer diameter, 5.5-mm inner diameter, and 25-mm height), magnetized through the height, and attached with duct tape to the shank of a hook. If any bait was removed or tampered with, all three treatments were rebaited with fresh bait of identical species. If a fish was found on any of the three lines, the remaining two lines were retrieved so that all three lines were in the water for the same duration. When a fish was caught, it was identified, measured (PCL, FL, TL, STL), the sex of elasmobranchs was determined, and treatment type was noted. Once the fish was de-hooked, all three lines were redeployed for the remaining minutes of the trial. Fishing occurred irrespective of tides and day or night.

Statistical analysis

For both the hook-and-line and longline experiments, total elasmobranch and teleost catches were analyzed separately. For the longline study, an individual chi-square analysis was used to compare the effectiveness of magnet type compared to the control. Also, a chi-square analysis was conducted on individual species if more than five individuals were caught during one treatment.

For the hook-and-line study, a chi-square analysis was conducted to compare control and procedural control hook data in order to determine whether the presence of an object (sham-magnet) on a hook altered fish capture. If no statistical difference was observed, further analysis was conducted on catches of control versus magnetic treatments. As with longline analyses, if more than five individuals from one species were captured during one treatment, a chi-square analysis was conducted for that species to determine species-specific trends.

Results

Longline: neodymium-iron-boron magnets

Five species of elasmobranchs were captured on longlines during the neodymium-iron-boron magnetic trials

Table 1

Elasmobranch catch composition from longline gear with neodymium-iron-boron magnets in 30 sets. No significant differences were found between control and magnetic treatments for any of the species or all species combined.

Species	*n*	No. of control treatments	No. of magnet treatments
Rhizoprionodon terraenovae	15	7	8
Carcharhinus limbatus	6	3	3
Carcharhinus plumbeus	4	2	2
Dasyatis americana	4	1	3
Negaprion brevirostris	1	0	1
Total elasmobranchs	30	13	17

Table 2

Elasmobranch catch composition from longline gear with barium-ferrite magnets in 54 sets. Asterisks indicate significant ($P<0.005$) differences between control and magnetic treatments in chi-square analyses.

Species	*n*	Control	Magnets
*Dasyatis americana**	11	9	2
*Carcharhinus limbatus**	11	9	2
Carcharhinus plumbeus	7	2	5
Negaprion brevirostris	2	2	0
Carcharhinus acronotus	2	0	2
Sphyrna tiburo	1	1	0
Total elasmobranchs*	34	23	11
Total teleosts	4	2	2

(n=30 sets): Atlantic sharpnose shark (*Rhizoprionodon terraenovae*), blacktip shark (*Carcharhinus limbatus*), sandbar shark (*Carcharhinus plumbeus*), southern stingray (*Dasyatis americana*), and lemon shark (*Negaprion brevirostris*). Total capture between magnetic and control treatments was not significant (χ^2=0.533, P=0.4652), nor was there a significant difference in catch for *R. terraenovae* (χ^2=0.067, P=0.7963), the only species for which sufficient catch allowed analysis by species (Table 1). No teleosts were caught on any hooks.

Longline: barium-ferrite permanent magnets

Seven different species were captured during the barium-ferrite permanent magnetic trials (n=54 sets): *C. limbatus*, *D. americana*, *C. plumbeus*, *N. brevirostris*, bonnethead shark (*Sphyrna tiburo*), blacknose shark (*Carcharhinus acronotus*), and one teleost—red drum (*Sciaenops ocellatus*). Elasmobranch catch with the use of barium-ferrite permanent magnets was significantly lower than the catch with controls (χ^2=4.235, P=0.0396). Among individual species with sufficient numbers to analyze, catches of *D. americana* and *C. limbatus* were significantly greater on control hooks than on magnetic treatment hooks (χ^2=4.455, P=0.0348). There was no difference in the catch of *C. plumbeus* (χ^2=1.286, P=0.257; Table 2).

Hook-and-line

Six elasmobranch species were captured by hook-and-line: *R. terraenovae,* spiny dogfish (*Squalus acanthias*), smooth dogfish (*Mustelus canis*), clearnose skate (*R. eglanteria*), *C. limbatus,* and scalloped hammerhead (*Sphyrna lewini*).

For all species combined, there was no statistical significance in capture found between control and procedural control hooks: *R. terraenovae* (χ^2=0.419, P=0.5175); *S. acanthias* (χ^2=0.019, P=0.8907); *M. canis* (χ^2=0.222, P=0.6374); *R. eglanteria* (χ^2=0.2860, P=0.5930); *C. limbatus* (χ^2=1.000, P=0.3173); and *S. lewini* (χ^2=0.000, P=1.000). Therefore, direct comparison between combined control and magnetic treatments was statistically warranted.

Table 3

Elasmobranch catch composition from hook-and-line gear with neodymium-iron-boron magnets in 660 trials. Procedural control data were not included because no significant difference in catch for control and procedural control treatments was observed. Asterisks indicate significant ($P<0.005$) differences between control and magnetic treatments in chi-square analysis.

Species	*n*	Control	Magnets
*Rhizoprionodon terraenovae**	169	67	30
*Mustelus canis**	21	10	1
Squalus acanthias	85	31	23
Raja eglanteria	16	6	3
Carcharhinus limbatus	7	4	0
Sphyrna lewini	2	1	0
Total elasmobranchs*	147	119	57
Total teleosts	16	6	5

Compared with control hooks, neodymium-iron-boron magnets significantly reduced elasmobranch capture (χ^2= 21.841, P=0.0001; Table 3). The capture of both *R. terraenovae* and *M. canis* was significantly reduced by magnets (*M. canis:* χ^2=7.364, P=0.0067; *R. terraenovae:* χ^2=14.113, P=0.0002). *Squalus acanthias* and *R. eglanteria* catch was not significantly different between control and magnet treatments (*S. acanthias*: χ^2=1.185, P=0.2763; *R. eglanteria*: χ^2=1.000, P=0.3173). Low *C. limbatus* and *S. lewini* catch did not allow experimental

analysis. Four species of teleost fishes were captured: Atlantic croaker (*Micropogonias undulatus: control (C)=3, procedural control (PC)=2, magnet (M)=1), oyster toadfish (Opsanus tau: C=1, PC=2, M=2), black sea bass (Centropristis striata: C=0, PC=0, M=1)*, and the bluefish (*Pomatomus saltatrix*: C=2, PC=1, M=1). There was no significant difference in the total number of teleost fish captured between control and procedural control treatments (χ^2=0.077, P=0.7815) nor between control and magnetic treatments (χ^2=0.077, P=0.7815; Table 3).

Discussion

Magnets were associated with a species-specific catch in elasmobranchs in both longline and hook-and-line studies. Longline hooks treated with neodymium-iron-boron magnets had no effect on any captured elasmobranchs (Table 1). Longline hooks with barium-ferrite permanent magnets produced a reduction in capture of *C. limbatus* and *D. americana,* whereas all other species were either not affected or were data-deficient (Table 2). In the hook-and-line study, neodymium-iron-boron magnets reduced the capture of two species, *R. terraenovae* and *M. canis,* compared with controls and procedural controls (Table 3). Teleost species were captured in both experiments and capture rate did not vary with treatment type.

Longline study

Barium-ferrite magnets repelled elasmobranchs, whereas neodymium-iron-boron magnets did not. Neodymium-iron-boron magnets ($Nd_2Fe_{14}B$) contain neodymium from the lanthanide group of elements, as well as iron (a ferromagnet) and boron. The neodymium-iron-boron magnets (grade N52) used in our study produced a maximum flux of 14,800 gauss at their surface. Barium-ferrite permanent magnets ($BaFe_{12}O_{19}$: grade C8) are also alloys with a solidified structure and produce a maximum flux of 3850 gauss at their surface.

A species-specific difference in catch was observed when using barium-ferrite magnets. Capture of *C. limbatus* and *D. americana* was significantly associated with control hooks; however, capture of *C. plumbeus* was not affected. Species-specific differences may be due to morphological (i.e., ampullary pore density or canal depth) or behavior (i.e., foraging strategy) (see additional discussion below). Because *D. americana* is a benthic elasmobranch whose vision is not the primary sense in locating buried prey (Raschi, 1986; Jordan, 2008; Jordan et al., 2009), especially in the turbid waters of our study sites, we hypothesize that *D. americana* may rely more heavily on electroreception, and therefore the strong induced current produced by the barium-ferrite magnets elicited a repellent response. O'Connell et al. (2010) conducted a study which examined the effects of grade C8 barium-ferrite permanent magnets, identical to the magnets used in the present longline study, on *D. americana* and found that the feeding response of this species was highly correlated with procedural control and control regions, and there were significantly greater quantities of avoidance behaviors toward the magnetic regions. Similarly, Rigg et al. (2009) showed that ferrite magnets induce repellent responses in five elasmobranch species, *S. lewini*, *C. tilstoni*, *C. amblyrhynchos*, *R. acutus*, and *G. glyphis*. These findings support the results obtained from field trials in the present study.

In addition to these results, it is unclear why *C. limbatus* catch was significantly associated with control hooks and *C. plumbeus* catch was not. One possible explanation for this result may be animal size and maturity. The size of the animal is directly correlated to ampullary canal length, resulting in differing electroreception capabilities (Sisneros et al., 1998; Sisneros and Tricas, 2002). Studies show that as the Atlantic stingray (*Dasyatis sabina*) and clearnose skate (*Raja eglanteria*) mature there is a gain of electrosensory primary afferents and, presumably, neural sensitivity (Sisneros et al., 1998; Sisneros and Tricas, 2002). More specifically, the neural sensitivity of *R. eglanteria* was five times greater in juveniles and eight times greater in adults than in embryos, (Sisneros et al., 1998). Similarly, in *D. sabina,* the neural sensitivity is three times greater in juveniles and four times greater in adults than in embryos (Sisneros and Tricas, 2002). All *C. plumbeus* captured in this experiment were juveniles (Sminkey and Musick, 1995), whereas all *C. limbatus* were adults (Killam and Parsons, 1989). It is possible that in the case of these two species, maturity was an important characteristic in determining the success of magnetic repellents and therefore could also explain why magnets successfully repelled *D. americana*, which were all adults. Intraspecific comparisons between animal maturity and repellent success could not be made because only one size class per species being was present in the catch; therefore we could not accurately conclude whether or not animal maturity reflects the effectiveness of the magnets as repellents.

Supporting our *C. plumbeus* findings, Brill et al. (2009) found that juvenile *C. plumbeus* catch was significantly reduced with the use of electropositive metals on longline hooks; however, preliminary laboratory investigations have demonstrated that juvenile *C. plumbeus* quickly habituate to magnetic stimulation (R. Brill, personal commun.[2])—a finding that serves as a possible explanation for the observed *C. plumbeus* results in our study. Lastly, differences in *C. plumbeus* and *C. limbatus* results may be an artifact of small sample size.

Hook-and-line study

Neodymium-iron-boron magnets polarized through the longitudinal axis repelled *M. canis* and *R. terraenovae*

[2] Brill, Richard. 2009. Virginia Institute of Marine Science, PO Box 1346, Gloucester Point, Virginia, 23062.

during the hook-and-line experiment. Other species of elasmobranchs did not show any significant responses to the magnetic treatment hook (*S. acanthias* and *R. eglanteria*) or were data deficient (*C. limbatus* and *S. lewini*).

The ineffectiveness of electrosensory stimuli on *S. acanthias* is supported by the results of Tallack and Mandelman (2009), who reported that the effectiveness of electrosensory stimuli was reduced owing to a high level of food deprivation (four days) for captive *S. acanthias*. Moreover, electrosensory stimuli had no affect in field studies involving this species. Because *S. acanthias* is found in dense schools, it is possible that the ineffectiveness of the magnetic stimuli in our experiment was due to factors such as social-facilitation (Guttridge et al., 2009). In teleosts fishes, social facilitation due to increasing group size increased intraspecific feeding activity (Major, 1978; Ryer and Olla, 1991); therefore these findings may correlate with our results for *S. acanthias* and indicate that high shark densities may influence conspecific feeding activity. Additionally, because *S. acanthias* may be found in dense schools, it is possible that the ineffectiveness of the electrosensory stimuli was due to the abundance of conspecific behavior and competition which simply overrode the electrosensory stimulation induced by the magnets. High densities of elasmobranchs have been previously postulated as a potential explanation for repellent ineffectiveness (Kaimmer and Stoner, 2008; Robbins et al., 2011) and therefore may explain our *S. acanthias* results.

Contrasting with *S. acanthias*, *M. canis* responded very differently to the treatment hooks and catch was significantly associated with control hooks. Kalmijn (1982) showed that *M. canis* was highly electroreceptive and oriented itself toward or bit electrodes, which mimicked the bioelectric fields produced by prey. An explanation for our findings may be that a stronger, induced voltage produced by an electrosensory stimulus, such as a barium-ferrite magnet, may repel *M. canis*.

Unlike our hypothesis above for *C. plumbeus* catch on longlines, the relationship between catch and animal size or ampullary canal length is weak and therefore cannot be used to explain catch in the hook-and-line study. For *M. canis,* ampullary canal length as a result of stage of maturity may explain the hook-and-line results because catch was significantly higher in controls and all animals were adults (Conrath et al., 2002); however, other examples of catch trends between an animal's maturity and magnetic effectiveness do not exist. For example, all *S. acanthias* were mature adults (Hammock et al., 1985), yet no significant trends in catch existed. Also, although catch of *R. terraenovae* was significantly higher for control hooks, catch was mixed between juvenile and adults (Parsons, 1985) and no distinct catch relationship was observed between control and treatment hooks, therefore minimizing the potential of animal maturity as a pertinent indicator of the effectiveness of the repellents.

Longline vs. hook-and line

Differences in catch rates for longlines and hooks-and-lines may be due to species-specific responses, as we discuss above. Additionally differences in magnetic characteristics, namely the axis of polarization, may have led to significant catch trends. Neodymium-iron-boron magnets used on longlines were polarized through the diameter, whereas barium-ferrite magnets and the hook-and-line neodymium-iron-boron magnets were polarized through a longitudinal axis (height)—a part of the experimental design that we initially overlooked. Because the longline neodymium-iron-boron magnets were placed approximately six centimeters away from the hook, the measurable magnetic field did not fully protect the bait, (peaks in magnetic flux occurred side to side instead of surface-to-substrate), whereas in the barium-ferrite magnets and hook-and-line neodymium-iron-boron magnets, the magnetic field covered the entire bait and hook, which may have been sufficient to deter elasmobranchs from feeding on the baited hooks.

Deployment methods may also be a possible explanation for these experimental differences. Because longlines are immersed (i.e., soaked) for longer time intervals, it is possible that elasmobranchs attracted by the bait were initially repelled but lingered owing to the continuous scent emanating from the bait. In this situation it is possible that sensory habituation to the magnetic field may have occurred, rendering the magnets less effective. Numerous studies have demonstrated that habituation is a common phenomenon in organisms subjected to repeated sensory stimulation (Myrberg et al., 1969; Myrberg et al., 1978; Givois and Pollack, 2000). Moreover, in a previous study, lemon sharks (*Negaprion brevirostris*) repeatedly exposed to a magnetic stimulus reacted at first but became unresponsive after several exposures (O'Connell et al., 2011). However, if repeated exposure to magnets during longline experiments resulted in sensory habituation with the use of neodymium-iron-boron magnets, this explanation is not supported by results with the use of barium-ferrite magnets, where there was significantly less elasmobranch catch on magnetic treatment hooks during the longline experiments.

Conclusion

In conclusion, magnets used as elasmobranch-selective repellents during both the longlining and hook-and-line fishing experiments produced positive result. Although the effectiveness of magnets may be influenced by animal density (Kaimmer and Stoner, 2008; Robbins et al., 2011) and by the level of satiation (Tallack and Mandelman, 2009), we found that magnetic polarization may effectively "protect" fish hooks and reduce unwanted elasmobranch capture in commercial and recreational fishing. Although promising, these results warrant further investigation before recommendations can be made to fishery managers and policy makers.

Acknowledgments

We thank Coastal Carolina University and the Georgetown County Environmental Protection Society for providing us with the RV *Brooks McIntyre*. Additionally, we acknowledge the National Science Foundation GK-12 Grant, Professional Association of Diving Instructors Foundation, and the Slocum-Lunz Foundation for providing us with additional funds. We also thank S. Gilman and K. Walters for their insightful comments on the manuscript. Lastly, we thank N. Simuro, M. K. Maxwell, M. Evans, R. Kercher, S. Pratt, B. Fishman, S. George, D. Young, C. Smith, J. Hord, J. Stevens, and many other volunteers who assisted us.

Literature cited

Anderson, E. D.
1990. Estimates of large shark catches in the Western Atlantic and Gulf of Mexico, 1960–1986. NOAA Tech. Rep. NMFS 90, 518 p.

Baum, J. K., and R. A. Myers.
2004. Shifting baselines and the decline of pelagic sharks in the Gulf of Mexico. Ecol. Lett. 7:135–145.

Bonfil, R.
1994. Overview of world elasmobranch fisheries. FAO Fish. Tech. Paper No. 341, 119 p. FAO, Rome.

Brill, R., P. Bushnell, L. Smith, C. Speaks, R. Sundaram, E. Stroud, and J. Wang.
2009. The repulsive and feeding deterrent effects of electropositive metals on juvenile sandbar sharks (*Carcharhinus plumbeus*). Fish. Bull. 107:298–307.

Conrath, C. L., J. Gelsleichter, and J. A. Musick.
2002. Age and growth of the smooth dogfish (*Mustelus canis*) in the northwest Atlantic Ocean. Fish. Bull. 100:674–682.

Dame, R. F., T. Chrzanowski, K. Bildstein, B. Kjerfve, H. Mckellar, D. Nelson, J. Spurrier, S. Stancyk, H. Stevenson, J. Vernberg, and R. Zingmark.
1986. The outwelling hypothesis and North Inlet, South Carolina. Mar. Ecol. Prog. Ser. 33:217–229.

Givois, V., and G. S. Pollack.
2000. Sensory habituation of auditory receptor neurons: implications for sound localization. J. Exp. Biol. 203:2529–2537.

Guttridge T. L., S. H. Gruber, K. S. Gledhill, D. P. Croft, D. W. Sims, and J. Krause.
2009. Social preferences in juvenile lemon sharks, *Negaprion brevirostris*. Anim. Behav. 78:543–548.

Hammock, M. F., J. A. Musick, and J. A. Colvocoresses.
1985. Life history of spiny dogfish off the northeastern United States. T. Am. Fish. Soc. 114:367–376.

Jordan, L. K.
2008. Comparative morphology of stingray lateral line canal and electrosensory systems. J. Morphol. 269:1325–1339.

Jordan, L. K., S. M. Kajiura, and M. S. Gordon.
2009. Functional consequences of structural differences in stingray sensory systems. Part II: electrosensory system. J. Exp. Biol. 212:3044–3050.

Kaimmer, S., and A. W. Stoner.
2008. Field investigation of rare-earth metal as a deterrent to spiny dogfish in the Pacific halibut fishery. Fish. Res. 94:43–47.

Kalmijn, A. J.
1982. Electric and magnetic field detection in elasmobranch fishes. Science 218:916–918.

Killam, K. A., and G. R. Parsons.
1989. Age and growth of the blacktip shark, *Carcharhinus limbatus*, near Tampa Bay, Florida. Fish. Bull. 87:845–857.

Klimley, A. P., S. C. Beavers, T. H. Curtis, and S. J. Jorgensen.
2002. Movements and swimming behavior of three species of sharks in La Jolla Canyon, California. Environ. Biol. Fishes 63:117–135.

Major, P. F.
1978. Predator prey interactions in two schooling fishes, *Caranx ignobilis* and *Stolephorus purpureus*. Anim. Behav. 26:760–777.

McKinnell, S., and M. P. Seki.
1998. Shark bycatch in the Japanese high seas squid driftnet fishery in the North Pacific Ocean. Fish. Res. 39:127–138.

Megalofonou, P., C. Yannopoulos, D. Damalas, G. De Metrio, M. Deflorio, and J. M. de la Serna.
2005. Incidental catch and estimated discards of pelagic sharks from the swordfish and tuna fisheries in the Mediterranean Sea. Fish. Bull. 103:620–634.

Murray, R. W.
1962. The response of the ampullae of Lorenzini of elasmobranchs to electrical stimulation. J. Exp. Biol. 39:119–128.

Musick, J. A., S. Branstetter, and J. A. Colvocoresses.
1993. Trends in shark abundance from 1974 to 1991 for the Chesapeake Bight region of the U.S. mid-Atlantic coast. NOAA Tech. Rep. NMFS 115, 18 p.

Myrberg, A. A., Jr., A. Banner, and J. D. Richard.
1969. Shark attraction using a video-acoustic system. Mar. Biol. 2:264–276.

Myrberg, A. A., Jr., C. R. Gordon, and A. P. Klimley.
1978. Rapid withdrawal from a sound source by open-ocean sharks. J. Acoust. Soc. Am. 64:1289–1297.

O'Connell, C. P., D. C. Abel, P. H. Rice, E. M. Stroud, and N. C. Simuro.
2010. Responses of the southern stingray (*Dasyatis americana*) and the nurse shark (*Ginglymostoma cirratum*) to permanent magnets. Mar. Freshw. Behav. Phys. 43:63–73.

O'Connell, C. P., D. C. Abel, S. H. Gruber, E. M. Stroud, and P. H. Rice.
2011. Response of juvenile lemon sharks, *Negaprion brevirostris*, to a magnetic barrier simulating a beach net. Ocean Coast. Manage. 54:225–230.

Parsons, G. R.
1985. Growth and age estimation of the Atlantic sharpnose shark, *Rhizoprionodon terraenovae*: a comparison of techniques. Copeia 1985:80–85.

Patchineelam, S. M., B. Kjerfve, and L. R. Gardner.
1999. A preliminary sediment budget for the Winyah Bay estuary, South Carolina, USA. Mar. Geo. 162:133–144.

Poisson, F.
2011. Catch, bycatch of sharks, and incidental catch of sea turtles in the reunion-based longline swordfish fishery (Southwest Indian Ocean) between 1997 and 2000, p. 163–165. *In* Global change: mankind-marine environment interactions; proceedings of the 13th French-Japanese oceanography symposium, September 4–8, 2008, Marseilles and Paris.

Raschi, W.
1986. A morphological analysis of the ampullae of Lorenzini in selected skates (Pisces, Rajoidei). J. Morphol. 189:225–247.
Rice, P.
2008. A shocking discovery: How electropositive metals (EPMs) work and their effects on elasmobranchs. NOAA Tech. Memo NMFS-PIFSC-16, 72 p.
Rigg, D. P., S. C. Peverell, M. Hearndon, and J. E. Seymour.
2009. Do elasmobranch reactions to magnetic fields in water show promise for bycatch mitigation? Mar. Freshw. Res. 60:942–948.
Robbins, W. D., V. M. Peddemors, and S. J. Kennelly.
2011. Assessment of permanent magnets and electropositive metals to reduce the line-based capture of Galapagos sharks, *Carcharhinus galapagensis*. Fish. Res. 109:100–106.
Ryer, C. H., and B. L. Olla.
1991. Information transfer and the facilitation and inhibition of feeding in a schooling fish. Environ. Biol. Fishes 30:317–323.
Sisneros, J. A., T. C. Tricas, and C. A. Luer.
1998. Response properties and biological function of the skate electrosensory system during ontogeny. J. Comp. Physiol. A:183:87–99.
Sisneros, J. A., and T. C. Tricas.
2002. Ontogenetic changes in the response properties of the peripheral electrosensory system in the Atlantic stingray (*Dasyatis sabina*). Behav. Ecol. 59:130–140.
Sminkey, T. R., and J. A. Musick.
1995. Age and growth of the sandbar shark, Carcharhinus plumbeus, before and after population depletion. Copeia 1995:871–883.
Smith, S., D. Au, and C. Snow.
1998. Intrinsic rebound potentials of 26 species of Pacific sharks. Mar. Freshw. Res. 49:663–678.
Stevens, J. D., R. Bonfil, N. K. Dulvy, and P. A. Walker.
2000. The effects of fishing on sharks, rays, and chimaeras (chondrichthyans), and the implications for marine ecosystems. J. Mar. Sci. 57:476–494.
Stoner A. W., and S. M. Kaimmer.
2008. Reducing elasmobranch bycatch: Laboratory investigation of rare earth metal and magnetic deterrents with spiny dogfish and Pacific halibut. Fish. Res. 92:162–168.
Tallack, S. M., and J. W. Mandelman.
2009. Do rare-earth metals deter spiny dogfish? A feasibility study on the use of electropositive "mischmetal" to reduce the bycatch of *Squalus acanthias* by hook gear in the Gulf of Maine. ICES J. Mar. Sci. 66:315–322.

Otolith morphometrics and population structure of Pacific sardine (*Sardinops sagax*) along the west coast of North America

Barbara Javor (contact author)
Nancy Lo
Russ Vetter

Email address for contact author: barbara.javor@noaa.gov

Southwest Fisheries Science Center
National Marine Fisheries Service, NOAA
8604 La Jolla Shores Drive
La Jolla, California 92037

Abstract—The broad distribution of Pacific sardine (*Sardinops sagax*) along the Pacific coast of North America makes it difficult for fisheries managers to identify regional stocks of this dominant small pelagic species. An investigation of morphometric characteristics of otoliths of Pacific sardine across most of their range revealed regional differences in populations. In a survey of over 2000 otoliths, all ages (with an emphasis on age-1 recruits) were compared. Principal components analysis, multivariate analysis of variance, and a novel method derived from regression and residuals calculations, termed perimeter-weight profiles (PWPs), revealed otolith similarities and differences. The results of the different approaches to statistical comparisons did not always agree. Sardine otoliths from Mexican waters were generally lighter and more lobate than those from U.S. and Canadian populations. Age-1 otoliths from northern California in 2006–07 tended to be heavier and smoother than those from other areas, including year-class cohorts from southern California. Comparisons of age-groups and year-classes of northern California otoliths with the use of the PWP models indicated significant trends in year-to-year patterns. In conjunction with other established indices of population structure, otolith PWPs are a useful tool for identifying local and regional stocks of Pacific sardine and may help distinguish populations of other fish species as well.

Manuscript submitted 23 November 2010.
Manuscript accepted 7 July 2011.
Fish. Bull. 109:402–415 (2011).

The distribution of Pacific sardine (*Sardinops sagax*) along approximately 5000 km of the Pacific coast of North America—an area spanning waters of Mexico, U.S.A., and Canada—poses an international challenge to understanding population structure and managing the fishery (Fig. 1; southeast Alaska not shown). The three countries regulate commercial fishing of this often dominant small, pelagic species under management plans based on annual stock assessments, but knowledge of sardine spawning, recruitment, and migratory habits is incomplete (Lo et al., 2010). After a peak in biomass of 3.6 million metric tons (t) in 1936, the commercial fishery collapsed in the 1940s and 1950s, possibly owing to overfishing or climatic changes in the California Current system (Norton and Mason, 2005; http://www.nmfs.noaa.gov/fishwatch/species/sardine.htm [accessed June 2011]). The population began to rebound in the 1970s, and a peak in biomass of 1.7 million t was recorded in 2000. The present existence of three North American stocks has been proposed (reviewed by Smith, 2005): 1) a stock along the California coast that migrates to the Pacific Northwest (Oregon to southeast Alaska; Wing et al., 2000); 2) a stock along the Pacific coast of Baja California, Mexico; and 3) a stock within the Gulf of California. Radovich (1982) proposed further dividing the California stock into northern and far northern races.

Despite a variety of methods, including egg, larval, and adult surveys, fish morphometrics, vertebral counts, tagging, and genetic, parasitic, and otolith studies, investigators have been unable to assign specific attributes and unique characteristics to identify regional stocks since the populations rebounded (Hedgecock et al., 1989; Grant and Bowen, 1998; Pereyra et al., 2004; Félix-Uraga et al., 2005; Smith, 2005; Lo et al., 2005, 2010; Valle and Herzka, 2008; Baldwin, 2010; Dorval et al., 2011). Further clues to stock structure might be found in more detailed surveys of the morphometry and microchemistry of sardine otoliths.

Since 1993 when a study of Atlantic cod (*Gadus morhua*) showed growth rates significantly correlated with otolith shape (Campana and Casselman, 1993), morphometric analysis has been used as a tool to detect stock structure and interannual variability in a number of fish species, including Pacific sardine (Félix-Uraga et al., 2005) and other Clupeiformes (Somarakis et al., 1997; Turan, 2000; Torres et al., 2000; Gonzalez-Salas and Lenfant, 2007; Burke et al., 2008). Linear measurements between landmark points (truss analysis), calculated geometries (e.g., circularity), and two-dimensional (Fourier series) shape analysis of otoliths are methods typically employed.

Otolith attributes are expressed under the control of genetic, physiological, and environmental factors.

Studies of tank-reared fish have led to insights into how specific environmental influences affect otolith shape and size. In some cases, feeding condition may affect growth and otolith morphology (Fletcher, 1995; Strelcheck et al., 2003; Gagliano and McCormick, 2004; Hüssy, 2008). Temperature influenced otolith size in tank-reared fish (Høie et al., 1999) and was inferred to regulate otolith growth in natural populations of *Merluccius* spp. and *Coelorhynchus* spp. (Lombarte and Lleonart, 1993; Bolles and Begg, 2000). Otolith morphometry, however, did not vary significantly with temperature or feeding condition in the Japanese flounder (*Paralichthys olivaceus*) (Katayama and Isshiki, 2007).

Pacific sardine inhabit coastal waters of a broad temperature range, from <10°C in Oregon and Washington (Emmett et al., 2005) to >25°C in southern Baja California (Félix-Uraga et al., 2004, 2005). Using temperature-at-catch data and otolith morphometry, Félix-Uraga et al. (2004, 2005) showed that the proposed north–south migration patterns of sardines supported the idea of three stocks in Baja California. The southern, warm-water otoliths were most differentiated from the rest, especially from those taken in coldest water catches. The authors performed multivariate discriminant analysis on over 1000 otoliths, using four straight linear measurements. Although they revealed statistical significance, the results showed a high degree of overlap between collection sites (Ensenada and Bahía Magdalena, ca. 500 km apart). That study did not address the cold-water stocks in the United States and Canada.

Our overall goal was to evaluate the efficacy of otolith morphometrics as a tool to identify Pacific sardine stocks for fishery management. One specific purpose of this investigation was to compare age-1 otoliths throughout their geographic range to detect regional differences and similarities by using several statistical approaches. Because sardine otoliths elongate asymmetrically as they grow, we applied a novel statistical approach that accommodated such changes, with the use of perimeter-weight profiles (PWPs), in addition to multivariate analysis of variance (MANOVA), principal component analysis (PCA), and generalized linear modeling (GLM). A second objective was to compare regional and age-related attributes in northern and southern California cohorts of recruits over multiple years. This research paralleled 1) a multiyear study of southern California sardine in the live bait industry, 2) an investigation of the microchemistry (trace elements and stable isotopes) of a subset of otoliths from the same multiyear study, and 3) genetic analysis of sardine tissues (Dorval et al., 2011; B. Javor, unpubl. data).

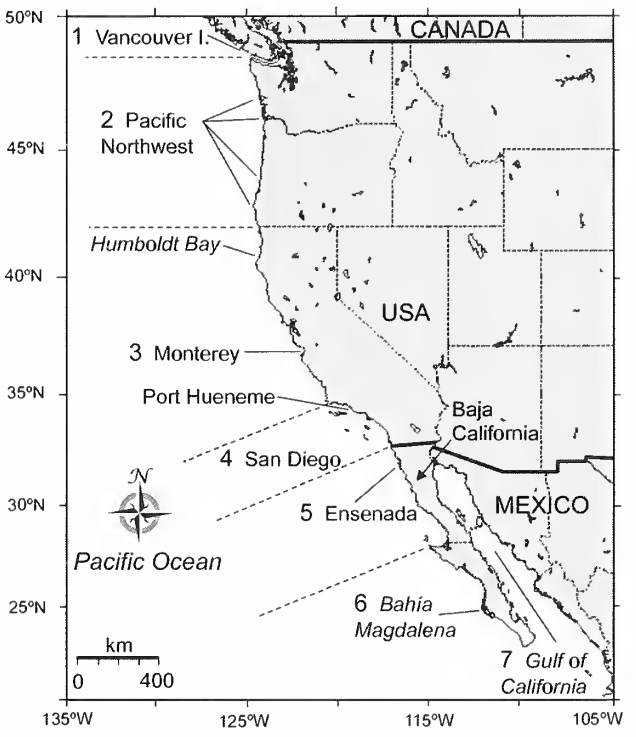

Figure 1

Map of the North American collection sites for Pacific sardine (*Sardinops sagax*) for determination of coast-wide population structure from otolith morphometrics. Details of the collections are given in Table 1.

Materials and methods

Collections

Either whole fish or otoliths were collected from sites between Vancouver Island, British Columbia, Canada, and the Gulf of California, Mexico (Table 1, Fig. 1). Samples from Canada, the Pacific Northwest, and Mexico were provided by other researchers investigating those populations. Samples from California were either specifically targeted in our study or were collected as part of regular port sampling by the California Department of Fish and Game (CDFG). No standard length (SL) or fish weight data were available for many of the otoliths obtained from archived CDFG collections.

The collections were divided into seven geographic groups that reflect oceanographic or political boundaries relevant to national fisheries: 1) Canada (Can); 2) Pacific Northwest (PNW), which includes Oregon and Washington; 3) Northern California (Monterey [Mon]); 4) Southern California Bight (SoCal), 32°–35°N, which includes San Diego (SD) and Los Angeles; 5) Ensenada (Ens); 6) Bahía Magdalena (BMag); and 7) Gulf of California (Gulf). Humboldt Bay (Hum, region 2\3 between the Pacific Northwest and Monterey) and Port Hueneme (PH, region 3\4 between northern and southern California) were considered to be transitional zones based on oceanographic features.

Otolith measurements

Sardine sagittal otoliths are asymmetric and lend themselves to measurements between multiple land-

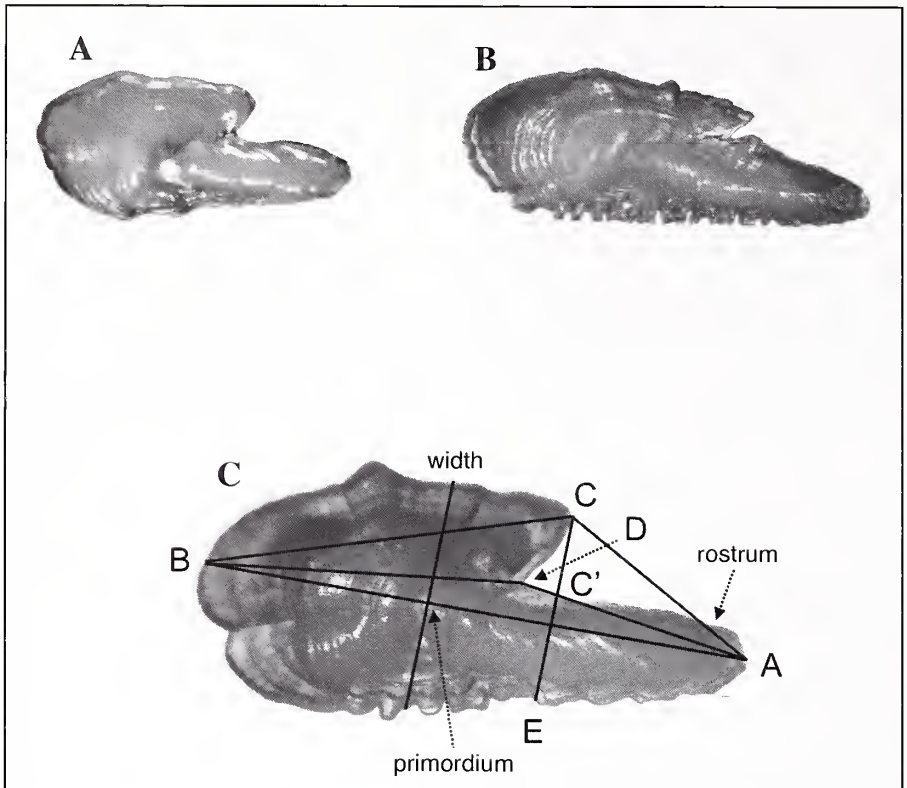

Figure 2

Otolith features and landmarks for morphometric measurements of Pacific sardine (*Sardinops sagax*). (**A**) Pacific Northwest specimen, age-0, 1.9 mm long, with a relatively smooth perimeter. (**B**) Gulf of California specimen, age-1, 3.1 mm long, with a relatively lobed perimeter. (**C**) Features for morphometry. Length is the distance from the midpoint of the rostrum at point A through the primordium to the posterior edge at point B. Width is the distance perpendicular to the length passing through the primordium. CE is the distance from the tip of the antirostrum to the ventral edge, parallel to the width; CC' is the segment of CE that represents the gap between the antirostrum (point C) and the rostrum; and D is the notch between the antirostrum and the rostrum.

mark points on the perimeter and through the primordium. The perimeter may develop rounded, irregular, or dentate protuberances, particularly along the ventral side, such that some otoliths are relatively smooth and others are relatively lobed (Fig. 2, A and B). Sagittal otoliths composed of vaterite, which are always clear and highly lobate, were omitted from the study.

We used both left and right otoliths. Age was determined by the method of Yaremko (1996). Age-1 otoliths weigh 0.73–1.30 mg based on our unpublished aging studies. After having been cleaned in distilled water, otoliths were dried, weighed on a Cahn C-33 microbalance (Thermo Electron Corp., Marietta, OH) with 0.005 mg accuracy and photographed with a reference scale for measuring otolith dimensions with Image-Pro Plus, vers. 4.5.1 or 6.3 software (Media Cybernetics, Inc., Bethesda, MD). The length (segment AB, Fig. 2C) was determined first, from the midpoint on the rostrum tip through the primordium to the posterior edge. Three segments perpendicular to the length included the width through the primordium, segment CE, and CE subsegment C–C' (a measure of the gap between the rostrum and antirostrum [point C]). Point D was the notch between the rostrum and the antirostrum. Other measured segments included AC, AD, BC, and BD. In addition to weight, the measurements included eight straight linear dimensions, perimeter, and area. The autotrace function of the software determined the perimeter and area.

Northern vs. southern California sardine populations

A synoptic study for 2006–07 of age-1 cohorts that turned age-2 during the spring of the calendar year was conducted to compare regional differences in sardine otoliths from Monterey Bay and from San Diego, about 700 km apart. Sardine from both regions presumably share the same spawning area offshore from central

Table 1

Dates and regions for collections of Pacific sardine (*Sardinops sagax*) from north to south. The number of otoliths obtained per site is given in Figure 4. Areas with two region numbers (e.g., 2\3) were considered transitional regions. DFO=Fisheries and Oceans; SWFSC=Southwest Fisheries Science Center; NWFSC=Northwest Fisheries Science Center; CDFG=California Department of Fish and Game; CICIMAR=Centro Interdisciplinario de Ciencias Marinas; CICESE=Centro de Investigación Científica y de Educación Superior de Ensenada.

Region no. and area	Year	Collections	Provider
1 Canada	2003	Vancouver I., 4 dates (adults)	C. Hrabek, DFO
	2005	Vancouver I., 1/28/05 area 24 (age 0)	C. Hrabek, DFO
2 Pacific Northwest	2003	Cruise FR0307 (3/03), 4 trawls	SWFSC
	2003	Cruise MF0313 (11/03), 6 trawls	R. Emmett, NWFSC
	2004	Cruise FR0403 (3/04), 3 trawls	SWFSC
	2010	Columbia River plume, 5/12 and 5/25	R. Emmett, NWFSC
2\3 Humboldt Bay	1996	Port samples, 3 dates	CDFG
3 Monterey	1996–97	Port samples, 8 dates	CDFG
	2006–97	Port samples, 21 dates	CDFG
	2008	Port samples, 4 dates	CDFG
3\4 Port Hueneme	2007	Port samples, 7 dates	CDFG
4 Los Angeles	1995–2003	Port samples, March–April (age 1)	CDFG
4 San Diego	2003–09	Bait receiver, monthly samples	SWFSC
5 Ensenada	1991–92	Port samples, spring and fall	CDFG
6 Bahía Magdalena	2004	Spring and fall, 4 dates	R. Félix-Uraga, CICIMAR
7 Gulf of California	2006	February and December	Y. Ríos, CICESE

and southern California (Lo et al., 2005). However, sea surface temperatures are markedly different at the two areas. The average annual temperature range in Monterey Bay at Pacific Grove is 11.8°–14.5°C, whereas 20 km south on the open coast, strong upwelling drives the temperatures lower (10°–13°C annual range; Breaker, 2005). The mean annual temperature range at the Scripps Institution of Oceanography pier in La Jolla (San Diego) is 13.9°–20.0°C (www.nodc.noaa.gov/dsdt/cwtg, accessed September 2010), whereas 23 km offshore from San Diego the temperatures are about 1°C warmer (www.calcofi.org, accessed September 2010). We also included sardine captured in 2007 near Port Hueneme (region 3\4), a landing in the Southern California Bight about midway between Monterey (region 3) and San Diego (region 4). Because regions 3 and 4 sardine reach a birthday during April, collections of cohorts during a calendar year are indicated as age 0–1, age 1–2, and age 2–3. Each sample set included 19–25 fish per collection, and both left and right otoliths were used when possible.

Statistical analysis

For coast-wide comparisons, several statistical approaches were used to ascertain patterns and regional characteristics of otoliths: principal components analysis (PCA), multivariate analysis of variance (MANOVA), and a method based on analysis of residuals described below. PCA was used initially to select the four most important otolith dimensions for the MANOVA and calculations of residuals. PCA and associated MANOVA statistics were applied only to age-1 otoliths (0.73–1.30 mg) because this age group was collected from all regions, whereas younger juveniles and older adults were not available from all areas. The coefficient of the characteristic vector of the product of contrast sum-of-square cross-product (SSCP) matrix (H) and the inverse of the error SSCP matrix (E) were used to determine the influential measurement among four variables. These selected measurements (length, area, perimeter, and weight) were then standardized (i.e., the correlation matrix rather than the covariance matrix) to be used in the MANOVA to test for possible differences in otolith dimensions with six orthogonal contrasts of individual regions or clusters of regions by using the Wilks's lambda test of significance: C1, regions 1–2 vs. 3–7; C2, region 1 vs. 2; C3, regions 3–5 vs. 6–7; C4, regions 3 vs. 4–5; C5, region 4 vs. 5; and C6, region 6 vs. 7. PCA and MANOVA were conducted with S-Plus (TIBCO Software, Palo Alto, CA) or SAS (SAS Institute, San Diego, CA) software.

In addition to MANOVA, we designed a method based on the residuals calculated from regression equations for measured otolith features in order to express morphometric data for comparisons with average data in simple models. Three regression equations with the use of the four most important dimensions determined by PCA (perimeter vs. area, perimeter vs. length, and weight vs. length) were derived from a data set of 2213 otoliths from all ages of sardine and all regions, whereas the MANOVA was performed for age-1 fish only. By applying these equations to the observed measurements of each otolith, the expected average perimeter and weight were calculated from the otolith area or length. The differences between observed and

calculated measurements (residuals) were employed to identify regional characteristics. According to the null hypothesis, 50% of the measurements for otoliths from a region should fall above the regression line and 50% below it if there is no regional bias for otolith perimeter or weight. We tested that hypothesis using the following equation expressed as a percentage:

$$PWP = \frac{\sum Z_i}{n}, \quad (1)$$

where Z_i = 1 if the observed measurement is greater than the calculated value from the regression line (otherwise scored as 0); and
n = the total number in the sample set.

We termed the results "perimeter-weight profiles," or PWPs.

PWPs reported this way correlated well with residuals expressed as plus or minus values in mm or mg. The correlation coefficients determined by comparing PWP (%) vs. average residuals (mm or mg) for 61 sample sets from San Diego collected monthly for over five years were the following: perimeter based on area, 0.876; perimeter based on length, 0.889; and weight based on length, 0.920. PWPs provide an advantage for categorizing the data on residuals, particularly when there is a wide spread of values and when the average residuals fall near zero.

Statistical significance of the three PWP calculations between geographic areas was determined by three-way chi-square tests and by using likelihood-ratio tests (or log linear model) with G^2 statistics (log-linear analysis, http://faculty.vassar.edu/lowry/abc.html, accessed September 2010). For the ABC chi-square matrix, we used pairs of values (i.e., 2×2×2): A=two locations; B=the number of otoliths above and the number below the regression line that describes the model otolith for each kind of measurement; and C=two kinds of measurements (PWP perimeter derived from the otolith area and PWP weight derived from the otolith length). Significance values (P) were determined from the G^2 statistic for AB(C) that represented the AB interaction when the AC and BC interactions were removed. It can be obtained by constructing a separate AB table for each level of C, calculating a separate G^2 measure for each AB table, and then summing the results.

Comparisons between northern and southern California sardine otoliths were conducted several ways. A GLM with logistic link was used to examine the possible differences between PWP for perimeter based on area (P/A), perimeter based on length (P/L), and weight based on length (W/L) for regions 3 and 4 (Monterey and San Diego, location effect) using cohorts collected in 2006 and 2007 (year effect):

$$g(PWP) = \beta_0 + \beta_1 x_1 + \beta_2 x_2 + \beta_3 x_1 x_2, \quad (2)$$

where g(PWP) is a logistic link function of the population proportion for each of the three equations (P/A), (P/L), and (W/L); and

$$g(PWP) = \log\left(PWP/(1-PWP)\right), \quad (3)$$

where x_1 and x_2 are categorical variables: x_1=0 for 2006 and 1 for 2007, and x_2=0 for Monterey and 1 for San Diego. The last term (β_3) is the interaction term. When the coefficient β_3 was significant, the GLM was performed to test the location effect for each year with x_2 as the only independent variable.

Because the multiyear data collected from Monterey area included more than one age, the GLM was also used to test age and year effect on otoliths sampled during 2006–07 by using the same methods described for Equations 2 and 3. The only difference between these two GLM applications was that here x_2 is the age category: x_2=0 for age-0 fish and 1 for age 1–2 fish. The coefficient β_2 was applied to measure the age effect, whereas in the previous GLM, x_2 was the indicator for the location.

Results

Coast-wide survey

PCA and MANOVA When otoliths of all ages and from all regions were compared, most measurements were highly correlated (coefficients≥0.90, n=2309 otoliths; data not shown). Length, perimeter, and area had the highest correlation coefficients (0.98–0.99). Otolith weight strongly correlated with length, perimeter, and area (0.94–0.98), and fish standard length similarly correlated with those four otolith features (0.95–0.97). When correlations were conducted for each of the seven areas, no regional patterns were detected (data not shown).

For the PCA of age-1 otoliths with all eleven measurements, the otolith dimensions (except C–C') had nearly equivalent PC1 coefficients (data not shown). When only the four most important dimensions were compared by PCA (area, length, perimeter, and weight), PC1 explained 86% of the variance and the coefficients were similar (Table 2). PC1 was the only component with an eigenvalue >1. These samples represented aggregated collections by region for all dates and provided one otolith per pair. When PCA was conducted with both otoliths per pair, the results were nearly identical (results not shown).

MANOVA on these four variables based on the correlation matrix indicated otolith sizes were not the same for all regions despite the selection of a single age class (0.73–1.30 mg, nearly a two-fold difference within the class). MANOVA results showed that all regions were not the same, and each of the six tested regional contrasts were significantly different (P<0.05) (Table 3). In three of the six regional contrasts, perimeter, or perimeter and weight together, contributed the most to the differences. Length was generally the least influential factor for any of these contrasts.

Although differences between widely spaced collection areas might be expected (contrasts 1, 3, and 4), the rea-

sons for the significant differences between neighboring regions that share spawning or oceanographic features (contrasts 2, 5, and 6) were not apparent. Small sample sizes may have biased some of the results. Age 0–1 otoliths from the northernmost areas were not well represented: n=30 from Canada (region 1), all from a single collection date; and n=20 from the Pacific Northwest (region 2). However, sample size might not explain why southern California and Ensenada (regions 4 and 5) otoliths were significantly different, and why Bahía Magdalena and Gulf of California (regions 6 and 7) were dissimilar.

We initially conducted PCA of over 1100 otoliths by aggregating all ages in a region, from juveniles to adults, which resulted in size-biased, significant differences within and between regions (data not shown). Otoliths from regions 1 and 2, the only areas with large adults in the collections, differed from all other regions. This response derived from the overall shape differences between young and older otoliths (Fig. 2). In order to compare otoliths of all sizes in collections that had different distributions of sizes, another approach was required.

Perimeter-weight profiles (PWPs) The regression lines between pairs of otolith features for sardine of all ages and regions were linear (perimeter vs. length) or curvilinear (perimeter vs. area, and weight vs. length) (Fig. 3). The regression equations used for calculating PWPs and their correlation coefficient (R^2) values for these features are as follows:

$$\textit{Perimeter} \text{ (based on area)} = -0.2250\ \textit{area}^2 + 3.1559\ \textit{area} + 1.9071,\ R^2=0.968 \quad (4)$$

$$\textit{Perimeter} \text{ (based on length)} = 2.6808\ \textit{length} + 0.118,\ R^2=0.975 \quad (5)$$

Table 2

Summary of principal components (comp) analyses of age-1 sardine (*Sardinops sagax*) otolith measurements based on the four most important features of length, area, perimeter, and weight. One otolith was examined per fish. The numbers of otoliths per region are as follows: region 1 (30), region 2 (20), region 3 (86), region 4 (280), region 5 (87), region 6 (36), region 7 (150), total (689).

	Importance of components			
	Comp 1	Comp 2	Comp 3	Comp 4
Standard deviation	1.86	0.59	0.32	0.29
Proportion of variance	0.864	0.088	0.026	0.022
Cumulative proportion	0.864	0.953	0.978	1.000
Eigenvalues	3.46	0.35	0.10	0.08
Coefficients				
Length	0.514	−0.229	0.732	0.384
Area	0.520			−0.850
Perimeter	0.496	−0.540	−0.639	0.233
Weight	0.468	0.810	−0.220	0.276

$$\textit{Weight} \text{ (based on length)} = (\textit{length}^{2.2429}) \times (0.1054),\ R^2=0.966, \text{ for otoliths <3 mm} \quad (6)$$

$$\textit{Weight} \text{ (based on length)} = 0.2709\ \textit{length}^2 - 0.605\ \textit{length} + 0.6084,\ R^2=0.947, \text{ for otoliths >3 mm} \quad (7)$$

PWPs showed several distinct regional and age patterns, particularly between northern California (regions 2\3 and 3, Humboldt Bay and Monterey) and regions 5–7

Table 3

Data from a coast-wide survey of the four most important Pacific sardine (*Sardinops sagax*) otolith dimensions (length, area, perimeter, and weight) determined by principal component analysis and multivariate analysis of variance to test the hypothesis of no overall region effects and in each of the six orthogonal contrasts of individual regions and clusters of regions. The coefficient of the characteristic vector of the product of contrast sum-of-square cross-product (SSCP) matrix (**H**) and the inverse of the error SSCP matrix (**E**) were used to determine the influential measurement among the four variables. The results include characteristic roots and vectors of **E**−1**H**. Significance ($PR>F$) was <0.0001 for no region effect and all contrasted regions. Denom.=denominator.

Contrasted regions Hypothesis: no effect	Wilks's lambda value	F value	No. of df	Denom. df	Characteristic root	Percent	Characteristic vector Standardized measurements			
							Length	Area	Perimeter	Weight
No region effect	0.61	15.13	24	2370	0.359	64.15	0.010	−0.003	0.055	−0.032
1: 1–2 vs. 3–7	0.94	10.02	4	679	0.071	100	0.010	−0.074	0.081	0.010
2: 1 vs. 2	0.92	14.61	4	679	0.059	100	−0.010	0.057	0.019	−0.033
3: 3–5 vs. 6–7	0.90	19.86	4	679	0.042	100	−0.170	−0.007	0.042	0.025
4: 3 vs. 4–5	0.93	12.06	4	679	0.116	100	0.001	0.042	0.029	−0.044
5: 4 vs. 5	0.90	19.74	4	679	0.086	100	0.011	−0.011	0.019	−0.026
6: 6 vs. 7	0.96	7.16	4	679	0.117	100	−0.026	0.039	−0.055	0.045

in Mexico (Fig. 4, Table 4). Most of the otoliths were from late age-0 and age-1fish, except those indicated as being from juvenile (all age-0) and adult (≥2 years) fish. Values close to 50% indicate the collection was close to the average of the entire population. Samples in Figure 4 were aggregated by collection area regardless of date, except for two sets: juveniles from region 2 separated by collection period, 2003–04 vs. 2010; and region 4 (San Diego) monthly otolith collections separated into 2006–07 and 2009–10 sets.

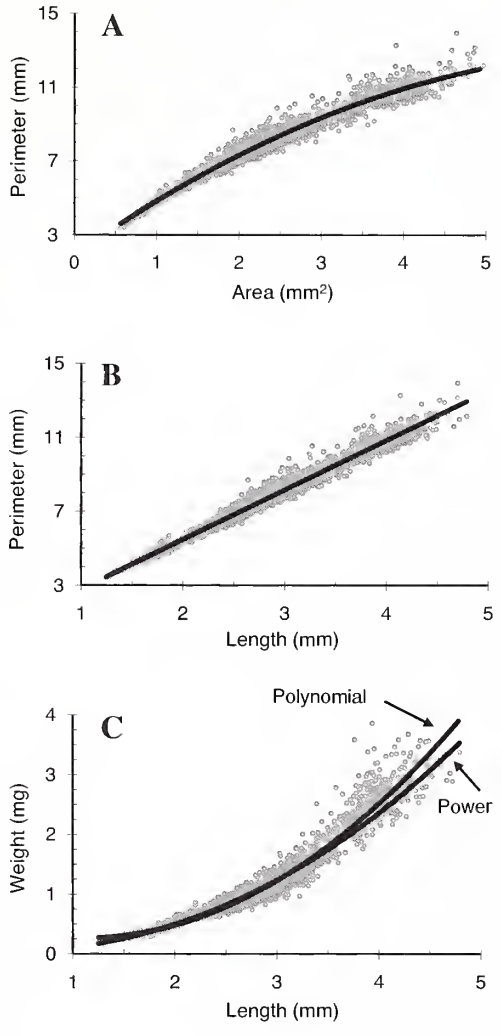

Figure 3

Pacific sardine (*Sardinops sagax*) otolith dimension relationships for 2213 otoliths from all ages and regions: (**A**) perimeter vs. area; (**B**) perimeter vs. length; and (**C**) weight vs. length relationships with two regression lines shown. The power equation best described otoliths <3 mm in length, and the polynomial equation best described larger otoliths. The regression equations are described in the text.

PWPs for Mexican sardine otoliths (regions 5–7) were distinct. Otolith weights from the three areas of collection were less than the predicted average. Perimeters of southern Baja California otoliths from Bahía Magdalena (pooled from spring and fall samples in 2004) and the Gulf of California (pooled from January and December, 2006 samples) were markedly lobed. Overall, the PWPs of sardine otoliths from region 6 and 7 resembled each other in the chi-square tests, unlike the results of the MANOVA described in Table 3. Region 5 otoliths had a PWP weight signature resembling the more southern fish and a PWP perimeter signature similar to that of southern California sardine. The chi-square test of the PWP factors indicated that region 5 otoliths were different (P=0.0002) from more southern sardine in regions 6 and 7.

Sardine otoliths from regions 1, 2 (2003–04 collection), and 4 resembled each other. These sets included both juveniles and adults. By contrast, region 1 and 2 otoliths were significantly different in the MANOVA presented in Table 3. Northern California otoliths (regions 2\3 and 3) were moderately similar to each other (P=0.03). The strongest similarities determined in the chi-square tests were between regions 2 and 4, and between regions 6 and 7 (P>0.8).

Correlation coefficients between the residuals (observed minus average values, ±mm or mg) for each

Table 4

Similarities in perimeter-weight profiles (PWPs) in the coast-wide survey of Pacific sardine (*Sardinops sagax*) determined by three-way chi-square tests contrasting perimeter based on area, perimeter based on length, and weight based on length; n=2213 otoliths. All otoliths were age 1–2 except those in collections described as juveniles (age-0) and adults (>age-2). Regions are shown in Figure 1. Region 2, 2003–04 collection; region 3, 1996–97 collection; region 4, San Diego collection. Dates of other collections are given in Table 1. Where indicated with +, the collections were aggregated.

Contrasted ages and regions	P
Region 1: juveniles vs. adults	0.0351
Region 2: juveniles vs. adults	0.3985
Region 1 vs. 2	0.1882
Region 1 adults vs. region 2 adults	0.0226
Region 1 vs. 4	0.2039
Region 2 vs. 3	<0.0001
Region 2 vs. 4	0.8025
Region 3 vs. 3\4	<0.0001
Region 3 vs. 2\3	0.0347
Region 3 + 2\3 vs. regions 6 + 7	<0.0001
Region 4 vs. 3\4	<0.0001
Region 4 vs. 5	<0.0001
Region 5 vs. 6 + 7	0.0002
Region 6 vs. 7	0.8781

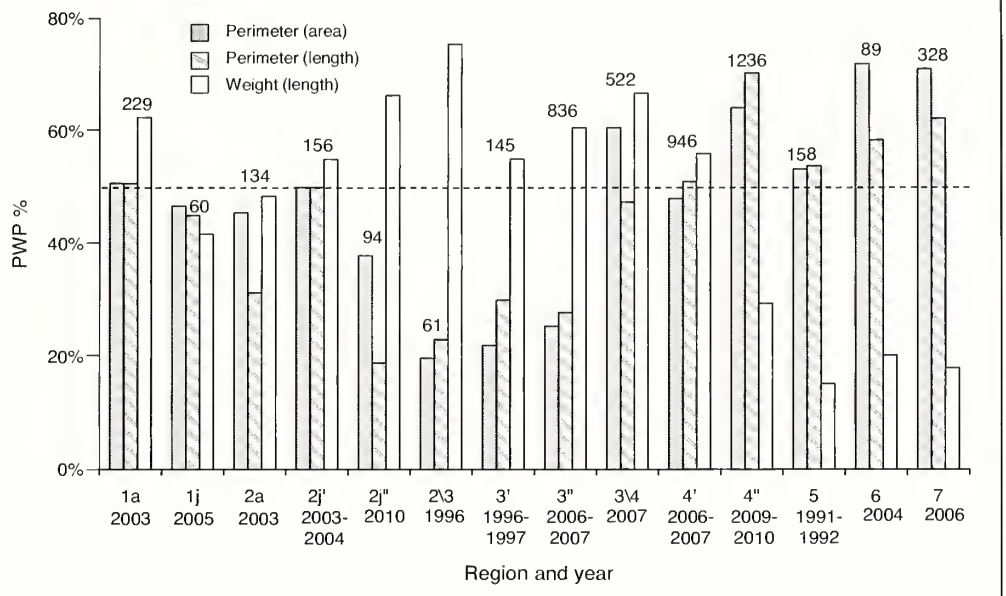

Figure 4

Regional perimeter-weight profiles (PWPs) of Pacific sardine (*Sardinops sagax*) otoliths. All are age 1–2, except age-0 juveniles (designated by a j) and adults >age-2 (designated by an a). Regions 2, 3, and 4 were divided by collection years (designated by ′ and by ″). The dashed line at 50% PWP represents the population average (i.e., 50% of the residuals lie above the regression line) as determined by the regression equations. The numbers above the columns represent the number of otoliths collected.

of the three PWP factors, compared for each otolith (n=2213), were largely similar across the seven geographic areas. They were positive between the two ways of conducting perimeter calculations (0.682) and negative or neutral between perimeter (P/A and P/L) and weight calculations (-0.382 and 0.071) (data not shown).

Northern vs. southern California sardine populations

The PWP perimeters calculated from otolith area and length in monthly or semimonthly collections were significantly different for Monterey and San Diego (regions 3 and 4) sardine in 2006–07 (Fig. 5, A and B). Monterey otoliths tended to have smoother perimeters. Distinctions between predicted and observed otolith weights for the two sites were not apparent (Fig. 5C). Fish standard lengths (SL) and condition factors were similar for the two sites as were the regressions for SL vs. otolith weight and SL vs. otolith length (data not shown). Because somatic and otolith growth rates were similar in the cohorts at the two locations, differences in otolith perimeters were likely due to environmental factors.

The Port Hueneme (region 3\4) samples in 2007 had perimeter profiles more like those of San Diego otoliths with the area-based regression and widely ranging perimeter attributes similar to both Monterey Bay and San Diego otoliths with the length-based regression. There was no distinction between weight profiles for the three sites during the same time period. The most salient feature of the 13 Port Hueneme collections over a five-month period was their nonuniformity.

A GLM with logistic link was used to examine the possible difference between PWPs for perimeter based on area (P/A), perimeter based on length (P/L), and weight based on length (W/L) between Monterey and San Diego (location effect) and between years 2006 and 2007 (year effect) (Table 5). For both cases of perimeter (P/A and P/L), the interaction term (*year*×*age*) was significant, and therefore two separate GLMs were performed to test for possible location effects, each for 2006 and 2007. The location effect for each of the two years was significant (P<0.001) with the difference between locations being greater in 2007 than in 2006. For the GLM analysis of PWP for W/L, location and year effects were not significant. Thus, only PWP perimeters (P/A and P/L) were dissimilar between regions 3 and 4 for these two years.

Fish age and collection year were factors for PWPs of sardine captured in Monterey. In a multi-year survey, age-1 and older otoliths tended to be smoother and heavier than average, but year-to-year PWPs were somewhat inconsistent (Fig. 6). Age-0 otolith PWPs did not show a predictable pattern that resembled that of older fish. The GLM was used to test age effect (age 0 and age 1–2) and year effect (2006 and 2007) for the three PWP factors P/L, P/A, and W/L of the region 3

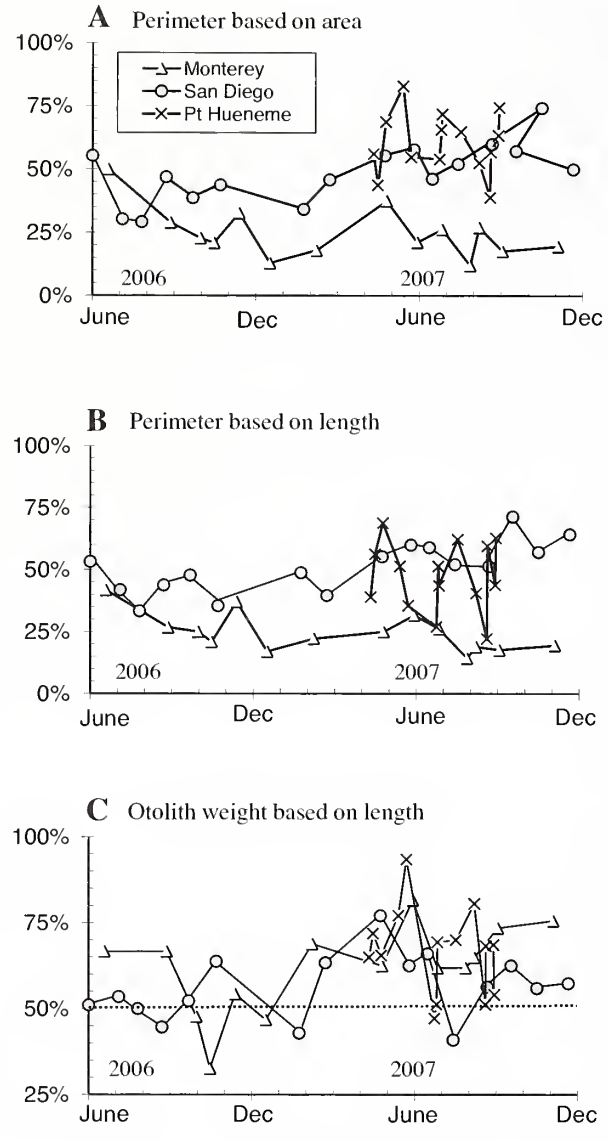

Figure 5

Perimeter-weight profiles (PWPs) of late age-0 and age-1 Pacific sardine (*Sardinops sagax*) otoliths from Monterey (region 3), San Diego (region 4), and Port Hueneme (region 3\4), 2006–07. (**A**) Perimeter based on area. (**B**) Perimeter based on length. (**C**) Weight based on length. The dashed line at 50% PWP represents the population average (i.e., 50% of the residuals lie above the regression line) as determined by the regression equations.

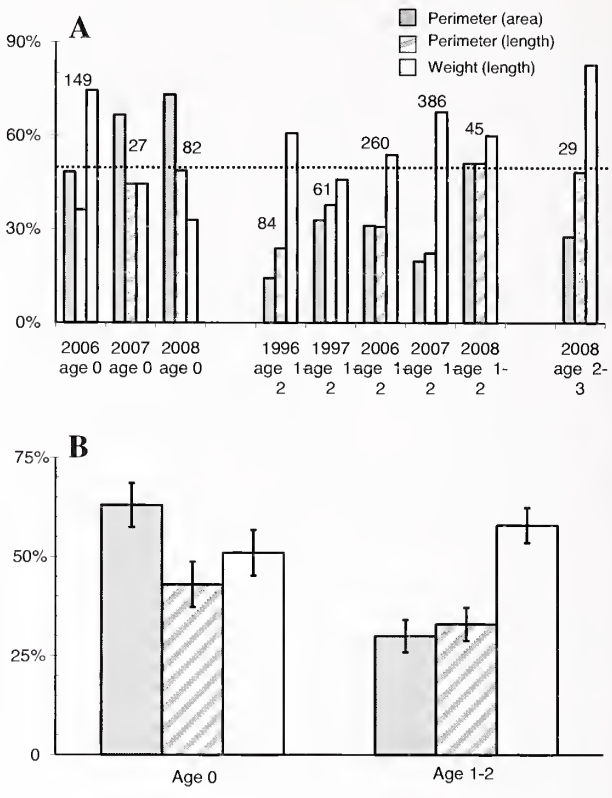

Figure 6

Multiyear comparisons of perimeter-weight profiles (PWPs) of Pacific sardine (*Sardinops sagax*) otoliths from Monterey (region 3). (**A**) Profiles by collection year and age (number of otoliths indicated). The dashed line at 50% PWP represents the population average (i.e., 50% of the residuals lie above the regression line) as determined by the regression equations. The number of otoliths is indicated above each set. (**B**) Averages by age: age-0 (mean of 3 years) and ages 1–2 (mean of 5 years). Each collection was normalized to 100 otoliths to remove year-based bias. Error bars are ±95% confidence intervals.

data in Figure 6. The age:year interaction term was not significant for perimeter (both P/L and P/A); therefore no further GLM was performed (Table 6). The age effect was significant for perimeter (both P/A and P/L); the year effect was significant for only P/A and not for P/L. For the GLM of W/L, the age and year interaction term was significant.

Discussion

PCA and PWP methods of comparison

We compared otolith characteristics from a large collection of Pacific sardine sampled from most of their North American range, which was divided into seven regions between Canada and the Gulf of California. Regional similarities and differences determined with MANOVA and perimeter-weight profile comparisons did not agree consistently with each other.

One of the inherent problems with this kind of survey is that sardine otoliths elongate asymmetrically as they grow. Including all sizes of otoliths in any statistical analysis resulted in significant differences between northern stocks (where large adult sardine are commercially captured and few juveniles were found) and

Table 5

General linear model (GLM) for year (β_1) and location (β_2) interactions effects of region 3 and 4 sardine (*Sardinops sagax*) otolith measurements for each perimeter-weight profile (PWP) factor: perimeter based on area, perimeter based on length, and weight based on length. Because the interaction term (β_3) was significant, GLM was performed for both 2006 and 2007 for the three PWP factors. Significance: *=P<0.05, **=P<0.005, ***=P< 0.001.

	Coefficient estimate	Standard error	z-value	P	Significance
Perimeter based on area, coefficients					
(Intercept)	−0.9163	0.1479	−6.195	5.82×10^{-10}	***
Location (β_1)	0.6286	0.1874	3.354	7.97×10^{-4}	***
Year (β_2)	−0.4773	0.2006	−2.380	0.0173	*
Location:year (β_3)	0.8760	0.2513	3.486	4.91×10^{-4}	***
Perimeter based on length, coefficients					
(Intercept)	−1.0515	0.1525	−6.894	5.42×10^{-12}	***
Location	0.8035	0.1909	4.209	2.57×10^{-5}	***
Year	−0.2702	0.2021	−1.337	0.1813	
Location:year	0.7360	0.2526	2.914	0.00357	**
Weight based on length					
(Intercept)	0.1791	0.1993	0.899	0.3763	
Location	0.0164	0.2620	0.063	0.9506	
Year	0.4879	0.2617	1.864	0.0724	
Location:year	−0.4265	0.3450	−1.236	0.2263	
Weight based on length after excluding interaction term					
(Intercept)	0.3226	0.1650	1.956	0.0599	
Location	−0.2305	0.1718	−1.342	0.1897	
Year	0.2427	0.1722	1.410	0.1690	
2006 Perimeter based on area, coefficients					
(Intercept)	−0.9163	0.1479	−6.195	5.82×10^{-10}	***
Location	0.6286	0.1874	3.354	7.97×10^{-4}	***
2007 Perimeter based on area, coefficients					
(Intercept)	−1.3936	0.1355	−10.286	2.00×10^{-16}	***
Location	1.5046	0.1674	8.988	2.00×10^{-16}	***
2006 Perimeter based on length, coefficients					
(Intercept)	−1.0515	0.1525	−6.894	5.42×10^{-12}	***
Location	0.8035	0.1909	4.209	2.57×10^{-5}	***
2007 Perimeter based on length, coefficients					
(Intercept)	−1.3218	0.1326	−9.965	2.00×10^{-16}	***
Location	1.5395	0.1654	9.310	2.00×10^{-16}	***

southern stocks (where large adults are rarely captured). These dissimilarities are likely due to age differences. Within the size-class defined to comprise mostly age-1 otoliths, the dimensional relationships spanned a smaller range, but they could have biased the results if all regions did not have a similar distribution of otolith sizes. The results may have also been biased by the relatively small number of age-1 representatives from regions 1 and 2. Any statistical analysis is most reliable when sample sizes are large and balanced (Osborne and Costello, 2004).

The predictability of dimensions of an average sardine otolith of any length or area was the premise for developing the PWP method to compare sets of otoliths as an alternative approach for analyzing the data. PWPs gave a picture of regional signatures and temporal trends within and between year classes. Juvenile otoliths from northern California (and in 2010, the Pacific Northwest) showed a regional signature as predominantly heavy and smooth, whereas juvenile otoliths from their southernmost distribution were predominantly light and lobate. Multiyear surveys showed trends in age-specific profiles for Monterey otoliths.

The PWP method, which permitted the comparison of individual otolith features, revealed unique profiles among Mexican sardine. Region 5 otoliths appeared to have weight characteristics of the more southerly region 6 and 7 populations and perimeter characteristics of region 4 southern California sardine. Migratory movements that could account for the uniformity of region 6

Table 6

General linear model (GLM) for year and age effect in region 3 (Monterey) Pacific sardine (*Sardinops sagax*) otoliths for each perimeter-weight profile (PWP) factor: perimeter based on area, perimeter based on length, and weight based on length. Significance: *= $P<0.05$, **=$P<0.005$, ***=$P<0.001$.

	Coefficient estimate	Standard error	*z*-value	*P*	Significance
Perimeter based on area					
(Intercept)	−0.0757	0.1471	−0.515	0.6069	
Year	−0.4729	0.2869	−1.648	0.0994	
Age	−0.8406	0.2086	−4.029	5.60×10^{-5}	***
Year:age	−0.0045	0.3501	−0.013	0.9898	
Perimeter based on area after excluding interaction term					
(Intercept)	−0.0749	0.1335	−0.561	0.575	
Year	−0.4759	0.1644	−2.894	3.80×10^{-3}	**
Age	−0.8422	0.1676	−5.026	5.01×10^{-7}	***
Perimeter based on length					
(Intercept)	−0.3606	0.1494	−2.413	0.0158	*
Year	−0.1880	0.2881	−0.652	0.5142	
Age	−0.6909	0.2135	−3.236	1.21×10^{-3}	**
Year:age	−0.0823	0.3520	−0.234	0.8152	
Perimeter based on length after excluding interaction term					
(Intercept)	−0.3458	0.1352	−2.557	0.0106	*
Year	−0.2431	0.1658	−1.467	0.1424	
Age	−0.7212	0.1701	−4.239	2.24×10^{-5}	***
Weight based on length					
(Intercept)	0.9391	0.1636	5.742	9.36×10^{-9}	***
Year	−0.2670	0.2995	−0.892	0.3726	
Age	−0.7601	0.2115	−3.593	3.27×10^{-4}	***
Year:age	0.7549	0.3475	2.173	0.0298	*
Weight based on length, 2006					
(Intercept)	0.9391	0.1636	5.742	9.36×10^{-9}	***
Age	−0.7601	0.2115	−3.593	3.27×10^{-4}	***
Weight based on length, 2007					
(Intercept)	0.6721	0.2509	2.679	7.39×10^{-3}	**
Age	−0.0051	0.2757	−0.019	0.9851	

and 7 otoliths and the mixed characteristics of region 4 and 5 otoliths were described by Félix-Uraga et al. (2005) in their study of Baja California populations. The results from our study support the generally accepted belief that southern Baja California sardine represent a distinct stock.

The PWP method clearly differentiated region 3 and 4 (Monterey and San Diego) cohorts collected in 2006–07. The mixed results of the Port Hueneme samples compared with Monterey and San Diego sardine could indicate that Port Hueneme is a zone of overlap where representatives are carried south by the cool California Current and others are transported north by the warm Southern California Countercurrent.

The PWP method has limitations for assigning fish to stocks or environments. Similar PWPs between region 2 and 4 age-1 sardine, but not region 3 fish, do not necessarily indicate a common stock, although it is generally believed adult sardine in California migrate north during the summer (Smith, 2005; Lo et al., 2010). Likewise, dissimilar perimeter profiles between age-0 and age-1 sardine otoliths from Monterey do not necessarily indicate two regions of origin. Some attributes of the PWP method need further study. For example, it is not obvious why the two equations to model otolith perimeters correlated differently with the weight model.

Factors affecting otolith morphometrics

In previous studies of otolith morphology, length, area, and perimeter were often the most important characteristics that defined fish stocks (Bolles and Begg, 2000; Torres et al., 2000; DeVries et al., 2002; Cardinale et al., 2004). When included in such studies, otolith weight

was also an important factor (Tuset et al., 2006; Jónsdóttir et al., 2006). In a morphometric study of Pacific sardine otoliths from Baja California, Mexico, Félix-Uraga et al. (2005) used length and other linear dimensions, but not area, perimeter, or weight. Because these factors were the most important in the first principal component that explained most of the variance in the present investigation, a re-evaluation of those otoliths might refine the results of the earlier study. However, those otoliths were permanently mounted on slides in clear resin that precluded weighing them and obtaining sharp digital images to measure area and perimeter with the autotrace tool of the image-processing software (R. Félix-Uraga[1]).

Both temperature and growth rate can be factors influencing otolith shape. In a study of two stocks of silver hake (*Merluccius bilinearis*), fish in the northern stock grew slower, probably due to colder temperatures, and their otoliths were subsequently larger (i.e., older) than those from southern-stock fish of the same standard length (Bolles and Begg, 2000). Similar phenomena have been noted in other fish (summarized by Strelcheck et al., 2003). Hüssy (2008) showed higher food consumption resulted in a higher number of lobes in otoliths of juvenile Atlantic cod (*Gadus morhua*).

In our 2006–07 synoptic study of region 3 and 4 cohorts, we found no apparent growth differences between recruits captured near Monterey and San Diego, although the higher percentage of smoother otoliths in Monterey was notable. Juveniles from both locations are believed to come from central and southern California coastal spawning grounds (Lo et al., 2005). An obvious explanation for the differences in otolith morphometrics between the two regions may be temperature.

Temperature has been tested and shown to affect otolith growth characteristics in other species. Positive effects of temperature on otolith weight have been observed in red drum (*Sciaenops ocellatus*) (Hoff and Fuiman, 1993) and herring (*Clupea harengus*) (Fey, 2001). Flounder (*Paralichthys olivaceus*) otoliths showed no significant difference in marginal coarseness between wild fish and experimental fish maintained at 15°, 20°, and 25°C (Katayama and Isshiki, 2007). Hoff and Fuiman suggested that otolith growth was more directly affected by metabolic rate than by growth rate. Our unpublished data indicate that otolith weights and perimeters of sardine reared in tanks at different temperatures are dissimilar to those same variables in otoliths of wild-caught sardine of the same age and they likely reflect artifacts of aquaculture that may be independent of water temperature.

Temperature may affect sardine otolith morphometrics in wild populations, but other factors may modify them. An improved survey to address possible temperature effects would compare all sardine sizes from their environmental ranges. Sardine do not regularly spawn successfully in the Pacific Northwest (McFarlane and Beamish, 2001; Emmett et al., 2005; Lo et al., 2010), and therefore further study to elucidate the environmental or growth factors that contribute to regional differences in otolith morphometrics in cold ocean environments would be hampered by the availability of samples of young fish. Likewise, older sardine are not usually collected in warmer Mexican waters.

[1] Félix-Uraga, Roberto. 2005. Personal commun. Centro Interdisciplinario de Ciencias Marinas, La Paz, Baja California Sur, Mexico.

Conclusion

Results from MANOVA indicated there were regional differences in age-1 otoliths between regions or clusters of regions when nearly 700 fish were compared. Based on comparisons with average otoliths of the same length or area, PWPs of young and adult sardine otoliths coupled with MANOVA and chi-square tests showed differences among some regions, as well as significant similarities. This investigation provided further evidence that *S. sagax* populations in their southernmost distribution in Mexican waters are a distinct stock from U.S. and Canadian populations (Félix-Uraga et al., 2004, 2005; Smith, 2005). Sardine from Ensenada (region 5) shared otolith features with both southern and northern stocks. Age-1 otoliths from northern California (region 3) tended to be heavier and smoother than those from other areas. Some regions showed variations in PWPs between years. PWPs were useful for describing relationships between and within local and regional sardine stocks and age cohorts. PWPs can be applied as a tool for understanding residence, migration, and population connectivity when used in combination with otolith chemistry, aging, genetics, and other traditional measures of population structures for sardine and other species of fish.

Acknowledgments

We gratefully acknowledge the individuals and agencies listed in Table 1 for the extensive collections of sardine otoliths. We thank L. Robertson of the NOAA Southwest Fisheries Science Center for monthly collections from the bait supplier for otolith extraction, and Z. Fan and Y. Gu for statistical analyses. We thank J. Hyde, M. Lowry, and J. Stewart for helpful reviews of early drafts of the manuscript.

Literature cited

Baldwin, R. E. B.
2010. Using parasite community data and population genetics for assessing Pacific sardine (*Sardinops sagax*) population structure along the west coast of North America. Ph.D. diss, 207 p. Oregon State Univ., Corvallis, OR.

Bolles, K. L., and G. A. Begg.
2000. Distinction between silver hake (*Merluccius bilinearis*) stocks in U.S. waters of the northwest Atlantic

based on whole otolith morphometrics. Fish. Bull. 98:451–462.

Breaker, L. C.
2005. What's happening in Monterey Bay on seasonal to interdecadal time scales. Cont. Shelf Res. 25:1159–1193.

Burke, N., D. Brophy, and P. A. King.
2008. Otolith shape analysis: its application for discriminating between stocks of Irish Sea and Celtic Sea herring (*Clupea harengus*) in the Irish Sea. ICES J. Mar. Sci. 65:1670–1675.

Campana, S. E., and J. M. Casselman.
1993. Stock discrimination using otolith shape analysis. Can J. Fish. Aquat. Sci. 50:1062–1083.

Cardinale, M., P. Doering-Arjes, M. Kastowsky, and H. Mosegaard.
2004. Effects of sex, stock, and environment on the shape of known-age Atlantic cod (*Gadus morhua*) otoliths. Can. J. Fish. Aquat. Sci. 61:158–167.

DeVries, D. A., C. B. Grimes, and M. H. Prager.
2002. Using otolith shape analysis to distinguish eastern Gulf of Mexico and Atlantic Ocean stocks of king mackerel. Fish. Res. 57:51–62.

Dorval, E., K. Piner, L. Robertson, C. S. Reiss, B. Javor, and R. Vetter.
2011. Temperature record in the oxygen stable isotopic composition of Pacific sardine otoliths: experimental vs. wild stocks from the Southern California Bight. J. Exper. Mar. Biol. Ecol. 397:136–143.

Emmett, R. L., R D. Brodeur, T. W. Miller, S. S. Pool, P. J. Bentley, G. K. Krutzikowsky, and J. McCrae.
2005. Pacific sardine (*Sardinops sagax*) abundance, distribution, and ecological relationships in the Pacific Northwest. Calif. Coop. Oceanic Fish. Invest. Rep. 46:122–143.

Félix-Uraga, R., V. M. Gómez-Muñoz, C. Quiñónez-Velázquez, F. N. Melo-Barrera, and W. García-Franco.
2004. On the existence of Pacific sardine groups off the west coast of the Baja California Peninsula and southern California. Calif. Coop. Oceanic Fish. Invest. Rep. 45:146–151.

Félix-Uraga, R., C. Quiñónez-Velázquez, K. T. Hill, V. M. Gómez-Muñoz, F. N. Melo-Barrera, and W. García-Franco.
2005. Pacific sardine (*Sardinops sagax*) stock discrimination off the west coast of Baja California and southern California using otolith morphometry. Calif. Coop. Oceanic Fish. Invest. Rep. 46:113–121.

Fey, D.
2001. Differences in temperature conditions and somatic growth rate of larval and early juvenile spring-spawned herring from the Vistula Lagoon, Baltic Sea manifested in the otolith to fish size relationship. J. Fish. Biol. 58:1257–1273.

Fletcher, W. J.
1995. Application of the otolith weight-age relationship for the pilchard, *Sardinops sagax neopilchardus*. Can. J. Fish. Aquat. Sci. 52:657–664.

Gagliano, M., and M. I. McCormick.
2004. Feeding history influences otolith shape in tropical fish. Mar. Ecol. Prog. Ser. 278:291–206.

Gonzalez-Salas, C., and P. Lenfant.
2007. Interannual variability and intraannual stability of the otolith shape in European anchovy *Engraulis encrasicolus* (L.) in the Bay of Biscay. J. Fish Biol. 70:35–49.

Grant, W. S., and B. W. Bowen.
1998. Shallow population histories in deep evolutionary lineages of marine fishes: Insights from sardines and anchovies and lessons for conservation. J. Heredity 89:415–426.

Hedgecock, D., E. S. Hutchinson, G. Li, F. L. Sly, and K. Nelson.
1989. Genetic and morphometric variations in the Pacific sardine *Sardinops sagax caerulea*: comparisons and contrasts with historical data and with variability in northern anchovy *Engraulis mordax*. Fish. Bull. 87:653–671.

Hoff, G. R., and L. A. Fuiman.
1993. Morphometry and composition of red drum otoliths: changes associated with temperature, somatic growth rate, and age. Comp. Biochem. Physiol. 106A:209–219.

Høie, H., A. Folkvord, and A. Johannessen.
1999. Maternal, paternal and temperature effects on otolith size of young herring (*Clupea harengus* L.) larvae. J. Exp. Mar. Biol. Ecol. 234:167–184.

Hüssy, K.
2008. Otolith shape in juvenile cod (*Gadus morhua*): Ontogenetic and environmental effects. J. Exp. Mar. Biol. Ecol. 364:35–41.

Jónsdóttir, I. G., S. E. Campana, and G. Marteinsdottir.
2006. Otolith shape and temporal stability of spawning groups of Icelandic cod (*Gadus morhua* L.). ICES J. Mar. Sci. 63:1501–1512.

Katayama, S., and T. Isshiki.
2007. Variation in otolith macrostructure of Japanese flounder (*Paralichthys olivaceus*): A method to discriminate between wild and released fish. J. Sea Res. 57:180–186.

Lo, N. C. H., B. J. Macewicz, and D. A. Griffith.
2005. Spawning biomass of Pacific sardine (*Sardinops sagax*), from 1994–2004 off California. Calif. Coop. Oceanic Fish. Invest. Rep. 46:93–112.
2010. Biomass and reproduction of Pacific sardine (*Sardinops sagax*) off the Pacific northwestern United States, 2003–2005. Fish. Bull. 108:174–192.

Lombarte, A., and J. Lleonart.
1993. Otolith size changes related with body growth, habitat depth and temperature. Environ. Biol. Fishes 37:297–306.

McFarlane, G. A., and R. J. Beamish.
2001. The re-occurrence of sardines off British Columbia characterizes the dynamic nature of regimes. Prog. Oceanogr. 49:151–165.

Norton, J. G., and J. E. Mason.
2005. Relationship of California sardine (*Sardinops sagax*) abundance to climate-scale ecological changes in the California Current system. Calif. Coop. Oceanic Fish. Invest. Rep. 46:83–92.

Osborne, J. W., and A. B. Costello.
2004. Sample size and subject to item ratio in principal components analysis. Prac. Assess. Res. Eval. 9(11). http://pareonline.net/getvn.asp?v=9&n=11

Pereyra, R. T., E. Saillant, C. L. Pruett, C. E. Rexroad, A. Rocha-Olivares, and A. R. Gold.
2004. Characterization of polymorphic microsatellites in the Pacific sardine *Sardinops sagax* (Clupeidae). Mol. Ecol. Notes 4:739–741.

Radovich, J.
1982. The collapse of the California sardine fishery. What have we learned? Calif. Coop. Oceanic Fish. Invest. Rep. 23:56–78.

Smith, P. E.
2005. A history of proposals for subpopulation structure in the Pacific sardine (*Sardinops sagax*) population off

western North America. Calif. Coop. Oceanic Fish. Invest. Rep. 46:75–82.

Somarakis, S., I. Kostikas, N. Peristeraki, and N. Tsimenides.
1997. Fluctuating asymmetry in the otoliths of larval anchovy *Engraulis encrasicolus* and the use of developmental instability as an indicator of condition in larval fish. Mar. Ecol. Prog. Ser. 151:191–203.

Strelcheck, A. J., G. R. Fitzhugh, F. C. Coleman, and C. C. Koenig.
2003. Otolith-fish size relationship in juvenile gag (*Mycteroperca microlepis*) of the eastern Gulf of Mexico: a comparison of growth rates between laboratory and field populations. Fish. Res. 60:255–265.

Torres, G. J., A. Lombarte, and B. Morales-Nin.
2000. Sagittal otolith size and shape variability to identify geographical intraspecific differences in three species of the genus *Merluccius*. J. Mar. Biol. Assoc. U.K. 80:333–342.

Turan, C.
2000. Otolith shape and meristic analysis of herring (*Clupea harengus*) in the North-East Atlantic. Arch. Fish. Mar. Res. 48:215–225.

Tuset, V. M., P. L. Rosin, and A. Lombarte.
2006. Sagittal otolith shape used in the identification of fishes of the genus *Serranus*. Fish. Res. 81:316–325.

Valle, R. S., and S. Z. Herzka.
2008. Natural variability in $\delta^{18}O$ values of otoliths of young Pacific sardine captured in Mexican waters indicates subpopulation mixing within the first year of life. ICES J. Mar. Sci. 65:174–190.

Wing, B. L., J. M. Murphy, and T. L. Rutecki.
2000. Occurrence of Pacific sardine, *Sardinops sagax*, off southeastern Alaska. Fish. Bull. 98:881–883.

Yaremko, M. L.
1996. Age determination in Pacific sardine, *Sardinops sagax*. NOAA Tech. Memo. NMFS-SWFSC-223, 32 p.

Population structure, long-term connectivity, and effective size of mutton snapper (*Lutjanus analis*) in the Caribbean Sea and Florida Keys

Evan W. Carson[1]
Eric Saillant[2]
Mark A. Renshaw[1]
Nancie J. Cummings[3]
John R. Gold (contact author)[1]

Email address for contact author: goldfish@tamu.edu

[1] Center for Biosystematics and Biodiversity
Texas A and M University
College Station, Texas 77843-2258

[2] Department of Coastal Sciences
Gulf Coast Research Laboratory
The University of Southern Mississippi
703 East Beach Drive
Ocean Springs, Mississippi 39564

[3] National Marine Fisheries Service
Southeast Fisheries Science Center
75 Virginia Beach Drive
Miami, Florida 33149

Abstract—Genetic structure and average long-term connectivity and effective size of mutton snapper (*Lutjanus analis*) sampled from offshore localities in the U.S. Caribbean and the Florida Keys were assessed by using nuclear-encoded microsatellites and a fragment of mitochondrial DNA. No significant differences in allele, genotype (microsatellites), or haplotype (mtDNA) distributions were detected; tests of selective neutrality (mtDNA) were nonsignificant after Bonferroni correction. Heuristic estimates of average long-term rate of migration (proportion of migrant individuals/generation) between geographically adjacent localities varied from 0.0033 to 0.0054, indicating that local subpopulations could respond independently of environmental perturbations. Estimates of average long-term effective population sizes varied from 341 to 1066 and differed significantly among several of the localities. These results indicate that over time larval drift and interregional adult movement may not be sufficient to maintain population sustainability across the region and that there may be different demographic stocks at some of the localities studied. The estimate of long-term effective population size at the locality offshore of St. Croix was below the minimum threshold size considered necessary to maintain the equilibrium between the loss of adaptive genetic variance from genetic drift and its replacement by mutation. Genetic variability in mutton snapper likely is maintained at the intraregional level by aggregate spawning and random mating of local populations. This feature is perhaps ironic in that aggregate spawning also renders mutton snapper especially vulnerable to overexploitation.

Manuscript submitted 11 April 2011.
Manuscript accepted 18 July 2011.
Fish. Bull. 109:416–428 (2011).

An understanding of the genetic structure of exploited, reef-associated marine fish species is important for their effective conservation and management. Many such species are known to have long larval phases (Boehlert, 1996)—a trait associated with either genetic cohesion or connectivity across regional geographic scales (Shulman and Bermingham, 1995; Rocha et al., 2002). However, many of these species also form stable spawning aggregations where assemblages of individuals gather in large densities with the specific purpose of reproducing, generally at approximately the same time and place each year (Domeier and Colin, 1997). For geographically widespread species, multiple spawning aggregations could tend to minimize connectivity at regional scales if adult movements are intraregionally localized. This effect would be pertinent to management of heavily exploited groups such as snappers and groupers in which spawning aggregations are common (Claro and Lindeman, 2003). Because fishing efforts commonly target spawning aggregations, participating species are at elevated risk of overexploitation and rapid population depletion (Domeier and Colin, 1997; Domeier, 2004; Sadovy de Mitcheson et al., 2008). Knowledge of population structure is thus of importance because separate management of subregional stocks, should they exist, is critical both to avoid over-exploitation and to maintain potentially adaptive genetic variation (Carvalho and Hauser, 1995; Hauser and Ward, 1998). Recent population-genetic studies of species that participate in spawning aggregations have included assessment of genetic variation (Rhodes et al., 2003) and the relationship between effective population size (N_e) and census size (Bekkevold et al., 2002).

In this study, we assessed genetic structure and average long-term connectivity and effective size of mutton snapper (*Lutjanus analis*) sampled from four localities in the northeastern Caribbean Sea and one locality in the Florida Keys. Mutton snapper are an important component of commercial fisheries in this region

(Matos-Caraballo et al., 2004), and fillets often sell for as much as US $12 per pound in Miami seafood markets (Watanabe, 2001). Landings of mutton snapper, however, have declined over the past decade in Puerto Rico (Matos-Caraballo et al., 2004; Cummings, 2007a,2007b) and in southern Florida. In the latter fishery, commercial landings between the years 2006 and 2009 dropped from 127.0 to 53.6 metric tons (http://www.st.nmfs.noaa.gov/st1/commercial/landings/annual_landings.html, accessed July 2011). Although mutton snapper are not considered overfished in U.S. waters of the western Atlantic Ocean and Caribbean Sea (Federal Register, 2005), concern regarding the condition of the fishery has prompted both seasonal and permanent closures off southwest Florida, Puerto Rico, and the U.S. Virgin Islands (http://www.edf.org/article.cfm?contentid=443; http://sero.nmfs.noaa.gov/sf/ClosedAreaCoordinates.htm, accessed March 2011). Finally, aggregate spawning of mutton snapper is well documented (Claro, 1981; Domeier et al.,1996), with known aggregations occurring at Riley's Hump in the Dry Tortugas National Park, Florida (Domeier, 2004; Burton et al., 2006), Gladden Spit, Belize (Graham et al., 2008), numerous sites along the coast of Cuba (Claro and Lindeman, 2003), Turks and Caicos (Mueller, 1994; Doemeier et al., 1997), off the southwest coast of St. Croix in the U.S. Virgin Islands, (SEDAR, 2007), and at La Parguera shelf along the southwest coast of Puerto Rico (Esteves, 2005). Other, less well-documented aggregations occur in the Cayman Islands and the Bahamas (Heyman[1]).

In a recent study by Shulzitski et al. (2009), variation at eight nuclear-encoded microsatellites was used to investigate population structure in mutton snapper sampled from localities off the Florida Keys, two localities in the western Caribbean Sea (Belize and Honduras), and the west coast of Puerto Rico. No evidence of genetic heterogeneity was found, leading these authors to suggest that larval dispersal or long-distance migration of adults maintained genetic homogeneity over such a broad geographic scale. However, simulation studies based on prevailing currents in the Caribbean Sea have indicated that larval transport of reef-associated species in most areas in the region is limited, with average distances of 145 and 212 km for one- and two-month periods of larval dispersal, respectively (Roberts, 1997), and with ecologically relevant larval dispersal distances in the 10–100 km range (Cowen et al., 2000, 2006). In addition, empirical studies in the region have shown that species with the capacity for long-range larval dispersal often exhibit high levels of larval retention (Taylor and Hellberg, 2003) and that the degree of dispersal can differ substantially between windward (high dispersal) and leeward (low dispersal) sides of islands (Swearer et al., 1999). Finally, the few data that exist (Beaumariage, 1969; Mueller, 1995; Farmer, 2009) indicate that movement of adult mutton snapper is generally limited to only a few kilometers.

The possibility of limited larval transport and long-distance adult movement among mutton snapper in the region may indicate that the genetic homogeneity observed by Shulzitski et al. (2009) at markers (microsatellites) presumed to be selectively neutral may obscure other differences that impact local population sustainability. The goal of the present study was to examine this possibility further by using genetic data to assess both long-term connectivity (migration) and effective population size (N_e) among the sampled localities. Populations with homogeneous allele frequencies at selectively neutral loci do not necessarily have the same effective sizes (Saillant and Gold, 2006) and differences in N_e could signal populations with reduced sustainability and capability to respond to environmental pressures such as over-exploitation or habitat degradation (Frankham, 1995).

Materials and methods

A total of 498 mutton snapper were sampled between 2007 and 2009 from four localities in the northern Caribbean Sea and one locality in the Florida Keys (Fig. 1). The locality in the Florida Keys is near a now annually protected mutton snapper spawning aggregation in the Dry Tortugas; the locality off the west coast of Puerto Rico is near several marine protected areas (MPAs) and a mutton snapper spawning aggregation off the southwest coast; the locality off the south coast of St. Thomas is near several MPAs; and the locality off the southwest coast of St. Croix is a seasonally protected mutton snapper spawning aggregation area. Samples from the Florida Keys (FK) were obtained from local fishermen or fish houses in or near Marathon, Florida. Samples from the west coast of Puerto Rico (PR-west) were procured from fish houses in or near Mayaguez, whereas samples from the east coast of Puerto Rico (PR-east) were obtained at fish houses in or near Fajardo. Samples from St. Croix (SC) were obtained as part of an ongoing project of the Caribbean Fishery Management Council (Kojis and Quinn[2]), and samples from St. Thomas (ST) came from the Gustave Quetel Fish House in Frenchtown (Charlotte Amalie) or local fishermen. Sample sizes were as follows: FK (118), PR-east (96), PR-west (94), ST (97), and SC (93). Except for samples from St. Croix (SC), small pieces (4–5 mm^3) of caudal fin were removed from each fish and fixed in 95% ethanol. Samples from St. Croix primarily were internal organs fixed in DMSO storage buffer (Seutin et al., 1991). DNA

[1] Heyman, W. D. 2010. Personal commun. Department of Geography, Texas A&M University, College Station, Texas 77843-3148.

[2] Kojis, B. L., and N. J. Quinn. 2011. Validation of a spawning aggregation of mutton snapper and characterization of the benthic habitats and fish in the mutton snapper seasonal closed area, St. Croix, U.S. Virgin Islands. [Available at http://www.caribbeanfmc.com/pdfs%202011/Mutton%20Snapper%20Report%20for%20CFMC%20-%2014%20Feb%2011%20, Final.pdf, accessed July 2011.]

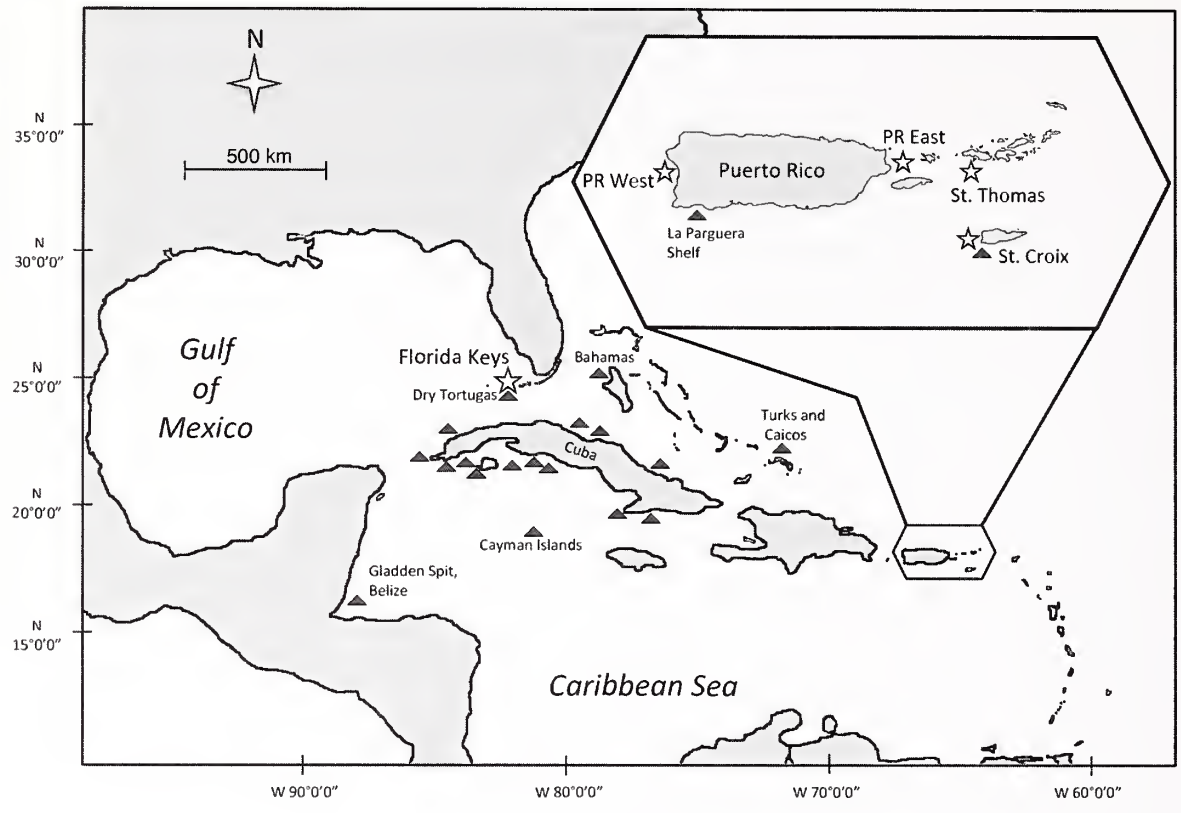

Figure 1

Map of mutton snapper (*Lutjanus analis*) collection sites and known sites of spawning aggregations in the Caribbean Sea and Florida Keys. Collection sites are represented by stars; known aggregation sites are represented by triangles.

was extracted by using a standard phenol-chloroform protocol (Sambrook et al., 1989).

Seventeen microsatellites were surveyed in three multiplex panels: panel 1 (*Lan*6, *Lan*11, *Lan*12, *Lan*13, *Och*4, and *Ra*6), panel 2 (*Lan*9, *Lca*22, *Lca*64, *Lsy*8, *Lsy*13, and *Ra*2), and panel 3 (*Lan*3, *Lca*20, *Lsy*4, *Prs*248, and *Ra*1). Touchdown polymerase-chain-reaction (PCR) protocols were as follows: 95°C for 3 min; 7 cycles at 95°C for 30 sec, annealing at T_{A1} for 1 min, and 72°C for 4 min; 7 cycles at 95°C for 30 sec, annealing at T_{A2} for 1 min, and 72°C for 4 min; and 28 cycles at 95°C for 30 sec, annealing at T_{A3} for 1 min, and 72°C for 4 min, with a final extension of 10 min at 72°C. Annealing temperatures T_{A1}, T_{A2}, and T_{A3}, respectively, were 55°C, 53°C, 51°C (Panel 1), 54°C, 52°C, and 50°C (Panel 2), and 52°C, 49°C, and 46°C (Panel 3). PCR primer sequences for individual microsatellites may be found as follows: *Ra*1, *Ra*2, and *Ra*6 (Bagley and Geller, 1998); *Lca20*, *Lca*22, *Lca*64, and *Prs*248 (Gold et al., 2001); and *Lan*3, *Lan*6, *Lan*9, *Lan*11, *Lan*12, *Lan*13, *Lsy*4, *Lsy*8, *Lsy*13, and *Och*4 (Renshaw et al., 2007). Details regarding fluorescent labeling of primers and amplification are described in Renshaw et al. (2006, 2007). An ABI Prism 377 DNA sequencer (Applied Biosystems Inc., Foster City, CA) was used to separate and visualize amplification products. Gel analysis was performed with Genescan Analysis, vers. 3.1.2® (Applied Biosystems), with allele-calling performed with Genotyper® software, vers. 2.5 (Applied Biosystems). Genotypes at the 16 polymorphic microsatellites assayed may be found at http://wfsc.tamu.edu/doc/, accessed July 2011, under the file name "Microsatellite genotypes of mutton snappers."

A 590 base-pair (bp) fragment of the mitochondrial NADH-dehydrogenase subunit 4 (ND-4) gene was amplified and sequenced for 134 individuals (25–29 from each locality). The primers NAP-2 (Arevalo et al., 1994) and ND4LB (Bielawski and Gold, 2002) were used for fragment amplification, and ND4BL was used for sequencing. Polymerase chain reaction amplifications were run in 30 µL reaction volumes, with ~100 ng whole genomic DNA, 1× GoTaq Flexi Buffer (Promega, Madison, Wisconsin), 1.5 mM $MgCl_2$, 0.5 µM of each primer, 250 µM of each dNTP, and 1.7U GoTaq *Taq* polymerase (Promega). The PCR protocol consisted of a 95°C initial denaturation, followed by 35 cycles of 95°C for 30 sec, 50°C for 45 sec, and 72°C for 1 min, with a 10 minute final extension at 72°C. Sequencing reactions were carried out with a Big Dye terminator kit®, vers. 3.1 (Applied Biosystems), according to the manufacturer's recommendations; products were separated and visualized on an ABI 3100 capillary sequencer

(Applied Biosystems) and sequences were aligned and edited in Sequencher, vers. 4.0 (Gene Codes Corp., Ann Arbor, MI).

For microsatellites, summary statistics, including number of alleles, allelic richness, unbiased gene diversity (expected heterozygosity), and the inbreeding coefficient F_{IS}, measured as f of Weir and Cockerham (1984), were generated in FSTAT (Goudet, 1995; vers. 2.9.3.2, http://www2.unil.ch/popgen/softwares/fstat.htm, accessed July 2011). Homogeneity in allelic richness and gene diversity among the five locations were assessed by using Friedman rank tests, with SPSS software (http://www-01.ibm.com/software/analytics/spss/products/statistics/, accessed July 2011). Departure from Hardy-Weinberg (HW) equilibrium expectations for each locality was tested with exact probability tests in Genepop (Raymond and Rousset, 1995; vers. 3.4, http://genepop.curtin.edu.au/, accessed March 2011), by using a Markov Chain approach (Guo and Thompson, 1992), with 10,000 dememorizations, 500 batches, and 5000 iterations per batch. Global and pairwise (between localities) exact tests of homogeneity of allelic (genic) and genotypic distributions also were conducted in Genepop; genetic homogeneity among locations was further tested by using analysis of molecular variance (AMOVA), with the program Arlequin (Excoffier and Lischer, 2010; vers. 3.5.1.2, http://cmpg.unibe.ch/software/arlequin35/, accessed March 2011). Sequential Bonferroni correction (Rice, 1989) of P values was applied for all simultaneous tests. Microchecker (van Oosterhout et al., 2004) was used to determine whether genotype scores at each locus were compromised by the presence of null alleles, stuttering, or genotyping errors.

For mitochondrial ND-4 DNA sequences, number of haplotypes and haplotype diversity were determined by using DnaSP, vers. 5.10.01 (Rozas et al., 2003; http://www.ub.edu/dnasp/, accessed March 2011); haplotype richness and nucleotide diversity for each sample locality were estimated following El Mousadik and Petit (1996) and using the software Rarefac (available at http://www.pierroton.inra.fr/genetics/labo/Software/Rarefac/, accessed July 2011) and Arlequin, respectively. A bootstrap resampling method (Dowling et al., 1996) was used to test homogeneity of haplotype number and diversity among localities. The observed haplotype number and diversity at each locality was compared to the distribution in 1000 bootstrap samples of a comparable size drawn from the entire population (all samples pooled); resampling was conducted in PopTools, a free add-in to Microsoft Excel and available at http://www.poptools.org/, accessed July 2011. Differences in average nucleotide diversity were considered significant if pairwise comparisons differed by more than two standard errors. Homogeneity in mtDNA haplotype distributions among localities was tested using global exact tests and analysis of molecular variance (AMOVA), as implemented in Arlequin. Pair-wise (between locations) estimates of Φ_{ST}, an analogue of F_{ST}, were generated by using Arlequin; Φ_{ST} estimates were based on pair-wise genetic distances, with significance determined by exact tests (Raymond and Rousset, 1995; Goudet et al., 1996), as implemented in Arlequin. Selective neutrality of mtDNA variation in each sample was tested by calculating Fu's (1997) F_S statistic and Fu and Li's (1993) D^* and F^* statistics, as implemented in the DnaSP program. Significance of F_S, D^*, and F^* was assessed in FSTAT by using 10,000 coalescent simulations (after Rozas et al., 2003) based on the observed number of segregating sites in each sample.

The coalescent-based program Migrate (Beerli and Felsenstein 2001; vers. 3.2.6, http://popgen.sc.fsu.edu/Migrate/Migrate-n.html, accessed July 2011) was used to generate maximum-likelihood estimates of both the average long-term (mutation-scaled) migration rate (M) between pairs of localities and the parameter theta (Θ) for each locality. Because the model used in Migrate explicitly accounts for migration, estimates of Θ can be generated for individual subpopulations within a larger metapopulation (Waples, 2010). The average long-term migration rate (m) between localities was estimated as $M = m/\mu$, where μ is the average, per gene mutation rate. Values of theta ($4N_e\mu$) were used to estimate average long-term effective population size (N_e) of each locality. To obtain estimates of m and N_e, the modal mutation rate (μ) of the microsatellite data set was obtained by using the Bayesian coalescent approach of Beaumont (1999) and Storz and Beaumont (2002) and the software MSVAR (vers. 0.4.1b, http://www.rubic.rdg.ac.uk/~mab/software.html, accessed July 2011). Because simulations in Migrate are computationally demanding, all parameter estimates were based on a random sample of 25 individuals from each location (125 individuals total). A preliminary analysis (short run) established initial estimates for both M and Θ that were then used as starting values in final long runs. Parameter estimates were obtained by averaging three replicate long runs that included 40 short Monte Carlo Markov chains (MCMC, 10^4 gene trees sampled) and three long chains (2.5×10^6 gene trees sampled). To ensure parameter stability, the first 1×10^4 steps of each chain were discarded as burn-in.

Results

Summary statistics for microsatellites are presented in Table 1. Microsatellite *Lca*64 was monomorphic for a 111-bp allele (scored with primers as 151 bp) and was excluded from further analysis. Of the remaining 16 microsatellites, the number of alleles ranged from 2–3 at *Lsy*8 to 19–25 at *Prs*248. Allelic richness ranged from 2.00–2.86 at *Lsy*8 and from 19.00–23.67 at *Prs*248, and expected (unbiased) gene diversity ranged from 0.050–0.118 at *Lsy*8 and from 0.860–0.901 at *Lan*11. Across all microsatellites and localities, number of alleles, allelic richness, and gene diversity averaged (±standard error [SE]) 10.05 (0.26), 9.80 (0.22), and 0.594 (0.01), respectively. No significant differences (Freidman's rank tests) in allelic richness (P=0.232) or gene diversity (P=0.373) were found among localities.

Table 1

Summary statistics for 16 nuclear-encoded microsatellites and a 590 base-pair sequence of the mitochondrially encoded ND-4 gene for mutton snapper (*Lutjanus analis*) sampled from four localities in the northeastern Caribbean Sea and one locality in the Florida Keys. For microsatellites, n is sample size , #A is number of alleles, A_R is allelic richness, H_E is gene diversity (expected heterozygosity), P_{HW} is the probability of conforming to expected Hardy-Weinberg genotypic proportions, and F_{IS} is an inbreeding coefficient (measured as f of Weir and Cockerham, 1984). For mitochondrial DNA (mtDNA): n is sample size, $\#_{Hobs}$ is observed number of haplotypes, H_R is haplotype richness, H_{Dobs} is observed haplotype (nucleon) diversity, and π_D is nucleotide diversity. $\#H_{exp}$ and H_{Dexp} are expected haplotype number and diversity (95% confidence interval [CI]), respectively, as determined by bootstrap resampling of the entire population.

Microsatellite	St. Croix	St. Thomas	Puerto Rico-east	Puerto Rico-west	Florida Keys
*Lan*3					
n	81	97	96	94	118
#A	14	14	15	13	13
A_R	13.98	13.81	14.58	12.84	12.78
H_E	0.849	0.857	0.829	0.838	0.857
P_{HW}	0.274	0.502	0.011	0.875	0.377
F_{IS}	0.026	−0.035	0.020	0.061	−0.009
*Lan*6					
n	93	97	96	94	114
#A	20	17	18	19	18
A_R	19.54	16.75	17.80	18.78	17.11
H_E	0.854	0.835	0.882	0.897	0.868
P_{HW}	0.033	0.282	0.776	0.838	0.676
F_{IS}	0.030	−0.024	0.032	0.016	−0.010
*Lan*9					
n	93	97	96	94	118
#A	13	12	12	12	12
A_R	12.69	11.56	11.80	11.93	11.75
H_E	0.776	0.774	0.781	0.746	0.795
P_{HW}	0.628	0.236	0.477	0.322	0.230
F_{IS}	0.058	−0.039	−0.027	−0.012	−0.003
*Lan*11					
n	91	96	96	94	116
#A	21	20	22	21	24
A_R	20.50	19.54	21.54	20.06	22.25
H_E	0.889	0.869	0.886	0.860	0.901
P_{HW}	0.002	0.766	0.743	0.968	0.151
F_{IS}	0.110	0.005	−0.070	−0.027	−0.004
*Lan*12					
n	93	97	96	94	118
#A	5	5	5	5	6
A_R	4.86	5.00	4.95	4.98	5.86
H_E	0.595	0.646	0.643	0.611	0.642
P_{HW}	0.208	0.823	0.193	0.080	0.057
F_{IS}	0.151	−0.022	0.011	−0.045	0.023
*Lan*13					
n	93	97	96	94	118
#A	4	4	5	3	5
A_R	3.98	3.83	4.81	3.00	4.36
H_E	0.295	0.297	0.378	0.380	0.341
P_{HW}	0.083	0.198	0.337	0.234	0.863
F_{IS}	0.161	0.064	0.063	0.076	−0.044

continued

Table 1 (continued)

Microsatellite	St. Croix	St. Thomas	Puerto Rico-east	Puerto Rico-west	Florida Keys
*Lca*20					
n	93	96	95	94	117
#A	12	14	13	14	12
A_R	11.84	13.80	12.96	13.64	11.86
H_E	0.589	0.646	0.683	0.677	0.659
P_{HW}	0.115	0.610	0.039	0.388	0.125
F_{IS}	0.032	−0.015	0.076	0.010	0.041
*Lca*22					
n	91	97	96	94	118
#A	5	4	5	4	6
A_R	4.88	3.83	4.83	3.85	5.35
H_E	0.546	0.465	0.483	0.481	0.507
P_{HW}	0.106	0.744	0.600	0.710	0.440
F_{IS}	0.074	0.003	0.072	0.005	0.013
*Lsy*4					
n	93	95	95	93	118
#A	4	4	4	4	4
A_R	4.00	4.00	4.00	4.00	4.00
H_E	0.270	0.331	0.386	0.329	0.355
P_{HW}	0.682	0.308	0.867	0.806	0.932
F_{IS}	−0.077	0.078	−0.090	−0.077	−0.050
*Lsy*8					
n	93	96	95	94	118
#A	3	2	2	3	2
A_R	2.86	2.00	2.00	2.85	2.00
H_E	0.083	0.118	0.052	0.102	0.050
P_{HW}	1.000	1.000	1.000	1.000	1.000
F_{IS}	−0.034	−0.062	−0.022	−0.046	−0.022
*Lsy*13					
n	91	96	96	94	118
#A	10	7	7	7	7
A_R	9.42	6.81	6.95	6.81	6.65
H_E	0.733	0.716	0.739	0.728	0.742
P_{HW}	0.007	0.875	0.037	0.010	0.633
F_{IS}	0.105	−0.018	−0.015	0.065	−0.073
*Och*4					
n	93	97	96	94	118
#A	5	4	4	4	5
A_R	4.98	4.00	4.00	4.00	4.68
H_E	0.559	0.576	0.535	0.553	0.565
P_{HW}	0.334	0.318	0.495	0.238	0.004
F_{IS}	0.115	−0.127	0.085	−0.039	0.160
*Prs*248					
n	80	97	94	91	117
#A	19	22	25	24	24
A_R	19.00	21.28	23.67	22.48	21.57
H_E	0.860	0.886	0.886	0.870	0.870
P_{HW}	0.011	0.583	0.507	0.190	0.818
F_{IS}	0.084	0.000	0.014	−0.015	0.007

continued

Table 1 (continued)

Microsatellite	St. Croix	St. Thomas	Puerto Rico-east	Puerto Rico-west	Florida Keys
*Ra*1					
n	93	97	96	94	118
#A	5	4	5	6	6
A_R	4.84	3.97	4.67	5.83	5.25
H_E	0.592	0.560	0.558	0.606	0.567
P_{HW}	0.877	0.327	0.150	0.308	0.410
F_{IS}	0.037	0.043	0.142	−0.019	0.059
*Ra*2					
n	93	94	96	94	118
#A	19	17	18	19	17
A_R	18.52	16.51	17.13	18.63	16.04
H_E	0.780	0.767	0.753	0.778	0.781
P_{HW}	0.345	0.873	0.466	0.549	0.436
F_{IS}	0.008	−0.013	0.073	−0.012	−0.020
*Ra*6					
n	93	97	92	94	118
#A	2	4	4	3	3
A_R	2.00	3.65	3.87	2.85	2.90
H_E	0.053	0.109	0.134	0.111	0.105
P_{HW}	1.000	0.106	1.000	1.000	1.000
F_{IS}	−0.022	0.050	−0.052	−0.051	−0.046
mtDNA					
n	27	26	29	25	27
$\#H_{obs}$	11	11	11	11	10
$\#H_{exp}$	9.6 (7–12)	9.9 (7–13)	9.5 (7–12)	9.6 (7–12)	9.7 (7–13)
H_R	10.97	10.99	10.92	11.00	9.97
H_{Dobs}	0.832	0.812	0.865	0.873	0.721
H_{Dexp}	0.835	0.818	0.873	0.818	0.835
(95% CI)	(0.732–0.915)	(0.709–0.900)	(0.788–0.934)	(0.693–0.897)	(0.731–0.916)
π_D	0.003	0.004	0.004	0.004	0.003

Significant deviations from Hardy Weinberg equilibrium were found before Bonferroni correction in nine of 80 tests (Table 1). Only one microsatellite (*Lan*11) at one locality (SC) deviated significantly (P=0.0019) from expectation after correction. Analysis with Microchecker indicated an excess of homozygotes, indicating possible null alleles, at *Lan*11 (in SC) and *Och*4 (in FK), a finding reflected in the F_{IS} values of 0.11 and 0.16 (Table 1), respectively, for these microsatellites at those localities. Sizes of observed alleles were compatible with the stepwise mutation model (SMM) for all microsatellites, except sizes of *Lca*20, *Lsy*13, and *Prs*248. Very rare alleles at *Lca*20 (allele 231) and *Prs*248 (allele 227) that differed by one base from their "regular" dinucleotide repeat were excluded from the analysis (Migrate) where a SMM was assumed. Two such alleles (alleles 118 and 120) were found at *Lsy*13; consequently, *Lsy*13 also was excluded from analysis with Migrate.

A total of 25 mtDNA haplotypes were observed among the 134 individuals sequenced. The number and distribution of mtDNA haplotypes across localities are given in Table 2; summary statistics for mtDNA may be found in Table 1. Haplotype richness ranged from 9.97 (FK) to 11.00 (PR-west), and haplotype diversity ranged from 0.72 (FK) to 0.87 (PR-west). Results of bootstrap resampling analysis indicated that observed haplotype number and diversity at each locality did not deviate significantly from expectations in random subsamples of the overall data set (Table 1). Estimates of haplotype richness and nucleotide diversity were essentially identical at all localities (Table 1).

Exact tests of homogeneity of both microsatellite allele and genotype distributions among localities were nonsignificant (P=0.225, alleles; P=0.288, genotypes), and the among-localities component of molecular variance (all microsatellites combined), estimated by AMOVA, did not differ significantly from zero (Φ_{ST}=−0.0001, P=0.644). Nearly identical results were obtained for mtDNA; an exact test of homogeneity of haplotype distribution was nonsignificant (P=0.590) and the among-locality component of molecular variance (from AMOVA) did not differ significantly from zero (Φ_{ST}=−0.010,

Table 2

Distribution of individual haplotypes in 134 mutton snapper (*Lutjanus analis*) sampled from four localities in the northeastern Caribbean Sea and one locality in the Florida Keys. Numbers below each locality indicate observed occurrence of each of 25 haplotypes identified across all localities. GenBank® is a genetic sequence database, available at http://www.ncbi.nlm.nih.gov/genbank/, accessed July 2011).

Haplotype	St. Croix	St. Thomas	Puerto Rico-east	Puerto Rico-west	Florida Keys	GenBank no.
1	1	0	1	0	1	JF514891
2	10	10	9	5	14	JF514892
3	1	0	0	1	0	JF514893
4	0	0	0	1	0	JF514894
5	0	0	0	1	0	JF514895
6	0	1	2	2	0	JF514896
7	0	0	1	0	0	JF514897
8	5	6	4	7	4	JF514898
9	0	1	0	0	1	JF514899
10	0	0	0	0	1	JF514900
11	1	0	0	0	0	JF514901
12	0	0	0	1	0	JF514902
13	1	0	0	0	0	JF514903
14	2	1	0	0	1	JF514904
15	1	0	1	0	0	JF514905
16	0	0	1	0	0	JF514906
17	0	1	0	1	1	JF514907
18	0	2	2	0	2	JF514908
19	3	1	5	4	1	JF514909
20	0	1	1	1	0	JF514910
21	0	0	0	0	1	JF514911
22	0	0	0	1	0	JF514912
23	1	0	0	0	0	JF514913
24	1	1	2	0	0	JF514914
25	0	1	0	0	0	JF514915
Total	27	26	29	25	27	

P=0.785). Pair-wise exact tests (between samples) for both microsatellites and mtDNA also were nonsignificant (data not shown but available from E. W. Carson). Finally, nine of 15 tests of selective neutrality were significant before Bonferroni correction; none remained significant after Bonferroni correction.

Estimates of average long-term mutation-scaled migration (M) between geographically adjacent pairs of sample localities are presented in Table 3. Estimates of M between adjacent localities were generated by averaging bidirectional estimates from Migrate, in part because bidirectional estimates generally were equivalent, and in part because confidence intervals for estimates of m, generated with Migrate, are generally compromised (Abdo et al., 2004). Based on a modal mutation rate (μ) over all microsatellites of 2.51×10^{-4}, generated with MSVAR, estimates of average long-term migration rate (m) between adjacent localities varied from 0.0033 (PR-west vs. PR-east) to 0.0054 (SC vs. ST). Higher estimates of m were found between ST and SC and between ST and PR-east (Table 3).

Estimates of average long-term, effective population size (N_e) for each locality (Table 3) were derived from Θ values generated in Migrate ($N_e=\Theta/4\mu$), with μ equal to the modal mutation rate of 2.51×10^{-4} obtained from the Bayesian coalescent approach of Beaumont (1999) and Storz and Beaumont (2002). Initial Migrate runs revealed that the sample from SC had by far the lowest estimate of N_e. Because genotypes at microsatellite *Lan*11 did not conform to Hardy-Weinberg expectations in the sample from SC (Table 1), values reported in Table 3 reflect Migrate runs without *Lan*11. Average long-term N_e among the five localities varied from a low of 341 (SC) to a high of 1066 (FK). Estimates from Migrate of 95% confidence intervals (CIs) indicate significant differences in average long-term N_e among localities (Table 3); the lower values for PR-west and SC are especially relevant because these two localities are close to known mutton snapper spawning aggregation sites in the U.S. Caribbean.

Discussion

Analysis of microsatellite and mtDNA variation in mutton snapper sampled from localities in the north-

eastern Caribbean Sea and the Florida Keys revealed no evidence of either genetic heterogeneity or population subdivision. Shulzitski et al. (2009) found similar results in their study of mutton snapper from the west coast of Puerto Rico, the Florida Keys, and localities in Belize and Honduras. Because two of the localities (one in the Florida Keys and one along the west coast of Puerto Rico) sampled by Shulzitski et al. (2009) were very near two of the localities sampled in this study, it appears that mutton snapper from the Leeward (northeastern) Islands in the Lesser Antilles to the Central American coast to the eastern Gulf of Mexico may be homogeneous in frequencies of alleles at microsatellite markers.

Shulzitski et al. (2009) suggested that genetic homogeneity among mutton snapper in the region stemmed from long-distance larval dispersal or adult migration to spawning aggregations. Estimates of long-term migration rates (m) in our study between geographically proximal localities, some separated by less than 100 km, ranged from 0.33% to 0.54%. These estimates of m, however, should be viewed as heuristic, in part because Migrate tends to underestimate m and because confidence intervals for m are generally unreliable (Abdo et al. 2004), and in part because of potential bias introduced by the necessity of running subsets of data owing to the computational demands of Migrate (Palstra et al., 2007). On the other hand, even if our estimates of m were 20 times higher, there still could be independent response of local populations to environmental or other (e.g., fishing) perturbations (Hastings, 1993, Hauser and Carvalho, 2008). Because the genetic markers used here and in Shulzitski et al. (2009) are presumed to be selectively neutral, genetic homogeneity in this case could be decoupled from genetic factors that affect adaptability and sustainability of local populations. That is, patterns of variation in genes affecting traits influenced by natural selection do not necessarily follow the same patterns as selectively neutral genes (or genetic markers) and geographic differences in adaptively useful genes (or alleles) can be maintained even in the face of substantial gene flow (Conover et al., 2005). Our estimates of average long-term migration also are consistent with the argument of Roberts (1997) that regional currents in the Caribbean Sea are insufficient for larval dispersal across the region.

The estimates of average long-term effective size varied three-fold among the localities sampled and the lowest and highest effective size was found in the samples from St. Croix (N_e=341) and the Florida Keys (N_e=1066), respectively. Briefly, N_e is the number of breeding individuals in an ideal population that experience the same amount of genetic drift and show the same dispersion of allele frequencies or inbreeding as the population under consideration (Wright, 1931) and is of importance as a measure of a population's response to evolutionary and ecological forces (Waples, 2010). For the conservation and management of exploited biological resources, effective size reflects fixation of deleterious alleles, loss of adaptive genetic variance, and the capacity to respond to either natural selection or environmental perturbation (Franklin, 1980; Anderson, 2005). Long-term estimates of N_e represent a harmonic mean of N_e over approximately $4N_e$ generations (Hare et al., 2011), meaning that 1) smaller values (that may have occurred either in the past or recently) will have a greater weight on average values, and 2) the time over which long-term N_e in mutton snapper was estimated ranged between ~1500 and >4000 generations. Because of the time period usually involved, estimates of long-term N_e are not necessarily reliable indicators of contemporary N_e but do provide a baseline for evaluating management planning (Hare et al, 2011). Differences in long-term N_e, however, do indicate possible differences in long-term demographic dynamics that potentially affect the number of individuals over time that produce surviving offspring (and hence population sustainability). Demographic factors that generate differences in effective size are difficult to assess empirically and can stem from varying numbers of breeding individuals across generations or from variance in reproductive success of either or both sexes (Charlesworth, 2009). In both cases, a number of factors including food availability, habitat quality, predation, or mortality are likely involved (Saillant and Gold, 2006).

The low effective size observed for the sample of mutton snapper taken off the southwest coast of St.

Table 3

Estimates of average long-term mutation-scaled migration (M) and rate of migration (m, proportion of migrant individuals/generation), and of average long-term effective size (N_e) for mutton snapper (*Lutjanus analis*). Estimates of M and m are presented for pair-wise comparison of geographically adjacent sample localities; distance (in km) between pairs of localities is approximate. Estimates of N_e and 95% confidence intervals (CI) are presented for each of five sample sites. PR=Puerto Rico.

Comparison	M	m	Distance
St. Croix and St. Thomas	21.46	0.0054	60
St. Croix and PR-east	15.16	0.0038	90
St. Thomas and PR-east	35.11	0.0053	90
PR-east and PR-west	13.27	0.0033	200
PR-west and Florida Keys	15.07	0.0038	>1,600

Site	N_e	Lower 95% CI	Upper 95% CI
St. Croix	341	314	372
St. Thomas	922	847	1007
PR-east	828	766	896
PR-west	646	607	689
Florida Keys	1066	987	1155

Croix is of possible concern for several reasons. First, the average long-term N_e estimate of 341 is below the upper bound of the "50/500" rule (Rieman and Allendorf, 2001), where an effective size of 500 or greater is needed to maintain the equilibrium between the loss of adaptive genetic variance from genetic drift and its replacement by mutation (Franklin, 1980; Schultz and Lynch, 1997). A potential consequence of sustained low effective size over time would be loss of adaptive genetic variance and reduced capacity to respond to perturbation (including exploitation). Second, this sample of mutton snapper came from a known spawning aggregation site that currently is under a joint territorial and federal closure during the spawning season (http://fw.dpnr.gov.vi/fish/Docs/Fisheries%20Master%20Plan/Sections/Appendix3.pdf, accessed July 2011). The estimate of effective size certainly indicates that the closure is appropriate and timely. Finally, St. Croix is near the northeastern edge of the Lesser Antilles and the spawning aggregation site is located on the leeward side of the island. Surface currents in the area are almost all to the west (Roberts, 1997) and include the Anegada Passage, a fairly wide channel that connects the Atlantic Ocean with the Caribbean Sea and runs westward between St. Thomas and St. Croix (Johns et al., 2002). Both the prevailing currents and the observation (Swearer et al., 1999) that leeward-island sites are prone to larval retention and less affected by larval immigration than windward locations would indicate that immigration into the spawning aggregation from locations outside of St. Croix could be limited. Limited immigration into St. Croix waters from outside potentially could impede recovery if the spawning aggregation becomes depleted. These inferences also are consistent with the findings of Wares and Pringle (2008) who found that N_e may be reduced in populations where there is unidirectional transport of individuals away from natal grounds.

The differences in long-term N_e among the samples of mutton snapper further indicate that at least historically there may have been distinct demographic stocks within the region. In addition to the low estimate of N_e for the sample from St. Croix, the estimate for the sample from St. Thomas (N_e=922) was nearly three times as large as the estimate for St. Croix, yet the distance between the two localities (60 km) is substantially less than the larval-dispersal ranges of Roberts (1999) and the ecologically relevant larval dispersal distances of Cowen et al. (2000, 2006). Saillant and Gold (2006) in their study of red snapper (*Lutjanus campechanus*) in the Gulf of Mexico defined demographic stocks as geographic samples that differed in dynamics that potentially affected N_e and the number of individuals that produce surviving offspring. In their study, estimates of N_e were negatively correlated with several critical fishery parameters, including size at age, maximum size, proportion of smaller and younger fish, and size and age of females at sexual maturity, reported by Fischer et al. (2004) and Woods et al. (2003), respectively. Similar age and growth and reproductive studies on mutton snapper in the U.S. Caribbean are clearly warranted.

At present, mutton snapper in the U.S. Caribbean (Puerto Rico, St. Thomas/St. John, and St. Croix) are managed as a single management unit, although island-specific management is under consideration. Based on data on prevailing surface currents, low probability of larval input, and restricted movements of adults, the life-history subgroup of a recent stock assessment (SEDAR, 2007) indicated a two-stock hypothesis, with one stock on the Puerto Rican platform (Puerto Rico and St. Thomas/St. John) and a second stock around St. Croix. The estimates of long-term N_e are consistent with the hypothesis that mutton snapper off St. Croix may represent a different demographic stock. In addition, the estimate of long-term N_e for mutton snapper of the west coast of Puerto Rico (N_e=646) is less than the estimate for the east coast of Puerto Rico (N_e=828) and nearly 1.5-fold less than the estimate for St. Thomas. This could indicate that there are different demographic stocks of mutton snapper on the Puerto Rican platform. Further study of mutton snapper off the west coast of Puerto Rico is likely justified because our sample locality is near a known spawning aggregation (Esteves, 2005). Finally, stock structure of mutton snapper in the U.S. Caribbean may follow metapopulation models suggested by Kritzer and Sale (2002), Hellberg et al. (2002), and Østergaard et al. (2003) where 1) subpopulations (stocks) may be asynchronous demographically but display homogeneity at selectively neutral (genetic) markers, and 2) subpopulations may be independent in terms of recruitment events and yet show no genetic differences because of sporadic gene flow.

Conclusions

Results of our study indicate that mutton snapper across the Caribbean Sea to the Florida Keys may be subdivided into a number of demographic stocks that differ in aspects that impact effective size and hence local sustainability. These differences could easily be both genetic and environmental, and in the future it will be of interest to apply new genomic tools (Allendorf et al., 2010) that allow identification of specific genomic regions responding to local adaptation. A second implication of our results is that neither larval drift nor inter-regional adult movement may be sufficient over time to offset these differences. Critical genetic variability in mutton snapper at the intraregional level, consequently, is likely maintained by aggregate spawning and random mating of local populations. It is perhaps ironic that the life-history characteristic (aggregate spawning) that makes mutton snapper especially vulnerable to overexploitation also could be a critical asset in maintaining local genetic diversity. This characteristic elevates the importance of securing the vitality of spawning aggregations in species such as mutton snapper. Protective measures for spawning aggregations, including seasonal closures and appropriately placed marine protected areas (MPAs),

are clearly critical steps to help ensure sustainability of species with this life history in the Caribbean Sea and Florida Keys.

Acknowledgments

We thank the following for their invaluable assistance in obtaining samples for this study: L. Anibal, J. Leon, H. Lopez, D. Matos-Caraballo, and A. Rosario of the of Department of Natural and Environmental Resources Fisheries Research Laboratory in Mayaguez, Puerto Rico; W. Ledee and D. Olsen of the St. Thomas Fishermen's Association; R. Nemeth of the University of the Virgin Islands; H. Rivera and W. Tobias of the U.S. Virgin Islands Division of Fish and Wildlife, and R. Beaver of the Florida Fish and Wildlife Commission. We especially thank B. Kojis for her efforts in obtaining the samples of mutton snapper from St. Croix. Work was supported by the Cooperative Research Program of the U.S. Department of Commerce (Grant NA06NMF4540061), and the Texas AgriLife Research Projects H-6703. Sampling by B. Kojis was supported by a grant (NA08NMF4410463) to the Caribbean Fishery Management Council under the NOAA Coral Reef Conservation Grant Program. We also thank the anonymous reviewers whose comments helped improve the manuscript. This article is number 79 in the series "Genetic Studies in Marine Fishes" and contribution number 197 of the Center for Biosystematics and Biodiversity at Texas A&M University.

Literature cited

Abdo, Z., K. A. Crandall, and P. Joyce.
2004. Evaluating the performance of likelihood methods for detecting population structure and migration. Mol. Ecol. 13:837–851.

Allendorf, F. W., P. A. Hohenlohe, and G. Luikart.
2010. Genomics and the future on conservation genetics. Nature Rev. Genetics 11:697–709.

Anderson, E. C.
2005. An efficient Monte Carlo method for estimating N_e from temporally spaced samples using a coalescent-based likelihood. Genetics 170:955–967.

Arevalo, E., S. Davis, and J. Sites Jr.
1994. Mitochondrial DNA sequence divergence and phylogenetic relationships among eight chromosome races of the *Sceloporus grammicus* complex (Phrynosomatidae) in Central Mexico. Syst. Biol. 43:387–418.

Bagley, M. J., and J. B. Geller.
1998. Characterization of microsatellite loci in vermillion snapper *Rhomboplites aurorubens* (Percoidei: Lutjanidae). Mol. Ecol. Notes 7:1089–1090.

Beaumariage, D. S.
1969. Returns from the 1965 Schlitz tagging program including a cumulative analysis of previous results. Florida Dept. Nat. Res. Tech. Ser. No. 59:1–38.

Beaumont, M. A.
1999. Detecting population expansion and decline using microsatellites. Genetics 153:2013–2029.

Beerli, P., and J. Felsenstein.
2001. Maximum likelihood estimation of a migration matrix and effective population sizes in *n* subpopulations using a coalescent approach. Proc. Nat. Acad. Sci. USA 98:4563–4568.

Bekkevold, D., M. M. Hansen, and V. Loeschke.
2002. Male reproductive competition in spawning aggregations of cod (*Gadus morhua*, L.). Mol. Ecol. 11:91–102.

Bielawski, J. P., and J. R. Gold.
2002. Mutation patterns of mitochondrial H- and L-strand DNA in closely related cyprinid fishes. Genetics 161:1589–1597.

Boehlert, G. W.
1996. Larval dispersal and survival in tropical reef fishes. *In* Tropical reef fisheries (N. V. C. Polunin and C. M. Roberts, eds.), p. 61–84. Chapman Hall, London.

Burton, M. L., K. J. Brennan, R. C. Múñoz, and R. O. Parker Jr.
2006. Preliminary evidence of increased spawning aggregations of mutton snapper (*Lutjanus analis*) at Riley's Hump two years after establishment of the Tortugas South Ecological Reserve. Fish. Bull.103:404–410.

Carvalho, G. R., and L. Hauser.
1995. Molecular genetics and the stock concept in fisheries. *In* Molecular genetics in fisheries (G. R. Carvalho and T. J. Pitcher, eds.), p. 55–80. Chapman and Hall, London.

Charlesworth, B.
2009. Effective population size and patterns of molecular evolution and variation. Nature Rev. Genetics 10:195–205.

Claro, R.
1981. Ecología y ciclo de vida del pargo criollo, *Lutjanus analis* (Cuvier), en la plataforma cubana. nf. Ceint.-Téc., Acad. Cienc. Cuba 186:1–83.

Claro, R., and K. C. Lindeman.
2003. Spawning aggregation sites of snapper and grouper species (Lutjanidae and Serrandidae) on the insular shelf of Cuba. Proc. Gulf Carib. Res. Inst. 14:91–106.

Conover, D. O., S. A. Arnott, M. R. Walsh, and S. B. Munch.
2005. Darwinian fishery science: lessons from the Atlantic silverside. Can. J. Fish. Aquat. Sci. 62:730–737.

Cowen, R. K., K. M. M. Lwiza, S. Sponaugle, C. B. Paris, and D. B. Olson.
2000. Connectivity of marine populations: open or closed? Science 287:857–859.

Cowen, R. K., C. B. Paris, and A. Srinivasan.
2006. Scaling of connectivity in marine populations. Science 311:522–527.

Cummings, N. J.
2007a. Updated commercial catch per unit effort indices for mutton snapper line and pot fisheries in Puerto Rico, 1983–2006. Sustainable Fisheries Division, Southeast Fisheries Science Center, NMFS, NOAA, Miami, FL, contribution no. SFD-2007-18, SEDAR14-AW-01. 9 p. [Available at: http://www.sefsc.noaa.gov/sedar/, accessed July 2011.]
2007b. An examination of mutton snapper, *Lutjanus analis*, commercial catch per unit of effort in Puerto Rico from 1983–2005 available for use in developing estimates of abundance. Sustainable Fisheries Division, Southeast Fisheries Science Center, NMFS, NOAA, Miami, FL, contribution no. SFD-2007-18, SEDAR 14 assessment workshop report no. 1, SEDAR14-AW-01-Addendum 1, 44 p. [Available at http://www.sefsc.noaa.gov/sedar/, accessed July 2011.]

Domeier, M. L.
2004. A potential larval recruitment pathway originating from a Florida marine protected area. Fish. Oceanog. 13:287–294.
Domeier, M. L., and P. L. Colin.
1997. Tropical reef fish spawning aggregations: defined and reviewed. Bull. Mar. Sci. 60:698–726.
Domeier, M. L., C. Koenig, and F. Coleman.
1996. Reproductive biology of the gray snapper (*Lutjanus griseus*), with notes on spawning for other western Atlantic snappers (Lutjanidae). *In* Biology, fisheries and culture of tropical groupers and snappers (F. Arreguin-Sanchez, J. L. Munro, M. C. Balgos, and D. Pauly, eds.), p. 189–201. Int. Cent. Living Aquat. Res. Mgmt. (ICLARM), Makati City, Philippines, and EPOMEX/ Univ. Autónoma de Campeche, Campeche, Mexico.
Dowling, T. E., W. L. Minckley, P. C. Marsh, and E. S. Goldstein.
1996. Mitochondrial DNA variability in the endangered razorback sucker (*Xyrauchen texanus*): analysis of hatchery stocks and implications for captive propagation. Conserv. Biol. 10:120–127.
El Mousadik, A., and R. J. Petit.
1996. High level of genetic differentiation for allelic richness among population of the argan tree (*Argania spinosa* (L.) Skeels) endemic to Morocco. Theoret. Appl. Genet. 92:832–839.
Esteves, R. F.
2005. Dispersal of reef fish larvae from known spawning sites in La Parguera. M.S. thesis, 53 p. Univ. Puerto Rico, Mayaguez.
Excoffier, L., and H. E. L. Lischer.
2010. Arlequin suite ver 3.5: A new series of programs to perform population genetics analyses under Linux and Windows. Mol. Ecol. Res. 10:564–567.
Farmer, N. A.
2009. Reef fish movements and marine reserve designs. Ph.D. diss., 217 p. Univ. Miami, Coral Gables, FL.
Federal Register.
2005. Fisheries of the Caribbean, Gulf of Mexico, and South Atlantic; Comprehensive Amendment to the Fishery Management Plans of the U.S. Caribbean; final rule. vol. 70, no. 208, October 28, p. 62073–62084. GPO, Washington, D.C.
Fischer, A. J., M. S. Baker Jr., and C. A. Wilson.
2004. Red snapper, *Lutjanus campechanus*, demographic structure in the northern Gulf of Mexico based on spatial patterns in growth rates and morphometrics. Fish. Bull. 102:593–603.
Frankham, R.
1995. Effective population-size adult-population size ratios in wildlife: a review. Genet. Res. 66:95–107.
Franklin, I. R.
1980. Evolutionary change in small populations. *In* Conservation biology: an evolutionary-ecological perspective (M. E. Soulé and B. A. Wilcox, eds.), p. 135–149. Sinauer, Sunderland, MA.
Fu Y.-X.
1997. Statistical tests of neutrality of mutations against population growth, hitchhiking, and background selection. Genetics 147:915–925.
Fu Y.-X, and W.-H. Li.
1993. Statistical tests of neutral mutations. Genetics 133:693–709.
Gold, J. R., E. Pak, and L. R. Richardson.
2001. Microsatellite variation among red snapper (*Lutjanus campechanus*) from the Gulf of Mexico. Mar. Biotech. 3:293–304.
Goudet, J.
1995. F-stat, a computer program to calculate F-statistics. J. Hered. 86 485–486.
Goudet, J., M. Raymond, T. de-Meeus, and F. Rousset.
1996. Testing differentiation in diploid populations. Genetics 144:1933–1940.
Graham R. T., R. Carcamo, K. L. Rhodes, C. M. Roberts, and N. Requena.
2008. Historical and contemporary evidence of a mutton snapper (*Lutjanus analis* Cuvier, 1828) spawning aggregation fishery in decline. Coral Reefs 27:311–319.
Guo, S., and E. Thompson.
1992. Performing the exact test of Hardy-Weinberg proportion from multiple alleles. Biometrics 48:361–372.
Hare, M. P., L. Nunney, M. K. Schwartz, D. E. Ruzzante, M. Burford, R. S. Waples, K. Ruegg, and F. Palstraa.
2011. Understanding and estimating effective population size for practical application in marine species management. Conserv. Biol. 25:438–449.
Hastings, A.
1993. Complex interactions between dispersal and dynamics: lessons from coupled logistical equations. Ecology 74:1362–1372.
Hauser, L., and G. R. Carvalho.
2008. Paradigm shifts in marine fisheries genetics: ugly hypotheses slain by beautiful facts. Fish Fish. 9:333–362.
Hauser, L., and R. D. Ward.
1998. Population identification in pelagic fish: the limits of molecular markers. *In* Advances in molecular mycology (G. R. Carvalho, ed.), p. 2191–2242. IOS Press, Amsterdam.
Hellberg, M. E., R. S. Burton, J. E. Neigel, and S. R. Palumbi.
2002. Genetic assessment of connectivity among marine populations. Bull. Mar. Sci. 70 (suppl.):273–290.
Johns, W. E., T. L. Townsend, D. M. Fratantoni, and W. D. Wilson.
2002. On the Atlantic inflow to the Caribbean Sea. Deep-Sea Res., pt. I, 49:211–243.
Kritzer, J. P., and P. F. Sale.
2004. Metapopulation ecology in the sea: from Levin's model to marine ecology and fisheries science. Fish Fish. 5:131–140.
Matos-Caraballo, D., M. Cartagena-Haddock, and N. Peña-Alvarado.
2004. Historical landings and biostatistical CFSP data analysis for five important species. Portrait of the fishery of mutton snapper *Lutjanus analis* in Puerto Rico during 1988–2001. [Available from Dept. Nat. Environ. Res. Fish. Res. Lab., Mayaguez, Puerto Rico.]
Mueller, K. W.
1994. Gregarious behavior in mutton snapper in the Exuma Cays. Bahamas J. Sci. 5:17–22.
1995. Size structure of mutton snapper, *Lutjanus analis*, associated with unexploited artificial patch reefs in the central Bahamas. Fish. Bull. 93:573–576.
Østergaard, S., M. M. Hansen, V. Loeschcke, and E. E. Nielsen.
2003. Long-term temporal changes of genetic composition in brown trout (*Salmo trutta* L.) populations inhabiting an unstable environment. Mol. Ecol. 12:3123–3135.
Palstra, F. P., M. F. O'Connell, and D. E. Ruzzante.
2007. Population structure and gene flow reversals in Atlantic salmon (*Salmo salar*) over contemporary and

long-term temporal scales: effects of population size and life history. Mol. Ecol. 16:4504–4522.

Raymond, M., and F. Rousset.
1995. Genepop (vers. 2.1): Population genetics software for exact tests and ecumenicism. J. Hered. 86:248–249.

Renshaw, M. A., S. Karlsson, and J. R. Gold.
2007. Isolation and characterization of microsatellites in lane snapper (*Lutjanus synagris*), mutton snapper (*Lutjanus analis*), and yellowtail snapper (*Ocyurus chrysurus*). Mol. Ecol. Notes 7:1084–1087.

Renshaw, M. A., E. Saillant, S. C. Bradfield, and J. R. Gold.
2006. Microsatellite multiplex panels for genetic studies of three species of marine fishes: red drum (*Sciaenops ocellatus*), red snapper (*Lutjanus campechanus*), and cobia (*Rachycentron canadum*). Aquaculture 253:731–735.

Rice, W. R.
1989. Analyzing tables of statistical tests. Evolution 43:223–225.

Rieman, B. E., and F. E. Allendorf.
2001. Effective population size and genetic conservation criteria for bull trout. N. Am. J. Fish. Manage. 21:756–764.

Rhodes, K.L., R. I. Lewis, R. W. Chapman, and Y. Sadovy.
2003. Genetic structure of camouflage grouper, *Epinephelus polyphekadion* (Pisces: Serranidae), in the western central Pacific. Mar. Biol. 142:771–776.

Roberts, C. M.
1997. Connectivity and management of Caribbean coral reefs. Science 278:1454–1457.

Rocha, L. A., A. L. Bass, D. R. Robertson, and B. W. Bowen.
2002. Adult habitat preferences, larval dispersal, and the comparative phylogeography of three Atlantic surgeonfishes (Teleostei: Acanthuridae). Mol. Ecol. 11:243–252.

Rozas, J., J. C. Sanchez-DelBarrio, X. Messeguer, and R. Rozas.
2003. DnaSP, DNA polymorphism analyses by the coalescent and other methods. Bioinformatics 19:2496–2497.

Sadovey de Mitcheson, Y., A. Cornish, M. Doreier, P. L. Colin, M. Russell, and K. C. Lindeman.
2008. A global baseline for spawning aggregations of reef fishes. Conserv. Biol. 22:1233–1244.

Saillant, E., and J. R. Gold.
2006. Population structure and variance effective size of red snapper (*Lutjanus campechanus*) in the northern Gulf of Mexico. Fish. Bull. 104:136–148.

Sambrook, J., E. F. Fritsch, and T. Maniatis.
1989. Molecular cloning. A laboratory manual, 2nd ed. Cold Spring Harbor Laboratory Press, Cold Spring Harbor, NY.

Schultz, S. T., and M. Lynch.
1997. Mutation and extinction: the role of variable mutational effects, synergistic epistasis, beneficial mutations, and degree of outcrossing. Evolution 51:1363–1371.

Shulman, M. J., and E. Bermingham.
1995. Early life histories, ocean currents, and the population genetics of Caribbean reef fishes. Evolution, 49:897–910.

Shulzitski, K., M. A. McCartney, and M. L. Burton.
2009. Population connectivity among Dry Tortugas, Florida, and Caribbean populations of mutton snapper (*Lutjanus analis*), inferred from multiple microsatellite loci. Fish. Bull. 107:501–509.

SEDAR (Southeast Data, Assessment, and Review).
2007. SEDAR 14: Caribbean mutton snapper. Stock assessment report 2. [Available at http://www.sefsc.noaa.gov/sedar/, accessed July 2011.]

Seutin, G., B. N. White, and P. T. Boag.
1991. Preservation of avian blood and tissue samples for DNA analyses. Can. J. Zool. 69:82–90.

Storz, J., and M. A. Beaumont.
2002. Testing for genetic evidence of population expansion and contraction: an empirical analysis of microsatellite DNA variation using a hierarchical Bayesian model. Evolution 56:154–166

Swearer, S. E., J. E. Caselle, D. W. Lea, and R. R. Warner.
1999. Larval retention and recruitment in an island population of a coral-reef fish. Nature 402:799–802.

Taylor, M. S., and M. E. Hellberg.
2003. Genetic evidence for local retention of pelagic larvae in a Caribbean reef fish. Science 299:107–109.

van Oosterhout, C., W. Hutchinson, D. Will, and P. Shipley.
2004. Micro-checker: software for identifying and correcting genotyping errors in microsatellite data. Mol. Ecol. Notes 4:535–538.

Waples, R. S.
2010. Spatial-temporal stratifications in natural populations and how they affect understanding and estimation of effective population size. Mol. Ecol. Res. 10:785–796.

Wares, J. P., and P. M. Pringle.
2008. Drift by drift: effective population size is limited by advection. BMC Evol. Biol. 8:235.

Watanabe, W. O.
2001. Species profile: mutton snapper. SRAG Publication 725, 9 p. Southern Regional Aquaculture Center, Stoneville, MS.

Weir, B. S., and C. C. Cockerham.
1984. Estimating F-statistics for the analysis of population structure. Evolution 38:1358–1370.

Woods, M. K., A. J. Fischer, J. H. Cowan Jr., and D. L. Nieland.
2003. Size and age of female red snapper *Lutjanus campechanus* in the northern Gulf of Mexico. Proc. Gulf Caribb. Fish. Inst. 54:526–537.

Wright, S.
1931. Evolution in Mendelian populations. Genetics 16:97–159.

Genetic and morphological differences between *Sebastes vulpes* and *S. zonatus* (Teleostei: Scorpaeniformes: Scorpaenidae)

Nozomu Muto[1]
Yoshiaki Kai[2]
Tetsuji Nakabo[3]

Email address for contact author: muto@inet.museum.kyoto-u.ac.jp

[1] Division of Applied Biosciences
Graduate School of Agriculture
Kyoto University
c/o The Kyoto University Museum
Kyoto University
Yoshida, Sakyo, Kyoto, 606-8501 Japan

[2] Maizuru Fisheries Research Station
Field Science Education and Research Center
Kyoto University
Nagahama, Maizuru, Kyoto, 625-0086 Japan

[3] The Kyoto University Museum
Kyoto University
Yoshida, Sakyo, Kyoto, 606-8501 Japan

Abstract—The taxonomic status of *Sebastes vulpes* and *S. zonatus* were clarified by comprehensive genetic (amplified fragment length polymorphisms [AFLP] and mitochondrial DNA [mtDNA] variation) and morphological analyses on a total of 65 specimens collected from a single locality. A principal coordinate analysis based on 364 AFLP loci separated the specimens completely into two genetically distinct groups that corresponded to *S. vulpes* and *S. zonatus* according to body coloration and that indicated that they are reproductively isolated species. Significant morphological differences were also evident between the two groups; 1) separation by principal component analysis based on 31 measurements, and 2) separation according to differences in counts of gill rakers and dorsal-fin spines without basal scales, and in the frequencies of specimens with small scales on the lower jaw. Restriction of gene flow between the two groups was also indicated by the pairwise Φ_{ST} values estimated from variations in partial sequences from the mtDNA control region although the minimum spanning network did not result in separation into distinct clades. The latter was likely due to incomplete lineage sorting between *S. vulpes* and *S. zonatus* owing to their recent speciation.

Manuscript submitted 21 May 2011.
Manuscript accepted 22 July 2011.
Fish. Bull. 109:429–439 (2011).

The genus *Sebastes*, containing the live-bearing rockfishes, is the most species-rich scorpaenid genus, comprising over 110 species worldwide, over 30 of which are known from the western North Pacific (Kai et al., 2003; Nelson, 2006; Hyde and Vetter, 2007). Exhibiting a relatively high diversity in number of closely related species in contrast to other genera of marine fishes, the genus has long attracted the attention of evolutionary biologists (e.g., Love et al., 2002). The greater part of such diversity has been ascribed to an ancient explosive speciation event and subsequent adaptive radiation. These species have been interpreted as representing an "ancient species flock"—an occurrence rarely seen in marine fishes (Johns and Avise, 1998; Rüber and Zardoya, 2005). However, an increasing number of recent studies have documented recently diverged sibling species pairs that are indicative of ongoing speciation within the genus (Kai et al., 2002a; Narum et al., 2004; Hawkins et al., 2005; Hyde et al., 2008; Burford, 2009; Stefánsson et al., 2009). These events present a series of "snapshots" of the speciation process, providing us with unique insights into evolutionary processes in the marine realm (Sobel et al., 2009).

Sebastes vulpes, S. ijimae, and *S. zonatus* are closely related and morphologically similar western North Pacific species (Chen and Barsukov, 1976; Nakabo, 2002b; Kai et al., 2003; Hyde and Vetter, 2007) that are subject to some taxonomic confusion. Döderlein in Steindachner and Döderlein (1884) first described *Sebastes vulpes*; Jordan and Metz (1913) subsequently listed *S. vulpes* as valid and described a new species, *S. ijimae*. Two color variants within *S. vulpes* recognized by Matsubara (1943) were later considered to represent separate species (*S. vulpes* and a new species, *S. zonatus*) by Chen and Barsukov (1976). They characterized *S. vulpes* as having a dark gray body with distinct dense white spots and *S. zonatus* as having a white to pinkish body with three distinct vertical dark bands. In addition, Chen and Barsukov (1976) also recognized *S. ijimae* as a distinct species, noting that the three species shared almost the same distributional range, being known from southern Hokkaido

southward to central Honshu on the Pacific coast of Japan and to the western coast of Honshu. Amaoka (1984) and Nakabo (2002b) recognized the three species as valid, following Chen and Barsukov (1976). Several authors recognized only *S. vulpes*—*S. ijimae* and *S. zonatus* being considered as synonyms (Kanayama and Kitagawa, 1983; Nagasawa, 2000; Kitagawa et al., 2008; Ishida, 2009). However, because comprehensive genetic or morphological studies have been lacking to date, taxonomic status of the three species remains uncertain.

Failure to recognize reproductively isolated populations within an exploited stock can introduce critical errors in management (Carvalho and Hauser, 1994). *Sebastes vulpes* and *S. zonatus* are both abundant across northern Japan, together representing an important fisheries component, whereas *S. ijimae* is relatively rare (Sekigawa et al., 2003). Because of their high commercial value, some Japanese fisheries organizations have attempted to enhance the stocks of *S. vulpes* and *S. zonatus* through aquaculture (Sasaki, 2003; Sekigawa et al., 2003). However, without reliable taxonomic information for both species, it is unlikely that enhancement of the fishery will be realized. In this context, as a first step toward fully resolving the taxonomic status of *S. vulpes*, *S. ijimae*, and *S. zonatus*, we focused on *S. vulpes* and *S. zonatus*, using comprehensive genetic and morphological analyses.

Mitochondrial DNA (mtDNA) has been used successfully as a primary marker to infer species boundaries among species of *Sebastes* (e.g., Alesandrini and Bernardi, 1999; Kai et al., 2002b), although recently evolved sibling species pairs that are nonmonophyletic with respect to the mtDNA gene tree have been frequently reported in *Sebastes* (e.g., Kai et al., 2002a; Narum et al., 2004; Burford and Bernardi, 2008). The delimitation of such pairs requires data from multiple independent loci (e.g., Nichols, 2001; Avise, 2004). In fact, *S. vulpes* and *S. zonatus* are primarily distinguished by body coloration, which has been demonstrated as a good indicator of recent speciation in *Sebastes* (e.g., Kai et al., 2002a; Narum et al., 2004; Hyde et al., 2008; Orr and Hawkins, 2008). Accordingly, a technique called AFLP (amplified fragment length polymorphisms) (Vos et al., 1995) has also been used, because it is a multilocus approach that produces hundreds of highly replicable independent dominant markers (Bensch and Åkesson, 2005) and therefore estimates genetic divergence across the whole genome. Such an approach has successfully resolved the species boundaries and phylogenetic relationships among recently diverged species complexes in various organisms, in which mtDNA sequencing alone was less informative (e.g., Seehausen et al., 2003; Mendelson and Shaw, 2005). Moreover, evaluating a mtDNA gene tree against the background of a multilocus approach allows further discussion on the evolutionary relationships and histories among closely related species (e.g., Kai et al., 2002a; Hyde et al., 2008; Burford, 2009).

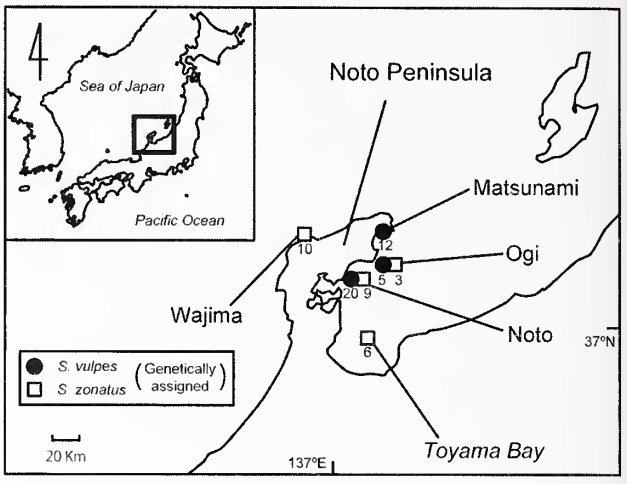

Figure 1

Collection sites around the Noto Peninsula, Island of Honshu, Japan, for the 65 *Sebastes* spp. specimens examined for genetic and morphological differences. Numbers below symbols represent sample sizes.

Materials and methods

Samples

In order to clearly demonstrate intrinsic reproductive isolation between *S. vulpes* and *S. zonatus*, a total of 65 specimens were collected from single locality around Noto, Ishikawa Prefecture, Japan (Fig. 1), thereby eliminating any geographical variations. The body coloration of each specimen was recorded with a photograph taken while the fish was alive or soon after death. Thirty-nine specimens with a grayish body were identified as *S. vulpes,* and the remaining 26 (with a brownish body) as *S. zonatus* (Fig. 2), generally by following the methods of Chen and Barsukov (1976). The two species are not usually caught together; *S. vulpes* is caught with set nets at ~60 m depth and *S. zonatus* with gill nets at ~150 m around the sampling locality (K. Sakai[1]). Muscle tissue was taken from each specimen before fixation and preserved in 99.5% ethanol. The specimens examined here were deposited in the Kyoto University Fish Collection (FAKU) (see Appendix for catalog numbers and collection data).

Genetic analysis

Genomic DNA was extracted from the preserved muscle tissue, by using the DNeasy Tissue Kit (Qiagen, Tokyo, Japan) according to the manufacturer's protocols.

AFLP profiles were generated with the AFLP Plant Mapping Kit (Applied Biosystems, Foster City, CA) by following the manufacturer's protocol slightly modified by Kai et al. (2002a). For the selective amplification

[1] Sakai, K. 2011. Personal commun. Noto Marine Center, 3-47 Ossaka, Noto, Ishikawa 927-0552, Japan.

step, 12 randomly chosen primer pairs were used (Mse I + Eco RI [ACA + CAA, AAG + CAG, ACA + CTT, ACA + CAC, ACT + CTA, ACA + CTG, AAG + CAC, AGG + CAT, ACC + CTT, ACG + CAC, AAG + CAT, AGG + CTT]). Selective amplification products were analyzed on an ABI PRISM 310 genetic analyzer (Applied Biosystems) together with a GeneScan-500 Rox size standard (Applied Biosystems). Fragment data were collected with Peak Scanner software, vers. 1.0 (Applied Biosystems). Electropherograms were scored for the presence (1) or absence (0) of fragments between 90 base pairs (bp) to 450 bp in size, so as to create binary matrices. Fragments were inferred as homologous if they differed by not more than 0.5 bp from the median. Euclidean pairwise genetic distances (Huff et al., 1993) were calculated from the binary matrices in GenAlEx, vers. 6.41 (Peakall and Smouse, 2006). Principal coordinate analysis (PCoA) with a covariance matrix and the data standardization method was performed on the basis of the Euclidean pairwise distance matrix, as implemented in GenAlEx, vers. 6.41 (Peakall and Smouse, 2006). By means of PCoA, we explored the genetic population structure among all 65 specimens without *a priori* grouping information.

The mitochondrial DNA sequence comprising 452 bp extending from the threonine transfer RNA ($tRNA^{Thr}$) gene to the middle conserved region of the control region (mtCR) was amplified with the primers L15876 (5′-AAG CAC TTG AAT GAG CTT G-3′) (Rocha-Olivares et al., 1999) and H16498 (5′-CCT GAA GTA GGA ACC AGA TG-3′) (Meyer et al., 1990). The polymerase chain reaction (PCR) proceeded for 30 cycles, with denaturation at 94°C for 1 min, annealing at 54°C for 1 min and extension at 72°C for 2 min, PCR products being purified with USB® ExoSAP-IT® (Affymetrix, Santa Clara, CA). DNA sequencing was performed with a BigDye Terminator Cycle Sequencing Kit (Applied Biosystems) on an ABI PRISM 310 genetic analyzer (Applied Biosystems). The DNA sequences were edited with the sequence alignment editor BioEdit 7.0.5.3 (Hall, 1999) and aligned with the program CLUSTAL X, vers. 2.1 (Larkin et al., 2007). Estimation of mitochondrial genetic structuring among specimens based on haplotype frequency and uncorrected genetic distances between haplotypes (Φ_{ST}) was performed by Arlequin, vers. 3.5 (Excoffier and Lischer, 2010). The significance of the Φ_{ST} value was tested by 10,000 random permutations. Arlequin 3.5 was also used to construct the minimum spanning network (MSN) of the haplotypes on the basis of minimum sequence differences. The sequences determined in this study have been deposited in GenBank (accession numbers AB614522–AB614526 and AB615270–AB615329).

Morphological analysis

Morphological characters were examined after fixation in 10% formalin and preservation in 70% ethanol. Measurements were made on 31 morphological characters, including standard length, which generally followed those described by Nakabo (2002a) except for the following: body depth 1 and 2 as defined by Kai and Nakabo (2002); upper peduncle length, lower peduncle length, spinous dorsal-fin base length, soft dorsal-fin base length, prepelvic length, and gill raker length as defined by Chen (1971); body width was taken as the distance between the uppermost bases of the right and left pectoral fins; pelvic-to-anal-fin length was taken as the distance from the anteriormost base of the pelvic fin to the origin of the anal fin.

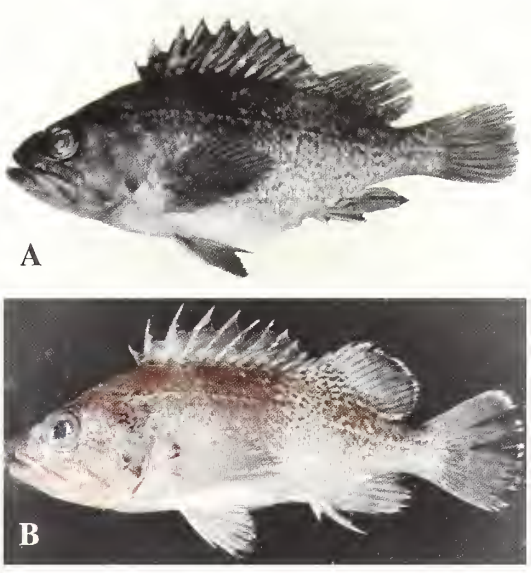

Figure 2

Coloration of fresh specimens of *Sebastes vulpes* and *S. zonatus*. (**A**) *S. vulpes*, FAKU 96090, 194.0 mm standard length; (**B**) *S. zonatus*, FAKU 97082, 167.9 mm standard length. Photo by N. Muto.

Analysis of covariance (ANCOVA) of log10 transformed measurements (with standard length as a covariate) was used to assess differences in morphometric characters between *S. vulpes* and *S. zonatus* when assumptions of normality and homogeneity of slopes were satisfied. The following characters met the assumptions required for ANCOVA: head length, snout length, orbit length, interorbital width, postorbital length, upper jaw length, body depth 1, body depth 2, body width, caudal peduncle depth, upper peduncle length, pectoral-fin length, pelvic-fin length, dorsal-fin base length, spinous dorsal-fin base length, soft dorsal-fin base length, preanal length, predorsal length, prepelvic length, pelvic-to-anal-fin length, 2nd dorsal-fin spine length, 3rd dorsal-fin spine length, and gill raker length. To provide an objectively defined score that summarizes the major components of variable measurements between the specimens, a principal component analysis (PCA) was conducted on the basis of all measurements. Raw measurement data were standardized by log transformation before PCA.

Counts were made on the dorsal-fin rays, anal-fin rays, pectoral-fin rays, pored lateral line scales, gill rakers, and dorsal-fin spines without basal scales. Significant differences in these characters were tested with the Mann-Whitney *U*-test. The presence or absence of small scales on the lower jaw was noted and the difference in frequencies between species assessed by Fisher's exact test. All statistical analyses were conducted using R language, vers. 2.11.1 (R Development Core Team, 2010). Differences were considered significant at $P<0.01$.

Results

Genetic analysis

The 12 primer sets yielded 364 AFLP fragments, of which 127 (34.9%) were polymorphic. All specimens tested displayed unique AFLP fragment patterns, indicating a high level of genetic variability. A PCoA based on the pairwise distance matrix clearly separated the specimens into two groups along the first principal coordinates (PCo) axis (accounting for 41.83% of the total variance) with no overlap (Fig. 3), which corresponded well with the initial identifications of *S. vulpes* and *S. zonatus* based on body coloration, except for two specimens (FAKU 82515 and FAKU 130236). The latter were initially identified as *S. vulpes*, but genetically assigned to *S. zonatus*. Because *S. vulpes* and *S. zonatus* were clearly distinguished by the PCo1 scores without any intermediate specimens, we regarded the above specimens as *S. zonatus*. Comparisons below were made between the two genetically assigned species (*S. vulpes*: 37 specimens, *S. zonatus*: 28 specimens). In contrast, the PCo2 and PCo3 scores (accounting for 13.52% and 12.56% of the total variance, respectively) did not result in separation of the two species (not shown). Despite the high polymorphism evident in the AFLP fragments, no diagnostic differences in fragment patterns were observed between genetically assigned *S. vulpes* and S. *zonatus*. Mean (± standard deviation) pairwise genetic distances estimated by the algorithm of Huff et al. (1993) were 22.63 ±3.95 within *S. vulpes*, 28.69 ±5.16 within *S. zonatus*, and 32.21 ±5.52 between them.

Within the amplified region of mtDNA, continuous sequences of part of the $tRNA^{Thr}$ gene (24 bp), the proline transfer RNA ($tRNA^{Pro}$) gene (70 bp), and part of the mtCR (358 bp) were aligned. The sequences contained 45 variable sites with three indels among 65 specimens, 29 of which were parsimony informative, defining a total of 41 haplotypes. Twenty-one haplotypes were found in *S. vulpes* and 22 in *S. zonatus*, two being shared by the two species. No transversions were observed. The nucleotide composition was AT-biased (A=38.4%, C=19.4%, G=13.6%, T=28.6%), as is common for fish mtDNA (McMillan and Palumbi, 1997). Pairwise sequence divergences between *S. vulpes* and *S. zonatus* varied from 0% to 3.1% (mean 1.5%). The haplotype diversities for *S. vulpes* and *S. zonatus* were 0.94 ±0.03 and 0.98 ±0.02, respectively, and nucleotide diversities (in %), 1.41 ±0.76 and 1.47 ±0.80, respectively. In the MSN inferred from mtDNA sequence variations, 41 haplotypes were connected to each other by one to six mutational steps, revealing a rather expanded topology in the network (Fig. 4). *Sebastes vulpes* and *S. zonatus* were not clearly separated in the network, but restricted gene flow between them was indicated by the low but significant pairwise Φ_{ST} value at $\alpha=0.05$ level ($\Phi_{ST}=0.053$, $P=0.011$ ±0.001).

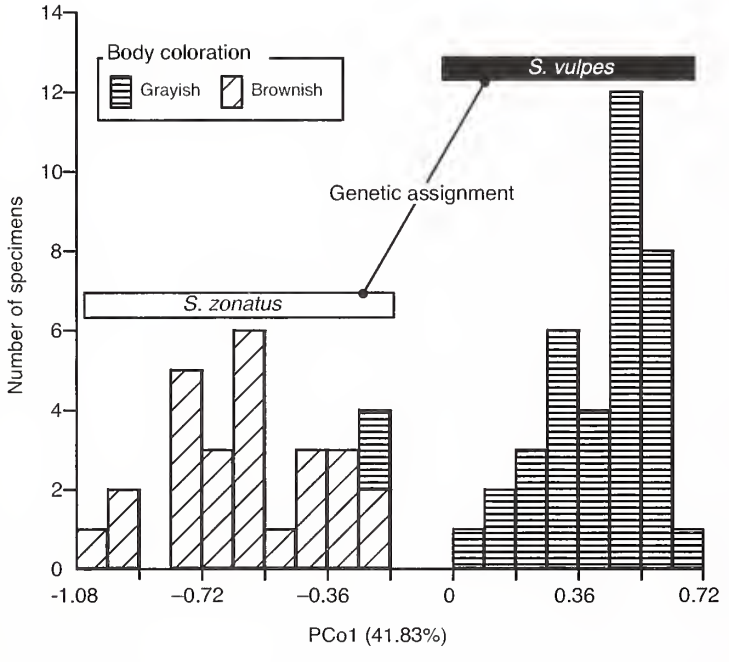

Figure 3

Distribution of first principal coordinate (PCo) scores based on 364 amplified fragment length polymorphisms fragments for *Sebastes zonatus* and *S. vulpes*. The amount of variance explained by PCo1 is given in parentheses. The body coloration of each specimen is designated by the fill pattern of the bars (grayish specimens, lateral stripes; brownish specimen, diagonal stripes). The present specimens were separated completely into two genetically distinct groups.

Morphological analysis

Measurements of *S. vulpes* and *S. zonatus* and results of the ANCOVA are shown in Table 1. Among measurements meeting the statistical assumptions for ANCOVA, four characters out of 23 differed significantly between the two species.

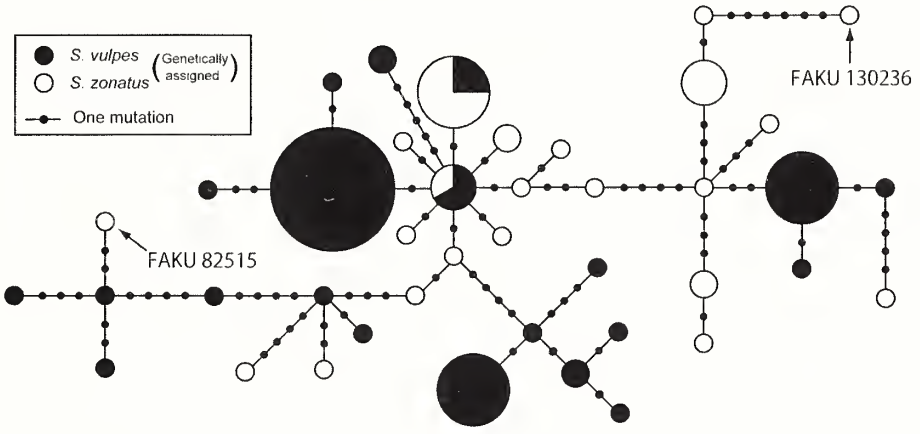

Figure 4

Minimum spanning network of mitochondrial DNA sequence haplotypes of *Sebastes vulpes* (filled circles) and *S. zonatus* (open circles). Each circle represents a unique haplotype (size proportional to number of specimens). The arrow indicates the specimen initially identified as *S. vulpes* by body coloration but genetically assigned to *S. zonatus* in the principal coordinate analysis of amplified fragment length polymorphisms. Black dots along branches represent nucleotide changes. The two species shared two haplotypes and did not exhibit clear separation in the network.

In the PCA, seven specimens were eliminated because they lacked one or more measurements, such as dorsal-fin spine length and anal-fin spine length. Nevertheless, plots of the PCA scores revealed marked differences between *S. vulpes* and *S. zonatus*. The first principal component (PC1) accounted for 87.5% of the variations. Because all loadings were negative, PC1 was considered a size component. PCs 2 and 3 were shape components, with both positive and negative loadings, and together accounted for an additional 4.9% of variation. These components were then visually assessed as dimensions of shape (Fig. 5). PC2 was heavily loaded on body width, 1st anal-fin spine length and 2nd anal-fin spine length (Table 2), providing separation between *S. vulpes* and *S. zonatus* with a narrow overlap. PC3 was heavily loaded on orbit length, prepelvic length, and 1st dorsal-fin spine length (Table 2), with the clusters of the two species broadly overlapping along PC3.

The results of countable characters are shown in Table 3. *Sebastes vulpes* had fewer gill rakers than *S. zonatus*. Counts of dorsal-fin spines without basal scales also differed significantly between *S. vulpes* and *S. zonatus*, as did the frequencies of specimens with small scales on the lower jaw (0.16 and 0.82, respectively). Other countable characters did not differ significantly between the species.

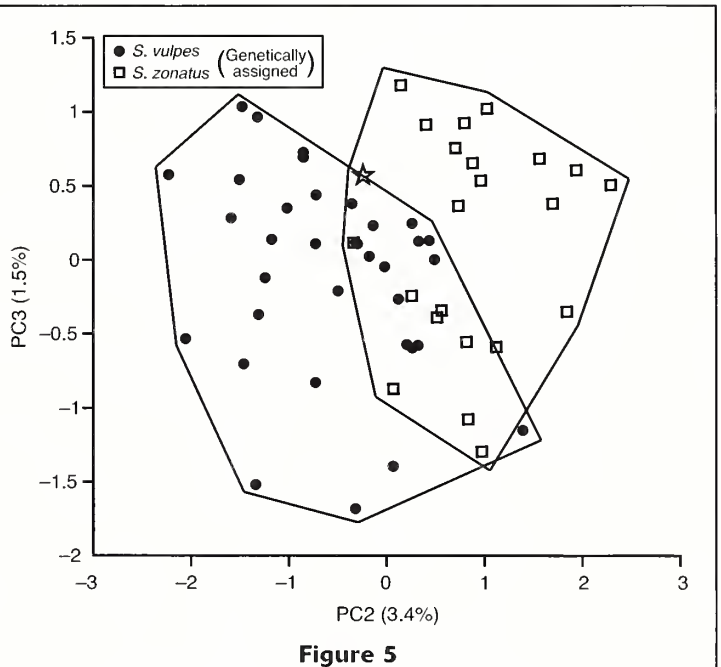

Figure 5

Plots of principal component (PC) scores based on 31 measurements for *Sebastes vulpes* (filled circles) and *S. zonatus* (open squares). The open star indicates one of the two specimens (FAKU 82515) initially identified as *S. vulpes* by body coloration but genetically assigned to *S. zonatus* in the principal coordinate analysis of amplified fragment length polymorphisms (FAKU 130236 was removed from analysis because it lacked a measurement for gill raker length). The two species were separated with a narrow overlap along the PC2 axis, the primary shape component.

Table 1

Measurements in proportion to standard length (SL) for *Sebastes vulpes* and *S. zonatus*. Data indicate ranges, means (in parentheses), and sample sizes (n). X indicates statistically a significant difference between the two species, demonstrated by analysis of covariance (ANCOVA) with standard length (SL) as a covariate. The specimens initially identified as *S. vulpes* by body coloration but genetically assigned to *S. zonatus* in the principal coordinate analysis of amplified fragment length polymorphisms are shown separately (FAKU 82515 and FAKU 130236). ns=not significant.

		S. zonatus (n=28)			
	S. vulpes (n=37)		FAKU 82515	FAKU 130236	ANCOVA
Standard length (mm)	156.4–249.9	137.3–286.4	189.0	154.8	
As % of SL					
Head length	38.0–41.1 (39.6, 37)	37.7–41.3 (39.3, 26)	41.4	40.4	ns
Snout length	10.1–12.4 (11.3, 37)	9.3–11.9 (10.7, 26)	11.2	11.6	X
Orbit length	8.9–11.3 (9.7, 37)	9.0–12.0 (10.4, 26)	10.7	10.2	X
Interorbital width	6.5–8.2 (7.4, 37)	6.6–8.3 (7.4, 26)	7.0	7.2	ns
Postorbital length	19.1–21.8 (20.3, 37)	18.8–21.9 (20.2, 26)	21.5	20.6	ns
Upper jaw length	19.1–21.6 (20.5, 37)	19.5–21.2 (20.1, 26)	20.3	21.6	X
Body depth 1	35.9–40.7 (38.3, 37)	35.8–41.2 (37.9, 26)	38.6	43.0	ns
Body depth 2	27.5–33.9 (30.3, 37)	29.3–33.4 (31.1, 26)	30.6	34.5	ns
Body width	17.5–24.0 (21.1, 37)	16.1–23.5 (18.7, 26)	18.9	22.2	X
Caudal peduncle depth	10.2–12.4 (11.5, 37)	10.4–12.3 (11.4, 26)	12.2	12.1	ns
Upper peduncle length	10.0–13.2 (11.7, 37)	10.4–13.0 (11.7, 26)	10.7	11.5	ns
Lower peduncle length	16.4–20.6 (18.6, 37)	16.6–19.8 (18.4, 26)	18.5	18.2	
Pectoral-fin length	24.9–31.2 (27.9, 37)	26.7–31.1 (28.8, 26)	28.4	27.8	ns
Pelvic-fin length	20.2–24.1 (22.1, 37)	20.9–24.4 (22.6, 26)	22.8	23.7	ns
Dorsal-fin base length	56.2–65.2 (60.3, 37)	57.2–65.4 (60.8, 26)	61.5	65.4	ns
Spinous dorsal-fin base length	34.0–43.1 (38.0, 37)	34.2–40.9 (37.7, 26)	38.2	41.5	ns
Soft dorsal-fin base length	19.5–25.2 (22.9, 37)	19.8–25.6 (22.8, 26)	23.4	24.7	ns
Preanal length	64.6–74.3 (68.3, 37)	63.7–72.2 (67.1, 26)	66.5	66.4	ns
Predorsal length	34.0–38.1 (35.8, 37)	33.0–40.0 (35.8, 26)	35.9	38.4	ns
Prepelvic length	39.1–52.5 (43.2, 37)	39.5–55.8 (43.5, 26)	43.4	44.1	ns
Anal-fin base length	12.9–16.7 (14.7, 37)	13.7–16.7 (14.9, 26)	13.8	14.4	
Pelvic-to-anal-fin length	26.6–40.5 (33.4, 37)	26.4–37.1 (33.0, 26)	33.5	32.9	ns
1st dorsal-fin spine length	5.3–8.6 (6.8, 37)	5.6–8.1 (7.0, 25)	6.8	7.1	
2nd dorsal-fin spine length	10.1–13.5 (11.5, 37)	10.6–13.9 (11.8, 25)	11.2	12.3	ns
3rd dorsal-fin spine length	13.5–18.2 (15.3, 36)	14.3–17.4 (15.7, 26)	15.8	18.0	ns
1st anal-fin spine length	5.0–8.2 (6.7, 37)	6.3–8.5 (7.3, 26)	7.4	7.8	
2nd anal-fin spine length	12.1–15.5 (13.4, 37)	13.1–17.0 (15.6, 26)	13.2	14.3	
3rd anal-fin spine length	12.2–15.8 (14.1, 37)	13.0–16.7 (14.8, 25)	13.7	15.1	
Pelvic-fin spine length	12.4–15.9 (13.6, 36)	13.2–15.6 (14.6, 26)	13.3	14.8	
Gill raker length	3.3–4.5 (3.8, 37)	3.0–4.7 (4.1, 25)	4.0	—	ns

Discussion

Genetic and morphological differentiation

Variations in AFLP loci across the whole genome revealed marked genetic structure among the specimens examined. The PCoA with AFLP disclosed two genetically distinct groups, which corresponded well with initial *S. vulpes* and *S. zonatus* identifications that were based on body coloration (Fig. 3). Because the present specimens were collected from a single sampling locality, the clear genetic differences between *S. vulpes* and *S. zonatus* indicated that they are reproductively isolated from each other and should be recognized as separate species. Notwithstanding, two specimens with grayish body coloration reminiscent of *S. vulpes* were clearly genetically assigned to *S. zonatus* on the basis of the PCoA with AFLP. Such discordance may be indicative of some intraspecific variation in body coloration in *S. zonatus,* or historical hybridization between *S. vulpes* and *S. zonatus*, as discussed below. Significant morphological differences also supported the validity of the two species. A PCA of body measurements resulted in clusters of *S. vulpes* and *S. zonatus* being almost completely separated, apart from a narrow overlap along the PC2 axis, the primary shape component (Fig. 5). Some countable characters also differed significantly between the two species. In addition, a restriction of gene flow between *S.*

Table 2

Factor loadings for principal component (PC) analysis of measurements of *Sebastes vulpes* and *S. zonatus* in specimens examined with all characters available for multivariate analysis.

	PC1	PC2	PC3		PC1	PC2	PC3
Standard length	−0.9895	−0.1027	0.0409	Soft dorsal-fin base length	−0.9445	−0.0692	0.1436
Head length	−0.9852	−0.1065	0.0703	Preanal length	−0.9567	−0.1952	−0.0632
Snout length	−0.9128	−0.2459	0.0786	Predorsal length	−0.9725	−0.0474	0.1441
Orbit length	−0.8875	0.1683	0.2684	Prepelvic length	−0.9080	−0.2030	−0.2424
Interorbital width	−0.9700	−0.0066	−0.0215	Anal-fin base length	−0.9390	−0.0077	−0.1620
Postorbital length	−0.9800	−0.0695	0.0980	Pelvic-to-anal-fin length	−0.8711	−0.1179	0.2136
Upper jaw length	−0.9783	−0.1367	0.0339	1st dorsal-fin spine length	−0.8878	0.2150	−0.2948
Body depth 1	−0.9768	−0.1375	−0.0715	2nd dorsal-fin spine length	−0.9371	0.1776	−0.0960
Body depth 2	−0.9727	−0.0285	−0.0632	3rd dorsal-fin spine length	−0.9357	0.2025	−0.0797
Body width	−0.8952	−0.3316	−0.1898	1st anal-fin spine length	−0.8194	0.3814	0.0470
Caudal peduncle depth	−0.9615	−0.1364	−0.0182	2nd anal-fin spine length	−0.8001	0.4780	0.0565
Upper peduncle length	−0.9401	−0.1069	0.0622	3rd anal-fin spine length	−0.9116	0.2521	−0.0827
Lower peduncle length	−0.9446	−0.0344	−0.0497	Pelvic-fin spine length	−0.9467	0.2192	−0.0177
Pectoral-fin length	−0.9686	0.0310	−0.0073	Gill raker length	−0.8520	0.1947	−0.0462
Pelvic-fin length	−0.9768	0.0100	−0.0085				
Dorsal-fin base length	−0.9792	−0.0444	0.1357				
Spinous dorsal-fin base length	−0.9644	−0.0373	0.1107				

Table 3

Distributions of countable characters in *Sebastes vulpes* and *S. zonatus*. Superscripts [a] and [b] indicate the counts of the two specimens initially identified as *S. vulpes* by body coloration but genetically assigned to *S. zonatus* (FAKU 82515 and FAKU 130236, respectively).

	Dorsal-fin rays		Anal-fin rays			Pectoral-fin rays (total)			Pectoral-fin rays (unbranched)						
Species	12	13	5	6	7	16	17	18	6	7	8	9	10	11	*n*
S. vulpes	19	18	—	36	1	5	31	1	1	—	11	22	3	—	37
S. zonatus	9	19[a,b]	1	26[a,b]	1	—	24[a,b]	4	—	1	4	17[b]	5[a]	1	28

	Pored lateral line scales									Gill rakers						
Species	28	29	30	31	32	33	34	35	36	24	25	26	27	28	29	*n*
S. vulpes	—	1	7	8	12	8	1	—	—	2	9	22	4	—	—	37
S. zonatus	1	—	4	5	6[a,b]	5	5	1	1	—	1	9[a,b]	9	8	1	28

	Dorsal-fin spines without basal scales												
Species	1	2	3	4	5	6	7	8	9	10	11	12	*n*
S. vulpes	3	–	1	1	1	3	3	3	9	4	—	5	33
S. zonatus	21	1[b]	2	1	1	—	—	1	—	—	1[a]	—	28

vulpes and *S. zonatus* was also indicated by the pairwise Φ_{ST} value based on mtDNA sequence variation although the MSN inferred from the mtDNA sequences did not clearly separate the two species and therefore indicated incomplete lineage sorting in mtDNA due to their recent speciation and the occurrence of introgression between them, or both (see below).

The difference in depth ranges between *S. vulpes* and *S. zonatus* also adds support to the recognition of two species. In the general sampling area, the different fish-

ing nets are indicative of the different depth habitats for the two species: adult *S. vulpes* are usually caught with set nets laid around 60 m depth, whereas *S. zonatus* are usually caught with gill nets laid around 150 m depth around the sampling locality (Sakai[1]); Similar habitat separation (by depth) is common for other closely related (sister) species of *Sebastes* (Narum et al., 2004; Orr and Blackburn, 2004; Burford and Bernardi, 2008; Hyde et al., 2008; Orr and Hawkins, 2008; Stefánsson et al., 2009)—ecologically based reproductive isolation having often been invoked for *Sebastes*. For example, Hyde et al. (2008) showed that *S. miniatus* and "S. crocotulus" were segregated by habitat depth and they hypothesized a speciation model for closely related species pairs of *Sebastes* in which truncation of depth-related ontogenetic migration may have led to speciation. More detailed ecological studies may provide further insights into the maintenance of independent gene pools by *S. vulpes* and *S. zonatus* and eventually provide clues for understanding the mechanisms underlying the considerable diversity within *Sebastes* (Ingram, 2011).

Incomplete lineage sorting and introgression

Although *S. vulpes* and *S. zonatus* are reproductively isolated from each other and should be treated as two distinct species, two specimens of *S. zonatus* had typical *S. vulpes* coloration. In addition, the two species shared two mtDNA haplotypes and did not exhibit clear separation in the MSN inferred from the mtDNA sequences (Fig. 4). This feature can be explained by 1) incomplete lineage sorting in mtDNA due to recent speciation, and 2) interspecific mtDNA gene flow mediated by hybridization and backcrossing (introgression), or both (Avise, 2000; Funk and Omland, 2003). Incomplete lineage sorting is a source of nonmonophyletic relationship among rapidly radiating species in a mtDNA gene tree (Funk and Omland, 2003) because newly diverged species are initially expected to be nonmonophyletic with respect to any gene tree owing to allelic separations predating the species split, thereafter progressing to reciprocal monophyly over time as ancestral haplotypes are sorted and unique mutations acquired (Avise, 2000). On the other hand, a mtDNA gene tree is also particularly susceptible to the effects of introgression because mtDNA is inherited maternally and does not recombine (Funk and Omland, 2003). In fact, both incomplete lineage sorting and introgression have been frequently reported within *Sebastes* (Roques et al., 2001; Kai et al., 2002a; Narum et al., 2004; Buonaccorsi et al., 2005; Hyde et al., 2008; Burford, 2009).

A rigorous statistical framework accounting for the stochastic variance of genetic processes is generally required to distinguish incomplete lineage sorting from introgression (Peters et al., 2007), although an *ad hoc* explanation can be given without the statistical rejection of alternative hypotheses (Avise, 2000; Donnelly et al., 2004). In this study, two lines of observations appeared to better support incomplete lineage sorting as the cause of the observed nonmonophyly of mtDNA, although the two processes are difficult to distinguish unequivocally and are not necessarily mutually exclusive.

First, the present MSN of mtDNA showed no distinct clades that corresponded with each species. The topology of the gene tree has often been used as an heuristic approach to determine the cause of lack of separation (e.g., Baker et al., 2003; Omland et al., 2006; Zakharov et al., 2009). A shallow genetic divergence between species without distinct clades, as observed in the present study, is generally interpreted as indicative of recent speciation and incomplete lineage sorting (e.g., Baker, 2003; Donnelley et al., 2004). The relatively small pairwise sequence divergences between *S. vulpes* and *S. zonatus*, corresponding closely to those of intraspecific variations found in some other species of *Sebastes* (Rocha-Olivares et al., 1999; Higuchi and Kato, 2002; Kai et al., 2002a; Burford and Bernardi, 2008), also indicate recent speciation between the two species. In addition, haplotype and nucleotide diversities within both *S. vulpes* and *S. zonatus* were relatively high compared with those of other species of *Sebastes* (Rocha-Olivares et al., 1999; Higuchi and Kato, 2002; Kai et al., 2002a), as well as other marine fishes (Grant and Bowen, 1998), indicating that the two species evolved from a large, genetically diverse ancestral population, thereafter maintaining large effective population sizes without recent bottlenecks (Grant and Bowen, 1998; Avise, 2000). Because the probability of complete sorting of ancestral haplotypes is a function not only of stochastic processes and time since speciation but also effective population sizes (Funk and Omland, 2003), it seems plausible that large, stable effective population sizes of those two species delayed lineage sorting, resulting in their present-day sharing of ancestral haplotypes.

Second, in the PCoA of AFLP, no specimens occupied positions intermediate between two clusters (=*S. vulpes* and *S. zonatus*) (Fig. 3). Because fragments detected in AFLP are inherited according to Mendelian expectations (Kakehi et al., 2005), hybridized specimens (F1) are generally expected to have intermediate fragment patterns between parental species (e.g., Congiu et al., 2001; Young et al., 2001). Therefore, the absence of intermediate specimens in PCoA indicated a lack of ongoing hybridization between the two species, although the possibility of historical introgression (including backcross) cannot be completely excluded. In fact, two specimens assigned to *S. zonatus* in the PCoA of AFLP had been initially identified as *S. vulpes* on the basis of body coloration (Fig. 3). One of those specimens (FAKU 82515) was plotted near the *S. vulpes* cluster in the PCA based on measurements (Fig. 5), the count of 11 dorsal-fin spines without basal scales for that specimen also being indicative of *S. vulpes* (usually more than six) rather than *S. zonatus* (usually one) (Table 3). Such equivocal morphological characters may be explained by traces of historical hybridization between *S. vulpes* and *S. zonatus*, which may have resulted in mtDNA introgression between them.

Conclusions

The recognition of *S. vulpes* and *S. zonatus* as two distinct species is the first step toward establishing a biologically based, species-specific management scheme for these commercially and recreationally important species. In order to demonstrate more detailed evolutionary relationships between the two species, specimens sampled throughout their overall distributional range are currently under examination.

Acknowledgments

We express our sincere gratitude to K. Sakai (Noto Marine Center, Ishikawa, Japan) and M. Matada (Kanazawa University) for their valuable discussion and help in sample collections. Special thanks also go to T. Noda (Miyako Station, National Center for Stock Enhancement, Fisheries Research Agency), and M. Tagawa and K. Nakayama (Kyoto University) for helpful comments. G. S. Hardy (Ngunguru, New Zealand) kindly reviewed the manuscript. This study was supported in part by a grant-in-aid for scientific research (B) from the Japan Society for the Promotion of Science (JSPS) (20370034).

Literature cited

Alesandrini, S., and G. Bernardi.
1999. Ancient species flocks and recent speciation events: What can rockfishes teach us about cichlids (and vice versa)? Mol. Evol. 49:814–818.

Amaoka, K.
1984. Genus *Sebastes*. *In* The fishes of the Japanese archipelago, English ed. (H. Masuda, K. Amaoka, C. Araga, T. Uyeno, and T. Yoshino, eds.), p. 310–313. Tokai Univ. Press, Tokyo.

Avise, J. C.
2000. Phylogeography: The history and formation of species, 464 p. Harvard Univ. Press, Cambridge, MA.
2004. Molecular markers, natural history, and evolution, 2nd ed., 684 p. Sinauer Associate, Sunderland, MA.

Baker, J. M., E. López-Medrano, A. G. Navarro-Sigüenza, O. R. Rojas-Soto, and K. E. Omland.
2003. Recent speciation in the orchard oriole group: divergence of *Icterus spurius spurius* and *Icterus spurius fuertesi*. Auk 120:848–859.

Bensch, S., and M. Åkesson.
2005. Ten years of AFLP in ecology and evolution: Why so few animals? Mol. Ecol. 14:2899–2914.

Buonaccorsi, V. P., C. A. Kimbrell, E. A. Lynn, and R. D. Vetter.
2005. Limited realized dispersal and introgressive hybridization influence genetic structure and conservation strategies for brown rockfish *Sebastes auriculatus*. Conserv. Genet. 6:697–713.

Burford, M. O.
2009. Demographic history, geographical distribution and reproductive isolation of distinct lineages of blue rockfish (*Sebastes mystinus*), a marine fish with a high dispersal potential. J. Evol. Biol. 22:1471–1486.

Burford, M. O., and G. Bernardi.
2008. Incipient speciation within a subgenus of rockfish (*Sebastosomus*) provides evidence of recent radiations within an ancient species flock. Mar. Biol. 154:01–717.

Carvalho, G. R., and L. Hauser.
1994. Molecular genetics and stock concept in fisheries. Rev. Fish Biol. Fish. 4:326–350.

Chen, L. C.
1971. Systematics, variation, distribution, and biology of rockfishes of the subgenus *Sebastomus* (Pisces, Scorpaenidae, *Sebastes*). Bull. Scripps Inst. Oceanogr. 18:1–107.

Chen, L. C., and V. V. Barsukov.
1976. A study of the western North Pacific *Sebastes vulpes* species complex (Scorpaenidae), with description of a new species. Japan. J. Ichthyol. 23:1–8.

Congiu, L., I. Dupanloup, T. Patarnello, F. Fontana, R. Rossi, G. Arlati, and L. Zane.
2001. Identification of interspecific hybrids by amplified fragment length polymorphism: The case of sturgeon. Mol. Ecol. 10:2355–2359.

Donnelly, M. J., J. Pinto, R. Girod, N. J. Besansky, and T. Lehmann.
2004. Revisiting the role of introgression *vs* shared ancestral polymorphisms as key processes shaping genetic diversity in the recently separated sibling species of the *Anopheles gambiae* complex. Heredity 92:61–68.

Excoffier, L., and H. E. L. Lischer.
2010. Arlequin suite, vers. 3.5: A new series of programs to perform population genetics analyses under Linux and Windows. Mol. Ecol. Resour. 10:564–567.

Funk, D. J., and K. E. Omland.
2003. Species-level paraphyly and polyphyly: Frequency, causes, and consequences, with insights from animal mitochondrial DNA. Annu. Rev. Ecol. Evol. Syst. 34:397–423.

Grant, W. S., and B. W. Bowen.
1998. Shallow population histories in deep evolutionary lineages of marine fishes: Insights from sardines and anchovies and lessons for conservation. J. Hered. 89:415–426.

Hall, T. A.
1999. BioEdit: A user-friendly biological sequence alignment editor and analysis program for windows 95/98/NT. Nucl. Acids Symp. Ser. 41:95–98.

Hawkins, S. L., J. Heifetz, C. M. Kondzela, J. E. Pohl, R. L. Wilmot, O. N. Katugin, and V. N. Tuponogov.
2005. Genetic variation of rougheye rockfish (*Sebastes aleutianus*) and shortraker rockfish (*S. borealis*) inferred from allozymes. Fish. Bull. 103:524–535.

Higuchi, M., and K. Kato.
2002. Sequence variability in the mitochondrial DNA control region of five *Sebastes* species. Fish. Sci. 68:643–650.

Huff, D. R., R. Peakall, and P. E. Smouse.
1993. RAPD variation within and among natural populations of outcrossing buffalograss [*Buchloë dactylides* (Nutt.) Engelem.]. Theor. Appl. Genet. 86:927–934.

Hyde, J. R., C. A. Kimbrell, J. E. Budrick, E. A. Lynn, and R. D. Vetter.
2008. Cryptic speciation in the vermilion rockfish (*Sebastes miniatus*) and the role of bathymetry in the speciation process. Mol. Ecol. 17:1122–1136.

Hyde, J. R., and R. D. Vetter.
2007. The origin, evolution, and diversification of rockfishes of the genus *Sebastes* (Cuvier). Mol. Phylogenet. Evol. 44:790–811.

Ingram, T.
2011. Speciation along a depth gradient in a marine adaptive radiation. Proc. R. Soc. Lond. B 278:613–618.
Ishida, M.
2009. Scorpaenidae. *In* Sea fishes of Japan, 3rd ed. (O. Okamura, K. Amaoka, eds.), p. 189–209. Yama to Keikoku Sha, Tokyo. [In Japanese.]
Johns, G. C., and J. C. Avise.
1998. Tests for ancient species flocks based on molecular phylogenetic appraisals of *Sebastes* rockfishes and other marine fishes. Evolution 52:1135–1146.
Jordan, D. S., and C. W. Metz.
1913. A catalog of the fishes known from the waters of Korea. Mem. Carnegie Mus. 6:1–65.
Kai, Y., and T. Nakabo.
2002. Morphological differences among three color morphotypes of *Sebastes inermis* (Scorpaenidae). Ichthyol. Res. 49:260–266.
Kai, Y., K. Nakayama, and T. Nakabo.
2002a. Genetic differences among three colour morphotypes of the black rockfish, *Sebastes inermis*, inferred from mtDNA and AFLP analyses. Mol. Ecol. 11:2591–2598.
Kai ,Y., N. Yagishita, H. Ikeda, and T. Nakabo.
2002b. Genetic differences between two color morphotypes of redfish, *Sebastes scythropus* (Osteichthyes: Scorpaenidae). Species Div. 7:371–380.
2003. Molecular phylogenetic perspective on speciation in the genus *Sebastes* (Scorpaenidae) from the Northwest Pacific and the position of *Sebastes* within the subfamily Sebastinae. Ichthyol. Res. 50:239–244.
Kakehi, Y., K. Nakayama, K. Watanabe, M. and Nishida.
2005. Inheritance of amplified fragment length polymorphism markers and their utility in population genetic analysis of *Plecoglossus altivelis*. J. Fish Biol. 66:1529–1544.
Kanayama, T., and D. Kitagawa.
1983. Fishes of Iwate II, Soi-Menukerui, 47 p. Iwate Fisheries Experimental Station, Iwate, Japan. [In Japanese.]
Kitagawa, D., H. Imamura, T. Goto, Y. Ishito, K. Fujiwara, and Y. Ueda.
2008. Field guide of the fishes from the Tohoku district, north-eastern waters of Japan, 140 p. Tokai Univ. Press, Tokyo. [In Japanese.]
Larkin, M. A., G. Blackshields, N. P. Brown, R. Chenna, P. A. McGettigan, H. McWilliam, F. Valentin, I. M. Wallace, A. Wilm, R. Lopez, J. D. Thompson, T. J. Gibson, and D. G. Higgins.
2007. Clustal W and Clustal X, vers. 2.0. Bioinformatics 23:2947–2948.
Love, M. S., M. Yoklavich, and L. Thorsteinson.
2002. The rockfishes of the northeast Pacific, 405 p. Univ. California Press, Los Angeles, CA.
Matsubara, K.
1943. Studies on the scorpaenoid fishes of Japan. Anatomy, phylogeny and taxonomy II. Trans. Sigenkagaku Kenkyusho 2:171–486.
McMillan, W. O., and S. R. Palumbi.
1997. Rapid rate of control-region evolution in Pacific butterflyfishes (Chaetodontidae). J. Mol. Evol. 45:473–484.
Mendelson, T. C., and K. L. Shaw.
2005. Rapid speciation in an arthropod. Nature 433:375–376.
Meyer, A., T. D. Kocher, P. Basasibwaki, and A. C. Wilson.
1990. Monophyletic origin of Lake Victoria cichlid fishes suggested by mitochondrial-DNA sequences. Nature 347:550–553.
Nagasawa, T.
2000. Early life history of kitsune-mebaru, *Sebastes vulpes* (Scorpaenidae), in the Sea of Japan. Ichthyol. Res. 47:311–320.
Nakabo, T.
2002a. Introduction to ichthyology. *In* Fishes of Japan with pictorial keys to the species, English ed. (T. Nakabo, ed.), p. xxi–xlii. Tokai Univ. Press, Tokyo.
2002b. Scorpaenidae. *In* Fishes of Japan with pictorial keys to the species, English ed. (T. Nakabo, ed.), p. 565–595, 1524–1528. Tokai Univ. Press, Tokyo.
Narum, S. R., V. P. Buonaccorsi, C. A. Kimbrell, and R. D. Vetter.
2004. Genetic divergence between gopher rockfish (*Sebastes carnatus*) and black and yellow rockfish (*Sebastes chrysomelas*). Copeia 2004:926–931.
Nelson, J. S.
2006. Fishes of the world, 4th ed., 601 p. John Wiley and Sons, Inc., Hoboken, NJ.
Nichols, R.
2001. Gene trees and species trees are not the same. Trends Ecol. Evol. 16:358–364.
Omland, K. E., J. M. Baker, and J. L. Peters.
2006. Genetic signatures of intermediate divergence: population history of Old and New World Holarctic ravens (*Corvus corax*). Mol. Ecol. 15:795–808.
Orr, J. W., and J. E. Blackburn.
2004. The dusky rockfishes (Teleostei: Scorpaeniformes) of the North Pacific Ocean: Resurrection of *Sebastes variabilis* (Pallas, 1814) and a redescription of *Sebastes ciliatus* (Tilesius, 1813). Fish. Bull. 102:328–348.
Orr, J. W., and S. Hawkins.
2008. Species of the rougheye rockfish complex: Resurrection of *Sebastes melanostictus* (Matsubara, 1934) and a redescription of *Sebastes aleutianus* (Jordan and Evermann, 1898) (Teleostei: Scorpaeniformes). Fish. Bull. 106:111–134.
Peakall, R., and P. E. Smouse.
2006. GENALEX 6: Genetic analysis in Excel. Population genetic software for teaching and research. Mol. Ecol. Notes 6:288–295.
Peters, J. L., Y. Zhuravlev, V. Fefelov, A. Logie, and K. E. Omland.
2007. Nuclear loci and coalescent methods support ancient hybridization as cause of mitochondrial paraphyly between gadwall and falcated duck (*Anas* spp.). Evolution 61:1992–2006.
R Development Core Team.
2010. R: A language and environment for statistical computing. URL http://www.R-project.org.
Rocha-Olivares, A., R. H. Rosenblatt, and R. D. Vetter.
1999. Cryptic species of rockfishes (*Sebastes:* Scorpaenidae) in the southern hemisphere inferred from mitochondrial lineages. J. Hered. 90:404–411.
Roques, S., J. M. Sevigny, and L. Bernatchez.
2001. Evidence for broadscale introgressive hybridization between two redfish (genus *Sebastes*) in the North-west Atlantic: A rare marine example. Mol. Ecol. 10:149–165.
Rüber, L., and R. Zardoya.
2005. Rapid cladogenesis in marine fishes revisited. Evolution 59:1119–1127.
Sasaki, M.
2003. Kitsune mebaru *Sebastes vulpes* Döderlein. *In* Shin kita no sakana tachi (Y. Ueda, K. Maeda, H. Shimada, and T. Takami, eds.), p. 194–195. Hokkaido Shinbun Sha, Hokkaido, Japan. [In Japanese.]

Seehausen, O., E. Koetsier, M. V. Schneider, L. J. Chapman, C. A. Chapman, M. E. Knight, G. F. Turner, J. J. M. van Alphen, and R. Bills.
2003. Nuclear markers reveal unexpected genetic variation and a Congolese-Nilotic origin of the Lake Victoria cichlid species flock. Proc. R. Soc. Lond. B 270:2637–2638.

Sekigawa, T., T. Takahashi, T. Takatsu, S. Nishiuchi, M. Sasaki, and F. Shiokawa.
2003. Age and growth of *Sebastes vulpes* in the coastal waters of western Hokkaido, Japan. Fish. Sci. 69:575–580.

Sobel, J. M., G. F. Chen, L. R. Watt, and D. W. Schemske.
2009. The biology of speciation. Evolution 64:295–315.

Stefánsson, M. Ö., T. Sigurdsson, C. Pampoulie, A. K. Daníelsdóttir, B. Thorgilsson, A. Ragnarsdóttir, D. Gíslason, J. Coughlan, T. F. Cross, and L. Bernatchez.
2009. Pleistocene genetic legacy suggests incipient species of *Sebastes mentella* in the Irminger Sea. Heredity 102:514–524.

Steindachner, F., and L. Döderlein.
1884. Beiträge zur kenntniss der fische Japan's. (III.). Denkschr. Akad. Wiss. Wien. 49:171–212, Pls. 1–7. [In German.]

Vos, P., R. Hogers, M. Bleeker, M. Reijans, T. van de Lee, M. Hornes, A. Friters, J. Pot, J. Paleman, M. Kuiper, and M. Zabeau.
1995. AFLP: A new technique for DNA fingerprinting. Nucl. Acids Res. 23:4407–4414.

Young, W. P., C. O. Ostberg, P. Keim, and G. H. Thorgaard.
2001. Genetic characterization of hybridization and introgression between anadromous rainbow trout (*Oncorhynchus mykiss irideus*) and coastal cutthroat trout (*O. clarki clarki*). Mol. Ecol. 10:921–930.

Zakharov, E. V., N. F. Lobo, C. Nowak, and J. J. Hellmann.
2009. Introgression as a likely cause of mtDNA paraphyly in two allopatric skippers (Lepidoptera: Hesperiidae). Heredity 102:590–599.

Appendix

Materials examined

Sebastes vulpes (genetically assigned) 37 specimens. FAKU 82514; Noto, Ishikawa Prefecture, Japan, 30 May 2002, 200.2 mm SL. FAKU 83188, 83189, 83193, 83195–83197; Noto, Ishikawa Prefecture, Japan, 31 May 2002, 200.9–243.2 mm SL. FAKU 96073; Noto, Ishikawa Prefecture, Japan, 8 April 2008, 203.5 mm SL. FAKU 96074–96078; Noto, Ishikawa Prefecture, Japan, 1 May 2008, 156.4–218.5 mm SL. FAKU 96082–96088, 96090–96094; Matsunami, Ishikawa Prefecture, Japan, 1 May 2008, 159.8–230.9 mm SL. FAKU 96097, 96099, 96100, 131566, 131567, 131569; Noto, Ishikawa Prefecture, Japan, 2 May 2008, 170.0–249.9 mm SL. FAKU 130099; Noto, Ishikawa Prefecture, Japan, 13 May 2004, 182.1 mm SL. FAKU 131533–131537; Ogi, Ishikawa Prefecture, Japan, 10 April 2006, 161.0–176.6 mm SL. *Sebastes zonatus* (genetically assigned) 28 specimens. *FAKU 82515; Wajima, Ishikawa Prefecture, Japan, 30 May 2002, 189.0 mm SL. FAKU 82516–82519, 82521; Wajima, Ishikawa Prefecture, Japan, 30 May 2002, 137.3–165.1 mm SL. FAKU 83185–83187; Noto, Ishikawa Prefecture, Japan, 30 May 2002, 252.1–286.4 mm SL. FAKU 85799; Noto, Ishikawa Prefecture, Japan, 11 February 2003, 257.5mm SL. FAKU 96095; Toyama Bay, Japan, 1 May 2008, 234.4 mm SL. FAKU 96096, 96098; Noto, Ishikawa Prefecture, Japan, 2 May 2008, 184.8–210.3 mm SL. FAKU 97077, 97080, 97082, 97083; Wajima, Ishikawa Prefecture, Japan, 7 July 2009, 147.9–170.3 mm SL. FAKU 129995, 130103–130105, 130349; Toyama Bay, Japan, 7 July 2004, 206.5–232.7 mm SL. FAKU 130100–130102; Ogi, Ishikawa Prefecture, Japan, 13 May 2004, 160.1–176.2 mm SL. FAKU 130235; Noto, Ishikawa Prefecture, Japan, 7 June 2004, 202.8 mm SL. *FAKU 130236; Noto, Ishikawa Prefecture, Japan, 12 May 2004, 154.8 mm SL. FAKU 131568; Noto, Ishikawa Prefecture, Japan, 2 May 2008, 204.2 mm SL. * indicates the specimen was initially identified as *S. vulpes* by body coloration but genetically assigned to *S. zonatus* in the principal coordinate analysis of amplified fragment length polymorphisms.

Ocean distribution of the American shad (*Alosa sapidissima*) along the Pacific coast of North America

William G. Pearcy (contact author)[1]

Joseph P. Fisher[2]

Email address for contact author: wgpearcy@coas.oregonstate.edu

[1] College of Oceanic and Atmospheric Sciences
Oregon State University
Corvallis, Oregon 97331

[2] Cooperative Institute for Marine Resources Studies
Hatfield Marine Science Center
Oregon State University
Newport, Oregon 97365

Abstract—We examined the incidental catches of American shad (*Alosa sapidissima*) taken during research cruises and in commercial and recreational landings along the Pacific coast of North America during over 30 years of sampling. Shad, an introduced species, was mainly found over the shallow continental shelf, and largest catches and highest frequency of occurrences were found north of central Oregon, along the coasts of Washington and Vancouver Island, and in California around San Francisco Bay. Migrations to the north off Washington and Vancouver were seen during spring to fall, but we found no evidence for large-scale seasonal migrations to the south during the fall or winter. The average weight of shad increased in deeper water. Sizes were also larger in early years of the study. Most were caught over a wide range of sea surface temperatures (11–17°C) and bottom temperatures (6.4–8.0°C). Abundance of shad on the continental shelf north of 44°N was highly correlated with counts of shad at Bonneville Dam on the Columbia River in the same year. Counts were negatively related to average weights and also negatively correlated with the survival of hatchery coho salmon (*Oncorhynchus kisutch*), indicating that survival of shad is favored by warm ocean conditions. Examining the catch during research cruises and commercial and recreational landings, we concluded that American shad along the Pacific coast have adapted to the prevailing environmental conditions and undertake only moderate seasonal migrations compared with the long seasonal migrations of shad along the Atlantic coast of North America. We suggest that the large spawning populations in the Columbia River and San Francisco Bay areas explain most of the distributional features along the Pacific coast.

Manuscript submitted 1 April 2011.
Manuscript accepted 22 July 2011
Fish. Bull. 109:440–453 (2011).

American shad (*Alosa sapidissima*), the largest member of the family Clupeidae, is a euryhaline, anadromous fish native to the east coast of North America, where it ranges from Florida to the Bay of Fundy. American shad undertake extensive ocean migrations along the east coast of North America to the north in the summer, and south in the fall and winter, before returning to natal rivers in the spring to spawn. Adults usually spend 3–6 years in the ocean before returning to spawn in natal rivers. Juveniles migrate downstream in the fall, but some may reside in estuaries more than a year (Talbot and Sykes, 1958; Walburg and Nichols, 1967; Leggett, 1973). According to tagging studies, their extensive ocean migrations, of sometimes thousands of kilometers during one season, are closely correlated with 13–18° sea surface isotherms (Leggett, 1973; Leggett and Whitney, 1972) and 7–13°C bottom temperatures (Neves and Depres, 1979).

Little is known about the ocean life of American shad (hereafter referred to as "shad") along the west coast of North America, although long migrations, like those in the Atlantic, have been postulated (Leggett and Whitney, 1972; Moyle, 1976; Petersen et al., 2003). We examine recent catches of American shad along the Pacific coast of North America from research surveys, 1977–2008, as well as from landings of shad by commercial or sport vessels, thus expanding the data provided for the Pacific coast by Petersen et al. (2003) and Leggett and Whitney (1972). We compare similarities in distributions and seasonal migrations along the Pacific coast with those along the Atlantic coast of North America.

American shad were first introduced to the Pacific coast of North America from the eastern United States in 1871. About ten thousand shad from the Hudson River were released into the Sacramento River after shipment across the country in 8-gallon (31.3-L) milk cans by the California Fish Commission (Green, 1874). Several other shipments were made between 1871 and 1881 (Smith, 1896). Shad migrated rapidly to the north and south. They were introduced into the Columbia River, and the Willamette and Snake rivers, in 1885 and 1886 (Skinner, 1962; Craig and Hacker, 1940). However, shad had appeared in the Columbia River several years before these introductions, and this occurrence indicated the rapid movements of fish planted earlier in California (Welander, 1940; Oregon Fish Commission, 1951). Shad eventually were found in British Columbia in 1891, and later as far north as Alaska and as far south as Baja California (Hart, 1973). They have been reported as far west as Kamchatka, Russia, but established spawning populations there are not known (Chereshnev and Zharnikov, 1989).

Adult and juvenile shad have been reported in many bays and estuaries along the west coast of United States from Grays Harbor, Washington, to San Francisco Bay, California (Emmett et al[1]). Their distribution in inland and coastal waters along the Pacific coast is known mainly from fishery landings. Large commercial catches of shad have been made in rivers in Oregon, Washington, and California. A fishery existed in the Columbia River, as well as in Oregon coastal streams in the early 1900s. Landings in other rivers (Siuslaw, Umpqua, Smith, Coos, and Coquille) in Oregon, where shad spawned, averaged 192 metric tons per year (t/yr) during 1962–72 (Mullen and Conover[2]). The fishery in the Umpqua River landed an average of 180 t annually after 1923 (Skinner, 1962). Each of these rivers apparently supported its own spawning run of shad, although some recoveries of tagged fish have been reported in other rivers (Mullen[3]). In the Columbia River, counts of shad passing Bonneville Dam to spawn during May through July have increased greatly over the past 70 years because of the completion of dams and creation of large reservoirs, from fewer than 17,000 before 1960 to over 2–5 million after 1990 (www.cbr.washington.edu/dart/, accessed November 2010). Several hundred thousand shad are landed annually by commercial and sport fisheries in the Columbia River (Petersen et al., 2003). Adults are even found in the Snake River above Lower Granite Dam, 600 km from the ocean (Quinn and Adams, 1996). However, the major spawning areas for shad in the Columbia River are thought to be below Bonneville Dam where large numbers of juvenile shad are found in the estuary (Cleaver, 1951; Oregon Fish Commission, 1951; Hamman, 1981; Petersen et al., 2003). In Washington, breeding populations of shad are known from Puget Sound, the Chehalis River, and Willapa Bay (Wydoski and Whitney, 2003; Emmett et al.[1]).

In California, large runs of shad migrate into the Sacramento–San Joaquin River Delta to spawn where juvenile shad have been collected. Smaller runs are found in the Klamath, Eel, Salinas, and Russian rivers (Skinner, 1962; Allen et al., 2006; CDFG[4]). The shad fishery in the San Francisco Bay area peaked in 1917 when over 2500 t were landed. Between 1918 and 1945 the catch averaged 362 to 1800 t and then declined. In 1957 the commercial fishery in the bay was closed and there now exists only a sport fishery (Skinner, 1962; Moyle, 1976).

Shad were first reported in British Columbia in 1891; small numbers were caught between 1914 and 1946 in fresh water. They were also reported from several regions in the ocean along the coast (Carl et al., 1959), but according to McPhail (2007), there is no evidence of reproduction in British Columbia.

Our objectives were to document the distributional patterns of American shad along the Pacific coast of North America and to compare these patterns with those known from the Atlantic coast.

Materials and methods

American shad were captured incidentally in both pelagic and benthic research surveys from 1977 through 2008 from California to British Columbia, as well as in commercial and recreational fisheries. National Oceanic and Atmospheric Administration's (NOAA) Alaska Fisheries Science Center (AFSC) triennial bottom trawl surveys from 1977 to 2004 provided extensive data on shad catches. Nor'eastern trawls (with 27.4-m head-rope and 12.7-cm mesh in the body, 9-cm mesh in the codend and a 3.2-cm stretch mesh liner) were fished during the day at about 5.6 km/h for one half hour and from depths of 55 to 500 m during the months of May through September, 1977–2004 (Stauffer, 2004). Cruises began during different months of the year, beginning in California and progressing northward to Vancouver Island.

Shad were also caught by the Northwest Fisheries Science Center (NWFSC) in bottom trawls (Aberdeen-style high-opening net, 26-m head rope, 3.8 cm liner in the codend), fished during the daytime to depths of 55–1280 m at a nominal tow duration of 15 min on the bottom at 4.0 km/h, mainly from late May to late July (early cruise) and again from late August to late October (late cruise), 2003–08. The trawl surveys were conducted according to a random-stratified sampling design (Keller et al., 2008). Biomass caught in both the AFSC and NWFSC trawls was converted to average weight per shad by dividing the total biomass by the total number of shad caught. Stepwise multiple regression models were used to relate size of shad to bottom depth, day of year, sea surface temperature (SST), and bottom (gear) temperature during the 10 years of AFSC surveys, and to bottom depth and day of year during the six years of the NWFSC surveys (SST data for the NWFSC cruises were not available). Catches were also related to the Pacific Decadal Oscillation (Mantua et al., 1997), Oregon Production Index (OPI) survival estimates generated from hatchery releases of coho salmon (*Oncorhynchus kisutch*) smolts and returns of adult coho salmon to hatcheries, and counts of shad passing the Bonneville Dam. Shad were also caught in pelagic surveys targeting juvenile salmonids from 1981 to 2008 off Oregon and Washington. The purse

[1] Emmett, R.L., S.A. Hinton, S.L. Stone and M.E. Monaco. 1991. Distribution and abundance of fishes and invertebrates in west coast estuaries. Volume 11: species life history summaries. ELME Report 8, 329 p. NOAA/NOS Strategic Environmental Assessments Division, Rockville, MD.

[2] Mullen, R. E., and K. R. Conover. 1973. Ecology of shad and striped bass in coastal rivers and estuaries, 12 p. Fish Comm. Oregon, Project No. AFC 53, Portland, OR.

[3] Mullen, R. E. 1974. A summary of American shad (*Alosa sapidissima*) tagging studies on the coastal streams of Oregon, 1946–70. Coastal Rivers Investigation, Inf. Rep. 74-3, 43 p. Fish Comm. Oregon, Portland, OR.

[4] CDFG (California Department of Fish and Game). 2010. Effects of delta inflow and outflow on several native, recreational, and commercial species. DFG Exhibit 1, unpubl. report, 39 p. California Department of Fish and Game, 830 S Street, Sacramento, CA 95811.

seine used during 1981–85 was 457–496 m long, had 32-mm or finer mesh, fished to a depth of 30–65 m, and sampled about 20,000 m^2 (Pearcy and Fisher, 1988). The midwater trawl deployed during 1998–2008 was a Nordic rope trawl that fished near the surface mainly during the day with a mouth opening 30 m wide×20 m deep and had a 0.8-cm fine mesh liner in the codend (Brodeur et al., 2005).

Shad catches and sizes were available from both commercial midwater and bottom trawling, 1997–2009, off British Columbia (Davidson and Fargo[5]), from commercial landings from bottom and midwater trawls and from gill nets, set nets, dip nets, and hook-and-line gear fished in the Columbia River and the Oregon coast, 1978–2009 (Karnowski and Hurtado[6]) and California (Larinto[7]). Catches in all regions were highly variable and shad discarded as bycatch were not reported. In addition, observer data on shad catches in the limited-entry trawl groundfish fishery in Washington, Oregon, and California for "summer" (April–October) and "winter" (November–March) seasons, 2002–2009 were also examined (Majewski and Bellman[8]; Olson[9]).

Shad, a schooling pelagic fish, undertake diel vertical migrations in the Atlantic (Neves and Depres, 1979). Such migrations are not known, however, for shad in the Pacific Ocean. We assumed that they would be more susceptible to capture during the daytime in bottom tows, or as the net descended or ascended to surface waters than in surface waters. Because schooling behavior may result in a few extremely large catches and many zero catches, we restricted our analyses mainly to $\log_{10}$ transformed numbers for fish caught and presence–absence data to deemphasize the rare catches of large numbers of shad. Although bottom trawls are designed to capture demersal species, catches may reflect major changes in abundance or availability of pelagic species, such as shad (Neves and Depres, 1979). In addition, shad migrate into estuaries and freshwater to spawn during May, June, and July along the Pacific coast (Hamman, 1981; Petersen et al., 2003) and hence adults and some juveniles were not available during the early months of ocean sampling. Also, small and young-of-the-year shad are unlikely to be retained by all sampling nets.

[5] Davidson, J., and J. Fargo. 2010. Personal commun. Department of Fisheries and Oceans, 200-401 Burrand St., Vancouver, British Columbia, Canada V6C 3S4.

[6] Karnowski, M., and N. Hurtado. 2010. Personal commun. Oregon Department of Fish and Wildlife, 2040 Southeast Marine Science Dr., Newport, OR 97365, and 3406 Cherry Ave NE, Salem, OR 97305.

[7] Larinto, T. 2010. Personal commun. California Department of Fish and Game, 4665 Lampson Ave Los Alamintos, CA 90720.

[8] Majewski, J., and M. Bellman. 2010. Personal commun. Northwest Fisheries Science Center, 2725 Montlake Blvd. E., Seattle, WA 98112.

[9] Olson, J. 2010. Personal commun. Pacific States Marine Fisheries Commission, 7600 Sand Point Way, Seattle, WA 98115.

Results

Shad were caught in 1178 of the 5612 tows by the AFSC (frequency of occurrence, FO=21%), and in 403 of 3762 tows by the NWFSC (FO=11%). Highest $\log_{10}$ catches were noted along the continental shelf off Washington and Vancouver Island and off San Francisco Bay during the AFSC cruises (Fig. 1A). Catches in NWFSC early season and late season tows were more uniformly distributed along the coast from northern Washington to northern California than were AFSC catches, but again with highest catches off Washington and lower catches to the south, with a cluster of catches off San Francisco (Fig 1, B and C). Large catches appeared to shift from Oregon to off Washington up to Vancouver Island between the early and late NWFSC cruises. This shift was consistent with the high catches off Vancouver Island also in late summer during the AFSC cruises (see also Fig. 2).

When the $\log_{10}(catch+1)$ and FO data were pooled across years, clusters of high shad catches became evident off the Washington coast (45–49°N lat.) and along the central California coast (37–38 °N lat.) during the AFSC sampling (Fig. 2A). Similar latitudinal trends in abundance were shown with the late-May to late-July NWFSC sampling (Fig. 2B), and this northward shift in abundance was also documented with the late-August to late-October NWFSC sampling (Fig. 2C). In addition to the two latitudinal centers of abundance seen in the AFSC sampling, the NWFSC sampling indicates a third center of abundance in northern California (41–42°N lat.). Despite interannual variations in the distribution of catches along the coast among years of sampling, this fairly consistent distributional pattern emerged. Note that catches in the AFSC tows were sometimes orders of magnitude higher than those in the NWFSC tows (Fig. 2), a difference related to the faster tow speeds, longer tow durations on the bottom, and the higher net opening of the AFSC tows.

Shad were also collected in purse seine surveys off Oregon and Washington during cruises conducted by Oregon State University from 1981 through 1985 (summarized by month in Fig. 3). Over 1100 shad were caught in 29 sets. Catches had a restricted distribution mainly near the Columbia River plume and close to shore. The largest catch comprised 883 shad in one purse seine set off Cape Disappointment in August 1981. In the daytime surface trawls by the NWFSC, only 139 shad were captured from 43 tows out of a total of 1536 tows (FO=2.8%) from central Oregon and the Washington coast during 1998–2008 (Fig. 4). These numbers and frequencies of occurrence were much lower than those seen during the demersal sampling (Fig. 2), supporting the observations in the Atlantic that shad undertake diel vertical migrations and are more available in subsurface than in surface waters by day.

An inshore–offshore gradient in abundance of shad was significant; most shad were caught in AFSC and NWFSC tows on the continental shelf (≤200 m) (Fig. 5,

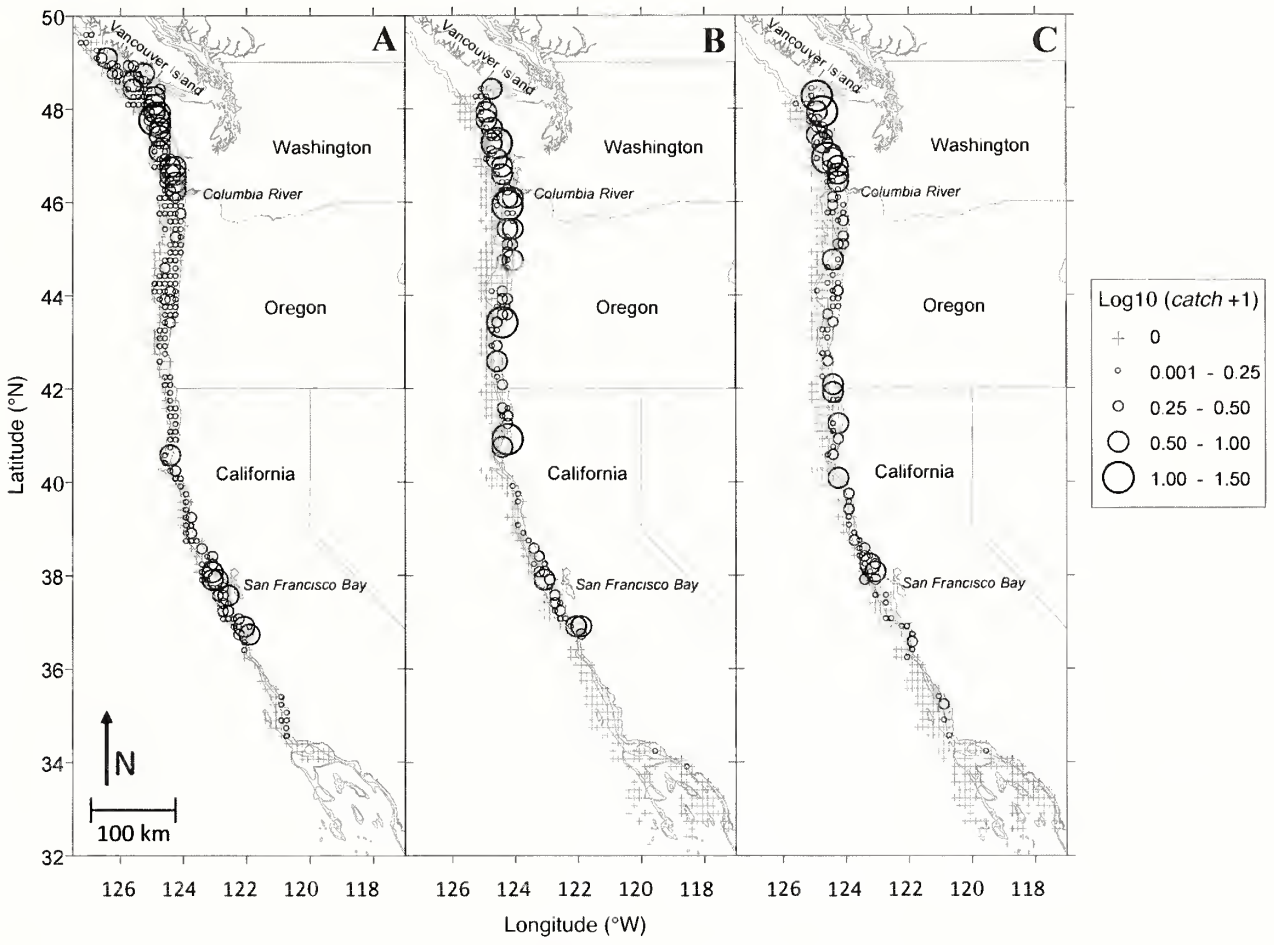

Figure 1

Average catch of American shad (*Alosa sapidissima*) in 10′ latitude×10′ longitude sampling areas during (**A**) 30-minute bottom tows conducted by the Alaska Fisheries Science Center for the years 1977–2004 combined, and (**B**) during 15-minute bottom tows conducted by the Northwest Fisheries Science Center for the years 2003–08 combined in early season sampling (May–July), and (**C**) late season sampling (August–October). Isobaths are 200 m and 500 m. Catch is transformed by $\log_{10}(catch+1)$.

Table 1). On the shelf shad were found in 28% of AFSC tows (1132 of 4010), whereas, off the shelf in deeper water they were found in only 2% of tows (36 of 1586). Similarly, shad were found in 24% of NWFSC tows (394 of 1669) on the shelf, but in <1% of off shelf tows (9 of 2093).

The average weight of individual shad caught in AFSC trawls increased with both latitude and day of year (Fig. 6, A and B). However, because latitude and day of year were highly correlated during each AFSC cruise (correlation coefficient [R]=0.90–0.99), it was impossible to separate the effects of these two variables on size. Average weight consistently increased with depth during both surveys and often with day of year during the AFSC sampling. An effect of sea surface temperature on size was evident in only a few years (Table 1). Similar increases in weight were obtained when latitude was substituted for day of year (not shown in Table 1). The increase in size of shad with depth was consistent in all sampling collections that we examined. Besides the increase in average weight of shad with depth in the AFSC and NWFSC tows (Table 1), shad weight in purse seines was also positively correlated with depth (R=0.40, n=43 hauls, P=0.007), and in the limited-entry trawl fisheries off Washington, Oregon, and California during both summer and winter seasons (linear regressions of average weight of shad by 5-m tow depth intervals: summer, n=36, slope =0.0026 kg/m, coefficient of determination [r^2]=0.53, P<0.001; winter, n=33, slope=0.0016 kg/m, r^2=0.56, P<0.001).

The weight of shad caught in later years, uncorrected for date of sampling or depth of tow, was also significantly less than that in early years (Fig. 7A). To correct weight for depth and date of sampling in the different years a general linear model was applied to the weight data from both the AFSC and NWFSC demersal surveys combined (Fig. 7B). Even when adjusted for bottom depth and date of capture (much earlier for 1995–2004),

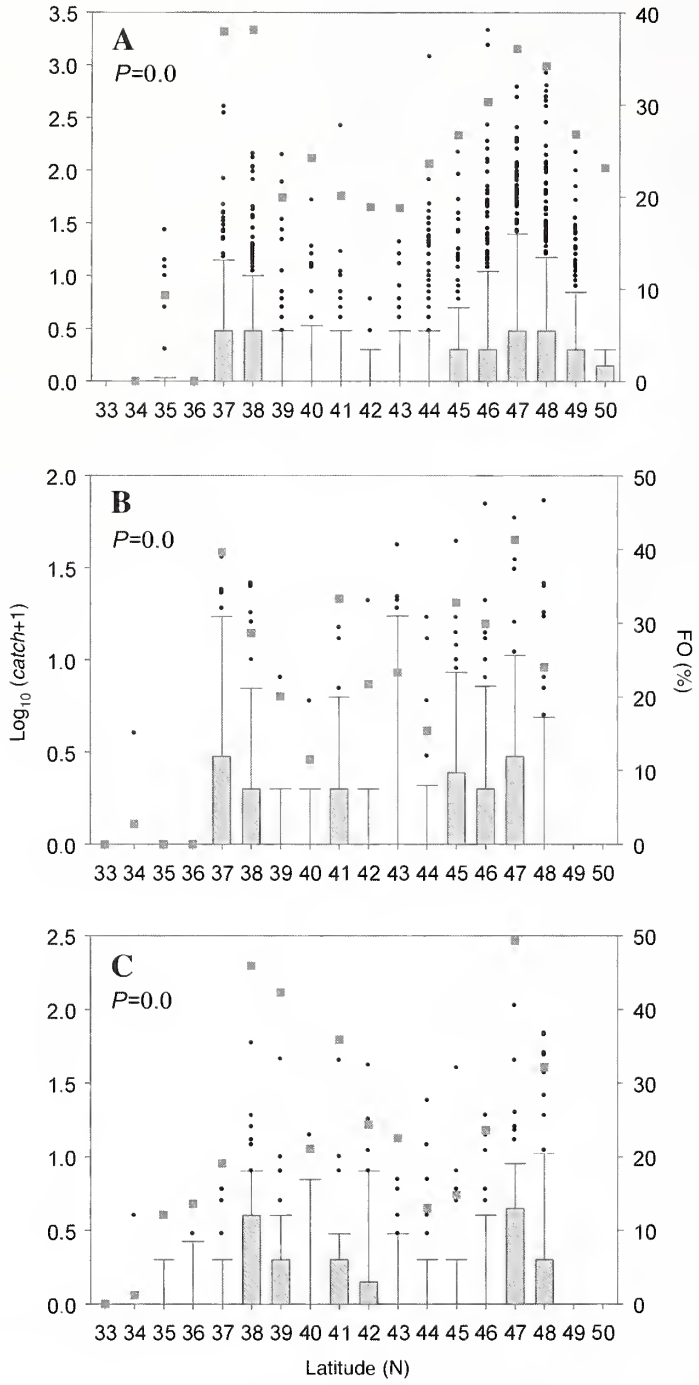

Figure 2

Log_{10}-transformed catch of American shad (*Alosa sapidissima*) and percent frequency of occurrence (FO) out to the 200-m isobath by one degree latitude ranges during (**A**) the 1977–2004 Alaska Fisheries Science Center triennial surveys, (**B**) the 2003–08 Northwest Fisheries Science Center early season (May–July) sampling, and (**C**) late season (August–October) sampling. Box plots show the 50th–75th percentile (shaded columns), the 10th–90th percentiles (whiskers), and outliers (dots). Small squares indicate FO of shad in tows. Kruskal-Wallace tests showed that catch differed by latitude ($P<0.05$) for all three studies.

a decline in size with year was still apparent (Fig. 7B). Shad caught in the surface trawls in 1998 were larger than those in the four subsequent years (2001, 2004, 2007, and 2008) when more than 10 fish were caught (Kruskal-Wallace test, $P=0.001$) and therefore also indicated a possible decrease in average weight of shad during this decade.

During the AFSC sampling survey over the shelf (≤200 m), shad were caught in tows over a wide range of sea surface temperatures (SSTs), from about 9° to 18°C, with the 10th and 90th percentiles of $\log_{10}(catch+1)$ occurring at 11.2° and 16.5°C, respectively (Fig. 8A). Cumulative frequency curves of $\log_{10}(catch+1)$ vs. SST and presence–absence vs. SST closely followed that of sampling, indicating that shad were widespread across most sea surface temperatures sampled on the shelf. However, the raw catch of shad (numbers per tow) indicated that the largest catches tended to occur where SSTs were from 13° to 17°C (Fig. 8A). This finding indicates that large schools of shad may be more abundant in areas where the SST is above 13°C. Conversely, the largest catches of shad also tended to occur where the bottom temperature (where gear was situated) was colder than that found in most other areas sampled; 80% of the raw catch occurred between 6.4°C and 8.0°C, whereas only 56% of sampling was in water that cold (Fig. 8, B and C). During both AFSC and NWFSC sampling surveys, bottom temperature was strongly negatively correlated with latitude ($R=0.78$ and 0.86, respectively). SST was weakly positively correlated with latitude ($R=0.36$). Therefore, the shad abundance vs SST patterns seen in Figure 8 (largest catches where bottom temperature is cool and SST is warm) are consistent with the generally larger catches seen north of 44°N and the smaller catches seen off central California (Fig. 2).

Discussion

Shad undertake long distance seasonal migrations along the Atlantic coast of the United States, swimming thousands of kilometers north in the summer and south in the winter (Talbot and Sykes, 1958; Walburg and Nichols, 1967; Leggett and Whitney, 1972; Leggett, 1973). Although little is known about shad migrations in the Pacific Ocean (Moyle, 1976), Leggett and Whitney (1972) speculated that shad in the Pacific Ocean migrate long distances within their preferred SST range of 13–18°C as they do in the Atlantic—migrating south of Point Conception into southern

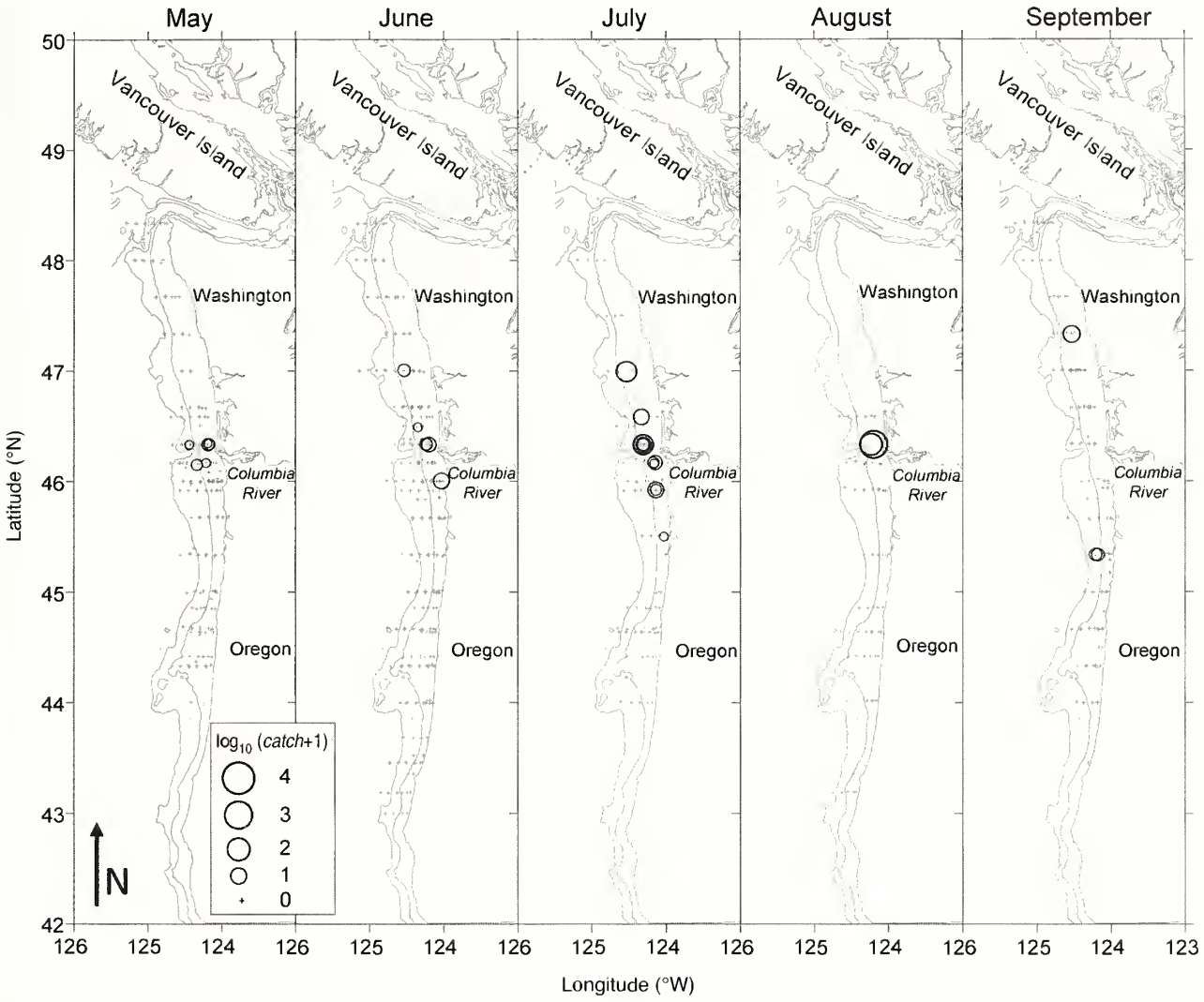

Figure 3

Catch of American shad (*Alosa sapidissima*) in round haul purse seine sets conducted by Oregon State University by month, for the combined years 1981–85. Catches are $\log_{10}$-transformed. Isobaths are 100 m and 200 m.

California and Baja Mexico during January–June, followed by migrations far to the north during July–October. Because ocean temperatures along the coast are often cooled by coastal upwelling during July, Leggett and Whitney thought that northward movements were diverted offshore to avoid these cool coastal waters. Data from our research surveys were collected mainly during the spring and summer; however, other data lend little support for shad migrations in the Pacific Ocean far to the south during the winter months. Data from commercial and sport landings of American shad along the Pacific coast indicate limited seasonal migrations along the West Coast.

In British Columbia, over 100 t of shad have been landed in some years in bottom and midwater trawls from 1997 to 2009 (Davidson andFargo[5]). This figure includes large catches from "unknown management" ocean areas in British Columbia (not shown in Table 2). From known ocean management areas, about 85% of the weight landed occurred between April and October ("summer" in Table 2) and most of these landings (95%) occurred during the months of August and October (see Figs. 1 and 2A). Shad were 260–580 mm fork length, most 400 mm or larger (about 0.8–3.0 kg; Davidson and Fargo [5]), mature, and over three years of age according to Petersen et al. (2003) and Hamman (1981). Large numbers of shad would not be expected in British Columbia waters during the fall when cool water temperatures below 13°C prevail if their migration patterns were similar to those predicted or shown for the Atlantic coast by Leggett and Whitney (1972). These large catches often found off the northern Washington and British Columbia coasts (Figs. 1 and 2) indicate that many shad from the Columbia River region move to the north after spawning. Surface currents to the north along the coast during winter months, or the deep

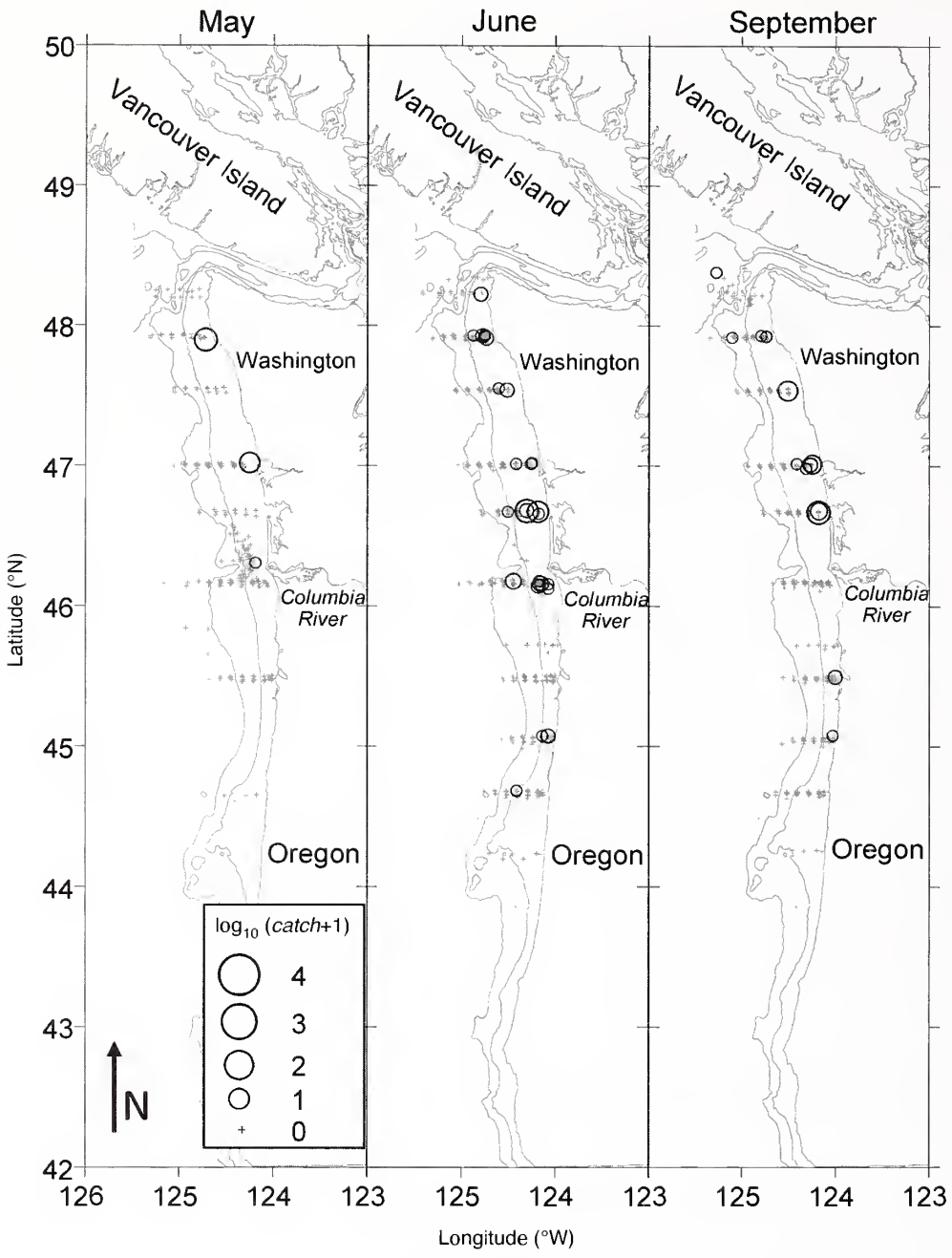

Figure 4

Catch of American shad (*Alosa sapidissima*) in Northwest Fisheries Science Center surface trawls (most 30 minutes) by month, for the combined years 1998–2008. Catches are $\log_{10}$-transformed. Isobaths are 100 m and 200 m.

countercurrent to the north during the spring and early summer off Oregon (Huyer et al., 1975) may passively transport shad to the north.

Most commercial landings of shad in Oregon are from gill nets fished in the Columbia River and along the Oregon coast during May and June when fishing effort is high and shad are migrating into the Columbia River (up to 40 to 172 t per month in some years between 1978 and 2009). Shad are also caught and landed in bottom and midwater trawls used to target Pacific whiting (*Merluccius productus*) during the summer, and some are landed in trawls or gill nets during the fall and winter, October–March (Table 3; Karnowski and Hurtado[6]). In northern California, where up to 32 t of shad are landed in some years, more shad were landed in the ocean and inland waters during the "winter" than the "summer" (Table 3; Larinto[7]). Observer data on shad catches in the limited-entry trawl groundfish

fishery (Majewski and Bellman[8]; Olson[9]) indicated that the percentage of tows with shad was higher in the "summer" (April–October) than in the "winter" (November–March). Although the average number of shad caught in positive tows was higher in California in the winter, catches were still taken in Oregon and Washington waters in the winter (Table 3). Lower catches per positive tows in the winter may be related to the deeper distribution of shad below 200 m in the winter, as found by Talbot and Sykes (1958).

Moreover, shad were rarely caught in fisheries targeting Pacific sardine (*Sardinops sagax*) and northern anchovy (*Engraulis mordax*) in southern California during any season of the year (Sweetman[10]), or in pelagic trawling off the central California coast (Brodeur et al., 2003). During eleven years of sampling (1995–2005) with variable mesh gill nets in bays and estuaries of California, Allen et al. (2006) and L. Allen[11] found shad in the Klamath and Eel rivers, but mainly in San Francisco Bay. These are apparently the only bays where shad spawn. In the southern California Bight, only 78 American shad were caught in thirteen years of sampling in shallow, protected embayments from Santa Barbara to Oceanside during the summer and fall. In summary, from all these observations of the geographic distribution of catches of shad, we see little evidence for long-distance seasonal migrations of stocks along the Pacific coast and a massive exodus from northern waters in the fall and large increases in southern California waters below 35°N. These differences are probably driven by the more extreme ranges of seasonal temperatures along the east coast in contrast to the temperature ranges along the west coast of North America.

In our study, most shad were also caught in bottom trawls in shallow water (<150 m depth), which is consistent with ocean catches in the Atlantic (Neves and Depres, 1979), and with the few catches of shad beyond the continental shelf in bottom and midwater trawls off California, Oregon and Washington (Brodeur et al., 2003, 2005; Ralston and MacFarlane[12]). We found no evidence that shad were more abundant offshore or that they avoided cooler nearshore waters along the Pacific coast during the upwelling season by migrating offshore as postulated by Leggettt and Whitney (1972).

Shad caught along the Pacific coast were generally larger in deep water along the outer continental shelf where bottom temperatures are cooler and surface temperatures are warmer during spring and summer months than inshore (Table 1). The lower catch number for shad off California (Fig. 2A) may also reflect their preference for cool bottom temperatures to the north. Although shad weight increased with latitude in the AFSC survey (Fig. 6A), it did not in the NWSC

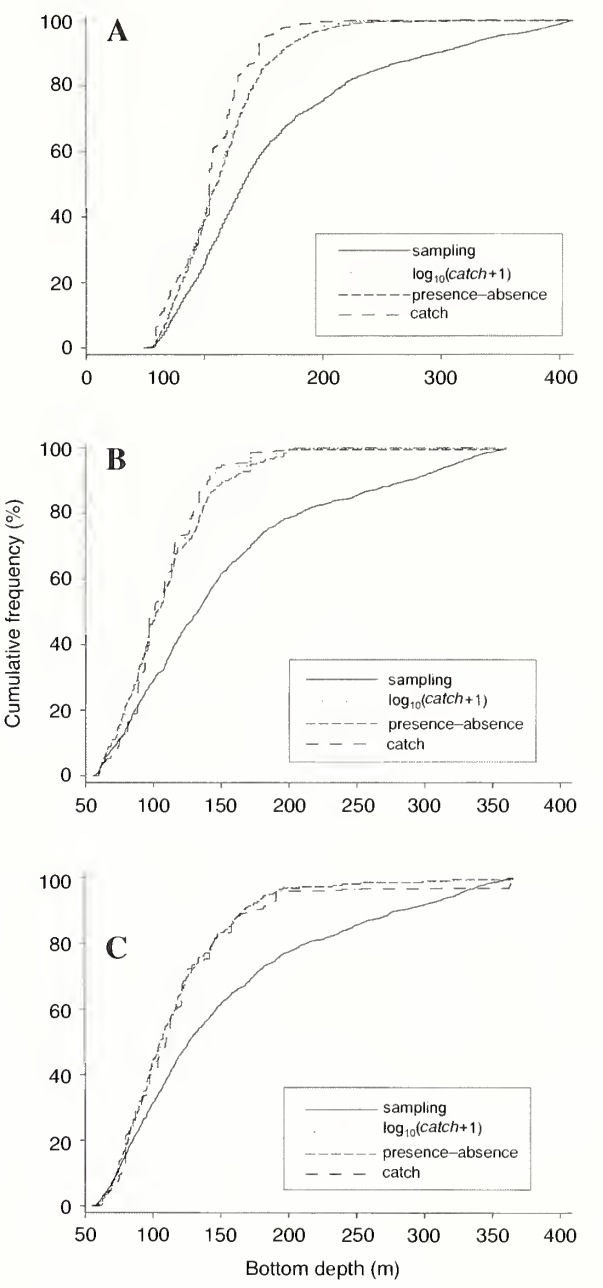

Figure 5

Cumulative frequency curves for sampling effort (number of tows), $\log_{10}$-transformed catch, presence–absence (1=present, 0=absent) of fish, and raw catch of American shad (*Alosa sapidissima*) vs. bottom depth out to the greatest depth of American shad catch during (**A**) the 1977–2004 Alaska Fisheries Science Center triennial surveys, and (**B**) the 2003–2008 Northwest Fisheries Science Center early season sampling, and (**C**) late season sampling surveys.

[10] Sweetman, D. 2010. Personal commun. California Dept. of Fish and Game, 8604 La Jolla Shores Dr., La Jolla, CA 92037.

[11] Allen, L. 2010. Personal commun. Southern California Marine Institute, 820 S. Seaside Ave, Terminal Island, CA 91330.

[12] Ralston, S., and B. MacFarlane. 2010. Personal commun. NOAA Southwest Fisheries Science Center, 110 Shaffer Rd., Santa Cruz, CA 95060.

Table 1

Results of forward selection multiple regression models relating the average weight (kg) of American shad (*Alosa sapidissima*) in Alaska Fisheries Science Center (AFSC) and Northwest Fisheries Science Center (NWFSC) sampling surveys in different years to sea-surface temperature (SST), bottom depth, and day of year. Shown for each model are the significant ($P<0.05$) coefficients and r^2 (coefficient of determination). SST was not available from the NWFSC sampling.

		Regression coefficients for weight on:			
Year	No of hauls	SST (kg/°C)	Depth (kg/m)	Day of year (kg/d)	r^2
AFSC					
1977–2004	1168	ns	0.0029	0.0027	0.23
1977	29	0.12	ns	ns	0.15
1980	26	ns	0.0120	ns	0.46
1983	133	ns	0.0024	0.0039	0.20
1986	152	ns	0.0044	ns	0.18
1989	94	0.04	0.0040	ns	0.38
1992	191	ns	0.0021	0.0057	0.36
1995	154	ns	0.0018	0.0056	0.35
1998	163	—[a]	0.0026	0.0050	0.43
2001	95	ns	0.0029	0.0025	0.25
2004	108	ns	0.0031	0.0025	0.23
NWFSC					
2003–08	387	—	0.0026	ns	0.15
2003	57	—	0.0038	ns	0.28
2004	76	—	0.0041	0.0020	0.36
2005	106	—	0.0025	ns	0.16
2006	60	—	0.0017	ns	0.08
2007	52	—	0.0030	ns	0.14
2008	36	—	ns	ns	0.00

[a] SST was removed from model because it was highly correlated ($R>0.5$) with the other, stronger variables.

Table 2

Total landings of American shad (*Alosa sapidissima*) in known management areas for British Columbia (1997–2010 provided by Department of Fisheries and Oceans), and Oregon, Washington and California (1981–2010 provided by the Pacific Fisheries Information Network database). Data for the United States are summarized for ocean, inland, and unknown areas and for the two seasons: April-October (summer) and November–March (winter).

Area	Ocean/ Inland	Season	Weight landed (t)	Area	Ocean/ Inland	Season	Weight landed (t)
BC	Ocean	Summer	17	CA	Ocean	Summer	13
	Ocean	Winter	3		Inland	Summer	23
OR and WA	Ocean	Summer	420		Ocean	Winter	27
	Inland	Summer	2307		Inland	Winter	51
	Unknown	Summer	577				
	Unknown	Winter	3				

sampling survey. However, shad landed off Vancouver Island were usually larger (2.0–3.0 kg; Davidson and Fargo[5]) than farther to the south (Figs. 6 and 7), indicating that larger shad may migrate farther to the north and remain in these cooler water longer, as do other pelagic species, such as Pacific whiting (Bailey et al., 1982; Dorn, 1995) and sardine (Emmett et al., 2005). Increased tolerances of cool water by large shad may explain both their extensive inshore–offshore and latitudinal distributions.

We found that shad occurred over a wide range of sea-surface temperatures; largest catches occurred

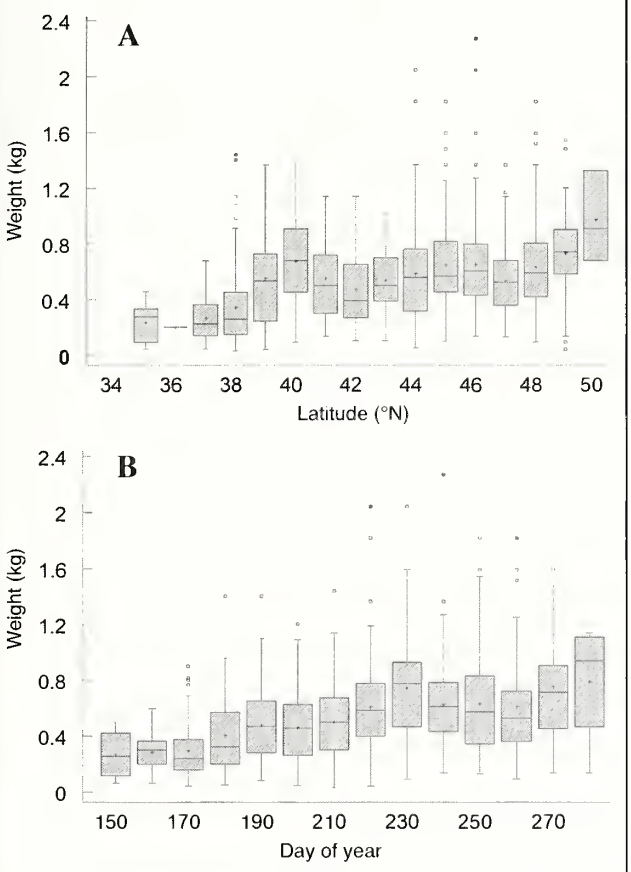

Figure 6

Trends in weight of American shad (*Alosa sapidissima*) by (**A**) latitude, and (**B**) day of year during the 1977–2004 Alaska Fisheries Science Center triennial surveys. Boxes span the 25th to 75th percentiles. The line and cross within each box indicate the median and mean weight, respectively. The whiskers indicate the minimum and maximum weights, except when outliers are present at more than 1.5 interquartile ranges (box heights) above or below the box. Small squares indicate outliers and small squares with crosses extreme outliers.

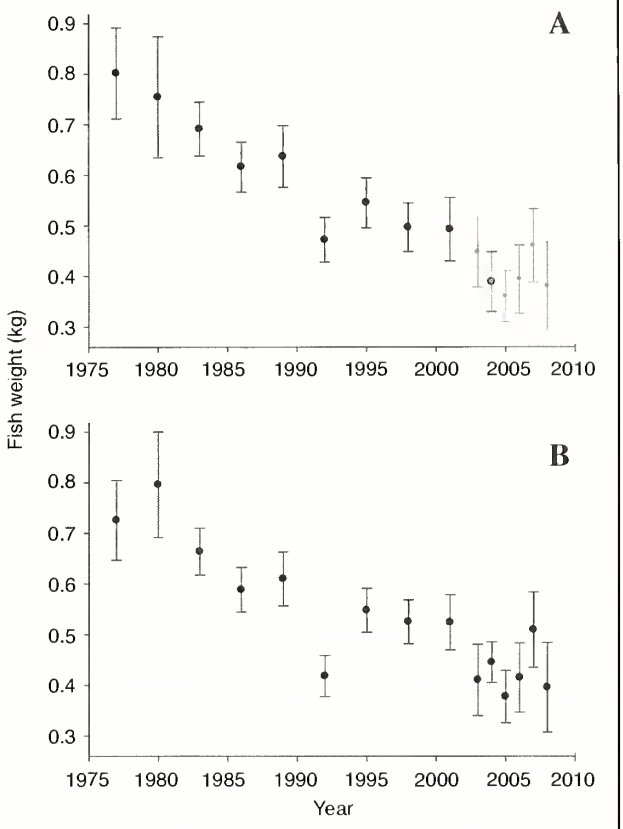

Figure 7

Mean weight (±2 standard errors) of American shad (*Alosa sapidissima*) by year during the 1977–2004 Alaska Fisheries Science Center triennial (black) and the 2003–08 Northwest Fisheries Science Center (gray) surveys: (**A**) uncorrected for date or depth of capture, and (**B**) results of a general linear model applied to both surveys combined where weight is the response variable, year is the categorical variable, and depth and day of year are quantitative variables (r^2=0.30). In (B) the mean weights are standardized to the average depth of 114 m and the average sample day 219 (August 7). In 2004 weights of shad in both surveys were very similar.

where SSTs were between 13° and 17°C and bottom temperatures were usually between 6.4° and 8°C. Neves and Depres (1979) caught Atlantic shad at SSTs of 2–23°C but concluded that bottom temperatures of 3–15°C provided a better basis for predicting movements of Atlantic shad in the ocean during all seasons of the year.

These differences in distributional and migration patterns of Pacific and Atlantic American shad are consistent with the phenotypic plasticity that has allowed adaptations to the unique environmental conditions along the Pacific coast over the past 100 years (see also Petersen et al., 2003). Rottiers et al. (1992) found that juvenile shad from the Columbia River had higher growth rates than did shad from the Delaware River and that the two stocks differed genetically. Quinn and Adams (1996) concluded that shad in the Columbia River have evolved a migratory pattern that allows greater behavioral response to environmental conditions because they now migrate into the river earlier in the year and at lower temperatures than during the prior 45 years. Future molecular and otolith microchemistry studies are needed to determine possible differences among spawning runs in different rivers, home stream fidelity, and distributional and migratory patterns at sea during their ocean migrations along the Pacific coast.

Counts of shad migrating past Bonneville Dam on the Columbia River provide important data on their abundances and interannual variability. The different indices of shad abundance (% FO, average $\log_{10}(catch+1)$, and average raw catch) during the AFSC and NWFSC demersal sampling on the shelf (≤200 m) between 44°N

and 50°N in different years were all strongly and positively correlated with shad counts at Bonneville Dam in the same years (Table 4). These positive correlations indicate that the abundance estimates of shad off northern Oregon and Washington during these surveys were good indicators of the spawning populations of Columbia River shad above Bonneville Dam, despite the fact that shad were not a target species of these demersal surveys. Average weight of shad in ocean surveys was also strongly negatively correlated with shad counts at Bonneville Dam (Table 4), indicating that the proportion of younger year classes in ocean sampling increased as the abundance of spawners increased.

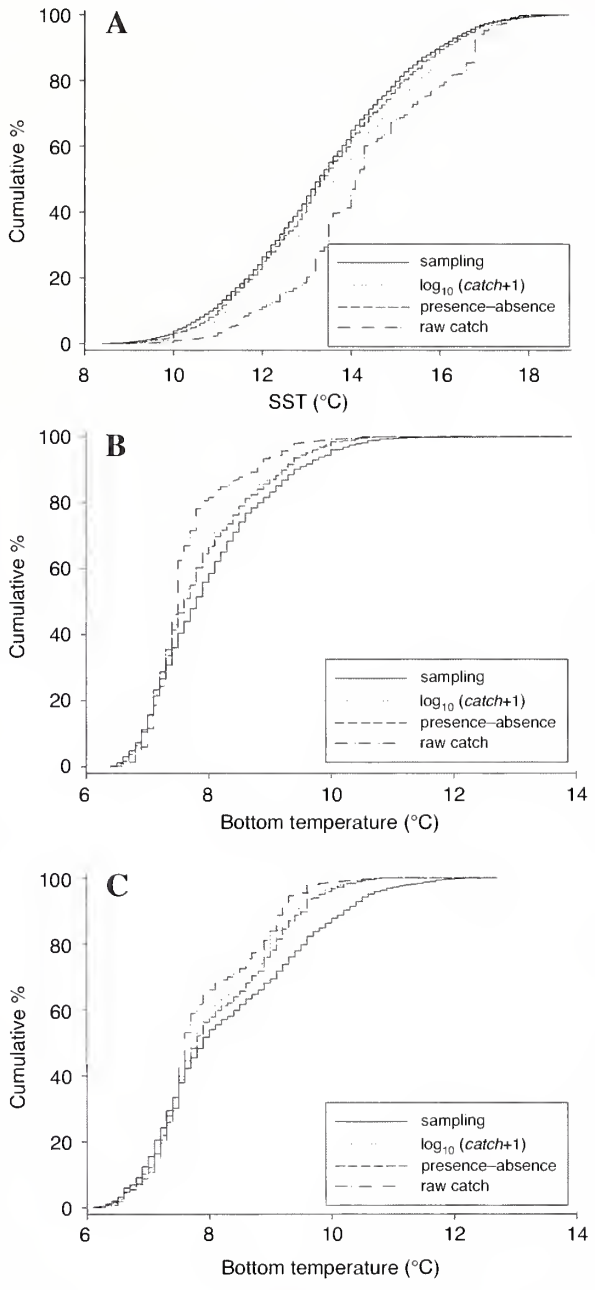

Figure 8

Cumulative frequency of sampling effort (number of tows), $\log_{10}$-transformed catch, presence–absence (1=present, 0=absent), and raw catch of American shad (*Alosa sapidissima*) vs. (**A**) sea-surface temperature (SST °C), and (**B**) bottom temperature during the Alaska Fisheries Science Center sampling, and (C) bottom temperature during the Northwest Fisheries Science Center sampling (both early and late season sampling combined).

The numbers of shad counted are related to ocean conditions and the survival of coho salmon as indicated by the Oregon Production Index or OPI (Fig. 9). The OPI is an index of smolt-to-adult survival of coho salmon mainly from Columbia River hatcheries. We assumed that ocean conditions that affect the survival of coho salmon may also affect the survival and return of Columbia River shad. During the cool Pacific Decadal Oscillation (PDO) regime between 1970 and 1976 shad counts were comparatively low. At this time coho salmon survival was high (Fig. 9, A and B). During the relatively warm PDO phase from 1977 to 1998 shad counts increased rapidly, whereas coho salmon survival was generally low, especially during the warm ocean conditions of the late 1990s. After 2000 shad counts increased markedly with warm PDOs, whereas coho salmon survival increased to high levels following several earlier years with cool PDOs and then declined. Shad counts at Bonneville were significantly negatively correlated with the OPI index (n=39 years, R=−0.45, P=0.004). From these trends we conclude that ocean survival of shad and coho salmon off Oregon and Washington are inversely related and that warm ocean conditions favor increased shad abundances and cool, more productive ocean periods favor coho salmon survival. In purse seine sets there was also a positive correlation between $\log_{10}(catch)$ of shad and SST (n=29 sets, R=0.43, P=0.02, SST from about 12.2° to 16.4°C). The occurrence of shad off Kamchatka in 1935–1939, and again in 1987, all during warm phases of the PDO (jisao.washington.edu/pdo, accessed July 2011), indicate that shad distributions may increase with predicted future climate change and a warmer ocean, just as Pacific hake, Pacific sardine, Pacific mackerel (*Scomber japonicus*), and jack mackerel (*Trachurus symmetricus*) increased off Oregon and Washington after ocean warming increased in 1977 (Ware and McFarlane, 1995; Emmett and Brodeur, 2000; Emmett et al., 2006).

In recent years, numbers of shad counted at Bonneville Dam have decreased dramatically. The run in 2010 was the lowest since 1982 (Columbia Basin Bulletin[13]). Reasons for this decline are unknown, but increased incidence of a protozoan parasite, endemic to the Pacific Ocean has been suspected (Columbia Basin Bulletin[13]).

[13] Columbia Basin Bulletin. 2011. American shad: nonnative to Columbia Basin, runs exceed one million fish, peaking at 6.5 million. The Columbia Basin Bulletin, May 13, 2011. [Available at: http://www.cbbulletin.com, accessed July 2011.]

Table 3

Data on counts of shad (*Alosa sapidissima*) in limited-entry groundfish catches, summarized for "summer" (April–October) and "winter" (November–March), by state (California, Oregon, and Washington) for as many as eight years, 2002–09. Counts were collected by onboard observers.

State	Season	Shad count	Years	Tows with shad	All observed tows	% of tows with shad	No. of shad per positive tow
CA	Summer	3224	8	324	4940	6.6	10
CA	Winter	1035	8	37	2002	1.8	28
OR	Summer	22,068	8	1056	11,147	9.5	21
OR	Winter	1853	8	133	4150	3.2	14
WA	Annual[a]	9381	3	96	620	15.5	98
WA	Summer	14,402	5	466	1969	23.7	31
WA	Winter	346	5	59	527	11.2	6

[a] For three of eight years only the annual catch off Washington was available.

Table 4

Correlation coefficients (R) between counts of American shad (*Alosa sapidissima*) at Bonneville Dam on the Columbia River and frequency of occurrence (FO) and abundance of shad determined from data from the Alaska Fisheries Science Center (AFSC) and Northwest Fisheries Science Center (NWFSC) demersal sampling survey over the continental shelf (≤200 m depth) from 44°N–50°N in different years. Tows that were negative for shad were included when calculating abundance. Shown also is the correlation (R) between average corrected weight of shad for the combined AFSC and NWFSC sampling survey in different years (Fig. 7B) and for the count of shad at Bonneville Dam.

	n	% FO	$\text{Log}_{10}(catch+1)$	Catch	Weight
AFSC	10 years	0.61, P=0.06	0.77, P=0.01	0.73, P=0.02	−0.77, P<0.001
NWFSC	6 years	0.84, P=0.03	0.88, P=0.02	0.89, P=0.02	

Prolonged infection by this parasite may cause mortality of larger adult fish that spend more years in the ocean and may relate to the decrease in size we observed in later years (Fig. 7, Table 4). Other possible explanations for declining numbers include changes in the temperature and river flows that may affect survival (Leggett and Whitney, 1972; Crecco and Savoy, 1986; Petersen et al., 2003), competition for zooplankton with forage fishes in the ocean that increase during cool ocean conditions (Emmett and Brodeur, 2000), dietary overlap with salmonids in the estuary (McCabe et al., 1983), and increased predation by seabirds in the Columbia River estuary (Petersen et al., 2003).

Conclusions

In conclusion, American shad along the Pacific coast of North America were mainly confined to the continental shelf and highest catches occurred from Oregon northward into British Columbia and near San Francisco Bay. Shad were bigger in deeper water. No evidence was found for large-scale seasonal migrations as reported along the Atlantic coast. The abundance of shad was highly correlated with the counts of shad passing Bonneville Dam on the Columbia River, and negatively correlated with the survival of coho salmon.

Acknowledgments

We are grateful to NOAA's Alaska Fisheries Science Center and Northwest Fisheries Science Center's West Coast Groundfish Survey for providing their databases for shad. We especially thank B. Horness and M. Wilkins for their cooperation. We also thank many others who generously provided data: M. Bellman and J. Majewski (NWFSC) and J. Olson (Pacific State Marine Fisheries Commission) for data obtained from bottom trawl surveys and observers in the limited entry trawl fisheries, J. Davidson and J. Fargo (Department of Fisheries and Oceans, British Columbia) for data from British Columbia, M. Karnowski and N. Hurtado (Oregon Department of Fish and Wildlife) for Oregon data, and T. Larinto (California Department of Fish and Game) for California data. We also thank D. Sweetman (California Depart-

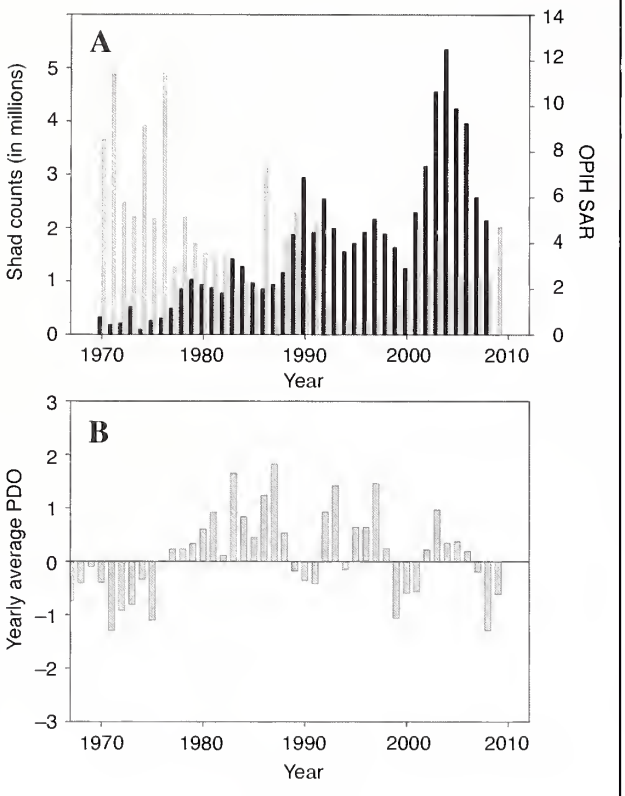

Figure 9

(**A**) American shad (*Alosa sapidissima*) counts at Bonneville Dam (black bars) and Oregon Production Index (OPI) coho salmon smolt-to-adult survival rates (SARs) (gray bars) along with (**B**) yearly average deviations of the Pacific Decadal Oscillation (PDO) index for the same years

ment of Fish and Game), L. Allen (Southern California Marine Institute), and S. Ralston and B. MacFarlane (Southwest Fisheries Science Center) for information. W. Wakefield, R. Brodeur, M. Parsley, and anonymous reviewers provided helpful comments on the manuscript.

Literature cited

Allen, L. G., M. M. Yoklavich, G. M. Cailliet, and M. H. Horn.
2006. Bay and estuaries. *In* The ecology of marine fishes: California and adjacent waters (L. G. Allen, D. J. Pondella, and M. H. Horn, eds.), p. 119–148. Univ. California Press, Berkeley, CA.

Bailey, K. M., R. C. Francis, and P. R. Stevens.
1982. The life history and fishery for Pacific whiting (*Merluccius productus*). Calif. Coop. Oceanic Fish. Invest. Rep. 23:81–98.

Brodeur, R. D., J. P Fisher, R. L Emmett, C. A. Morgan and E. Casillas.
2005. Species composition and community structure of pelagic nekton off Oregon and Washington under variable oceanographic conditions. Mar. Ecol. Prog. Ser. 298:41–57.

Brodeur, R. D., W. G. Pearcy, and S. Ralston.
2003. Abundance and distribution patterns of nekton and micronekton in the northern California Current transition zone. J. Oceanogr. 59:515–535.

Carl, G. C., W. A. Clemens, and C. C. Lindsey.
1959. The fresh-water fishes of British Columbia. British Columbia Provincial Museum, Handbook No. 5, 192 p. British Columbia Provincial Museum, Victoria, B.C., Canada.

Chereshnev, I. A., and S. I. Zharnikov.
1989. On the first record of the American shad, *Alosa sapidissima*, in the Anadyr' River. Voprosy Ikhtiologii 3:501–503.

Cleaver, F. C.
1951. Fisheries statistics of Oregon. Oregon Fish Comm. Contrib. No. 16:53–153.

Craig, J. A. and R. L. Hacker.
1940. The history and development of the fisheries of the Columbia River. Fish. Bull. 49:133–216.

Crecco, V., and T. Savoy.
1986. Effects of climatic and density-dependent factors on the intra-annual mortality of larval American shad. *In* 10th annual larval fish conference (R. D. Hoyt, ed.), p. 69–81. Am. Fish. Soc. Symp. 2, Bethesda, MD.

Dorn, M. W.
1995. The effects of age composition and oceanographic conditions on the annual migration of Pacific whiting, *Merluccius productus*. California Coop. Oceanic Fish. Invest. 36:95–105

Emmett, R. L., and R. D. Brodeur.
2000. Recent changes in the pelagic nekton community off Oregon and Washington in relation to some physical oceanographic conditions. N. Pac. Anad. Fish Comm. Bull. 2:11–20.

Emmett, R. L., R. D. Brodeur, T. W. Miller, S. Pool, G. K. Krutzikowski, P. J. Bentley, and J. McCrae.
2005. Pacific sardine (*Sardinops sagax*) abundance, distribution, and ecological relationships in the Pacific Northwest. Calif. Coop. Oceanic Fish. Invest. Rep. 46:122–143.

Emmett, R. L., G. K. Krutzikowski and P. Bentley.
2006. Abundance and distribution of pelagic piscivorous fishes in the Columbia River plume during spring/early summer 1998–2003: Relationship to oceanographic conditions, forage fishes, and juvenile salmonids. Prog. Oceanogr. 68:1–16.

Green, S.
1874. Fish culture. *In* Report of the Commissioner of Agriculture, 1982, p. 248–274. U.S. Dept. Agriculture, Washington, D.C.

Hamman, M. G.
1981. Utilization of the Columbia River estuary by American shad, *Alosa sapidissima*. M.S. thesis, 48 p. Oregon State Univ., Corvallis, OR

Hart, J. L.
1973. Pacific fishes of Canada. Fish. Res. Board Can. Bull. 180, 480 p.

Huyer, A., R. D. Pillsury, and R. L. Smith.
1975. Seasonal variation of the alongshore velocity field over the continental shelf off Oregon. Limnol. Oceanogr. 20:90–95.

Keller, A. A., B. H. Horness, E. L. Fruh, V. H. Simon, V. J. Tuttle, K. L. Bosley, J. C. Buchanan, D. J. Kamikawa, and J. R. Wallace.
2008. The 2005 U.S. West Coast bottom trawl survey of groundfish resources off Washington, Oregon, and

California: Estimates of distribution, abundance, and length composition. NOAA Tech. Memo. NMFS-NWFSC-93, 136 p.

Leggett, W.C.
1973. The migrations of the shad. Sci. Am. 228:92–98.

Leggett, W. C., and R. R. Whitney.
1972. Water temperature and the migrations of American shad. Fish. Bull. 70:659–670.

Mantua, N., S. Hare, Y. Zhang, J. Wallace, and R. Francis.
1997. A Pacific interdecadal climate oscillation with impacts on salmon production. Bull. Am. Meteorol. Soc. 78: 1069–1079.

McCabe, G. T., W. D. Muir, R. L. Emmett, and J. T. Durkin.
1983. Interrelationships between juvenile salmonids and nonsalmonid fish in the Columbia River estuary. Fish. Bull. 81:815–826.

McPhail, J. D.
2007. The freshwater fishes of British Columbia, 620 p. Univ. Alberta Press, Alberta, Canada.

Moyle, P. B.
1976. Inland fishes of California, 405 p. Univ. California Press, Los Angeles and Berkeley, CA.

Neves, R. J., and L. Depres.
1979. The oceanic migration of American shad, *Alosa sapidissima,* along the Atlantic coast. Fish. Bull. 77: 199–212.

Oregon Fish Commission.
1951. Fisheries statistics of Oregon, 176 p. Oregon Fish Comm. Contrib. No. 16, Fish Commission of Oregon, Portland, OR.

Pearcy, W. G., and J. P. Fisher.
1988. Migrations of coho salmon *Oncorhynchus kisutch*, during their first summer in the ocean. Fish. Bull. 86:173–195.

Petersen, J. H., R. A. Hinrichsen, D. M. Gadomski, D. H. Fell, and D. W. Rondorf.
2003. American shad in the Columbia River. *In* Biodiversity, status, and conservation of the world's shads (K. E. Limburg and J. R. Waldman, eds.), p. 141–155. Am. Fish. Soc. Symp. 35, Bethesda, MD.

Quinn, T. P., and D. J. Adams.
1996. Environmental changes affecting the migratory timing of American shad and sockeye salmon. Ecology 77:1151–1162.

Rottiers, D. V., L. A. Redell, H. E. Booke, and S. Amaral.
1992. Differences in stocks of American shad from the Columbia and Delaware rivers. Trans. Am. Fish. Soc. 121:132–136.

Skinner, J. E.
1962. Anadromous fisheries. *In* An historical review of the fish and wildlife resources of the San Francisco Bay area (J. E. Skinner, ed.), p. 57–93. California Bay-Delta Authority Science Program and the John Muir Institute of the Environment. [Available at http://www.estuary archve.org/archive/skinner_1962, accessed August 2010.]

Smith, H. M.
1896. A review of the history and results of the attempts to acclimate fish and other water animals in the Pacific states. U.S. Fish Comm. Bull. 15:379–472.

Stauffer, G. (compiler).
2004. NOAA protocols for groundfish bottom trawl surveys of the Nation's fishery resources. NOAA Tech. Memo. NMFS-F/SPO-65, 205 p.

Talbot, G. B. and J. E. Sykes.
1958. Atlantic coast migrations of American shad. Fish. Bull. 58:473–490.

Walburg, C. H., and P. R. Nichols.
1967. Biology and management of the American shad and status of the fisheries, Atlantic coast of the United States, 1960. U.S. Fish Wildlife Serv. Spec. Sci. Rept. Fisheries 550, 105 p. U.S. Dept. Interior, Bureau of Commercial Fisheries, Washington, D.C.

Ware, D. M., and G. A. McFarlane.
1995. Climate-induced changes in Pacific hake (*Merluccius productus*) abundance and pelagic community interactions in the Vancouver Island upwelling system. Can. Spec. Pub. Fish. Aquat. Sci. 121:509–521.

Welander, A. D.
1940. Notes on the dissemination of shad, *Alosa sapidissima* (Wilson), along the Pacific Coast of North America. Copeia 1940:221–223.

Wydoski, R. S., and R. R. Whitney.
2003. Inland fishes of Washington, 322 p. Am. Fish. Soc., Bethesda, MD, and Univ. of Washington, Seattle, WA.

Bomb radiocarbon and tag-recapture dating of sandbar shark (*Carcharhinus plumbeus*)

Allen H. Andrews (contact author)[1]
Lisa J. Natanson[2]
Lisa A. Kerr[3]
George H. Burgess[4]
Gregor M. Cailliet[5]

Email address for contact author: allen.andrews@noaa.gov

[1] NOAA Fisheries, Pacific Islands Fisheries Science Center
99-193 Aiea Heights Drive #417
Aiea, Hawaii 96701

[2] NOAA Fisheries, Apex Predators Program
28 Tarzwell Drive
Narragansett, Rhode Island 02882

[3] University of Massachusetts Dartmouth
School for Marine Science and Technology
200 Mill Road, Suite 325
Fairhaven, Massachusetts 02719

[4] Florida Program for Shark Research
Florida Museum of Natural History
University of Florida
Gainesville, Florida 32611

[5] Moss Landing Marine Laboratories
8272 Moss Landing Road
Moss Landing, California 95039

Abstract—The sandbar shark (*Carcharhinus plumbeus*) was the cornerstone species of western North Atlantic and Gulf of Mexico large coastal shark fisheries until 2008 when they were allocated to a research-only fishery. Despite decades of fishing on this species, important life history parameters, such as age and growth, have not been well known. Some validated age and growth information exists for sandbar shark, but more comprehensive life history information is needed. The complementary application of bomb radiocarbon and tag-recapture dating was used in this study to determine valid age-estimation criteria and longevity estimates for this species. These two methods indicated that current age interpretations based on counts of growth bands in vertebrae are accurate to 10 or 12 years. Beyond these years, we could not determine with certainty when such an underestimation of age begins; however, bomb radiocarbon and tag-recapture data indicated that large adult sharks were considerably older than the estimates derived from counts of growth bands. Three adult sandbar sharks were 20 to 26 years old based on bomb radiocarbon results and were a 5- to 11-year increase over the previous age estimates for these sharks. In support of these findings, the tag-recapture data provided results that were consistent with bomb radiocarbon dating and further supported a longevity that exceeds 30 years for this species.

Manuscript submitted 3 June 2011.
Manuscript accepted 8 August 2011.
Fish. Bull. 109:454–465 (2011).

Bomb radiocarbon dating has evolved as a useful method for validating the age of fishes. The validation of age relies on a preserved record of the rapid increase in radiocarbon (^{14}C) that occurred in the world's oceans as a result of atmospheric testing of thermonuclear devices in the 1950s and 1960s (Broecker and Peng, 1982). The uptake of bomb-produced ^{14}C by the marine environment, reported as $\Delta^{14}C$ in reference to an established prenuclear ^{14}C record (Stuiver and Pollach, 1977), was virtually synchronous in the mixed layer of mid-latitude oceans and was first recorded from marine carbonates in hermatypic corals (Druffel and Linick, 1978). Application for the dating of fishes began with an innovative comparison of $\Delta^{14}C$ values recorded in otolith carbonate in relation to regional $\Delta^{14}C$ records from hermatypic corals (Kalish, 1993). The temporal specificity of otolith $\Delta^{14}C$ provided an independent determination of age and corroborated age estimates determined from counting growth zones in otoliths (Campana, 2001). Bomb radiocarbon dating has since been successfully applied to validate age estimates of numerous teleost fishes (e.g., Andrews et al., 2007; Ewing et al., 2007; Neilson and Campana, 2008), elasmobranchs (e.g., Campana et al., 2002, 2006; Kneebone et al., 2008), and other marine organisms (e.g., Frantz et al., 2005; Roark et al., 2006; Stewart et al., 2006; Kilada et al., 2007).

The first application of bomb radiocarbon dating to validate ages in long-lived sharks addressed the porbeagle (*Lamna nasus*) and, preliminarily, the shortfin mako (*Isurus oxyrinchus*; Campana et al., 2002). Unlike the otoliths of bony fishes, in which the source of ^{14}C is inorganic and uptake is mostly synchronous with the marine environment, the vertebrae of porbeagle provided evidence for a phase lag of approximately three years in the timing of the rise in $\Delta^{14}C$. This lag was attributed to a trophic-level delay in the propagation of ^{14}C or to depth-related dilution of carbon sources, or to both, in relation to the

formation of vertebrae from organic carbon sources. Use of measurements from known-age individuals, in relation to measurements made in adult vertebrae, ruled out the possibility of reworked vertebral carbon throughout the life of the shark. This procedure enabled age validation for porbeagle and shortfin mako (Campana et al., 2002; Ardizzone et al., 2006). By contrast, a study of the white sharks (*Carcharodon carcharias*) of the eastern North Pacific Ocean indicated that aspects of life history, such as large-scale movements and feeding below the ocean mixed layer, can lead to mixed $\Delta^{14}C$ results that confound attempts to validate age (Kerr et al., 2006).

The sandbar shark (*Carcharhinus plumbeus*) is a cosmopolitan species of subtropical and tropical seas and was the cornerstone large coastal shark taken in the western North Atlantic (WNA) and Gulf of Mexico (GOM) bottom longline shark fisheries from the early 1980s until 2008 when they were allotted to a research-only fishery (NMFS, 2008). Modeling regional population dynamics has led to conclusions that the population is in need of rebuilding (Brewster-Geisz and Miller, 1999; Cortes, 1999). The most recent stock assessment of the large coastal shark complex of this region revealed that sandbar sharks are currently overfished, and overfishing is occurring (NMFS, 2006). Because fishing authorities set management measures using stock assessment models that increasingly and necessarily rely on age data (Cailliet and Andrews, 2008), even greater importance must be placed on age validation as a requirement for stock assessments (Payne, 2006). Validated age data enable stock assessment scientists 1) to understand and monitor long-term changes in population age-structure; 2) to determine the timing of important life history events (e.g., age at first maturity); 3) to measure vital rates (e.g., growth and natural mortality); and 4) to monitor fishing mortality rates and their long-term effects on the population.

Some validated age and growth information exists for sandbar shark, but more comprehensive information on its biological development is needed. Age has been validated for juvenile sandbar sharks in Hawaii by using marginal increment analysis and oxytetracycline (OTC) marking (Romine et al., 2006), and for adults up to approximately 17 years in Australia with the use of tag-recapture data (McAuley et al., 2006). However, studies geographically removed from the WNA are of limited use for that region. In the WNA–GOM region, one laboratory study validated growth up to 112 cm (Branstetter, 1987). Estimates of age, growth, and longevity were primarily "unvalidated" by using vertebral centra and observations of growth in tag-recapture programs (Casey et al., 1985; Casey and Natanson, 1992; Sminkey and Musick, 1995; Merson and Pratt, 2001). Use of tag-recapture data to determine growth characteristics can be complicated because revisions may be needed as additional recaptures continue to provide new data over time (*cf.* growth parameters presented in Casey and Natanson [1992] with those in Casey et al. [1985]). In addition, maximum size (L_{max}) is typically underestimated in tag-recapture studies, although the tag-recapture method offers several advantages, including a useful verification of younger age classes, estimates of longevity, and valid measures of age and growth when used in concert with OTC-marked growth bands. Therefore, use of both bomb radiocarbon and tag-recapture dating methods can produce a series of age and growth determinations that can facilitate accurate growth modeling throughout ontogeny of a species. The sandbar shark is not known to move into deep water; thus it is a good candidate for bomb radiocarbon dating because complications from greatly depleted ^{14}C sources with depth are unlikely (i.e., Kerr et al., 2006). It was hypothesized that an application of bomb radiocarbon dating would 1) provide independent estimates of age that either corroborate or refute age estimates from counting growth band-pairs; and 2) provide a minimum longevity for sandbar shark. It was further hypothesized that additional tag-recapture age and growth data from OTC-injected sandbar sharks would be in agreement with the bomb radiocarbon age data.

Materials and methods

Bomb radiocarbon dating

Sandbar shark vertebrae, collected from the WNA and stored frozen, with capture years ranging from 1965 to 1985 were obtained from 1) the Apex Predators Program of the National Marine Fisheries Service (NMFS; n=4); and 2) the Florida Program for Shark Research (n=1) for bomb radiocarbon analyses (Table 1). Successful application of bomb radiocarbon dating requires that structures used to determine age come from sharks that were alive during some portion, or all, of the period of rapid increase in $\Delta^{14}C$ from atmospheric bomb testing (~1955 to 1970 for the marine environment). Five sharks collected between 1965 and 1981 were selected for analysis on the basis of estimated age from sex specific growth curves (Casey et al., 1985) and collection dates, to estimate birth year (Table 1). Age estimates from growth band counts for four of these sharks were made before our study by using histological techniques described elsewhere (Casey et al., 1985). Contiguous vertebrae were used for the ^{14}C analyses.

Vertebrae from the five individual sharks were sampled for ^{14}C analysis by using accelerator mass spectrometry (AMS). A section of the vertebral centrum was removed from the corpus calcareum of each vertebra along the sagittal plane. Sections were cut thicker than typically used for age estimates (2–3 mm) to ensure that there was adequate material to meet minimum sample size requirements. Sections were mounted on glass microscope slides with fine-meshed, double-stick nylon tape. A New Wave® (Electro Scientific Industries, Fremont, CA) micromilling machine with a 0.3-mm diameter bit (Brassler®, Savannah, GA) was used to drill a series of overlapping holes around the circumference of the targeted growth band pair (one opaque and one translucent band; *sensu*

Table 1

Size, year of capture, estimated age, and sex of sandbar shark (*Carcharhinus plumbeus*) sampled in this study.

Specimen number	Fish fork length (cm)	Year of capture	Estimated age (yr)	Estimated birth year	Sex
SB 43	136.5	1965	10.3	1955	F
SB 47970	160.0	1985	14.2	1971	F
SB 745	167.0	1976	16.4	1960	M
SB 118	167.5	1966	15.6	1950	F
SB 749	170.0	1981	16.1	1965	F

Cailliet et al., 2006). The location of the series of drill holes was carefully chosen to extract the targeted growth-band pair within the corpus calcareum and to minimize the possibility of including external vertebral material not formed during that year of growth. The intermedialia of the vertebral centrum was avoided because banding is poorly defined near the corpus calcareum. The width of growth-band pairs was used as the target size for extraction therefore, the amount of material extracted decreased as the width of growth band pairs decreased. Drilling depth was just short of the depth required to pass completely through the section to provide a secure mount for the extracted block of vertebral material. Final removal of the sample was made with a razor blade, firmly pressed to the slide.

A total of thirteen growth-band pairs were extracted from the corpus calcareum of the five sandbar shark vertebrae. The first growth-band pair after the birth band (estimated to be the first year of growth after birth) and one to four subsequent growth band pairs farther toward the outer edge of the corpus calcareum were extracted from each vertebra. The last band pair, corresponding to the last year of growth, was targeted to provide a sample where time of formation was constrained by the collection date. The location for extraction of the most recent vertebral sample was usually proximal to the distal tip of the corpus calcareum because of reduced band width and poor edge condition at the tip, The extracted samples weighed approximately 10 mg; the specific values were not specifically recorded owing to an oversight.

Demineralization of vertebral samples was performed to isolate the organic portion (collagen) by dissolving the inorganic component that can increase carbon yield from the accelerator mass spectrometry (AMS) graphitization process (Brown et al., 1988). Samples were soaked in 0.25 N HCl for 24 hours at refrigerator temperatures to reduce reaction rate. Treated samples were dried in an oven at 60°F (16°C) and placed in clean quartz tubes. Copper oxide (CuO, oxidizing agent) and silver (Ag, for impurity removal: SOx and NOx) were added to the treated organic samples at levels specified for AMS (Center for Accelerator Mass Spectrometry [CAMS], Lawrence Livermore National Laboratory). Quartz tubes were evacuated, sealed, and heated for 2 hours at 900°C to convert the organic carbon to CO_2. Sample CO_2 was converted to graphite (Vogel et al., 1984, 1987) and measured for ^{14}C content with AMS at the CAMS. The ^{14}C values were reported as $\Delta^{14}C$ (Stuiver and Polach, 1977) and age corrected by using the estimated year of formation in relation to 1950. The ^{14}C values were then adjusted for fractionation by using an assumed $\partial^{13}C$ value of –15‰ based on a previous study (Campana et al., 2002) and other standards (Stuiver and Polach, 1977).

Sandbar shark $\Delta^{14}C$ data were compared with existing hermatypic coral $\Delta^{14}C$ records for the WNA for a temporal alignment. Because this species is known to cover great distances along the Atlantic seaboard seasonally and ontogenetically (Grubbs et al., 2007), the $\Delta^{14}C$ records from hermatypic coral off the Florida Keys and Bermuda (Druffel and Linick, 1978; Druffel, 1989) and validated shark vertebrae (porbeagle from western North Atlantic; Campana et al., 2002) were used as reference chronologies for comparison to the measured values from aged sandbar shark vertebrae. Fish otolith $\Delta^{14}C$ records were also considered for calibration purposes (i.e., Campana et al., 2008) but were not used in our analysis because the $\Delta^{14}C$ record was intermediate in time and magnitude to the coral and shark $\Delta^{14}C$ records and did not provide additional temporal clarity. Age of sandbar sharks was calibrated by aligning measured $\Delta^{14}C$ values with the $\Delta^{14}C$ reference chronologies, and estimated age was adjusted for some sharks according to the temporal alignment of these data.

OTC tag-recapture dating

Tag-recapture data were obtained and analyzed by using the methods of Casey et al. (1985) and by using only recaptures obtained since the publication by Casey and Natanson (1992). In addition, vertebrae were processed from OTC-injected and recaptured specimens. Two adjacent vertebrae were sectioned and examined concurrently to align band pairs with the OTC mark. One section was removed for histological examination (Casey et al., 1985) and the other, a thicker section, was made to preserve the OTC mark. The thicker section was made by using a gem saw (Raytech, Middleton, CT)

Table 2

Summary of results from radiocarbon analyses. Estimated shark age from growth band counts with calculated birth year, year of growth-band formation, and ages for each sandbar shark (*Carcharhinus plumbeus*) vertebra. Resultant $\Delta^{14}C$ values and the adjusted year of growth-band (GB) formation for each sample are given along with bomb radiocarbon age of the shark, where applicable. SD=standard deviation

	Age determined from growth bands				Age determined from radiocarbon data	
Sample number	Shark age (yr)	Year of GB formation	Age sampled	$\Delta^{14}C$ (SD) (‰)	Adjusted year	Shark age (yr)
SB 43		1955			N.C.[1]	
		1957	2	−67.6 (4.2)	N.C.[1]	
		1963	8	−21.2 (3.6)	N.C.[1]	
	10.3	1965				10.3
SB 47970		1971			1960	
		1972	1	−79.8 (4.1)	1962	
		1977	6	125.3 (5.9)	1967	
	14.2	1985				25 (23–27)
SB 745		1960			1955	
		1961	1	−64.3 (4.0)	1956	
		1967	7	−78.6 (3.9)	1962	
	16.4	1976				≥20
SB 118		1950			N.C.[2]	
		1951	1	−53.3 (4.2)	N.C.[2]	
		1965	15	N.M.[3]		
	15.6	1966				N.C.[2]
SB 749		1965			1954	
		1966	1	−7.8 (4.4)	1955	
		1967	2	−110.9 (3.9)	1956	
		1970	5	−70.6 (3.9)	1959	
		1974	9	−61.7 (4.0)	1963	
		1980	15	16.6 (4.6)	1980	
	16.1	1981				≥26

[1] No change: Values in alignment with calibration curves.
[2] No change: Not enough information to assess an adjustment (with prebomb reference)
[3] Not measured: Sample was lost during preparations for accelerator mass spectrometry.

with two diamond blades separated by a 0.6-mm spacer. Photographs of both sections were taken—the thicker sections under UV light and the thinner histological sections under reflected lighting. Resulting photographs were superimposed to determine the location of the OTC mark on the histological section and counts and measurements were determined from the combined images.

Results

Bomb radiocarbon dating

Values of $\Delta^{14}C$ measured in sandbar shark vertebrae, provided in parts per million (‰) ±1 standard deviation [SD]), ranged from prebomb to peak and postbomb levels (Table 2). Prebomb levels were similar to those in the porbeagle record, with values as low as −110.9‰ (SD=3.9). The peak $\Delta^{14}C$ value exceeded expectations and was similar in magnitude to hermatypic coral $\Delta^{14}C$ records (125.3‰, SD=5.9). Despite the strong indication of bomb-produced radiocarbon in several vertebrae, the growth-band derived years of formation for many of the samples were not in agreement with the bomb radiocarbon dating $\Delta^{14}C$ references (Fig. 1). One sample was lost from specimen SB 118; therefore, the vertebra was useful only as a prebomb $\Delta^{14}C$ reference value. The age of the youngest specimen (SB 43), estimated at 10.3 years, was supported by the $\Delta^{14}C$ results; yet the estimated ages of the other three adult

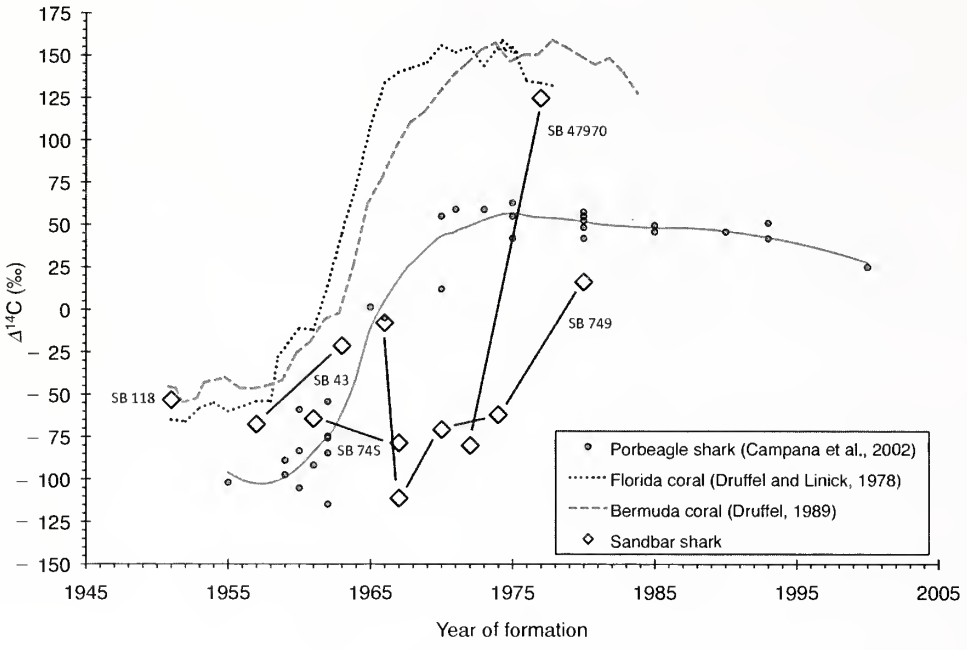

Figure 1

Plot of sandbar shark (*Carcharhinus plumbeus*) $\Delta^{14}C$ measured from vertebrae in relation to the estimated year of formation (determined from growth band counts). Observations from individual sharks are connected with lines and labeled accordingly. For calibration purposes two regional hermatypic coral records and the porbeagle (*Lamna nasus*) $\Delta^{14}C$ records were used. In addition, a LOESS curve was fitted to the porbeagle $\Delta^{14}C$ data to provide a central distribution reference (LOESS, P=0.5, 2-parameter regression). Note that the sandbar shark $\Delta^{14}C$ values, plotted in relation to estimated age, were phase lagged by up to 11 years. Calibration of age was necessary for some sandbar shark age estimates (see Figs. 2–4).

sharks were not in agreement with the reference $\Delta^{14}C$ chronologies.

The age of three adult sandbar sharks (SB 745, SB 749, SB 47970) was underestimated by approximately five to 11 years in relation to the reference $\Delta^{14}C$ chronologies and resulted in an increase in age to at least 20 to 26 years. The age of specimen SB 749 was underestimated by at least 11 years after alignment with the porbeagle $\Delta^{14}C$ reference record for a revised age of at least 26 years. To make the alignment, we had to assume that the innermost sample (year-1) of the vertebra was an inaccurate extraction that included more recent (postbomb) material (Fig. 2). This conclusion was supported by the measured postbomb $\Delta^{14}C$ level from the innermost sample of the corpus calcareum (–7.8‰, SD=4.4) when compared to more recently formed samples that were clearly prebomb and further into the life of the shark (Table 2). The age of specimen SB 47970 was underestimated, requiring adjustment of 10 to 12 years based on a simultaneous alignment of the measured $\Delta^{14}C$ values in relation to the coral and porbeagle shark $\Delta^{14}C$ reference chronologies. The near peak $\Delta^{14}C$ value could not have been formed earlier than 1965 (based on the maximum rise in $\Delta^{14}C$ from the Florida coral record), yet the measured prebomb $\Delta^{14}C$ value could be no later than 1962 (based on the rise in $\Delta^{14}C$ from the porbeagle record; Fig. 3). With these alignment constraints, and with the assumption that there was no problem with interpreting age from the early growth between the two samples (five years), a median age of 25 ±2 years was determined for this shark. The age for specimen SB 745 was underestimated by at least five years to align with the porbeagle $\Delta^{14}C$ record, but this shark could have been older because prebomb values alone are not diagnostic (Fig. 4).

OTC tag-recapture dating

Since 1992, 173 tagged sandbar sharks have been recaptured as part of the NMFS Apex Predators Program. Ten of these sharks were estimated to have lived more than 20 years (20.1–31.1 years) based on time-at-liberty (TAL) and the estimated age at time of release determined from the sex-specific growth curves of Casey et al. (1985). These sharks were tagged at 80–183 cm fork length (FL) and had a TAL of 2.6–26.9 years (Table 3). In addition, 22 sharks with estimated lengths at tagging

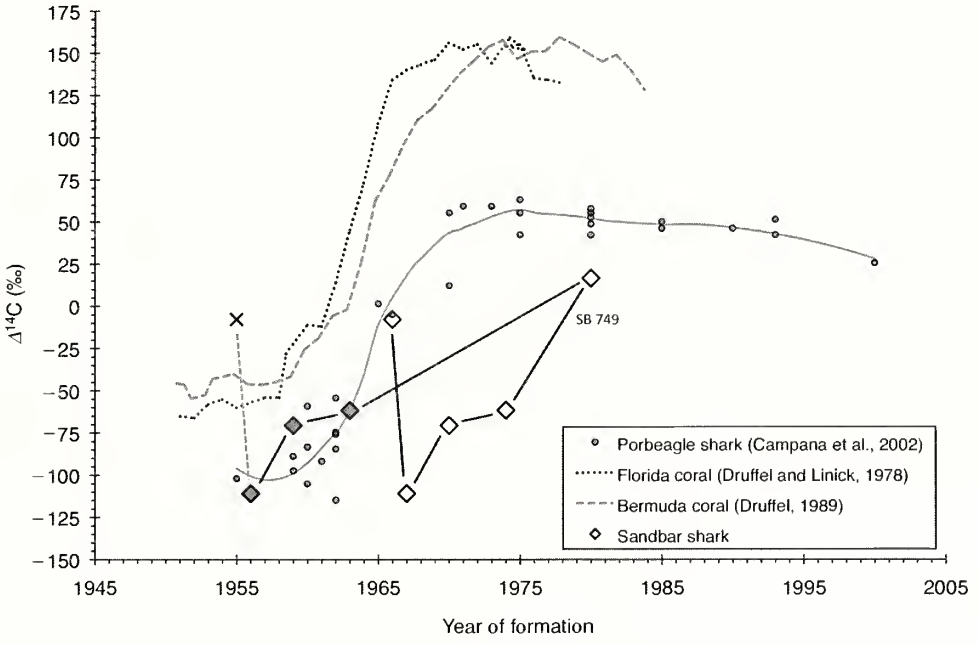

Figure 2

Plot of sandbar shark (*Carcharhinus plumbeus*) $\Delta^{14}C$ measured from vertebrae in relation to the estimated year of formation (determined from growth band counts), showing that an adjustment of formation dates for sandbar shark specimen SB 749 (by an additional 10 years) was necessary to match the porbeagle (*Lamna nasus*) $\Delta^{14}C$ record (filled diamonds). Minimum adjusted age was 26 years. The assumption was made that the missing years were those in the late-adult years (as reflected in the outer part of corpus calcareum where band resolution can be lost) and that early growth was well quantified. 10 years was added to the time between the known-age edge material and the next sample inward in the corpus calcareum (*cf.* 1974 with 1963). For this sample series, the youngest sample (juvenile portion of corpus calcareum) was classified as contaminated with older (postbomb) adult material and was eliminated from consideration because of its unexpectedly high $\Delta^{14}C$ value (denoted as an X in the projected growth scenario).

of 73–140 cm FL were recaptured after a minimum of 10 years at liberty (TAL 10.0–27.7 years). Ages for these sharks ranged from 13.1 to 36.0 years (Table 3). The tag of the shark at liberty 27.7 years was compromised over time: the last of 3 digits on the tab was worn off by the time of recapture. This shark was one of ten sandbar sharks measured and tagged on the same day within this number series. These sharks ranged in size from 99 to 122 cm FL at recapture and longevity was estimated at 33 to 36 years for these sharks for this longest period before recapture.

One OTC-tagged recaptured shark was examined that measured 68 cm at tagging and 150.4 cm FL at recapture. Time at liberty was 11.8 years and the estimated age at tagging was 1.6 years. Twelve band pairs were visible after the OTC mark as determined by the criteria of Casey et al. (1985) and the total estimated age was 13.6 years. This estimate was one year more than the growth curve estimate (12.6 years), but was within the margin of uncertainty of the growth function.

Re-examination of vertebrae

Because the bomb radiocarbon analyses revealed discrepancies in age, four of the original histological sections were re-examined to determine whether banding existed in the sections that would correspond with the bomb radiocarbon ages. Many additional band pairs were visible in the vertebrae of these specimens and support the ages indicated by the bomb radiocarbon analyses. These band pairs were not considered to represent annual growth in the early study because they did not fit the criteria defined in the study and were not counted. If an approach were used to count all band pairs, this would also indicate that the age-validated specimen SB 43 was more than 10 years old (maximum addition of three years in relation to coral $\Delta^{14}C$ records). In addition, the recently collected OTC-marked specimen would necessarily have an age greater than the known TAL and lead to the conclusion that early growth was not underestimated. These findings indicate that the band pair counts with the Casey et al. (1985) criteria

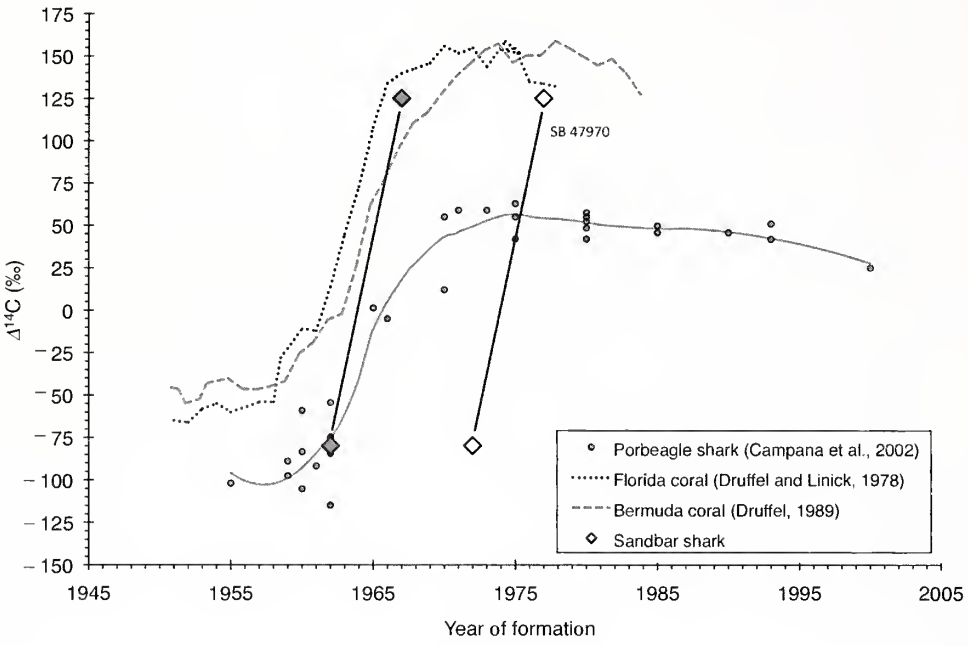

Figure 3

Plot of sandbar shark (*Carcharhinus plumbeus*) $\Delta^{14}C$ measured from vertebrae in relation to the estimated year of formation (determined from growth band counts), showing that an adjustment of formation dates for sandbar shark specimen SB 47970 (by an additional 11 years) was necessary to match the porbeagle (*Lamna nasus*) $\Delta^{14}C$ record (filled diamonds). Adjusted age was increased to 25 years. The assumption was made that the missing years were those in the late-adult years (as reflected in the outer part of corpus calcareum) and that early growth was well quantified. This span in $\Delta^{14}C$ values is perhaps the most diagnostic in terms of age determination; age could not be older by more than 2 years because of limits to the rise in $\Delta^{14}C$ from the Florida coral record (~1965 for the measured $\Delta^{14}C$ level), and the prebomb sample could not have been younger by more than 1 year because of the limits of the porbeagle (*Lamna nasus*) $\Delta^{14}C$ record (~1964 for the measured $\Delta^{14}C$ level). Age for this sandbar shark was likely constrained to a range between 23 and 27 years.

were reliable as a measure of annual growth to at least 12 years (10 and 12 years validated in this study with bomb radiocarbon and OTC marking, respectively). After this time of band formation in the vertebrae, either growth-band pairs do not provide an accurate measure of annual growth or the criteria for counting must be changed to incorporate a finer growth band structure. Until all sizes and ages can be validated, it would not be possible to determine how the growth-band counting criteria need to change.

Discussion

The comparisons of measured $\Delta^{14}C$ values from sandbar shark vertebrae with regional reference chronologies provided age determinations that exceeded age estimates from visual growth-band counts for three of the largest sharks in this study. Levels of $\Delta^{14}C$ recorded in sandbar shark vertebrae during the rise in marine $\Delta^{14}C$ and postbomb periods were unexpectedly low based on their estimated year of band formation determined from growth-band counts. This finding led us to conclude that ages had been underestimated for these adult sandbar sharks by 5 to 11 years, thereby providing explanation for the temporal offset and providing evidence that these individuals were considerably older.

Considerable evidence shows that diet is the primary source of carbon in the skeletal structure of sharks and that collagen retains its time specificity in respect to its deposition in vertebrae (Fry, 1988; Campana et al., 2002, 2006); hence, an alternative explanation for the unexpectedly attenuated $\Delta^{14}C$ values measured in sandbar shark vertebrae could be a shift or mix in dietary carbon sources. To address this potential explanation for sandbar sharks, we turned to the well-documented study of white sharks from the eastern North Pacific Ocean (Kerr et al., 2006). For white sharks, the unexpectedly low $\Delta^{14}C$ values in the vertebrae could not be explained as problems with age estimation; collection year and known-age juvenile samples provided temporal constraints that eliminated

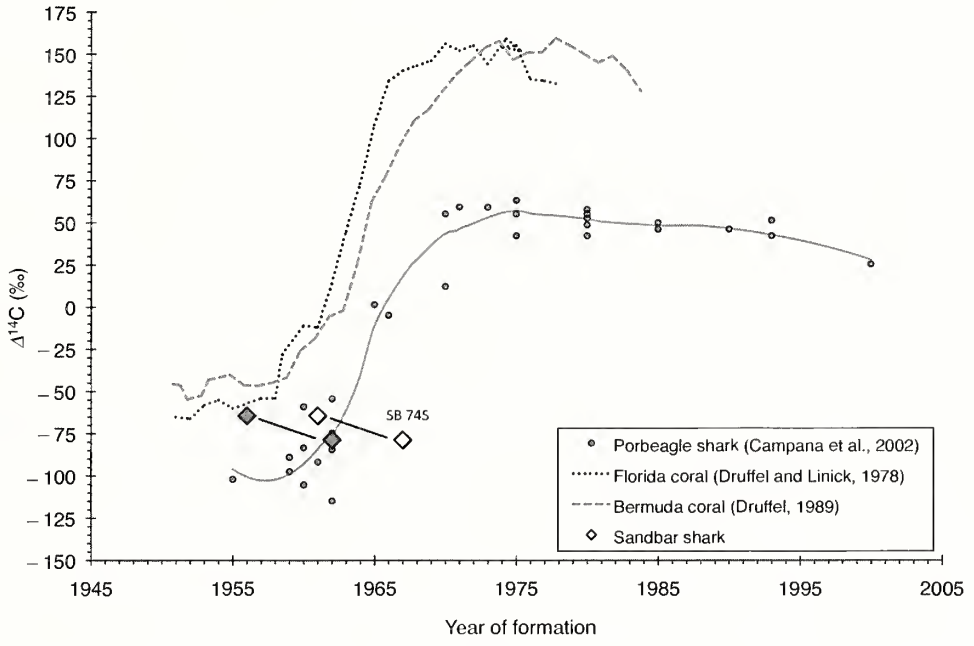

Figure 4

Plot of sandbar shark (*Carcharhinus plumbeus*) $\Delta^{14}C$ measured from vertebrae in relation to the estimated year of formation (determined from growth band counts), showing that an adjustment of formation dates for sandbar shark specimen SB 745 (by 5 years) was necessary to match the porbeagle (*Lamna nasus*) $\Delta^{14}C$ record (filled diamonds). Adjusted age was increased to a minimum of 20 years. The assumption was made that the missing years were those in the late-adult years (as reflected in the outer part of corpus calcareum) and that early growth was well quantified. This determination does not preclude an older age because there are no limits to the prebomb levels measured in these samples.

age-related discrepancies. Instead, feeding habits of these sharks in deep offshore waters appear to explain the observations.

For the sandbar shark, a scenario similar to that of the white shark would be possible if the single sample from year-1 of specimen SB 749 was considered uncontaminated. This $\Delta^{14}C$ value was clearly postbomb value at −7.8‰ (SD=4.4). Including this sample would preclude an increase in age for this sandbar shark, as well as the other sharks in our study and explain the unexpectedly low $\Delta^{14}C$ values. Based on the growth band age estimates alone, the temporal distribution of the $\Delta^{14}C$ data for sandbar shark would be similar to that of the white shark (*cf.* Fig. 1 of this study with Fig, 1 of Kerr et al. [2006]). However, the well-documented feeding behavior and depth-related life history of sandbar shark do not support this hypothesis (Springer, 1960; Stillwell and Kohler, 1993; Conrath and Musick, 2007). In addition, although it is certain there was some non-surface–derived ^{14}C included in the sandbar shark diet based on the lowest measured $\Delta^{14}C$ values (−78.6‰ to −110.9‰ *cf.* −40.2‰ to −66‰ for corals), the levels were similar to the lowest $\Delta^{14}C$ values measured in the porbeagle $\Delta^{14}C$ reference chronology (−74.6‰ to −114.7‰). Because of important life history considerations, it was concluded that the innermost sample (year-1) from the vertebra from specimen SB 749 was inaccurately extracted and included more recently formed vertebral material. In support of this conclusion is the series of three additional samples that would have formed after this sample, all of which were clearly classified as prebomb material.

The most plausible explanations for underestimated ages of sandbar sharks in this study are either a lack of band pair formation at the oldest adult ages or a problem with the interpretation of growth bands. The validated age of the youngest specimen (SB 43) provides some evidence that age can be determined visually with growth-band counts in the earliest years of growth. A validated age of ten years for this shark provides evidence that the missing years for the larger shark were most likely those from the latter years of life. This argument was well documented for porbeagle shark off New Zealand, for which age estimation was accurate to approximately 20 years but was underestimated by several decades for older sharks (Francis et al., 2007). Estimation of age from band pair counts was not possible for older sharks because as somatic growth of the shark slowed or ended, vertebral growth ceased. A similar scenario was described for school shark or

Table 3

Tag and recapture data for sandbar shark (*Carcharhinus plumbeus*) over a period of several decades. Specimen IDs 1–10 revealed life spans exceeding 20 years and the remaining specimens had time at liberty (TAL) exceeding 10 years. Age at tagging was estimated from the Casey et al. (1985) growth function. Age at recapture was the sum of estimated age at capture and time at liberty. Italicized lengths were estimated. NR=not reported. U=unidentified.

Specimen ID	Sex	Fork length (cm)			TAL (yr)	Estimated age (years)	
		Tagging	Recapture	Growth		Tagging	Recapture
1	F	183	160	–23	2.6	19	21.4
2	F	152	170	18	7.6	13	20.5
3	M	139	*140*	1	9.0	11	20.1
4	F	152	145	–7	10.2	13	23.0
5	F	156.6	*169*	12	12.1	14	25.7
6	M	154	NR		12.1	14	25.9
7	M	127	*203*	76	12.7	9	21.8
8	M	80	141	61	24.9	3	27.8
9	M	106	*136*	30	24.9	6	31.1
10	F	87	*166*	79	26.9	4	30.6
11	M	*137*	*152*	15	11.0	11	21.7
12	F	*73*	*202*	129	11.0	2	13.1
13	M	*82*	154	72	11.0	3	14.2
14	M	*90*	127	37	11.0	4	15.1
15	F	*131*	*127*	–4	11.1	10	20.6
16	U	*102*	*131*	29	11.1	6	16.7
17	F	*127*	*162*	35	11.5	9	20.4
18	U	*115*	178	63	11.5	7	18.9
19	M	*137*	148	11	11.7	11	22.4
20	F	*102*	*202*	100	12.1	6	17.7
21	M	*115*	156	41	12.8	7	20.2
22	F	*91*	*140*	49	13.2	4	17.4
23	M	*140*	155	15	13.4	11	24.6
24	F	*127*	*169*	42	13.5	9	22.4
25	F	*90*	152	62	13.6	4	17.7
26	F	*102*	*152*	50	14.5	6	20.1
27	F	*123*	*165*	42	15.6	8	24.0
28	F	*122*	160	38	16.8	8	25.0
29	F	*102*	*167*	65	17.5	6	23.1
30	U	*115*	*183*	68	18.0	7	25.4
31	F	*91*	168	77	18.4	4	22.6
32	U	*99–122*	*146*	47–24	27.8	5–8	33–36

tope shark (*Galeorhinus galeus*) in Australia (Kalish and Johnston, 2001).

There is evidence to support a similar conclusion in terms of reduced or ceased somatic growth of the vertebrae. Two of the sandbar sharks in this study could be older because once prebomb $\Delta^{14}C$ levels were attained there was no limit to maximum age. In contrast, the age of specimen SB 47970 was well constrained by the upper and lower limits of the $\Delta^{14}C$ reference chronologies for an age of 25 ±2 years. The five years estimated from band pair counts between the measured values for SB 47970 is consistent with the validated early growth from SB 43 (10 years old). Therefore, the addition of 11 years, as part of the age estimate that was not quantified for late adult life, was chosen to shift the observed five-year early growth period to match the $\Delta^{14}C$ reference records.

In general, bomb radiocarbon dating of sharks must be qualified with empirical evidence to support a temporal correlation with a regional $\Delta^{14}C$ reference chronology. Complexities tied to ontogenetic changes in feeding were recently observed to varying degrees in bomb radiocarbon dating studies of other sharks. Bomb radiocarbon dating of tiger shark (*Galeocerdo cuvier*) not only validated age estimates up to 20 years, but also provided information about carbon sources from the measured levels of $\Delta^{14}C$ (Kneebone et al., 2008). The interesting finding with tiger shark in terms of ^{14}C uptake was in the differences and similarities of values between juveniles and an adult shark. Measured $\Delta^{14}C$ values from

juvenile tiger sharks were in agreement over time with a hermatypic coral record from Florida, indicating there was no phase lag in terms of the timing of the $\Delta^{14}C$ signal for the early growth of vertebrae. In contrast, the older adult, one that lived through the period of bomb testing to nearly the end of the marine $\Delta^{14}C$ record, was mostly in phase with the porbeagle record as an adult, and deviated to match the coral record in what would have been the juvenile portion of the adult vertebrae. These findings can be logically attributed to tiger shark juveniles feeding on short-lived and near-surface food sources and adults shifting to older food sources, represented as a phase lag that can be attributed to trophic-level changes (Kneebone et al., 2008). A similar scenario was observed for the great hammerhead (*Sphyrna mokarran*), where there was close agreement with a coral $\Delta^{14}C$ record in some years and attenuation of the $\Delta^{14}C$ signal in others (Passerotti et al., 2010). For the sandbar shark, carbon is derived from mixed sources throughout ontogeny and $\Delta^{14}C$ values range from agreement with the attenuated and phase-lagged porbeagle record to agreement with the elevated and timely coral records. In general, no time-specific correlation was observed with either record, and this finding is consistent with the wide-range of sandbar shark feeding habits.

The use of vertebrae as an exclusive tool to age sandbar shark has well-documented limitations. Casey et al. (1985) used strict age-estimation criteria and noted that ages may be underestimated owing to a large number of uncounted growth bands at the margin. The uncounted banding pattern did not fit the criteria formulated from observed early growth; therefore, the bands were not counted at the time. A subsequent tag-recapture study provided support for the notion that age was underestimated and evidence was presented for much slower growth and greater longevity (Casey and Natanson, 1992). Tag-recapture data generated since Casey and Natanson's publication and presented herein provides an indication of an even greater longevity (33–36 years). These data were further supported by the bomb radiocarbon results that indicated ages were underestimated late in adult life.

For age determination of smaller sharks, Casey and Natanson (1992) suggested that the band counts may have an annual periodicity until a threshold size and age, at which the deposition rate changes. At the time of the Casey and Natanson's study, the only age validation was from a laboratory OTC study for sharks no larger than 112 cm (Branstetter, 1988), and the conclusion was that periodicity of band-pair deposition changed after 5–6 years. Branstetter (1988) argued that the Casey et al. (1985) criteria were limited to early growth and this view is supported by the bomb radiocarbon and OTC findings of the present study.

Conclusion

In light of these results, it is important to emphasize the need for age validation across all size (and age) classes for the sandbar shark. Given the potential for changes in the periodicity of band pair formation throughout ontogeny, the application of complementary age validation methods is preferred in order to provide a verifiable and defensible position for the determination of important life history parameters for sharks and other fishes.

Acknowledgments

We would like to thank F. F. Snelson (Florida Program for Shark Research, retired) for help with project logistics. Prior work and data provided by the long-term tagging of J. Casey, H. Pratt, and C. Stillwell, and the original histological sections to which we refer, made longevity estimates possible. We appreciate the contribution of tag-recapture data by N. Kohler (Apex Predators Program). We also thank R. Humphreys, E. DeMartini, R. Nichols, and three anonymous reviewers for comments that improved the manuscript. Moss Landing Marine Laboratories provided infrastructure support. T. Brown at Lawrence Livermore National Laboratory handled ^{14}C measurements. This work benefitted greatly from NMFS funding of the National Shark Research Consortium.

Literature cited

Andrews, A. H., L. A. Kerr, G. M. Cailliet, T. A. Brown, C. C. Lundstrom, and R. D. Stanley.
2007. Age validation of canary rockfish (*Sebastes pinniger*) using two independent otolith techniques: lead-radium and bomb radiocarbon dating. Mar. Freshw. Res. 58:531–541.

Ardizzone, D. A., G. M. Cailliet, L. J. Natanson, A. H. Andrews, L. A. Kerr and T. A. Brown.
2006. Application of bomb radiocarbon chronologies to shortfin mako (*Isurus oxyrinchus*) age validation. Environ. Biol. Fishes 77:355–366.

Branstetter, S.
1987. Age and growth validation of newborn sharks held in laboratory aquaria, with comments on the life history of the Atlantic sharpnose shark, *Rhizoprionodon terraenovae*. Copeia 1987:291–300.

Brewster-Geisz, K. K. and T. J. Miller.
1999. Management of the sandbar shark, *Carcharhinus plumbeus*: implications of a stage-based model. Fish. Bull. 98:236–249.

Broecker, W. S. and T. -H. Peng.
1982. Tracers in the sea, 690 p. Lamont-Doherty Geological Observatory, Palisades, NY.

Brown, T. A., D. E. Nelson, J. S. Vogel, and J. R. Southon.
1988. Improved collagen extraction by modified Longin method. Radiocarbon 30:171–177.

Cailliet, G. M., and A. H. Andrews.
2008. Age-validated longevity of fishes: Its importance for sustainable fisheries. *In* Fisheries for Global Welfare and Environment (K. Tsukamoto, T. Kawamura, T. Takeuchi, T. D. Beard Jr., and M. J. Kaiser, eds.), p. 103–120. TERRAPUB, Tokyo, Japan.

Cailliet, G. M., W. D. Smith, H. F. Mollet, and K. J. Goldman.
2006. Age and growth studies of chondrichthyan fishes: the need for consistency in terminology, verification,

validation, and growth function fitting. Environ. Biol. Fishes 77:211–228.

Campana, S. E.
2001. Accuracy, precision and quality control in age determination, including a review of the use and abuse of age validation methods. J. Fish Biol. 59:197–242.

Campana, S. E., J. M. Casselman, and C. M. Jones.
2008. Bomb radiocarbon chronologies in the Arctic, with implications for the age validation of lake trout (*Salvelinus namaycush*) and other Arctic species. Can. J. Fish. Aquat. Sci. 65:733–743.

Campana, S. E., C. Jones, G. A. McFarlane, and S. Myklevoll.
2006. Bomb dating and age validation using the spines of spiny dogfish (*Squalus acanthias*). Environ. Biol. Fishes 77:327–336.

Campana S. E., L. J. Natanson, and S. Myklevoll.
2002. Bomb dating and age determination of large pelagic sharks. Can. J. Fish. Aquat. Sci. 59:450–455.

Casey, J. G., and L. J. Natanson.
1992. Revised estimates of age and growth of the sandbar shark (*Carcharhinus plumbeus*) from the western North Atlantic. Can. J. Fish. Aquat. Sci. 49:1474–1477.

Casey, J. G., H. L. Pratt Jr., and C. Stillwell.
1985. Age and growth of the sandbar shark (*Carcharhinus plumbeus*) from the western North Atlantic. Can. J. Fish. Aquat. Sci. 42:963–975.

Conrath, C. L., and J. A. Musick.
2007. The sandbar shark summer nursery within bays and lagoons of the eastern shore of Virginia. Trans. Am. Fish. Soc. 136:999–1007.

Cortes, E.
1999. A stochastic stage-based population model of the sandbar shark in the western North Atlantic. AFS Symposium 23:115–136.

Druffel, E. M.
1989. Decadal time scale variability of ventilation in the North Atlantic: high-precision measurements of bomb radiocarbon in banded corals. J. Geophys. Res. 94:3271–3285.

Druffel, E. R. M., and T. W. Linick.
1978. Radiocarbon in annual coral rings of Florida. Geophys. Res. Lett. 5:913–916.

Ewing, G. P., J. M. Lyle, R. J. Murphy, J. M. Kalish, and P. E. Ziegler.
2007. Validation of age and growth in a long-lived temperate reef fish using otolith structure, oxytetracycline and bomb radiocarbon methods. Mar. Freshw. Res. 58:944–955.

Francis, M. P., S. E. Campana, and C. M. Jones.
2007. Age under-estimation in New Zealand porbeagle sharks (*Lamna nasus*): Is there an upper limit to ages that can be determined from shark vertebrae? Mar. Freshw. Res. 58:10–23.

Frantz, B. R., M. S. Foster, and R. Riosmensa-Rodriguez.
2005. *Clathromorphum nereostratum* (Corralinales, Rhodophyta): The oldest alga? J. Phycol. 41:770–773.

Fry, B.
1988. Food web structure on Georges Bank form stable C, N and S isotopic conditions. Limnol. Oceanogr. 33:1182–1190.

Grubbs, R. D., J. A. Musick, C. L. Conrath, and J. G. Romine.
2007. Long-term movements, migration, and temporal delineation of summer nurseries for juvenile sandbar sharks in the Chesapeake Bay region. *In* Shark nursery grounds of the Gulf of Mexico and the East Coast waters of the United States (C. T. McCandless, N. E. Kohler,and H. L. Pratt Jr., eds.), p. 87–108. Am. Fish. Soc. Symp. 50, Bethesda, MD.

Kalish, J. M.
1993. Pre and post bomb radiocarbon in fish otoliths. Earth Planet. Sci. Lett. 114:549–554.

Kalish, J. M., and J. Johnston.
2001. Determination of school shark age based on analysis of radiocarbon in vertebral collagen. *In* Use of the bomb radiocarbon chronometer to validate fish age (J. M. Kalish, ed.), p. 116–122. Fisheries Research and Development Corporation, Canberra, Australia.

Kerr, L. A., A. H. Andrews, G. M. Cailliet, T. A. Brown, and K. H. Coale.
2006. Investigations of $\Delta^{14}C$, $\delta^{15}N$, and $\delta^{13}C$ in vertebrae of white shark (*Carcharodon carcharias*) from the eastern Pacific Ocean. Environ. Biol. Fishes 77:337–353.

Kilada, R., S. E. Campana, and D. Roddick.
2007. Validated age, growth and mortality estimates of the ocean quahog (*Arctica islandica*) in the western Atlantic. ICES J. Mar. Sci. 64:31–38.

Kneebone, J., L. J. Natanson, A. H. Andrews, and H. Howell.
2008. Using bomb radiocarbon analyses to validate age and growth estimates for the tiger shark, *Galeocerdo cuvier*, in the western North Atlantic. Mar. Biol. 154:423–434.

McAuley, R. B., C. A. Simpfendorfer, G. A. Hyndes, R. R. Allison, J. A. Chidlow, S. J. Newman, and R. C. J. Lenanton.
2006. Validated age and growth of the sandbar shark *Carcharhinus plumbeus* (Nardo 1827) in the waters off western Australia. Environ. Biol. Fishes 77:385–400.

Merson, R. R. and H. L. Pratt.
2001. Distribution, movements and growth of young sandbar sharks, *Carcharhinus plumbeus*, in the nursery grounds of Delaware Bay. Environ. Biol. Fishes 61:13–24.

NMFS (National Marine Fisheries Service).
2006. SEDAR 11, Stock assessment report: large coastal shark complex, blacktip and sandbar shark, 387 p. NOAA/NMFS Highly Migratory Species Management Division, 1315 East-West Highway, Silver Spring, MD 20910.

NMFS (National Marine Fisheries Service).
2008. Final amendment 2 to the consolidated Atlantic Highly Migratory Species Fisheries Management Plan, 1 p. U.S. Dept. Comm., NOAA, NMFS, Silver Spring, MD.

Neilson, J. D. and S. E. Campana.
2008. A validated description of age and growth of western Atlantic bluefin tuna (*Thunnus thynnus*). Can. J. Fish. Aquat. Sci. 65:1523–1527.

Payne, A. I. L (ed.).
2006. Consensus summary report. *In* NMFS, SEDAR 11, Stock assessment report: large coastal shark complex, blacktip and sandbar shark. Section IV: review workshop consensus summary, 31 p. NOAA/NMFS Highly Migratory Species Management Division, 1315 East-West Highway, Silver Spring, MD 20910.

Passerotti, M. S., J. K. Carlson, A. N. Piercy, and S. E. Campana.
2010. Age validation of great hammerhead shark (*Sphyrna mokarran*), determined by bomb radiocarbon analysis. Fish. Bull. 108:346–351.

Roark, E. B., T. P. Guilderson, R. B. Dunbar, and B. L. Ingram.
2006. Radiocarbon based ages and growth rates: Hawaiian deep sea corals. Mar. Ecol. Prog. Ser. 327:1–14.

Romine, J. G., R. D. Grubbs, and J. A. Musick.
2006. Age and growth of the sandbar shark, *Carcharhinus plumbeus*, in Hawaiian waters through vertebral analysis. Environ. Biol. Fishes 77:229–239.
Sminkey, T. R., and J. A. Musick.
1995. Age and growth of the sandbar shark, *Carcharhinus plumbeus*, before and after population depletion. Copeia 1995:871–883.
Springer, S.
1960. Natural history of the sandbar shark *Eulamia milberti*. Fish. Bull., Fish Wildl. Ser. U.S. 178:1–38.
Stewart, R. E. A., S. E. Campana, C. M. Jones, and B. E. Stewart.
2006. Bomb radiocarbon dating calculated beluga (*Delphinapterus leucas*) age estimates. Can. J. Zool. 84:1840–1852
Stillwell, C. E., and N. E. Kohler.
1993. Food habits of the sandbar shark *Carcharhinus plumbeus* off the U.S. northeast coast, with estimates of daily ration. Fish. Bull. 91:138–150.
Stuiver, M., and H. A. Polach.
1977. Discussion: Reporting of ^{14}C data. Radiocarbon 19:355–363.
Vogel J. S., D. E. Nelson, and J. R. Southon.
1987. ^{14}C background levels in an accelerator mass spectrometry system. Radiocarbon 29:323–333.
Vogel J. S., J. R. Southon, D. E. Nelson, and T. A. Brown.
1984. Performance of catalytically condensed carbon for use in accelerator mass spectrometry. Nucl. Instr. Meth. Phys. Res. Sec. B. 5:289–293.

Acknowledgment of reviewers

The editorial staff of *Fishery Bulletin* would like to acknowledge the scientists who reviewed articles published in 2010–11. Their contributions have helped ensure the publication of quality science.

Allen H. Andrews
Seiji Arakaki

Kevin M. Bailey
Terry D. Beacham
James R. Bence
Ewann Bernston
Donna Marie Bilkovic
Richard W. Brill
Jeffrey A. Buckel
John S. Burke
Michael L. Burton
Chris Butler

Michael Canino
Nick Caputi
Massimiliano Cardinale
R. Christopher Chambers
Unai Cotano
George Cutter
Ivone Alejandra Czerwinski

Douglas A. DeVries
Antony W. Diamond
Jan Dierking
Ellen Druffel
William Duffy
Keith J. Dunton

Rana W. El-Sabaawi
Robert L. Emmett

Robert J. Feller
Michael L. Fine
Gary R. Fitzhugh

Damon P. Gannon
Susana Garrido
Patrick J. Gearin
R. Grant Gilmore, Jr.
Kenneth J. Goldman
W. Stewart Grant
Churchill B. Grimes
Juan C. Gutierrez-Estrada

Jon Hare
Euan Sinclair Harvey
Daniel Hasselman
Doug Hay
Mikko Heino
John Hess
John R. Hyde

Mattias Johansson
Marc A. Johnson

Craig R. Kastelle
Christopher Kelley
Neala Kendall
James Kennedy
David W. Kerstetter
Olav S. Kjesbu

Chi H. Lam
Timothy Langlois
Marisa N. C. Litz
Kwang Ming Liu
John Logan
Flavia M. Lucena

Romney McPhie
Frederic Menard
Richard L. Merrick
Bruce S. Miller
Todd W. Miller
Richard D. Methot
Roldan C. Muñoz
Hilario Murua

Anna Neuheimer
David L. Nieland

Jeffrey B. Olsen
James W. Orr
Joseph A. Orsi

Wayne Palsson
Michelle S. Passerotti (Andrews)
William F. Patterson, III
Pierre Pepin
Clay E. Porch
Steven Pothoven

Nicole Richoux
William Robbins
Christopher N. Rooper
Gregg Rosenkranz
Paul J. Rudershausen

Keith M. Sakuma
Jameal Farouq Samhouri
Lawrence E. Schaufler
Piper Schwenke
George R. Sedberry
Lisa W. Seeb
Kathryn Shulzitski
M. Shareef M. Siddeek
Dongwha Sohn
Stylianos Somarakis
Ingrid Spies
Allan W. Stoner
Stephen T. Szedlmayer

Ian Taylor
Mark Terceiro
Josie Thompson
Charles E. Tilburg
Cindy Tribuzio
Andrew W. Trites
Efthymia V. Tsitsika
Jefferson Turner
Victor M. Tuset

Sebastien Villeger

William Watson
Winsor Watson
Curt E. Whitmire
Erik H. Williams
Trevor Willis
Peter Witthames
Mark Wuenschel

Ronald M. Yoshiyama

Fishery Bulletin

Guidelines for authors

Manuscript Preparation

Contributions published in *Fishery Bulletin* describe original research in marine fishery science, fishery engineering and economics, as well as the areas of marine environmental and ecological sciences (including modeling). Preference will be given to manuscripts that examine processes and underlying patterns. Descriptive reports, surveys, and observational papers may occasionally be published but should appeal to an audience outside the locale in which the study was conducted. Although all contributions are subject to peer review, responsibility for the contents of papers rests upon the authors and not on the editor or publisher. *Submission of an article implies that the article is original and is not being considered for publication elsewhere.* **Articles** may range from relatively short contributions (10–15 typed, double-spaced pages, tables and figures not included) to extensive contributions (20–30 typed pages). Manuscripts must be written in English; authors whose native language is not English are strongly advised to have their manuscripts checked by English-speaking colleagues before submission.

Title page should include authors' full names and mailing addresses and the senior author's telephone, fax number, and e-mail address, and a list of key words to describe the contents of the manuscript. **Abstract** should be limited to 200 words (one-half typed page), state the main scope of the research, and emphasize the author's conclusions and relevant findings. Do not review the methods of the study or list the contents of the paper. Because abstracts are circulated by abstracting agencies, it is important that they represent the research clearly and concisely.

Text must be typed in 12 point Times New Roman font throughout. A brief introduction should convey the broad significance of the paper; the remainder of the paper should be divided into the following sections: **Materials and methods**, **Results**, **Discussion**, **Conclusions**, and **Acknowledgments**. Headings within each section must be short, reflect a logical sequence, and follow the rules of multiple subdivision (i.e., there can be no subdivision without at least two items). The entire text should be intelligible to interdisciplinary readers; therefore, all acronyms, abbreviations, and technical terms should be written out in full the first time they are mentioned. Include FAO common names for species in the list of keywords and in the introduction. Regional common names may be used throughout the rest of the text if they are different from FAO common names which can be found at http://www.fishbase.org/search.html. Follow the U.S. Government Printing Office Style Manual (2000 ed.) and Scientific Style and Format: the CSE Manual for Authors, Editors, and Publishers (7^{th} ed.) for editorial style; for fish nomenclature follow the most current issue of the American Fisheries Society's Common and Scientific Names of Fishes from the United States, Canada, and Mexico, 6^{th} ed. Dates should be written as follows: 11 November 2000. Measurements should be expressed in metric units, e.g., 58 metric tons (t); if other units of measurement are used, please make this fact explicit to the reader. Write out the numbers zero through nine unless they form part of measurement units (e.g., nine fish but 9 mm). Refrain from using the shorthand slash (/), an ambiguous symbol, in the general text.

Equations and mathematical symbols Set equations from a standard mathematical program (MathType) or tool (Equation Editor in MS Word). LaTex is acceptable for more advanced computations. For mathematical symbols in the general text (α, χ^2, π, $\pm$, etc.), use the symbols provided by the MS Word program and italicize all variables. Do not use the photo mode when creating these symbols in the general text.

Literature cited comprises published works and those accepted for publication in peer-reviewed literature (in press). Follow the name and year system for citation format in the "Literature cited" section (that is say, citations should be listed alphabetically by the authors' last names, and then by year if there is more than one citation with the same authorship). If there is a sequence of citations in the text, list chronologically: (Smith, 1932; Green, 1947; Smith and Jones, 1985). Abbreviations of serials should conform to abbreviations given in Cambridge Scientific Abstracts (http://www.csa.com/ids70/serials_source_list.php?db=biolclast-set-c). Authors are responsible for the accuracy and completeness of all citations. Literature citation format: Author (last name, followed by first-name initials). Year. Title of report or manuscript. Abbreviated title of the series to which it belongs. Always include number of pages. Cite all software and special equipment or chemical solutions used in the study, not in a footnote but within parentheses in the text (e.g., SAS, vers. 6.03, SAS Inst., Inc., Cary, NC).

Footnotes are used for all documents that have not been formally peer reviewed and for undocumented observations and communications. These types of references should be cited sparingly in manuscripts submitted to the journal. All reference documents, administrative reports, internal reports, progress reports, project reports, contract reports, personal observations, personal communications, unpublished data, manuscripts in review, and council meeting notes are footnoted in 9 pt font and placed at the bottom of the page on which they are first cited. Footnote format is the same as that for formal literature citations (e.g., Ref Doc. 10-65, 35 p.). A link to the online source (e.g., [Available at http://www/..... , accessed July, 2007.]), or the mailing address of the agency or department holding the document, should be provided so that readers may obtain a copy of the footnoted document.

Tables are often overused in scientific papers; it is seldom necessary or even desirable to present all the data associated with a study. Tables should not be excessive in size and must be cited in numerical order in the text. Headings should be short but ample enough to allow the table to be intelligible on its own. All unusual symbols must be explained in the table legend. Other incidental comments may be footnoted with italic numeral footnote markers. Use asterisks to indicate significance in statistical data. Do not type table legends on a separate page; place them above the table data. *Do not submit tables in photo mode.*

Figures include line illustrations, photographs (or slides), and computer-generated graphs and must be cited in numerical order in the text. Graphics should aid in the comprehension of the text, but they should be limited to presenting patterns rather than raw data. Figures should not exceed one figure for every four pages of text. Figures must be labeled with author's name and number of the figure. Avoid placing labels vertically (except for *y* axis). Figure legends should explain all symbols and abbreviations and should be double-spaced on a separate page at the end of the manuscript. Color is allowed in figures to show morphological differences among species (for species identification), to show stain reactions, and to show gradations in temperature contours within maps. Color is discouraged in graphs, and for the few instances where color may be allowed, the use of color will be determined by the Managing Editor.

- Zeros should precede all decimal points for values less than one.
- Sample size, *n*, should be italicized.
- Capitalize the first letter of the first word in all labels within figures.
- Do not use overly large font sizes in maps and for units of measurements along axes in figures.
- Do not use bold fonts or bold lines in figures.
- Do not place outline rules around graphs.
- Use a comma in numbers of five digits or more (e.g. 13,000 but 3000).
- Maps require a North arrow and degrees latitude-longitude (e.g., 170°E).

Failure to follow these guidelines and failure to correspond with editors in a timely manner will delay publication of a manuscript.

Copyright law does not apply to *Fishery Bulletin*, which falls within the public domain. However, if an author reproduces any part of an article from *Fishery Bulletin* in his or her work, reference to source is considered correct form (e.g., Source: Fish. Bull. 97:105).

Submission

Submit manuscript online at http://mc.manuscriptcentral.com/fisherybulletin. Commerce Department personnel should submit papers under a completed NOAA Form 25-700. For further details on electronic submission, please contact the Scientific Editorial Office directly at

julie.scheurer@noaa.gov

Once the manuscript has been accepted for publication, you will be asked to submit a final electronic copy of your manuscript. When requested, the text and tables should be submitted in Word format. Figures should be sent as PDF files, Windows metafiles, tiff files, or EPS files. Send a copy of figures in the original software if conversion to any of these formats yields a degraded version.

Questions? If you have questions regarding these guidelines, please contact the Managing Editor, Sharyn Matriotti, at

Sharyn.Matriotti@noaa.gov

Questions regarding manuscripts under review should be addressed to Julie Scheurer, Associate Editor.

Fishery Bulletin

Subscription form

Superintendent of Documents **Publications** Order Form

*5178

☐ YES, please send me the following publications:

____ Subscriptions to *Fishery Bulletin*
for $36.00 per year ($50.40 foreign)

The total cost of my order is $ _____ . Prices include regular domestic postage and handling and are subject to change.

_____
(Company or Personal Name) (Please type or print)

_____
(Additional address/attention line)

_____
(Street address)

_____
(City, State, ZIP Code)

_____
(Daytime phone including area code)

_____
(Purchase Order No.)

Charge your order. IT'S EASY!

VISA

MasterCard

Please Choose Method of Payment:

☐ Check Payable to the Superintendent of Documents
☐ GPO Deposit Account ☐☐☐☐☐☐☐–☐
☐ VISA or MasterCard Account
☐☐☐☐☐☐☐☐☐☐☐☐☐☐☐☐
☐☐☐☐ (Credit card expiration date)

To fax your orders (202) 512-2250

_____
(Authorizing Signature)

Mail To: Superintendent of Documents
P.O. Box 371954, Pittsburgh, PA 15250-7954

Thank you for your order!

Also available online at http://bookstore.gpo.gov/collections/fishery-bulletin